DISSERTATION

Cellular Signaling in Fungi

Ausgeführt zum Zwecke der Erlangung des akademischen Grades einer

Doktorin der Naturwissenschaften unter der Leitung von

PD. Dr.in Monika Schmoll

Institut für Verfahrenstechnik, Umwelttechnik und

technische Biowissenschaften, E166

eingereicht an der Technischen Universität Wien

Fakultät für Technische Chemie

von

Miriam Schalamun

01140758

Wien, am 13. 01. 2024

Affidavit

I declare in lieu of oath, that I wrote this thesis and performed the associated research myself, using only literature cited in this volume. If text passages from sources are used literally, they are marked as such.

I confirm that this work is original and has not been submitted elsewhere for any examination, nor is it currently under consideration for a thesis elsewhere.

I acknowledge that the submitted work will be checked electronically-technically using suitable and state-of-the-art means (plagiarism detection software). On the one hand, this ensures that the submitted work was prepared according to the high-quality standards within the applicable rules to ensure good scientific practice "Code of Conduct" at the TU Wien. On the other hand, a comparison with other student theses avoids violations of my personal copyright.

_____   _____

City and Date   *Signature*

Acknowledgements

Table of Contents

English abstract

Fungi are able to grow in various environments, including nutrient scarce, hostile surroundings. This is achieved by quickly adjusting their growth and metabolism to changing external signals, including the presence of nutrients, light, competitors or mating partners. These signals are received and conveyed by cellular signaling cascades, triggering fine-tuned responses by initiating gene expression and production of specialized metabolites and enzymes. This thesis examines the role of signaling components in the biotechnological workhorse *Trichoderma reesei* in response to the presence or absence of light and upon growth on cellulose and other carbon sources. The regulator of G-protein signaling (RGS4) was investigated for the part it plays in altered gene expression on cellulose in varying light conditions, in iron metabolism, asexual development and stress response. Furthermore, the analysis revealed that the MAPkinases TMK1, TMK2 and TMK3 are involved in sexual development, light depended cellulase gene expression and cellulase activity and the synthesis of secondary metabolites. This overlaps with functions of the transcription factor STE12, downstream of the MAPkinases. With a more ecological focus further investigations into interkingdom signaling were conducted, which led to elucidation of the early chemical communication and interaction between the agriculturally applied biocontrol agent *Trichoderma harzianum* B97 and plants, and the impact of a secondary metabolite gene cluster on plant root-colonization.

Deutsche Kurzfassung

Pilze sind in der Lage, in verschiedenen Umweltbedingungen zu wachsen, auch in nährstoffarmen, Umgebungen. Dies wird erreicht, indem sie ihr Wachstum und ihren Stoffwechsel schnell an sich ändernde externe Reize anpassen, z. B. an das Vorhandensein von Nährstoffen, Licht, Konkurrenten oder potentiellen Reproduktionspartnern. Diese Umweltreize werden von zellulären Signalkaskaden empfangen, weitergeleitet und lösen fein abgestimmte Reaktionen aus, indem sie die Genexpression und die Produktion spezialisierter Stoffwechselprodukte und Enzyme in Gang setzen. In dieser Arbeit wird die Rolle von Signalkomponenten in dem biotechnologisch vielfach eingesetzten Pilz, *Trichoderma reesei* als Reaktion auf die An- oder Abwesenheit von Licht und auf das Wachstum auf Zellulose und anderen Kohlenstoffquellen untersucht. Der regulator of G-Protein-signaling (RGS4) wurde auf seine Rolle bei der veränderten Genexpression auf Zellulose unter verschiedenen Lichtbedingungen, beim Eisenstoffwechsel, der asexuellen Entwicklung und der Stressreaktion untersucht. Weiters konnte gezeigt werden, dass die MAPkinasen TMK1, TMK2 und TMK3 an der sexuellen Entwicklung, der lichtabhängigen Cellulase-Genexpression und Cellulase-Aktivität sowie an der Synthese von Sekundärmetaboliten beteiligt sind, was sich mit der Rolle des MAPkinse-Downstream-Transkriptionsfaktors STE12 überschneidet. Darüber hinaus untersuchten wir die frühe chemische Kommunikation und Interaktion zwischen dem landwirtschaftlich eingesetzten Biokontroll Pilz *Trichoderma harzianum* B97 und Pflanzen sowie die Auswirkungen eines Sekundärmetabolit-Genclusters auf die Wurzelbesiedlung von Pflanzen.

Co-authorship statement

Chapter 1: My contribution to the review article "Trichoderma – genomes and genomics as treasure troves for research towards biology, biotechnology and agriculture" was revision and editing of the manuscript.

Chapter 2: My contribution to the publication "RGS4 impacts carbohydrate and siderophore metabolism in *Trichoderma reesei*" was the experimental work, bioinformatic analysis, including pre-processing of raw files and differential gene expression analysis, figure design and writing of the manuscript.

Chapter 3: My contribution to the publication "MAPkinases regulate secondary metabolism, sexual development and light dependent cellulase regulation in *Trichoderma reesei*" was RT-qPCR, chemotropic response analysis, figure design and writing of the manuscript.

Chapter 4: My contribution to the preprint "The transcription factor STE12 influences growth on several carbon sources and production of dehydroacetic acid (DHAA) in *Trichoderma reesei*" was RT-qPCR, bioinformatic analysis including pre-processing of raw files and differential gene expression analysis, figure design and writing of the manuscript.

Chapter 5: My contribution to the preprint "Plant recognition by *Trichoderma harzianum* elicits upregulation of a novel secondary metabolite cluster required for colonization" was gene deletion, colonization assay and confocal microscopy and editing of the manuscript.

Chapter 6: My contribution to the data analysis pipeline "Differential gene expression analysis optimized for Trichoderma reesei RNA sequencing data" was the development and implementation of the analysis script in R, as well as the creation and maintenance of the corresponding Github repository.

Aim and outline

This thesis aims to elucidate the complex signaling mechanisms in two filamentous fungi, *Trichoderma reesei* and *Trichoderma harzianum* in response to their environment. This includes understanding how these fungi react to environmental cues like light and different carbon sources, influencing their metabolism and interactions with plants.

To better understand the mechanisms of signal transmission, leading to fine-tuned responses in *T. reesei*, the role of a thus so far uncharacterized regulator of G-protein signaling (RGS4), the three MAPkinases TMK1, TMK2 and TMK3 and the downstream transcription factor STE12 were investigated. Deletion mutants, lacking these proteins were cultivated under the presence and absence of light on different carbons sources, evaluating growth and development, gene expression and synthesis of secondary metabolites. In addition, the role of the Plant Communication Associated (PCA) secondary metabolite gene cluster in *T. harzianum* is explored, to elucidate its impact on early fungus-plant communication and root colonization. Thereby, the topic of signaling in fungi should be covered with different aspects, from signal reception and transmission by components of G-protein and MAPkinase pathways, gene regulation by a transcription factor to output in the form of a secondary metabolite gene cluster and root colonization.

In summary, this thesis aims to enhance our understanding of fungal cellular signaling and demonstrating its potential in promoting sustainable biotechnological and agricultural practices.

Introduction

1. From natural habitats to biotechnological applications – the genus *Trichoderma* with workhorses in enzyme production and biocontrol

Fungi can adapt to a wide range of environments and are present in almost every part of the world. Even though we only know a fraction about the many different types and species, it is clear that they not only play a crucial role in natural ecosystems but also human life. Fungi are currently used across various sectors, including medicine, the food and beverage industry, the biofuel industry and in agriculture (Meyer et al., 2020). Particularly, filamentous fungi are vital in these sectors due to their rapid growth and their ability to produce enzymes, organic acids, and antibiotics (Alberti et al., 2017).

This thesis examines two such ascomycetous, filamentous fungi: *Trichoderma reesei* and *Trichoderma harzianum*. *T. reesei* is widely employed for its efficient enzyme production, specifically cellulases, while *T. harzianum*, is used in agriculture for biological pest control (Bischof et al., 2016; Xiao et al., 2023). Due to this widespread use, *Trichoderma* species are subject to diverse genomic studies to better understand the underlying biological mechanisms that are the basis to their efficacy (Chapter 1).

2. Cellulolytic enzyme production in *T. reesei*

In the natural ecosystem, filamentous fungi play a crucial role as primary decomposers of a wide variety of substances, with a particular emphasis on plant biomass. Lignocellulosic plants represent the most abundant biomass on earth (Bar-On et al., 2018). The main components of lignocellulose are polysaccharides such as cellulose, hemicellulose and pectin and the polyphenolic biopolymer lignin (Glass et al., 2013). For fungi to use lignocellulosic biomass as carbon source for their metabolism, they produce different cellulolytic enzymes that extracellularly hydrolyze the lignocellulose into simpler sugars, like glucose, that can then be taken up into the cells. In industrial applications, these enzymes are used in the textile industry, production of detergents, food and animal feed processing, the paper and pulp industry as well as in the generation of biofuels (El-Gendi et al., 2021; Kuhad et al., 2011).

Since the isolation of the *T. reesei* strain QM6a in the 1950s, it has become a highly utilized fungus for industrial enzyme production (Bischof et al., 2016). In the biofuel industry, cellulolytic enzymes produced by *T. reesei*, are used to pretreat recalcitrant plant substrates by breaking down the cellulose components into fermentable sugars which allows other microorganisms to convert these sugars into biofuels (Glass et al., 2013; Lange, 2017; Wilson, 2009). This approach not only breaks down cellulosic waste like crop residues or fruit peels but also transforms it into a valuable and renewable energy source (Belal, 2013; Saravanakumar & Kathiresan, 2014; Saravanan et al., 2012; Vasic et al., 2021).

To improve the protein production capabilities of the natural *T. reesei* isolate QM6a, optimizations by random mutagenesis created hypersecreting strains such as QM9414 and RUT-C30 with substantially higher cellulase activities (Peterson & Nevalainen, 2012). A significant characteristic of Rut-C30 is its reduced carbon catabolite repression, resulting from a truncation in the carbon catabolite repressor gene *cre1* (Rassinger et al., 2018). Upon presence of readily available simple sugars, carbon catabolite repression (CCR) is activated by CRE1 within minutes and inhibits the secretion of lignocellulolytic enzymes (Brown et al., 2014; Hinterdobler et al., 2021). For fungi, this represents an efficient control of its scarce energy resources, as enzyme production is an energetically expensive process. In the industrial enzyme production however, this is an unfavorable condition because upon cultivation on plant biomass, which consists of a mixture of carbohydrates, including simple sugars, CCR impairs the secretion of cellulolytic enzymes. Therefore, its regulation is studied in detail, showcasing the involvement of different components of the signaling machinery in the activation of CCR (Brown et al., 2014; Cupertino et al., 2015; de Assis et al., 2021; Kunitake et al., 2022; Wang et al., 2004). While the enhanced secretion is crucial for the industrial use of *T. reesei*, studies revealed that RUT-C30 possesses significant genomic alterations that limit its utility for basic research studies. These alterations include an 85 kb deletion affecting multiple genes and a truncation in *cre1*, which both complicate the study of naturally underlying molecular mechanisms (Ilmen et al., 1996; Seidl et al., 2008). Recent research has also shown that epigenetic mechanisms could be at play in the spontaneous degeneration observed in RUT-C30 cultures, leading to an irreversible and undesirable loss of cellulase producing capabilities. This phenomenon appears to be attributable to chromatin condensation in key

promoter regions, resulting in reduced transcript levels for the corresponding genes (Martzy et al., 2021).

Another strain commonly used both, in industrial applications and basic research is QM9414. Unlike RUT-C30, this strain is not subject to carbon catabolite repression but exhibits reduced responsiveness to light, a critical environmental cue in *T. reesei* cellulase regulation (Schmoll, 2018a; Stappler, Walton, et al., 2017). In summary, the strains currently of interest for industrial strain development carry considerably alterations in their genomes, which results in difficulties to draw conclusions as to the natural/biological roles of signaling processes. Due to these complexities, the natural isolate QM6a serves as the preferred *T. reesei* strain for this thesis, allowing investigations of the cellular mechanisms that govern primary and secondary metabolism with particular emphasis on the modulatory influence of light. In addition to discovery of the biological role of the processes we investigate, regulation of genes with mutations in RutC30 or QM9414 seen in our studies helps to narrow down the relevance of individual mutations in these strains for their high-enzyme production phenotype.

3. *Trichoderma harzianum*: a key player in biocontrol and explorations into fungus-plant communication

With an increasing global demand for food production also the agricultural productivity needs to grow which often leads to an increased use of chemical pesticides and fertilizers (van Dijk et al., 2021). To avoid further damage to our soils with chemicals, naturally occurring microorganisms play a crucial role as they can be utilized for biological pest control and as plant growth promoting agents (Yao et al., 2023). *Trichoderma* species are widely used for these purposes due to their ability to parasitize other fungi (mycoparasitism), through the action of cell wall degrading enzymes and by inhibiting their growth with bioactive compounds (Hermosa et al., 2012; Xiao et al., 2023). Furthermore, it was shown that the presence of *Trichoderma* species in the soil stimulates plant growth, increases resistance to disease as well as to abiotic stresses (Hermosa et al., 2012). Among *Trichoderma*, *T. harzianum* is one of the most extensively used species in biocontrol applications (Rush et al., 2021). While *T. harzianum* mycoparasitism and antagonism are well described, there is still a lack of understanding in the early interactions between fungus and plant. Chapter 5 investigates the function of a previously uncharacterized Plant Communication Associated (PCA) secondary

metabolite gene cluster in *T. harzianum* B97 (Compant et al., 2017). Furthermore, its role in fungus-plant communication with respect to chemotropic reactions of the fungus to the plant, plant root colonization and secondary metabolite production in both, the fungus and the plant are investigated.

4. Environmental sensing and signaling in fungi

The ability to efficiently react to and transmit environmental signals is crucial for fungi to swiftly adapt their metabolism to changes in their surroundings (Macias-Rodriguez et al., 2020). Membrane bound receptors receive these signals and transmit them downstream through signaling pathways, triggering a fine-tuned response. The individual signals sensed range from nutrient sources to pheromones to secondary metabolites to light in the environment (Carreras-Villaseñor et al., 2012; Herrera-Estrella & Horwitz, 2007). Whereas the output is equally complex, including the adjustment of enzyme and metabolite production, growth, morphology and many more. In only a few cases the signals from the environment could so far be connected to downstream pathways and output – for example in case of the pheromone response, but the ligands of the majority of receptors are unknown as are the targeted downstream pathways (Bardwell, 2004).

A key environmental signal for fungi is the presence or absence of light, which influences growth, differentiation, virulence, carbohydrate- and secondary metabolism as well as stress responses (Schmoll, 2018a; Yu & Fischer, 2019). The production of mycotoxins e.g., aflatoxins but also of antibiotics and other fungal metabolites are repressed by the presence of light (Moreno-Ruiz et al., 2020; Tisch & Schmoll, 2010). The mycoparasitic abilities of *Trichoderma atroviride* on the plant pathogen *Botrytis cinerea* is controlled by the circadian clock of both fungi, depended on nutrient availability, and inhibited by excessive light (Henriquez-Urrutia et al., 2022). This is in agreement with reduced metabolite production under exposure to white light (Moreno-Ruiz et al., 2020). Light also reduces *B. cinerea* virulence on plants and affects its morphology and resistance to oxidative stress (Canessa et al., 2013).

In *T. reesei*, the presence of light significantly impacts the expression and production of plant cell wall degrading enzymes through the action of photoreceptors at a transcriptional level (Schmoll, 2018a, 2018b; Schmoll et al., 2010). The three main photoreceptors in *T. reesei* are the two zinc-finger transcription factors BLR1 and BLR2 (blue light receptor 1 and 2) and the

small PAS/LOV domain containing protein ENV1 (Envoy) (Schmoll et al., 2005; Schuster et al., 2007). ENV1 is a key regulator in light signal transduction and exerts its function through the interconnection and regulation of the G-protein and cAMP pathway (Schmoll, 2018a; Schuster et al., 2012; Tisch et al., 2011a; Tisch et al., 2014).

4.1. G-protein signaling is involved in cellular responses to the environment

In eukaryotes, external signals are perceived by cell surface receptors such as G-protein coupled receptors (GPCRs) that transmit signals through the heterotrimeric G-protein complex (Figure 1). In *T. reesei,* 58 GPCRs coding genes, three G-alpha subunits, one G-beta and one G-gamma subunit are described (Schmoll, 2008; Schmoll et al., 2016; Schmoll & Hinterdobler, 2022). The binding of a ligand causes a conformational change of the GCPR and the activation of the G-proteins inside the cell (Li et al., 2007). This activation occurs via the exchange of GDP for GTP at the G-alpha subunit and leads to the dissociation of the G-beta-gamma complex. The three subunits then detach from the membrane bound GPCR and are free to interact with their downstream targets (Cabrera-Vera et al., 2003). The signal transmission is terminated by the intrinsic GTPase activity of the G-alpha subunits that hydrolyzes the GTP to GDP and causes a reassociation of the G-protein heterotrimer (Li et al., 2007). The duration of signal transmission depends on the hydrolysis rate of GTPase activity of the G-alpha subunit which is accelerated by the presence of regulators of G-protein signaling (RGS) proteins (Syrovatkina & Huang, 2019).

In *T. reesei*, G-protein signaling was investigated on multiple levels, including the GPCRs CSG1 and GPR8 which respectively are required for glucose sensing and in posttranscriptional regulation of cellulase production and the regulation of the SOR-cluster a secondary metabolite gene cluster, responsible for the secretion of sorbicillinoids (Derntl et al., 2016; Hinterdobler et al., 2020; Hitzenhammer et al., 2019; Monroy et al., 2017; Salo et al., 2016). The G-alpha subunits GNA1 and GNA3 and G-beta and -gamma subunits GNB1 and GNG1 play a critical role in connecting light response and nutrient signaling by modulating cellulase transcript levels in a light dependent manner (Tisch et al., 2011a; Tisch et al., 2014). To further investigate components of G-protein signaling, the phosducin-like protein PhlP1 which acts as co-chaperones for G-protein beta-gamma folding was functionally characterized and shown to also be involved in a light depended cellulase regulation (Tisch et al., 2011b). The deletion of PHLP1, GNB1 and GNG1 decrease transcript levels of the RGS-protein RGS1 which was

hypothesized to lead to an increased GNA1 activity, drawing overlaps in the connection of G-alpha and G-beta-gamma signal transmission (Tisch et al., 2011a). Since then, however, the four different RGS proteins and three GPCRs with RGS-domain were not further functionally characterized in *T. reesei* (Schmoll et al., 2016). In other filamentous fungi, RGS-proteins are involved in conidiation, stress response, pheromone response, toxin production, pathogenicity and nematode trapping (Kim et al., 2017; Y. Kim et al., 2019; Ma et al., 2021; Park et al., 2020; Y. Wang et al., 2013). To start the elucidation of the roles of RGS proteins in *T. reesei*, we investigated the role of the SNX/H-type RGS4 in cellulase regulation, stress response growth on different carbon sources and further found a light dependent involvement on the transcriptional regulation on a siderophore gene cluster (chapter 2).

4.2. MAPkinases in conserved regulatory mechanisms and individual responses

An alternative pathway downstream of G-protein coupled receptors for intracellular signal transmission involves the MAPkinase pathway, consisting of three protein kinases that form a phosphorylation cascade (Schmoll & Hinterdobler, 2022). The initial component in this cascade is a MAPkinase kinase kinase (MAPKKK), which, upon activation, phosphorylates serine/threonine residues on the MAPkinase kinase (MAPKK). In turn the MAPKK phosphorylates the MAPkinase (MAPK) which undergoes conformational change, is translocated into the nucleus and activates its target (Gustin et al., 1998). In many cases these targets are transcription factors which, upon phosphorylation, adjust the transcriptional pattern of the cell by inducing or repressing gene expression, according to the activating stimulus (Martinez-Soto & Ruiz-Herrera, 2017).

While the principle of phosphorylation cascades is conserved among eukaryotes, the quantity of MAPkinases and the variety of target molecules differ across fungal species (Avruch, 2007; Rispail et al., 2009; Tong & Feng, 2019). Furthermore, their precise subcellular localization plays a pivotal role in their functionality and the formation of regulatory feedback loops and feedback inhibition, a mechanism that enhances signal accuracy (Serrano et al., 2018). This inhibition is often orchestrated by phosphatases, which dephosphorylate and consequently deactivate MAPkinases (Gonzalez-Rubio et al., 2019). This complex interplay explains their involvement in nearly all essential physiological processes, including growth, sexual development, stress response, secondary metabolite production, metabolism, circadian

rhythmicity and light response (Bardwell, 2004; Lamb et al., 2011; Lengeler et al., 2000; Ma et al., 2022; Martinez-Soto & Ruiz-Herrera, 2017; Medina-Castellanos et al., 2018; Turra et al., 2014; Vitalini et al., 2007; Yu et al., 2016). In filamentous fungi, the three main MAPK pathways described are the pheromone response pathway, the cell wall integrity (CWI) pathway and the high osmolarity glycerol (HOG) pathway (Martinez-Soto & Ruiz-Herrera, 2017; Rispail et al., 2009; Schmoll et al., 2016; Tong & Feng, 2019). The physiological output of these pathways varies between species. In the yeast *S. cerevisiae*, the MAPK, Fus3 pheromone response pathway regulates cell-cell fusion in response to a pheromone signal transmitted by G-protein beta and gamma subunits (Lengeler et al., 2000). In filamentous fungi such as *N. crassa* and *Aspergillus* species, an additional involvement of other MAPkinase pathways has been shown to be required for sexual development (Frawley & Bayram, 2020). Additionally, the pheromone response pathway is implicated in pathogenicity (Jin et al., 2014; Zheng et al., 2000), secondary metabolite production (Bayram et al., 2012; Ma et al., 2022) and in *Trichoderma* species in the production of mycoparasitism related cell wall degrading enzymes (Mendoza-Mendoza et al., 2003; Moreno-Ruiz et al., 2021; Mukherjee et al., 2003; Reithner et al., 2007). Similarly, the MAPkinase homologues Slt2 in the CWI pathway and Hog1 in the HOG pathway are involved in cell wall integrity maintenance and in high osmolarity resistance but also in a variety of different other cellular responses, including circadian rhythm and light response (Bennett et al., 2013; Hohmann, 2015; Valiante, 2017; Yu et al., 2016).

In *T. reesei,* MAPkinase pathways were characterized for their roles in stress response, cell wall integrity, growth and regulation of cellulase gene expression (de Paula et al., 2018; Wang et al., 2014; Wang et al., 2017; M. Wang et al., 2013). However, as mentioned above, light plays a crucial role in *T. reesei* physiology but was not considered as environmental cue in previous studies. Therefore, we investigated the role of *T. reesei* MAPkinases TMK1 (Fus3-like), TMK2 (Slt2-like) and TMK3 (Hog1-like) in the light dependent regulation of cellulase production, in sexual development and the production of secondary metabolites (chapter 3).

In the world of signal transmission, transcription factors serve as the final component responsible for implementing the signal by enhancing or inhibiting gene transcription. With respect to cellulase gene expression, many transcription factors have been investigated in detail (Benocci et al., 2017). Downstream of the MAPkinase pheromone response pathway the Ste12 and Ste12-like transcription factors, which are unique to fungi, are potential targets

(Wong Sak Hoi & Dumas, 2010). In many fungi Ste12-like transcription factors are involved in pathogenicity and development (Rispail et al., 2009; Wong Sak Hoi & Dumas, 2010). In *T. atroviride* it was already shown that Ste12 acts downstream of the pheromone response pathway and mediates the effects of the MAPK Tmk1 in mycoparasitism, hyphal fusion, and expression of cell wall degrading enzymes involved in mycoparasitism and carbon source dependent growth (Gruber & Zeilinger, 2014). In chapter 4 we discuss the effects of deletion of STE12 in *T. reesei* with respect to gene expression upon growth on cellulose and its role in the production of secondary metabolites.
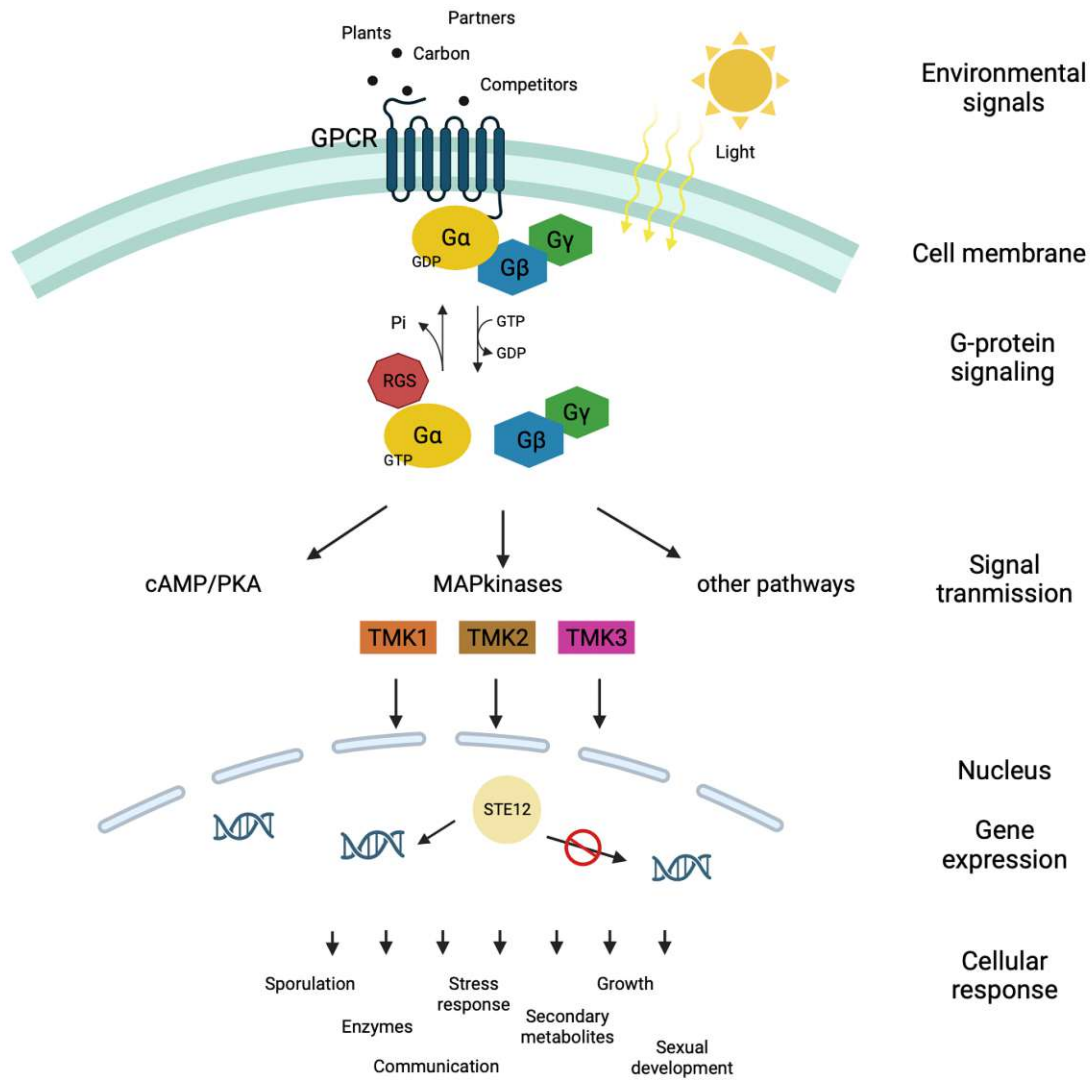
Figure 1. Schematic representation of signaling in *T. reesei.* Environmental signals are received at the cell membrane by GPCRs which activate the G-proteins by an exchange of GDP for GTP and dissociation of G-alpha subunit from the G-beta-gamma complex. RGS proteins accelerate the termination of signal transmission by increasing the intrinsic GTPase activity of the G-alpha subunits that hydrolyzes the GTP to GDP and leads to a reassociation of the G-protein complex. The signal is further transmitted downstream through various signaling cascades, including the MAPkinase phosphorylation cascade (cascade not shown), ending in the activation of the MAPkinases TMK1, TMK2 and TMK3 which further activate transcription factors such as STE12. Transcription factors trigger or inhibit gene expression which lead to cellular responses. The figure was created using biorender.com.

Chapter overview

Signaling cascades modulate responses to the environment by regulating carbon- and secondary metabolism in *Trichoderma*

The upcoming chapters investigate the regulatory roles of the regulator of G-protein signaling protein RGS4, the three MAPkinases TMK1, TMK2 and TMK3 and the transcription factor STE12 in *T. reesei*, examining their role in light dependent growth, gene expression, enzyme production and secondary metabolism (chapter 2 – 4). Additionally, we show that early communication between *T. harzianum* and plants is mediated by the PCA secondary metabolite gene cluster, which is required for plant root colonization (chapter 5). These studies would not possible without the advancements in genomics which have improved our understanding of *Trichoderma* evolution and physiology (chapter 1). These findings, along with ongoing research, will deepen our understanding of fungal regulatory processes and expand their potential in biotechnology and biocontrol, contributing to the advancement of a sustainable, bio-based economy.

Chapter 1: Trichoderma – genomes and genomics as treasure troves for research towards biology, biotechnology and agriculture

Miriam Schalamun[1], Monika Schmoll[1,2]

[1] AIT Austrian Institute of Technology, Center for Health and Bioresources GmbH, Tulln, Austria

[2] Department of Microbiology and Ecosystem Science, Division of Terrestrial Ecosystem Research, University of Vienna, Vienna, Austria

Trichoderma – genomes and genomics as treasure troves for research towards biology, biotechnology and agriculture

Miriam Schalamun[1] and Monika Schmoll[2]*

[1]Center for Health and Bioresources, AIT Austrian Institute of Technology GmbH, Tulln, Austria,
[2]Department of Microbiology and Ecosystem Science, Division of Terrestrial Ecosystem Research,
University of Vienna, Vienna, Austria

The genus *Trichoderma* is among the best studied groups of filamentous fungi, largely because of its high relevance in applications from agriculture to enzyme biosynthesis to biofuel production. However, the physiological competences of these fungi, that led to these beneficial applications are intriguing also from a scientific and ecological point of view. This review therefore summarizes recent developments in studies of fungal genomes, updates on previously started genome annotation efforts and novel discoveries as well as efforts towards bioprospecting for enzymes and bioactive compounds such as cellulases, enzymes degrading xenobiotics and metabolites with potential pharmaceutical value. Thereby insights are provided into genomes, mitochondrial genomes and genomes of mycoviruses of *Trichoderma* strains relevant for enzyme production, biocontrol and mycoremediation. In several cases, production of bioactive compounds could be associated with responsible genes or clusters and bioremediation capabilities could be supported or predicted using genome information. Insights into evolution of the genus *Trichoderma* revealed large scale horizontal gene transfer, predominantly of CAZyme genes, but also secondary metabolite clusters. Investigation of sexual development showed that *Trichoderma* species are competent of repeat induced point mutation (RIP) and in some cases, segmental aneuploidy was observed. Some random mutants finally gave away their crucial mutations like *T. reesei* QM9978 and QM9136 and the fertility defect of QM6a was traced back to its gene defect. The *Trichoderma* core genome was narrowed down to 7000 genes and gene clustering was investigated in the genomes of multiple species. Finally, recent developments in application of CRISPR/Cas9 in *Trichoderma*, cloning and expression strategies for the workhorse *T. reesei* as well as the use genome mining tools for bioprospecting *Trichoderma* are highlighted. The intriguing new findings on

evolution, genomics and physiology highlight emerging trends and illustrate worthwhile perspectives in diverse fields of research with *Trichoderma*.

Introduction

The genus *Trichoderma* belongs to the most beneficial group of fungi for humanity, which explains the extensive research efforts dedicated to biology and biotechnology with these fungi (Schuster and Schmoll, 2010; Druzhinina et al., 2011; Bischof et al., 2016; Guzman-Guzman et al., 2019). While industrial application of *Trichoderma* for protein production is limited to the descendants of a single species (Bischof et al., 2016; Paloheimo et al., 2016; Arnau et al., 2020), applications in agriculture for biocontrol and plant protection involve numerous species and strains (Kashyap et al., 2017; Lahlali et al., 2022; Tyskiewicz et al., 2022) and their high performance made *Trichoderma* the biocontrol agent with the highest market performance in terms of value, even higher than bacterial biocontrol agents together[1] [2]. Due to their versatility, *Trichoderma* species serve as models for such important topics like mechanisms regulating plant cell wall degradation (Glass et al., 2013; Bischof et al., 2016), biocontrol (Harman et al., 2004a; Guzman-Guzman et al., 2019; Harman et al., 2021), effector like molecules (Ramirez-Valdespino et al., 2019) and light response (Schmoll et al., 2010; Carreras-Villaseñor et al., 2012; Schmoll, 2018a; 2018b). Additionally, *Trichoderma* spp. are a valuable source for natural products leveraged by screening genomes with constantly enhanced software tools (Rush et al., 2021). Recently, even a connection between the innate immune system of animals and *Trichoderma* was drawn (Medina-Castellanos et al., 2018). Interestingly, *Trichoderma* can initiate heritable plant priming responses, which are attributed to epigenetic regulation (Moran-Diez et al., 2021). Not only the active fungi themselves, but also extracts of *Trichoderma* spp. can inhibit growth and/or production of mycotoxins by pathogens (Stracquadanio et al., 2021). However, only a few years ago also a potential downside of the distribution of *Trichoderma* in nature became obvious with

the detection of *T. afroharzianum* causing maize ear rot disease (Pfordt et al., 2020; Sanna et al., 2022). Consequently, species identification and genomic competences of these fungi deserve particular attention. *Trichoderma* spp. show an exceptional versatility in their preferred habitats and substrates with lifestyles ranging from mycoparasitism to plant saprotrophy and accordingly life in habitats characterized by feeding on fungi or decaying plant material, in soil or even as endophytes in living plant tissue, which changed during evolution several times (Chaverri and Samuels, 2013)

Starting from the genome sequence of *T. reesei*, which was published in 2008 (Martinez et al., 2008), the genomes of numerous *Trichoderma* model strains for enzyme production and biocontrol followed (Figure 1). The availability of the genome sequences of major model fungi of *Trichoderma* considerably contributed to detailed investigation of mechanisms of action and regulation of pathways (Sood et al., 2020), which is focused on systemic resistance of plants (Shoresh et al., 2010), colonization (Hinterdobler et al., 2021b; Taylor et al., 2021; Hafiz et al., 2022; Taylor et al., 2022), effector molecules (Ramirez-Valdespino et al., 2019) and plant-fungus-pathogen interactions (Mendoza-Mendoza et al., 2018; Macias-Rodriguez et al., 2020; Alfiky and Weisskopf, 2021) among others.

One crucial task in the future will be to seriously investigate both competences of *Trichoderma* strains that can be applied for human benefit and to balance these benefits with potential threats by strains with harmful characteristics for human and plant health. The imminent climate crisis and the aim of more sustainable and safe agriculture require increased research efforts to safely develop biocontrol applications and support of plant health by microbes without risking ecological or human adversities.

The NCBI taxonomy browser (https://www.ncbi.nlm.nih.gov/Taxonomy/Browser/; accessed on July 11, 2022) lists more than 400 *Trichoderma* species and additionally over 1800 unclassified *Trichoderma* species. The ecophysiology and evolution of a first batch of more than 30 *Trichoderma* species is currently subject to a large scale sequencing effort with the Joint Genome Institute (JGI community sequencing project CSP-503464), which will be followed by analyses of another several hundred species to be analyzed.

---

1   https://www.marketsandmarkets.com/Market-Reports/biofungicide-market-8734417.html

2   https://www.mordorintelligence.com/industry-reports/global-fungi-based-agricultural-microbial-market
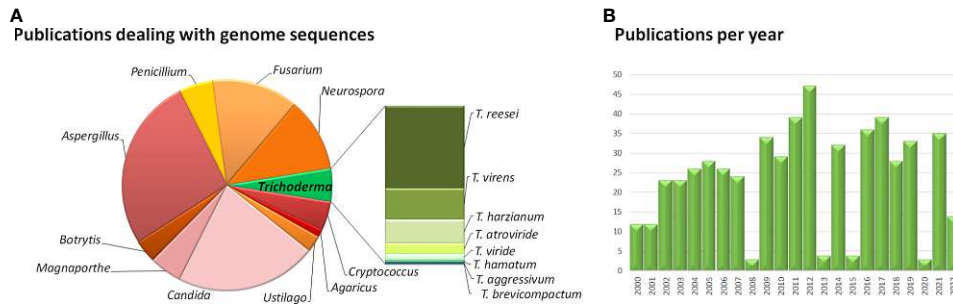
FIGURE 1
Overview of studies dealing with fungal genomes. **(A)** Results of a Pubmed search for "genome sequences" of the respective fungi. **(B)** Number of studies dealing with „*Trichoderma* genome sequences" per year published in Pubmed. The website pubmed.ncbi.nlm.nih.gov/was accessed in August 2022.

Large scale research efforts for many species of *Trichoderma* revealed the evolutionary basis of the versatility of the fungi in this genus and provided important insights into their evolution. The genus evolved about 66 million years ago with later formation of the sections Longibrachiatum and Trichoderma and the clade Harzianum/Virens (Kubicek et al., 2019). Evolution of the genus was dominated by considerable gene gain (predominantly encoding ankyrins, HET domain proteins and transcription factors) and loss events around a core genome of exactly 7000 genes, which formed the basis for the diverse competences of *Trichoderma* (Kubicek et al., 2019). This core genome is dominated by genes involved in metabolism, with an important share of genes assigned to the KOG families "posttranslational modification, protein turnover and chaperones", "transcription" and "carbohydrate transport and metabolism", but also high numbers of glycoside hydrolases and fungal specific transcription factors (Kubicek et al., 2019). The constant adaptation and optimization of *Trichoderma* genomes is reflected in the finding that of the 105 orphan genes found in the core *Trichoderma* genome by comparing fungi out of this genus, most are under strong purifying selection (Kubicek et al., 2019).

Trichoderma – fungal pirates with a taste for plants

Being among the most important genera for industry and agriculture, the evolution of *Trichoderma* and their metabolic consequences is highly relevant for research. In recent years, enabled by sequencing efforts for several important *Trichoderma* species, intriguing new aspects on evolution in the genus *Trichoderma* were revealed, which in part explain their special characteristics. Horizontal or lateral gene transfer (HGT/LGT) has long been known to play a role in evolution, also in fungi, although it was considered to be more important in bacteria at

first (Wang et al., 2015b). However, discrepancies of gene content or presence of whole clusters in closely related species can also be due to selective pressure and loss of genes, or a combination of selection and HGT (Hou et al., 2022).

An intriguing example for the latter phenomenon was found with the sorbicillin secondary metabolite gene cluster in *T. reesei* (Figure 2) (Druzhinina et al., 2016). Sorbicillinoids are yellow to orange secondary metabolites (Derntl et al., 2016; Salo et al., 2016; Guzman-Chavez et al., 2017), with weak antagonistic effects against bacteria (Duan et al., 2022; Hou et al., 2022) and pharmacological activity (Meng et al., 2016). The respective gene cluster contains two polyketide synthases, an FAD dependent monooxygenase, an MSF transporter and two transcription factors as most important components (Druzhinina et al., 2016; Monroy et al., 2017). The cluster is transcriptionally regulated by light and in response to different carbon sources (Monroy et al., 2017; Stappler et al., 2017) as well as by the two transcription factors in the cluster, YPR1 (Derntl et al., 2016; Derntl et al., 2017) and YPR2 (Hitzenhammer et al., 2019), by the carbon catabolite repressor CRE1 (Monroy et al., 2017) and by LAE1 (Karimi Aghcheh et al., 2013).

The genes of this cluster are only in part present in other *Trichoderma* spp, but closely related to clusters in *Penicillium notatum* and other Eurotiomycetes as well as a few Sordariomycetes (Maskey et al., 2005; Harned and Volp, 2011) and their phylogeny is not in accordance with the Ascomycota phylogeny, which hints at HGT events from different ancestors. Investigation of the evolution of the SOR cluster revealed several HGT events between *Acremonium chrysogenum, Penicillium rubens, Ustilaginoidea virens, Colletotrichum graminicola* and *Trichoderma*, in which *Trichoderma* spp. appears to only have received SOR2 (Druzhinina et al., 2016). To explain the evolution of the remaining genes of the cluster, selection and gene loss were analyzed, which showed that the cluster arose in early Hypocreales, was complemented by HGT and is under strong purifying selection (Druzhinina et al., 2016). In *T. reesei*
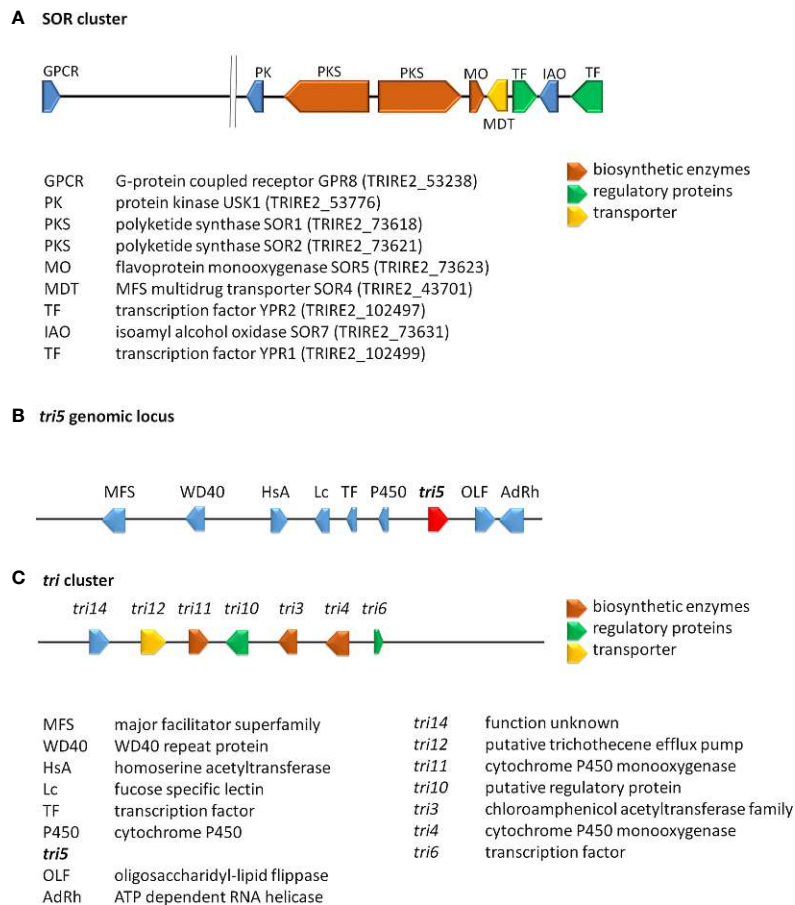
FIGURE 2

Schematic representation of selected secondary metabolite clusters in *Trichoderma*. **(A)** The SOR cluster in *T. reesei* along with characterized flanking genes. Functions and JGI protein IDs (*T. reesei* v2.0) are listed below the scheme. **(B)** The genomic locus of *tri5* in *T. arundinaceum* and *T. brevicompactum* (Gutierrez et al., 2021). **(C)** The *tri* cluster in *T. arundinaceum* (Cardoza et al., 2011). Encoded proteins of the *tri* cluster and the *tri5* genomic locus are given below the scheme.

two additional genes with clear relations to the cluster and located close to it in the genome were detected. The gene encoding protein kinase USK1 (unique SOR cluster kinase) is located only 2.3 kb upstream of *sor1* and is not syntenic in other fungi, not even in *Trichoderma* spp. (Beier et al., 2020). USK1 regulates VEL1 which is crucial for coordination of secondary metabolism with development (Bayram and Braus, 2012; Bazafkan et al., 2015) and several genes of the SOR cluster. Accordingly, lack of USK1 decreases production of sorbicillins considerably, but is also required for normal levels of alamethicine and paracelsins (Beier et al., 2020).

In a distance of about 60 kb upstream of the SOR cluster, the G-protein coupled receptor GPR8 (Hinterdobler et al., 2020a) is located, which is largely co-regulated with the SOR cluster under several conditions (Stappler et al., 2017). Although homologues of GPR8 are encoded in other *Trichoderma* spp. and related fungi, their locus in the genome is not syntenic and the

homologous genes are mostly located on different scaffolds or chromosomes (Hinterdobler et al., 2020a). GPR8 is the only member of class VII (secretin like) G-protein coupled receptors in the currently investigated *Trichoderma* spp. (Gruber et al., 2013; Schmoll et al., 2016). While the ligand of GPR8 is not yet known, transcriptome analysis showed a considerable impact on gene regulation predominantly in darkness, which not only impacts secondary metabolism, but also carbon metabolism (Hinterdobler et al., 2020a). In accordance with its impact on the SOR cluster genes, the regulatory targets of GPR8 overlap also with those of the SOR cluster transcription factor YPR2 (Hitzenhammer et al., 2019) and production of sorbicillinoids, alamethicine, orsellinic acid and paracelsins is strongly decreased (Hinterdobler et al., 2020a). Despite their clear relations to the SOR cluster, the phylogenetic characteristics of both GPR8 and USK1 do not align with the phylogeny of *Trichoderma* within the ascomycetes, which hints at an

involvement of either HGT or selection pressure on these genes during evolution as shown for the SOR cluster genes, which remains to be investigated.

In summary, the question remains, why this cluster was retained and even complemented during evolution in *T. reesei*, but not in closely related species. Since sorbicillins only have a relatively weak antagonistic function towards other microbes (Derntl et al., 2017), it is unlikely that their major relevance lies in competition and defense. Interestingly, transcriptome analyses revealed that the core SOR cluster genes are among those most strongly transcribed under conditions of sexual development in *T. reesei* (Dattenböck et al., 2018). Additionally, mutual transcriptional regulation of *sor1*, *sor2* and *sor5* establishes a pattern reminiscent of a feedback cycle, which acts positively in light and negatively in darkness (Monroy et al., 2017). Since deletion of *gpr8* resulted in altered regulation of several sensing and signaling genes including eight G-protein coupled receptor genes, the function of sorbicillinoids as signaling molecules and of the SOR cluster as a tool for communication warrants further investigations.

A history of gene loss and potential re-acquisition *via* HGT was also proposed for a gene involved in trichothecene production. Trichothecenes are harmful mycotoxins, which are produced by several genera of the fungal order Hypocreales (Cardoza et al., 2011). The terpene synthase gene *tri5* (Malmierca et al., 2013), which catalyzes formation of trichodiene is present in a part of *Trichoderma* species, but not in all cases with a functional copy (Vicente et al., 2020) (Gutierrez et al., 2021). In contrast to other fungi, the gene in *Trichoderma* is located outside of the trichothecene biosynthesis cluster (Figure 2) (Lindo et al., 2018; Proctor et al., 2018). This interesting evolution of gain and loss of *tri5*, sometimes even if the associated trichothecene biosynthesis cluster was not present in the genome, suggests a competitive advantage of trichodiene production, justifying the acquisition of the whole and parts of the cluster (Gutierrez et al., 2021).

A further case for the occurrence of LGT is the group of ceratoplatanins with three members in the core genome of *Trichoderma* (some *Trichoderma* species have also 4 ceratoplatanin genes) of which only one is efficiently expressed (Gaderer et al., 2014; Gaderer et al., 2015; Gao et al., 2020). Ceratoplatanins of *Trichoderma* are involved in the activation of plant defences and induce expression of peroxidase and dioxygenase encoding genes (Salas-Marina et al., 2015), reduce surface hydrophobicity and negatively affect root colonization (Gao et al., 2020). Analysis of evolution of EPL1-like ceratoplatanins in 37 *Trichoderma* genomes and numerous other genomes revealed their likely origin in Basidiomycota with a distribution to Ascomycota by several ancient events of LGT (also within Ascomycota) and subsequent diversification by birth-and-death evolution. Moreover, all four *Trichoderma* ceratoplatanins were found to be under purifying selection pressure (Gao et al., 2020).

For the evolution of hydrophobins, which form hydrophobic layers that cover fungal bodies and spores (Bayry et al., 2012; Guzman-Guzman et al., 2017) and broadly affect fungal physiology (Cai et al., 2021) a differential impact on fungal fitness was proposed (Cai et al., 2020). Especially *T. harzianum* HFB4 was shown to evolve under strong positive selective pressure, while most other hydrophobins were subject to purifying selection. Consequently, evolution of hydrophobins is suggested as an example of fitness tradeoffs during evolution (Kubicek et al., 2008; Cai et al., 2020).

However, the genomes of *Trichoderma* hold remnants of even more intriguing events, which shaped their physiological characteristics. *Trichoderma* species are known for their exceptional abilities to feed on a broad range of substrates from plant debris to dead fungi to parasitism on living pathogens and diverse degradation products related to these materials (Druzhinina et al., 2011; Druzhinina et al., 2018). Although at first different species were considered specialists for either degradation of cellulosic plant material or fungal biomass (Kubicek 2011), later studies showed that these metabolic competences are present in all *Trichoderma* species (Druzhinina and Kubicek, 2013). In fact, *Trichoderma* shares a last common ancestor with entomoparasitic fungi and the phylogenetic branch leading to the plant associated Nectriaceae diverged earlier in evolution (Druzhinina et al., 2018). Intriguingly, in depth analysis of nine *Trichoderma* genomes revealed that more than 40% of the plant cell wall degrading genes encoding CAZymes (Carbohydrate Active enZymes) of *Trichoderma* was gathered from other plant associated filamentous Ascomycota by LGT. The auxiliary protein swollenin (Saloheimo et al., 2002; Brotman et al., 2008) was even likely obtained from green plants by LGT (Druzhinina et al., 2018), which is supported by the finding that *Trichoderma* spp. are frequently found as members of endophytic fungal communities (Gazis and Chaverri, 2010; Yadav et al., 2022) and generally plant symbionts living in their rhizosphere (Harman et al., 2004a). In contrast to numerous genes encoding enzymes, their major regulators XYR1, ACE2 and ACE3 (Benocci et al., 2017) evolved by vertical gene transfer, but not by LGT (Druzhinina et al., 2018). The results of this study further suggest that *Trichoderma* spp. originally represented potent mycoparasites and that this very lifestyle allowed them to broaden their metabolic competences by collecting, combining and optimizing novel genes they encountered when feeding on fungal prey. Hence the plant cell wall degradation related CAZome of *Trichoderma* is distinct from other hypocrealean fungi. In addition to genes extending the nutrient versatility of *Trichoderma*, 123 further genes were detected, which were putatively obtained by other fungi. They include genes encoding four GPCRs of the PTH11 type, two of which were tested for a relevance in cellulase regulation previously (Stappler et al., 2017), the small unique protein OOC1 (Schmoll and

Kubicek, 2005; Pang et al., 2021), the dehydrogenase GRD1, which impacts cellulase regulation in a light dependent manner (Schuster et al., 2011), the high affinity nitrate transporter NIT10, CIP1, which was identified as one of the VIP genes limiting hydrolysis performance of cellulase mixtures (Lehmann et al., 2016) and CON-13, which is putatively involved in asexual reproduction (Hager and Yanofsky, 1990).

With respect to CAZymes and polysaccharide degradation, the description of a novel glucuronan lyase system in *T. parareesei* (Druzhinina et al., 2010) adds a further highlight to the versatility of the genus (Pilgaard et al., 2022). Detailed analyses of activity and degradation products confirmed that this degradation system enables complete degradation of glucoronan, which is found in fungi like *Agaricus bisporus* – a possible prey of the mycoparasite *T. parareesei*, to easily absorbable dimers and monomers (Pilgaard et al., 2022).

A further interesting aspect of evolution was reported for the processivity of cellulases with *T. reesei* CEL6A and CEL7a as examples. While in fungi, family 7 glycoside hydrolases are highly processive, the same characteristic is adopted by bacteria for family 6 cellulases. In both cases, the presence of highly processive and less processive cellulases avoids "traffic jams" on the cellulose fibers, which would decrease efficiency. Consequently, the high relevance of efficient cellulose degradation for competitive success in nature obviously led to convergent evolution of cellulases in which the structural features of cellulases was shaped to optimize processivity and interplay of the cellulose degrading machinery in bacteria and fungi (Uchiyama et al., 2020).

Recombination and mating as tools of evolution – repeat induced point mutation and segmental aneuploidy in *Trichoderma*

Sexual development is crucial for propagation and evolution of a species (Bennett and Turgeon, 2016; Wallen and Perlin, 2018), especially if environmental conditions deteriorate (Debuchy et al., 2010; McDonald et al., 2016). In *Trichoderma*, numerous strains of diverse species were isolated from fruiting bodies (Jaklitsch and Voglmayr, 2015) – indicating that mating happens in nature – but only for *T. reesei* induction of sexual development was achieved under laboratory conditions (Seidl et al., 2009; Hinterdobler et al., 2020b). Although this novel tool for strain improvement opens up intriguing perspectives for industry, in that strains can be bred for enhanced performance, also drawbacks became obvious. Besides the female sterility of QM6a, which is due to a defect in the

scaffolding protein HAM5 (Seidl et al., 2009; Linke et al., 2015; Tisch et al., 2017), the process of repeat induced point mutation may hamper optimization of genetically already modified production strains.

RIP was first discovered in *Neurospora* (Selker et al., 1987) as a mechanism for protection of the genome from transposable elements and mobile DNA (Gladyshev, 2017) and is operative in most Ascomycota (van Wyk et al., 2020). In case of a functional RIP mechanism, repetitive DNA sequences >400 bp cause C-5 cytosine methylation and deamination by the methyltransferases *rid1* and *dim2* prior to meiosis (Kouzminova and Selker, 2001; Li et al., 2018). Nevertheless, RIP was also observed for smaller duplicated regions (Gladyshev and Kleckner, 2014).

Genomes of organisms in which RIP is operative show a low number of repetitive sequences or transposon remnants (Gladyshev, 2017) as for example *N. crassa* (Krumlauf and Marzluf, 1980; Borkovich et al., 2004), which is also true for the genome of *T. reesei* (Martinez et al., 2008) although RIP was not unequivocally detected at first (Schuster et al., 2012). Nevertheless, operation of RIP is different in *T. reesei* compared to *N. crassa* (Li et al., 2018) with different dinucleotide preference and requirement of the methyltransferase genes *rid1* and *dim2* for normal sexual development in *T. reesei* but not *N. crassa*. Interestingly, *T. reesei* QM6a was found to have comparatively few transposon sequences, which are mostly located in AT-rich regions (Li et al., 2017).

Consequently, this mechanism is of utmost importance for evolution, especially considering the history of lateral gene transfer as well as gain and loss of genes as seen in *Trichoderma*. Additionally, evolution of the genome by gene duplication would be counteracted in a sexually propagating population of *Trichoderma*.

Besides RIP, another phenomenon decreased the enthusiasm after the achievement of sexual development under laboratory conditions. Already in the first crosses of QM6a with the fertile CBS999.97 (MAT1-1) strain, the diverse phenotypes of the progeny were obvious (M. Schmoll, unpublished). Detailed analysis then showed that of the 16 ascospores generated by meiosis and two rounds of postmeiotic mitosis four to eight were inviable and segmentally aneuploid ascospores were found (Chuang et al., 2015; Schmoll and Wang, 2016). The segmental duplication and deletion in the respective genome area caused loss of the polyketide synthase *pks4*, which is responsible for spore coloration (Atanasova et al., 2013) and loss of a xylanase and hence lignocellulosic biomass degradation efficiency increased in these progeny (Chuang et al., 2015). However, this process is not easily predictable in crosses between other nature isolates of *T. reesei* or among production strains.

High quality genome sequences of important plant symbionts

Besides strains of *T. reesei*, also strains of prototypical biocontrol agents were recently re-sequenced to get high quality genome sequences for reliable analysis of genome synteny and evolutionary events (Li et al., 2021b). This analysis revealed that the telomeric sequences are conserved between *T. reesei* CBS999.97, *T. reesei* QM6a, *T. virens* Gv29-8, *T. virens* FT-333, *T. atroviride* P1 and *T. asperellum* FT-101. Third generation sequencing now also enabled analysis of AT-rich blocks, which can hardly be aligned based on the short NGS-sequence reads. Interestingly, the *T. reesei* strains have a lower percentage of AT-rich blocks than the four other strains (7-8% versus 11-13%), which in part explains their larger genome sizes (Li et al., 2021b). Generally, the genome contents of the four *Trichoderma* species are highly divergent, with 2000 – 3000 species specific genes each and obviously all seven tested high quality *Trichoderma* genomes underwent extensive transposon invasions followed by RIP mutations. Additionally, evidence for considerable chromosome shuffling in *Trichoderma* was found (Li et al., 2021b). In addition to the previously reported 7000 core *Trichoderma* genes (Druzhinina et al., 2018), the four biocontrol agents possess 800 more conserved genes (Li et al., 2021b). An important divergence in gene content was observed for transcription factor genes, with variations in the subfamilies of fungal zinc-binuclear cluster domains and fungal specific transcription factor domains, while the gene numbers of the other transcription factor families were identical among the seven genomes. Moreover, the investigated high quality genome sequences support the hypothesis that CAZyme genes form physically linked CAZyme gene clusters in polysaccharide utilization loci. Besides several species specific clusters, *T. reesei* and *T. virens* were found to share 14 common CAZyme gene clusters whereas *T. atroviride* and *T. asperellum* share 18 (Li et al., 2021b). As for secondary metabolite gene clusters, *T. reesei* and *T. virens* share 27 common clusters and *T. atroviride* and *T. asperellum* have 37 clusters in common (Li et al., 2021b).

The frequent presence of genes associated with secondary metabolism in such clusters was already noted with the first genome analysis of *T. reesei* and also specific secondary metabolite clusters were detected (Martinez et al., 2008). Investigation of the distribution and evolution of Cytochrome P450 genes in several *Trichoderma* spp. now allowed for additional insights into clustering of secondary metabolite genes complemented by Cytochrome P450s. In the *Trichoderma* Cypome (the genome content of Cytochrome P450 encoding genes), 12 specific families of this functional group were detected (Chadha et al., 2018).

Intriguing news about well-known model *Trichoderma* species

In recent years, improvement of the quality of genome sequencing was subject to intensive research. The genome of *T. reesei* QM6a was subjected to proximity ligation scaffolding (Jourdier et al., 2017) using the GRAAL software tool (Marie-Nelly et al., 2014), which already yielded an improvement compared to the initial assembly (Martinez et al., 2008). Approximately at the same time, long read sequencing using the PacBio or Nanopore (ONT; flowcell 10.4) technologies (supported by Illumina short read sequencing to enhance quality) was increasingly used to improve the quality of genome sequences and so called "gold-standard" genomes became available for many organisms. For *T. reesei* QM6a (Li et al., 2017), this high quality sequence revealed numerous sequencing errors, indels and inversions in older genome assemblies (Martinez et al., 2008; Marie-Nelly et al., 2014; Jourdier et al., 2017) and yielded more than 1000 previously undetected genes. Telomer-to-telomer sequences became available for all seven chromosomes along with the sequence of the mitochondrial genome which is identical with that published previously (Chambergo et al., 2002), confirming the high quality of the sequence. Additionally, a comparison to the RutC30 genome indicates that the number of translocation in this strain is lower than reported earlier (Seidl et al., 2008; Peterson and Nevalainen, 2012). The long reads obtained with third generation sequencing even allowed for correct sequencing of the highly AT-rich centromere region, in which several genes were detected (Li et al., 2017).

Since the achievement of sexual development under laboratory conditions, this process is subject to detailed investigation for important determinants as well as its consequences in the *Trichoderma* genomes (Schmoll, 2013; Hinterdobler et al., 2020b). In the course of investigation of recombination during meiosis, high quality genome sequences of CBS999.97(MAT1-1) and CBS999.97 (MAT1-2) (Lieckfeldt et al., 2000; Seidl et al., 2009) were prepared by third generation sequencing (Li et al., 2021a). Like QM6a, they also have seven chromosomes. As RIP (Gladyshev, 2017) is operative in *Trichoderma*, the CBS999.97 genomes only contain 62 transposable elements (Li et al., 2021a). Phenotypes of QM6a and CBS999.97 strains show considerable differences and their progeny are unexpectedly diverse (Seidl et al., 2009; Li et al., 2017). Accordingly, a very high number of SNPs and indels (ca. 1 Mio) were detected between QM6a and the CBS999.97 strain, but only around 2700 between CBS999.97(MAT1-1) and CBS999.97(MAT1-2). However, during analysis, problems with "difficult to align" sequences were observed and therefore the specifically developed software tool TSETA (TGS to Enable Tetrad Analysis; (Liu et al., 2021)) was used, which then

identified around 6 fold more alterations between QM6a and CBS999.97 with sizes of up to 61 kb (Li et al., 2021a). Interestingly, for QM6a more than 3000 nucleotides were subject to RIP, while in CBS999.97 (MAT1-1) this was the case for only 92 nucleotides (Li et al., 2021a).

Although QM6a represents a nature isolate, it still carries an important mutation in its genome: sexual development was hampered by female fertility (Seidl et al., 2009). Ten rounds of backcrossing of QM6a with the fertile CBS999.97 allowed for narrowing down the genomic locus which contains the mutation (Schmoll et al., 2013). Subsequently it could be confirmed that the MAPKinase scaffold protein HAM5, which is encoded by a gene in this very locus, shows several mutations causing frame shifts and lead to an unfunctional gene, which renders QM6a female sterile (Linke et al., 2015; Tisch et al., 2017). This knowledge now enables a complementation of the defect to facilitate strain improvement by breeding. However, QM6a and recombinant strains derived from it can now also be used as a female sterile test strains to evaluate male and female fertility and knowledge-based crossings to remove the HAM5 defect serve to investigate mating in homozygous crosses (Hinterdobler et al., 2020b).

Delving into the past – elucidation of the genetic basis of early and later random mutants

Since the advent of genome sequencing, the quest to elucidate the characteristics of high performance mutant strains of *Trichoderma* continues (Seidl and Seiboth, 2010). The number of mutations in these strains was greatly underestimated prior to knowledge on the genomes and hence, although many crucial functions of the mutated genes are already known (Seidl and Seiboth, 2010; Peterson and Nevalainen, 2012; Bischof et al., 2016), there are still numerous genes left, which are altered, but without deeper knowledge on their function or contribution to the phenotype of the respective mutant. Nevertheless, there was quite some progress in recent years.

One of the most important topics upon investigation of random mutants is gaining insight into the mechanism of cellulase regulation, both because of their relevance as homologously produced enzymes in *Trichoderma* and due to the efficiency of their promotors for heterologous protein production (Gudynaite-Savitch and White, 2016; Paloheimo et al., 2016; Arbige et al., 2019).

The random mutant strain QM9978 produces cellulases at a very low basic level, but cannot be induced under usual cellulase inducing conditions (Torigoi et al., 1996) and hence was used for comparative studies for decades (for example (Zeilinger et al., 2003; Schmoll et al., 2004)). Finally, in 2017,

the defect of QM9978 was identified due to genome sequencing (Ivanova et al., 2017). Comparison with QM6a revealed 43 mutations, among them a translocation between chromosomes V and VII upstream of the transcription factor gene *vib1*, which caused the lack of cellulase induction in QM9978 (Ivanova et al., 2017). The homologue of VIB1 was previously reported as a link between glucose signaling and carbon catabolite repression and to be involved in regulation of plant cell wall degrading enzymes in *N. crassa* (Xiong et al., 2014). While overexpression of VIB1 did not increase cellulase gene expression in *T. reesei* (Ivanova et al., 2017), the same strategy led to significantly increased secreted cellulase activity in *T. orientalis* EU7-22 (Han et al., 2020).

The early random mutant *T. reesei* RUT C30 (Peterson and Nevalainen, 2012) is the most extensively studied mutant strain, as it serves as parental strain for many industrial production strains. Moreover, the considerable genomic rearrangements in this strain (Seidl et al., 2008) provided numerous hypothesis for strain improvement to be tested. Although quite some details on the basis for enhanced cellulase production of this strain are already known (Peterson and Nevalainen, 2012), it is still subject to research with the most recent finding, that the truncation of CRE1 present in RutC30 turns the repressor into an activator (Rassinger et al., 2018). Re-assembly and re-annotation of its genome showed diverse chromosomal rearrangements (Jourdier et al., 2017). The industrial application of derivatives of RUT C30 is also the reason for this strain to be used as parental strain for gene regulation studies. However, in this case, it has to be kept in mind that the numerous mutations of RUT C30, which also cause a considerably altered physiology including decreased growth and sporulation as well as weakened cell wall stability, do not allow for a reliable generalization of functional characteristics of individual genes to *Trichoderma* as a whole.

A less well known cellulase negative strain is *T. reesei* QM9136, which cannot grow on cellulose or form cellulases, but otherwise has a normal phenotype (Mandels et al., 1971; Nevalainen and Palva, 1978). In this strain, a frameshift mutation in the crucial cellulase transcription factor XYR1, which causes a truncation by 140 amino acids is responsible for the defect in cellulase production (Lichius et al., 2015). Additionally, 14 mutations have been detected which are likely irrelevant for cellulase production.

A descendant of the cellulase overproducer QM9414, which was subjected to several more mutagenic rounds is *T. reesei* PC-3-7 (Kawamori et al., 1985). Sequencing of this strain and comparison with the QM6a genome sequence yielded 260 SNPs in PC-3-7, of which most were located in non-coding regions. However, also in the important cellulase regulator genes *ace1* and *cre1* SNPs were detected. The SNP in CRE1 at amino acid 78 indeed caused a decrease in binding affinity of CRE1 to the *cbh1* promotor, which in turn negatively affected cellulase production (Porciuncula Jde et al., 2013).

Bioprospecting in genomes of nature isolates

Investigation of the genome of novel biocontrol agents or biofertilizers is becoming increasingly interesting. On the one hand, these organisms are being distributed in nature in considerably larger amounts than would occur naturally. On the other hand, they can be sources for novel bioactive molecules (Karwehl and Stadler, 2016). In both cases the metabolic competences of a microbe can be a benefit or a threat to humanity. Especially the widespread application of biocontrol agents in the form of spores in low income countries raised questions as to the safety for farm workers there, but also the burden on consumers as well as nature in general (Konstantinovas et al., 2017; Hatvani et al., 2019). Clinically relevant *Trichoderma* strains are assumed to be limited to certain species (Kredics et al., 2003; Sandoval-Denis et al., 2014), but detailed knowledge on relevant secondary metabolite gene clusters is important to rule out selection of a potential harmful isolate for commercial application in agriculture. However, fungi including *Trichoderma* represent a potential source for valuable compounds to fight cancer or the counteract microbial resistance against common antibiotics (Viglas et al., 2021).

In all these cases detailed knowledge on the gene content of a given strain is crucial for knowledge based decisions on application (for an overview on recent genome level analyses of Trichoderma spp. aimed at biocontrol issues see Table 1). Additionally, a higher number of available genome sequences will enhance specificity of developed methods to detect biocontrol agents in agriculture (Kabani et al., 2002; Kredics et al., 2018), especially if identification of individual strains of a species is required – for example for following up distribution and habitat colonization of a biocontrol agent in the field. Unfortunately, genome level studies on health issues due to distribution of *Trichoderma* as biocontrol agents or of clinical isolates are still very rare.

Besides biocontrol and health related targets, also novel enzymes still remain an important commercial topic for which Trichoderma spp. are valuable (for an overview on recent genome level analyses of Trichoderma spp. aimed at bioprospecting see Table 2). Consequently, bioprospecting for novel, more efficient enzymes under diverse conditions – as required for various applications in industry – are still actively sought (enzymes reviews (Wilson, 2009; Singh et al., 2015; Arnau et al., 2020)).

Importantly, numerous additional newly sequenced genomes of the genus *Trichoderma* became available in JGI mycocosm (https://mycocosm.jgi.doe.gov/mycocosm/home) recently, which are not specifically described here.

Mitochondrial genomes of *Trichoderma*

Mitochondria represent the powerhouse of every eukaryotic cell and are responsible for the production of ATP through the oxidative phosphorylation pathway and the aerobic citric acid (TCA) cycle and biosynthesis of metabolites like amino acids (Medina et al., 2020). Moreover, besides respiratory metabolism and energy production, mitochondria are also relevant for senescence during the cell cycle and maintenance of ion homeostasis (Basse, 2010; Chatre and Ricchetti, 2013). The mitogenome was shown to play a role in fungal virulence and emerged as an important target of fungicides (Medina et al., 2020).

In contrast to other cell organelles, mitochondria have their own genome, which can be present in multiple copies, also depending on growth conditions and is capable of independent replication and inheritance (Burger et al., 2003). Mitochondrial genomes have their own codon usage (Medina et al., 2020) and are highly variable, also with the extent of introns and their different sizes (Burger et al., 2003; Aguileta et al., 2014). Both high conservation of intronic sequences and their location within genes and species-specific introns were detected in Hypocreales, hence indicating an origin from a common ancestor as well as an alternative mechanism for intron evolution/transfer (Fonseca et al., 2020). Comparative analyses further showed a correlation between mitogenome length and the number and size of non-coding sequences in the mitochondrial genome of Hypocreales (Fonseca et al., 2020). Detailed sequence analysis revealed several cases of HGT of bacterial genera to fungi (Megarioti and Kouvelis, 2020). The different distribution of heavier and lighter nucleotides in the two strands of the mitochondrial genome enables their isolation by differential centrifugation (Garber and Yoder, 1983; Chambergo et al., 2002). The introns can contain so called homing endonucleases responsible for intron splicing (Megarioti and Kouvelis, 2020), of which the classes of LAGLIDADG and GIY-YIG are present also in fungal mtDNAs (Belfort et al., 2002; Stoddard, 2014). Such a gene conversion can happen through intron invasion and leads to altered size and composition of the mitochondrial genome (Wu and Hao, 2019; Medina et al., 2020). In fungi, mitochondrial genomes can be circular or linear with sizes from little more than 10 kb up to 200 kb (Pramateftaki et al., 2006; Losada et al., 2014; Liu et al., 2020), although the typical mitochondrial genome is much smaller. As for evolution of mitochondrial genomes, they were found to evolve more slowly than their nuclear genomes (Clark-Walker, 1991; Gaillardin et al., 2012), despite the high variability of non-coding regions.

In some cases, transfer of mitochondrial genes from the mitochondrial genome to the nuclear genome was observed and concerns genes like *nad5*, while for other genes no transfer

events were detected (Fonseca et al., 2020; Medina et al., 2020). Over evolutionary time, a considerable number of the initially endosymbiotic genes were transferred to the nuclear genome and mitochondrial proteins are encoded by the nuclear genome and transported to the mitochondria (Burger et al., 2003). In the order Hypocreales, also duplication of mitochondrial genes is a common phenomenon as among the 17 core genes, only *atp8*, *atp9* and *cox3* were not detected in the respective nuclear genome (Fonseca et al., 2020).

The interest on research towards mitochondrial genomes remained very low with until recently just very few mitochondrial genomes published for the genus *Trichoderma* (Kwak, 2020; Kwak, 2021). In the last few years, with the advent of efficient and affordable genome sequencing methods, especially third generation sequencing, the numbers increased. Mitochondrial genomes in the Hypocreales are circular and range from about 24 kb to more than 100 kb in size (Fonseca et al., 2020). Thereby, the size of introns contributes to the variance of genome sizes (Medina et al., 2020).

Already in the 1990s, the relevance of mitochondrial functions for physiology of *Trichoderma* was investigated, which revealed a significant impact on cellulase production, in that a low oxygen tension negatively influenced their biosynthesis (Abrahao-Neto et al., 1995). This sensitivity of *T. reesei* to the functional state of mitochondria was subsequently associated with the 5' region of the major cellulase gene, *cbh1* (Carraro et al., 1998). A few years thereafter, the mitochondrial genome of *T. reesei* (Figure 3) was published (Chambergo et al.,

2002). In *T. reesei* a role in oxidative stress resistance was proposed for mitochondria as well (Wang et al., 2015a). Recently, third generation sequencing yielded an update of mitochondrial genomes in *T. reesei*. The female sterile MAT1-2 strain QM6a (Li et al., 2017) was sequenced along with both mating types of *T. reesei* CBS999.97 (Seidl et al., 2009), which showed strikingly different sizes of the mitochondrial genomes yet a similar set of genes essential for mitochondrial functions (Li et al., 2021a). The mitochondrial genome of QM6a has 42 kb, while that of CBS999.97 (MAT1-1) has only 39 kb and only shares 75% of nucleotide sequence identity with that of QM6a. In contrast, the mitochondrial genomes of CBS999.97 (MAT1-1) and CBS999.97 (MAT1-2), which arose from the same crossing event (Seidl et al., 2009), are identical except for only six SNPs, hence reflecting maternal inheritance (Li et al., 2021a). Moreover, the mitochondrial genome sequences of *T. atroviride* P1, *T. asperellum* FT-101, *T. virens* Gv29-8 and *Tvirens* FT-333 vary considerably in size and analysis of high quality genomes of these strains indicates that mobile genetic elements played key roles in shaping the mitochondrial genomes in *Trichoderma* (Li et al., 2021b). Also three nuclear encoded mitochondrial sequences (NUMTs) were detected in *Trichoderma*, which are all located within an AT-rich block, which suggests that filamentous fungi and mammalian cells may have an evolutionarily conserved origin of NUMTs (Tsuji et al., 2012; Li et al., 2021b).

The mitochondrial genome of *T. harzianum* HB324 is circular and has a size of 32kb, with a GC content of 28%
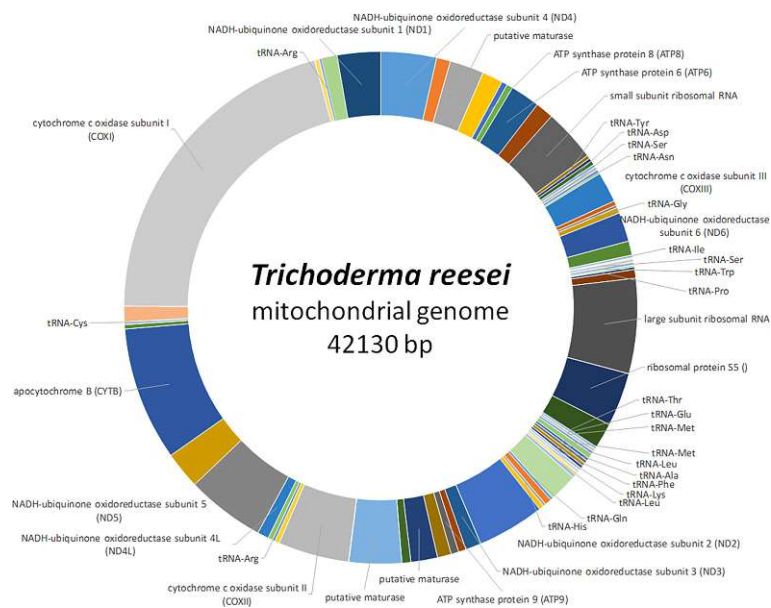
FIGURE 3

Schematic representation of the mitochondrial genome of *T. reesei*. The complete mitochondrial genome of *T. reesei* (GenBank accession number NC_003388) is shown along with encoded genes (Chambergo et al., 2002). Areas without label represent intergenic regions.

(Fonseca et al., 2020), which is in accordance with a generally high AT content in fungal mitogenomes (Medina et al., 2020). Fourteen genes associated with oxidative phosphorylation, 28 tRNA encoding genes as well as two ribosomal RNAs were detected in addition to a few hypothetical genes (Fonseca et al., 2020). As in many ascomycetes (Medina et al., 2020) all the genes were encoded on the same DNA strand in *T. harzianum* HB324. A comparison with other *Trichoderma* mitochondrial genomes showed a considerable variation in their structure and size even within the genus (Fonseca et al., 2020).

Another *T. harzianum* strain, CBS226.95, has a considerably smaller circular mitochondrial genome with only around 28 kb (Kwak, 2021). This mitogenome was further predicted to have evolved earlier than other *Trichoderma* species' mitogenomes. It was further proposed that the evolution of *Trichoderma* mitochondria is influenced by their adaptive diversification depending on the diverse habitats from which *Trichoderma* strains were isolated concerning oxygen availability like soil, wood or living plants and fungi (Kwak, 2021).

Trichoderma atroviride ATCC26799 has a mitochondrial genome of 33 kb comprising the usual content of mitochondrial genes in the genus (Kwak, 2020). Gene order in the mitochondrial genomes of five *Trichoderma* spp. (*T. reesei* QM9414 (GenBank accession number AF447590), *T. asperellum* B05 (NC_037075), *T. hamatum* (MF287973), and *T. gamsii* KUC1747 (KU687109) is highly conserved, while intergenic regions, nucleotide composition bias, number of protein coding sequences and size of mitochondrial genomes was more variable (Kwak, 2020). Recently, also a mitochondrial genome of *T. simonsii* was reported (Chung et al., 2022), which clusters with several other *Trichoderma* mitogenomes including *T. cornu-damae* (Genbank accession number MW525445), *T. lixii* (NC_052832) and *T. hamatum* (NC_036144), most of which are not yet described in detail.

Mycoviruses of *Trichoderma*

Viruses are able to infect living organisms from bacteria to humans and are present in fungi as well (Myers and James, 2022). Viruses of fungi have been known for more than 5 decades (Ghabrial et al., 2015), but the detection of them in *Trichoderma* spp. happened quite recently. In most cases, infection of a fungus with a virus does not change the phenotype (Ghabrial and Suzuki, 2009; Son et al., 2015), which is a likely reason that viruses in *Trichoderma* did not receive much attention so far. Nevertheless, there are some intriguing examples of mycoviruses considerably altering physiology and organismic interactions: If *Sclerotinia sclerotiorum* is infected with the small DNA mycovirus SsHADV-1, it turns from a pathogen of *Brassica* spp. into a beneficial endophyte due to downregulation of major pathogenicity factor genes (Zhang et al., 2020). Even more

fascinating is the three-way symbiosis of the endophytic fungus *Curvularia protuberata*, which allows its host plant *Dichanthelium lanuginosum* to grow at high temperatures only if it is infected by the mycovirus CThTV (Marquez et al., 2007). Although it was initially thought that mycoviruses have a relatively narrow host range, detection of a virus first described in *Botrytis porri* in *B. squalosa* and *Sclerotinia sclerotiorum* suggests that this is not the case and that mycoviruses can be transmitted between species (Wu et al., 2012; Nerva and Chitarra, 2021). Intriguingly, also mycoviruses from endophytes were found to replicate in a plant, although this phenomenon was so far only shown *in vitro*, not in nature (Nerva et al., 2017).

The model fungus for studying the interaction of mycoviruses with their hosts is *Cryphonectria parasitica*, the chestnut blight pathogen, in which infection by a so called hypovirus decreases virulence (Dawe and Nuss, 2013; Eusebio-Cope et al., 2015). Similar effects were shown in other plant pathogens, hence making mycoviruses an interesting subject to research towards biocontrol applications (Milgroom and Cortesi, 2004). In this respect, treatment of chestnut blight with mycoviruses exemplified the problem with such an application. No natural vectors are known for mycoviruses (Ghabrial and Suzuki, 2009; Son et al., 2015). They spread predominantly vertically by propagation *via* conidiospores, less efficiently *via* ascospores in ascomycetes (Ghabrial et al., 2015). Alternatively, infection occurs by hyphal anastomosis, which is limited by vegetative incompatibility, leading to programmed cell death if two incompatible fungi fuse (Daskalov et al., 2017). In case of multiple incompatibility groups in fungal population, spread of the viruses is very inefficient as is biocontrol in such a case (Xie and Jiang, 2014). The limited success of treatment of *C. parasitica* in the US compared to the imported strains in Europe is attributed to this problem (Myers and James, 2022). In *Trichoderma*, vegetative incompatibility was shown previously (Gomez et al., 1997), but is not yet sufficiently investigated to draw any conclusions as to the impact on biocontrol enhancements by mycovirus applications.

Another natural defense mechanism that limits infection of pathogens by mycoviruses is RNAi, meant to destroy intruding foreign nucleic acids (Segers et al., 2007). Interestingly, although mycoviruses often only have two genes encoded, they can counteract programmed cell death and vegetative incompatibility as well as RNAi (Hammond et al., 2008; Daskalov et al., 2017), which tips the balance again towards their benefit. Often, the presence of a mycovirus in a fungus causes lower growth rates which is interpreted as a lack of fitness (Ghabrial and Suzuki, 2009). Nevertheless, also co-evolution of mycoviruses with their hosts has been observed, although this observation cannot be generalized (Nerva and Chitarra, 2021).

In *Trichoderma*, the first mycovirus was described in 2009 (Jom-in and Akarapisan, 2009) and only a few followed thereafter. However, a study of more than 300 fungal isolates

TABLE 1 Recent genome level analyses of *Trichoderma* spp. targeted at biocontrol related issues.

Species	Strain	Topic	Key findings	Reference
T. harzianum	B97	biocontrol	Genes with non-synonymous SNPs compared to the reference strain are enriched in metabolic functions including secondary metabolism and DNA repair	(Compant et al., 2017)
T. atrobrunneum	ITEM 908	biocontrol	abundance of genes encoding CAZymes, secondary metabolite-, peptaibole-epidithiodioxopiperazine- and siderophore producing proteins is comparable to other *T. harzianum* complex associated species	(Fanelli et al., 2018)
T. asperelloides	T 203	mycoparasitism	genome announcement only	(Gortikov et al., 2022)
T. virens	FT-333	biocontrol, defense and nutrient utilization	gene content related to reactions to the environment varied compared to *T. virens* Gv29-8 and to other *Trichoderma* species	(Kuo et al., 2015)
T. gracile	HK011-1	biocontrol	antagonistic activity against several pathogens, gene annotation provided, secondary metabolite clusters detected	(Li and Liu, 2022)
T. virens	M7	biocontrol	deletion of 250 kb of the genome in five locations with 71 predicted genes	(Pachauri et al., 2020)
T. koningiopsis	UKM-M-UW RA5	biocontrol against *Erwinia mallotivora*	fungi controlling *E. mallotivora* identified, potential secondary metabolite pathways underpinning the antimicrobial properties of three antagonistic strains delineated	(Tamizi et al., 2022)
	UKM-M-UW RA6			
	UKM-M-UW RA3a			
T. afroharzianum	T11-W	control of nematodes and fungal plant pathogens	PacBio genome sequencing, annotation and basic comparative analysis to the high-quality genome of *T. reesei* QM6a	(Zhou et al., 2020)
T. cyano-dichotomus	TW21990-1			
T. afroharzianum	BFE349	mycoparasitism	genome announcement only	(Landeis and Schmidt-Heydt, 2021)
T. asperellum	TAIK1 TAIK4 TAIK5	biocontrol and plant growth promotion	genome announcement only	(Kannan et al., 2022)

causing green mold disease revealed evidence for potential dsRNA mycoviruses of diverse groups in 32 isolates, indicating that mycoviruses are not uncommon in *Trichoderma* (Yun et al., 2016). The genomes of these mycoviruses are relatively small and they mostly encode only two proteins, a coat protein and an RNA dependent RNA polymerase (RdRp) (Figure 4). As reported from other fungi, mycoviruses often do not influence the phenotypes of their hosts or just have a minor impact on pyhsiology, which was also observed for several isolates from *Trichoderma* (Table 3).

In several cases however, presence of the mycovirus in the *Trichoderma* strain did cause phenotypic alterations, mostly enhanced mycoparasitic abilities:

A mycovirus in *T. harzianum* (ThMV1) was investigated in more detail and caused a decrease in biomass production, a slightly positive effect on plant health if *T. harzianum* was applied alone and somewhat better biocontrol activity against *Fusarium oxysporum* f. sp. *cucumerinum* in cucumber (Liu et al., 2019). The *T. atroviride* mycovirus TaMV1, a member of the proposed family *Fusagraviridae* does not impact conidiation or growth, but supported enhanced antifungal activity against the plant pathogen *Rhizoctonia solani* (Chun et al., 2020). For the *T. harzianum* mycovirus ThHV1, which

shares similarity with betahypoviruses, an influence on mycoparasitism was shown in case of the presence of a defective genome. This mycovirus could be transmitted vertically to conidia, but could also infect another *T. harzianum* isolate as well as *T. koningiopsis* (You et al., 2019). The *T. harzianum* partitivirus 1 (ThPV1) enhances growth inhibition of co-cultured plant pathogens as well as glucanase activity (Chun et al., 2018b).

The still few reports on mycoviruses in *Trichoderma* indicate that investigation of mycoviruses and their interaction with the host as well as their influence on biocontrol of plant pathogens are emerging as an important new topic of research. Since it was shown that mycoviruses can have a broad host spectrum, transmission of a mycovirus from a pathogen to a mycoparasite like *Trichoderma* or vice versa is likely to be possible, yet the consequences for plant health, population structure and ecology are currently completely unknown. Additionally, the effects of mycovirus infections in *Trichoderma* are hardly predictable and loss of a mycovirus can easily happen during industrial cultivation, potentially leading to altered characteristics of the fungus. Consequently, it will be crucial to be aware of a potential mycovirus in a fungus if it is part of a commercial product in order to guarantee a stable,
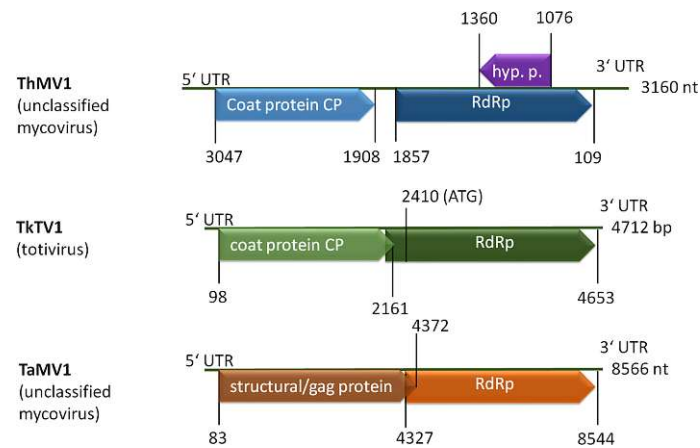
FIGURE 4
Schematic representation of selected mycovirus genomes. ThMV1 (Liu et al., 2019), TkTV1 (Khalifa and MacDiarmid, 2019) and TaMV1 (Lee et al., 2017) genomes comprise two ORFs coding for a coat protein (CP or GAG) and an RNA dependent RNA polymerase (RdRp). ThMV1 additionally comprises a small ORF encoding a hypothetical protein of unknown function.

efficient product and knowledge on susceptibility of the fungus for mycovisuses abundant in the target pathogen will be beneficial.

In this respect, the increasing performance of next generation sequencing of transcriptomes (revealing RNA viruses) comes in handy, as a previous screening of available GenBank data shows (Gilbert et al., 2019). Detection of mycoviruses as a by-product of gene regulation studies is a worthwhile effort to gain important information on model organisms as well as production strains and biocontrol agents.

TABLE 2 Recent genome level analyses of *Trichoderma* spp. targeted at bioprospecting of enzymes and bioactive compounds.

Species	Strain	Topic	Key findings	Reference
T. harzianum	B13-1	lipolytic activity	50 putative lipases detected; lipase gene inducable with olive oil identified	(Canseco-Perez et al., 2018)
T. koningiopsis	POS7	cellulase production in solid state fermentation	genome announcement only	(Castrillo et al., 2017)
T. hamatum *T. hamatum*	YYH13 YYH16	cellulase production - variations in different strains	thirteen functionally important genes are under positive selection in the higher producing strain, 15 protease families are different and 10 further families of enzyme functionalities are subject to stronger positive selection	(Cheng et al., 2017)
T. simonsii	GH-Sj1	asparaginase production	seven putative asparaginase-encoding genes detected, three of them are significantly upregulated under conditions enhancing asparaginase activity	(Chung et al., 2021)
T. harzianum	IOC-3844	biomass degradation	genes located in vicinity of those encoding biomass degrading enzymes were identified	(Crucello et al., 2015)
T. harzianum	T6776	enzymes for biofuel production	CAZymes identified, transcript levels analyzed (cellulose, lactose, sugar cane bagasse), phylogenetic analysis of AA9, CE5 and GH55 families showed high functional variation	(Ferreira Filho et al., 2017)
T. harzianum	IOC-3844	cellulose degradation	PacBio long read sequencing for genome, annotation, *clr2* is differentially expressed between glucose and cellulose, regulation network inferred	(Ferreira Filho et al., 2020)
T. viride	J1-030	sesquiterpene production	a novel sesquiterpene synthase was identified and characterized and the biosynthetic products of this enzyme were determined	(Sun et al., 2019)
Trichoderma sp. (*harzianum complex*)	MMS1255	peptaibol production	Pentadecaibin production associated with biosynthetic gene and antimicrobial activity detected	(van Bohemen et al., 2021)

TABLE 3 Reports on detection of mycoviruses in diverse *Trichoderma* species.

Species	Strain	Virus	Type	Key findings	Reference
T. atroviride	NFCF028	TaMV1	dsRNA	8 kb mycovirus with two open reading frames detected, member of a distinct species, unclassified	(Lee et al., 2017)
T. harzianum	137	ThBMV1	dsRNA	ThBMV1 clusters with other unclassified dsRNA mycoviruses	(Liu et al., 2019)
T. asperellum	JLM45-3	TaRV1	dsRNA	Virus, approximately 10 kb in size, with two open reading frames associated to a taxonomically unassigned mycovirus group, new family proposed as *Fusagraviridae*	(Zhang et al., 2018)
T. atroviride	NFCF394	TaPV1	dsRNA	TaPV1 belongs to the genus *Alphapartitivirus* in the family *Partitiviridae*. Virus cured strains did not show phenotypic alterations.	(Chun et al., 2018a)
T. koningiopsis	Mg10	TkTV1	dsRNA	TkTV1 represents a novel Totivirus of approximately 5 kb and is highly similar to a mycovirus from *Clonostachys rosea* isolated from the same sample. TkTV1 could infect both strains.	(Khalifa and MacDiarmid, 2019)
T. harzianum	M6	ThHV2	(+) ssRNA	The 14 kb mycovirus contains one large open reading frame with five conserved motifs and likely belongs to the proposed genus Alphahypovirus	(Chun et al., 2022)

Genomic aspects of mycoremediation with *Trichoderma*

As the awareness of the community towards a healthy environment increases, contaminated sites, which could previously hardly be treated efficiently, comes into focus (Febbraio, 2017; Ford et al., 2022a; Sharma et al., 2022). The genomes of *Trichoderma* spp., originating from diverse habitats represent a treasure trove for the quest for enzymes and metabolic competences to detoxify or even mineralize dangerous chemicals (Tripathi et al., 2013; Zafra and Cortes-Espinosa, 2015; Repas et al., 2017; Mishra et al., 2021) and *Trichoderma* species are well known for their efficiency in remediation of soil and water pollution (Harman et al., 2004b). Fungi are generally very potent organisms for bioremediation (Kour et al., 2021), even outperforming bacteria (Dell'Anno et al., 2022). The decades-long application of *Trichoderma* spp. in biocontrol and in industry led to an in depth knowledge of their environmental safety (Nevalainen et al., 1994; Frisvad et al., 2018; Shenouda and Cox, 2021), which makes fungi of this genus prime candidates for application at natural contaminated sites with limited negative effects on the surrounding flora and mostly without the need for genetic modification. The chemical composition of pollutants is diverse, representing a considerable challenge for strain selection. In case of plastic degradation however, suitable enzyme classes for degradation of the respective structures can be defined beforehand (Verschoor et al., 2022).

Genome mining and omics analyses allow for delineating regulation pathways of suitable target enzymes, which is important for performance of a given strain, as not only the presence of degradative enzymes, but also their appropriate regulation under commercially viable conditions is crucial for applicability. This strategy is not yet routinely applied in *Trichoderma*, but in recent years, several interesting examples

of detailed investigation of genomes, enzymes targeting certain pollutants and delineation of degradation pathways were reported.

Trichoderma lixii MUT3171 was isolated from a highly polluted environment and comparison of its genome was used to gain insight into potential degradation pathways of polycyclic aromatic hydrocarbons (PAHs) (Venice et al., 2020). Orthologues of genes encoding oxidoreductases, CAZymes and proteins responsible for biosurfactant biosynthesis were screened in 14 *Trichoderma* species. Additionally, also unique genes of MUT3171 including a quinoprotein alcohol dehydrogenase and a specialized mechanism of DNA repair were determined which may contribute to the ability of *T. lixii* to survive in this habitat (Venice et al., 2020). The dichlorodiphenyltrichloroethane (DDT) resistant *T. hamatum* strain FBL587 was investigated for its transcriptomic reaction to the pollutant (Davolos et al., 2021). This strain could degrade DDT and enhance degradation by *Cucurbita* phytoremediation. Especially Cytochrome P450 enzymes encoding genes were upregulated in the presence of DDT, but also transforming enzymes such as epoxide hydrolases, FAD-dependent monooxygenases, glycosyl and glutathione transferases as well as transporters (Davolos et al., 2021). The example of this detailed analysis shows how crucial genes for xenobiotic remediation can be narrowed down, which can represent an important step for strain screening and selection for future bioremediation purposes by fungal cultures or their isolated enzymes.

Currently, approaches to realize circular economy by valorization are in development – for example with *Trichoderma* spp. degrading waste biomass for production of metabolites (Shenouda and Cox, 2021; Shenouda et al., 2022), which should be extended to degradation of more problematic waste materials (Verschoor et al., 2022) like plastics or composites. In this respect the ability of adaptation of fungal strains to the substrate by crossing (Ashton and Dyer, 2016) can

be a valuable tool for strain improvement towards plastics degradation and detoxification of pollutants. So far, only for *T. reesei* crossing was achieved under laboratory conditions (Seidl et al., 2009) and the method has successfully been applied to increase cellulase production by at least 10fold compared to RutC30 (M. Schmoll and S. Basyouni-Khamis, unpublished results). The availability of European nature isolates of *T. reesei*, which are sexually fertile (Hinterdobler et al., 2021a) is an important prerequisite to test a crossing approach for using plastics and/or their degradation products as carbon source to produce higher value chemicals and enzymes. Such a scheme of circular economy could serve as a blueprint for avoiding pollution and creating high value products with minimal pollution in the future, which makes further genome mining and efforts to achieve crossing with other *Trichoderma* spp. as well a worthwhile effort.

Tools for genome screening and manipulation

Fungal genomes are constantly subject to manipulation – mostly of course in nature in order to achieve optimal adaptation to the habitat or just to enable survival if environmental conditions deteriorate. Sexual development represents the major strategy of nature to modify the genome, but also a valuable tool for strain improvement in the lab (see above). However, also artificial methods for genome manipulation of fungi were developed further in recent years.

Functional analysis of genes and whole pathways are especially important to understand the physiology of *Trichoderma* and consequently, strategies for increasing the ease and efficiency of genome manipulation are constantly optimized (Guangtao et al., 2009; Schuster et al., 2012; Chum et al., 2017). A more recent addition is the TrichoGate cloning strategy which is mainly an adaptation of the Golden Gate cloning system to *Trichoderma* (Nogueira-Lopez et al., 2019). Using this system, vectors for different promotors, deletions, protein localization studies and overexpressions are introduced along with a vector for *Agrobacterium* mediated transformation.

Also the SES (synthetic expression system), which was previously established for *Saccharomyces cerevisiae* (Rantasalo et al., 2016; Rantasalo et al., 2019) represents an interesting addition to the toolset for genome manipulation in *Trichoderma*, which is focused on protein expression (Rantasalo et al., 2018). In this system induction of protein synthesis involves two cassettes for low and constitutive production of a synthetic transcription factor, which activates a promotor in a second cassette with strong and tunable expression (Rantasalo et al., 2018).

CRISPR – adaptation to Trichoderma and optimization

Traditionally, genome manipulation in *Trichoderma* spp. was done using protoplast transformation, electroporation, agrobacterium mediated transformation or biolistic transformation (Rodriguez-Iglesias and Schmoll, 2015; Schmoll and Zeilinger, 2021). However, in recent years, the versatile method of clustered regularly interspaced short palindromic repeat (CRISPR)-associated Cas9 (Hoof et al., 2018; Wang and Coleman, 2019; Rozhkova and Kislitsin, 2021) was also established for *Trichoderma*, particularly *T. reesei* (Liu et al., 2015; Zou and Zhou, 2021) and *T. harzianum* (Vieira et al., 2021) and subsequently optimized. Usually, the specific gRNA and the Cas9 protein are introduced as DNA into the host organisms which leads to constitutive exposure of the fungus to active Cas9. This can cause decreased viability and genome integrity of the host, but most importantly also unintended genome modifications. It was shown that *in vitro* assembly of Cas9 and gRNA prior to transformation of the nucleoprotein complex with a marker plasmid or the donor DNA was less prone to off target gene disruption than intracellular expression of Cas9 (Hao and Su, 2019; Rantasalo et al., 2019). Later on, the 5S rRNA promotor of *A. niger* was suggested for expression of the guide RNA, which enabled gene deletion using a donor DNA carrying only a 40 bp homology sequence and no selectable marker gene (Wang et al., 2021). Similarly, the promotors of two RNA polymerase III U6 snRNA genes were confirmed to be suitable for gRNA expression in *T. reesei* (Wu et al., 2020). Although the method of genome editing has become quite popular for modifications in fungi, the method *via* Cas9-CRISPR gRNA ribonucleoprotein complexes assembled *in vitro* is relatively low. Addition of chemicals like Triton X-100, inositol or benomyl led to increased efficiency in transformation as well as homologous integration (Zou et al., 2021). Nevertheless, the method is still relatively young and more improvements – for example as developed for *Saccharomyces cerevisiae* (Antony et al., 2022) – await adaptation and establishment in *Trichoderma*. Moreover, application CRISPR has not been established in several other *Trichoderma* species, which may be due to the capability of *Trichoderma* to clear their genomes of foreign DNA elements and hence further efforts are required.

Tools for genome mining

Secondary metabolites of fungi are generally an important resource for novel pharmaceuticals and antibiotics, but can also represent a threat to human health (Karwehl and Stadler, 2016; Bhattarai et al., 2021; Juraschek et al., 2022). Therefore it is very important to tackle new ways of genome mining and

investigation, as was done for Ribosomally synthesized and posttranslationally modified peptides, RiPPs, in *Trichoderma* (Vignolle et al., 2020). These compounds add a further way of biosynthesis to polyketides and non-ribosomal peptides in that they are encoded within a precursor and subsequently processed after posttranslational modification. However, evaluation of the biological function of RiPPs is still at its beginnings and roles in defense, deterring mycophagy, support of nutrient acquisition, competition, but also in symbioses (Ford et al., 2022b). Despite the relevance of for example alpha-amanitin or phallacidin, which are formed by *Amanita* spp., current screening software is focused on bacterial sequences and reports on biosynthesis in fungi is scarce (Kessler and Chooi, 2022). The multistep approach now presented (Vignolle et al., 2020) and including manual inspection yielded a wide range of RiPP candidates for *Trichoderma* spp., from 6 in *T. reesei* to 222 in *T. harzianum*, which indicates a considerable relevance of these compounds for physiology of *Trichoderma*. Together with the potential importance of novel RiPPs as bioactive substances, their biological relevance to fungi and especially *Trichoderma* warrants further investigation.

A novel tool for screening for essential biosynthetic genes was developed to enable determination of biosynthetically relevant genes in clusters versus those which are not needed for secondary metabolite production within the cluster – the so-called gap genes (Vignolle et al., 2021). The tool "FunOrder" (Vignolle et al., 2021) was also tested for *Trichoderma* and applies computational molecular co-evolution to distinguish between biosynthetic genes and gap genes. Thereby FunOrder facilitates efficient heterologous expression of biosynthetic gene clusters as well as functional analysis of the underlying biochemical pathways.

Generally, for screening for secondary metabolite clusters responsible for novel bioactive compounds in *Trichoderma* several software packages are useful (Rush et al., 2021). Besides the well-known tool antiSMASH (Blin et al., 2019), which detects biosynthetic clusters for secondary metabolites, the tool amPEPpy (Lawrence et al., 2021) can be used for screening for antimicrobial peptides.

Author contributions

MoS drafted the manuscript, MiS edited the manuscript and all authors agreed on the final version of the manuscript.

Funding

Conflict of interest

The authors declare that the research was conducted in the absence of any commercial or financial relationships that could be construed as a potential conflict of interest.

Publisher's note

All claims expressed in this article are solely those of the authors and do not necessarily represent those of their affiliated organizations, or those of the publisher, the editors and the reviewers. Any product that may be evaluated in this article, or claim that may be made by its manufacturer, is not guaranteed or endorsed by the publisher.

References

Abrahao-Neto, J., Rossini, C. H., El-Gogary, S., Henrique-Silva, F., Crivellaro, O., and El-Dorry, H. (1995). Mitochondrial functions mediate cellulase gene expression in *Trichoderma reesei*. *Biochemistry* 34, 10456–10462. doi: 10.1021/bi00033a018

Aguileta, G., De Vienne, D. M., Ross, O. N., Hood, M. E., Giraud, T., Petit, E., et al. (2014). High variability of mitochondrial gene order among fungi. *Genome Biol. Evol.* 6, 451–465. doi: 10.1093/gbe/evu028

Alfiky, A., and Weisskopf, L. (2021). Deciphering *Trichoderma*-plant-pathogen interactions for better development of biocontrol applications. *J. Fungi (Basel)* 7 (1):61. doi: 10.3390/jof7010061

Antony, J. S., Hinz, J. M., and Wyrick, J. J. (2022). Tips, tricks, and potential pitfalls of CRISPR genome editing in *Saccharomyces cerevisiae*. *Front. Bioeng Biotechnol.* 10, 924914. doi: 10.3389/fbioe.2022.924914

Arbige, M. V., Shetty, J. K., and Chotani, G. K. (2019). Industrial enzymology: the next chapter. *Trends Biotechnol.* 37, 1355–1366. doi: 10.1016/j.tibtech.2019.09.010

Arnau, J., Yaver, D., and Hjort, M. C. (2020). "Strategies and challenges for the development of industrial enzymes using fungal cell factories," in *Grand challenges in fungal biotechnology*. Ed. H. Nevalainen (Switzerland: Springer Nature Switzerland AG), 179–210.

Ashton, G. D., and Dyer, P. (2016). "Sexual development in fungi and its uses in gene expression systems," in *Gene expression systems in fungi: Advancements and applications*. Eds. M. Schmoll and C. Dattenböck (Switzerland: Springer International Publishing), 335–350.

Atanasova, L., Knox, B. P., Kubicek, C. P., Druzhinina, I. S., and Baker, S. E. (2013). The polyketide synthase gene *pks4* of *Trichoderma reesei* provides pigmentation and stress resistance. *Eukaryot Cell* 12, 1499–1508. doi: 10.1128/EC.00103-13

antiSMASH 5.0: updates to the secondary metabolite genome mining pipeline. *Nucleic Acids Res.* 47 (W1), W81–W87. doi: 10.1093/nar/gkz310

Basse, C. W. (2010). Mitochondrial inheritance in fungi. *Curr. Opin. Microbiol.* 13, 712–719. doi: 10.1016/j.mib.2010.09.003

Bayram, O., and Braus, G. H. (2012). Coordination of secondary metabolism and development in fungi: the velvet family of regulatory proteins. *FEMS Microbiol. Rev.* 36, 1–24. doi: 10.1111/j.1574-6976.2011.00285.x

Bayry, J., Aimanianda, V., Guijarro, J. I., Sunde, M., and Latge, J. P. (2012). Hydrophobins–unique fungal proteins. *PloS Pathog.* 8, e1002700. doi: 10.1371/journal.ppat.1002700

Bazafkan, H., Dattenböck, C., Böhmdorfer, S., Tisch, D., Stappler, E., and Schmoll, M. (2015). Mating type dependent partner sensing as mediated by VEL1 in *Trichoderma reesei*. *Mol. Microbiol.* 96, 1103–1118. doi: 10.1111/mmi.12993

Beier, S., Hinterdobler, W., Monroy, A. A., Bazafkan, H., and Schmoll, M. (2020). The kinase USK1 regulates cellulase gene expression and secondary metabolite biosynthesis in *Trichoderma reesei*. *Front. Microbiol.* 11, 974. doi: 10.3389/fmicb.2020.00974

Belfort, M., Derbyshire, V., Parker, M. M., Cousineau, B., and Lambowitz, A. (2002). "Mobile introns: pathways and proteins," in *Mobile DNA II*. Eds. N. L. Craig, R. Craigie, M. Gellert and A. M. Lambowitz (Washington, DC: ASM Press), 761–783.

Bennett, R. J., and Turgeon, B. G. (2016). Fungal sex: The ascomycota. *Microbiol. Spectr.* 4(5). doi: 10.1128/microbiolspec.FUNK-0005-2016

Benocci, T., Aguilar-Pontes, M. V., Zhou, M., Seiboth, B., and De Vries, R. P. (2017). Regulators of plant biomass degradation in ascomycetous fungi. *Biotechnol. Biofuels* 10, 152. doi: 10.1186/s13068-017-0841-x

Bhattarai, K., Bhattarai, K., Kabir, M. E., Bastola, R., and Baral, B. (2021). Fungal natural products galaxy: Biochemistry and molecular genetics toward blockbuster drugs discovery. *Adv. Genet.* 107, 193–284. doi: 10.1016/bs.adgen.2020.11.006

Bischof, R. H., Ramoni, J., and Seiboth, B. (2016). Cellulases and beyond: the first 70 years of the enzyme producer *Trichoderma reesei*. *Microb. Cell Fact* 15, 106. doi: 10.1186/s12934-016-0507-6

Blin, K., Shaw, S., Steinke, K., Villebro, R., Ziemert, N., Lee, S. Y., et al. (2019). antiSMASH 5.0: updates to the secondary metabolite genome mining pipeline. *Nucleic Acids Res.* 47(W1), W81–W87.

Borkovich, K. A., Alex, L. A., Yarden, O., Freitag, M., Turner, G. E., Read, N. D., et al. (2004). Lessons from the genome sequence of *Neurospora crassa*: tracing the path from genomic blueprint to multicellular organism. *Microbiol. Mol. Biol. Rev.* 68, 1–108. doi: 10.1128/MMBR.68.1.1-108.2004

Brotman, Y., Briff, E., Viterbo, A., and Chet, I. (2008). Role of swollenin, an expansin-like protein from *Trichoderma*, in plant root colonization. *Plant Physiol.* 147, 779–789. doi: 10.1104/pp.108.116293

Burger, G., Gray, M. W., and Lang, B. F. (2003). Mitochondrial genomes: anything goes. *Trends Genet.* 19, 709–716. doi: 10.1016/j.tig.2003.10.012

Cai, F., Gao, R., Zhao, Z., Ding, M., Jiang, S., Yagtu, C., et al. (2020). Evolutionary compromises in fungal fitness: hydrophobins can hinder the adverse dispersal of conidiospores and challenge their survival. *ISME J.* 14, 2610–2624. doi: 10.1038/s41396-020-0709-0

Cai, F., Zhao, Z., Gao, R., Chen, P., Ding, M., Jiang, S., et al. (2021). The pleiotropic functions of intracellular hydrophobins in aerial hyphae and fungal spores. *PloS Genet.* 17, e1009924. doi: 10.1371/journal.pgen.1009924

Canseco-Perez, M. A., Castillo-Avila, G. M., Chi-Manzanero, B., Islas-Flores, I., Apolinar-Hernandez, M. M., Rivera-Munoz, G., et al. (2018). Fungal screening on olive oil for extracellular triacylglycerol lipases: Selection of a *Trichoderma harzianum* strain and genome wide search for the genes. *Genes (Basel)* 9(2):62. doi: 10.3390/genes9020062

Cardoza, R. E., Malmierca, M. G., Hermosa, M. R., Alexander, N. J., McCormick, S. P., Proctor, R. H., et al. Identification of loci and functional characterization of trichothecene biosynthesis genes in filamentous fungi of the genus Trichoderma. *Appl Environ Microbiol.* (2011) 77(14):4867–77. doi: 10.1128/AEM.00595-11

Carraro, D. M., Ferreira Junior, J. R., Schumacher, R., Pereira, G. G., Hollenberg, C. P., and El-Dorry, H. (1998). A region of the cellobiohydrolase I promoter from the filamentous fungus *Trichoderma reesei* mediates glucose repression in *Saccharomyces cerevisiae*, dependent on mitochondrial activity. *Biochem. Biophys. Res. Commun.* 253, 407–414. doi: 10.1006/bbrc.1998.9758

Carreras-Villaseñor, N., Sanchez-Arreguin, J. A., and Herrera-Estrella, A. H. (2012). *Trichoderma*: sensing the environment for survival and dispersal. *Microbiology* 158, 3–16. doi: 10.1099/mic.0.052688-0

Castrillo, M. L., Bich, G. A., Modenutti, C., Turjanski, A., Zapata, P. D., and Villalba, L. L. (2017). First whole-genome shotgun sequence of a promising cellulase secretor, *Trichoderma koningiopsis* strain POS7. *Genome Announc* 5 (37):e00823-17. doi: 10.1128/genomeA.00823-17

Chadha, S., Mehetre, S. T., Bansal, R., Kuo, A., Aerts, A., Grigoriev, I. V., et al. (2018). Genome-wide analysis of cytochrome P450s of *Trichoderma* spp.: annotation and evolutionary relationships. *Fungal Biol. Biotechnol.* 5, 12. doi: 10.1186/s40694-018-0056-3

Chambergo, F. S., Bonaccorsi, E. D., Ferreira, A. J., Ramos, A. S., Ferreira, J.R.J.J.R., Abrahao-Neto, J., et al. (2002). Elucidation of the metabolic fate of glucose in the filamentous fungus trichoderma reesei using expressed sequence tag (EST) analysis and cDNA microarrays. *J. Biol. Chem.* 277, 13983–13988. doi: 10.1074/jbc.M107651200

Chatre, L., and Ricchetti, M. (2013). Prevalent coordination of mitochondrial DNA transcription and initiation of replication with the cell cycle. *Nucleic Acids Res.* 41, 3068–3078. doi: 10.1093/nar/gkt015

Chaverri, P., and Samuels, G. J. (2013). Evolution of habitat preference and nutrition mode in a cosmopolitan fungal genus with evidence of interkingdom host jumps and major shifts in ecology. *Evolution* 67, 2823–2837. doi: 10.1111/evo.12169

Cheng, P., Liu, B., Su, Y., Hu, Y., Hong, Y., Yi, X., et al. (2017). Genomics insights into different cellobiose hydrolysis activities in two *Trichoderma hamatum* strains. *Microb. Cell Fact* 16, 63. doi: 10.1186/s12934-017-0680-2

Chuang, Y. C., Li, W. C., Chen, C. L., Hsu, P. W., Tung, S. Y., Kuo, H. C., et al. (2015). *Trichoderma reesei* meiosis generates segmentally aneuploid progeny with higher xylanase-producing capability. *Biotechnol. Biofuels* 8, 30. doi: 10.1186/s13068-015-0202-6

Chum, P. Y., Schmidt, G., Saloheimo, M., and Landowski, C. P. (2017). Transient silencing of DNA repair genes improves targeted gene integration in the filamentous fungus *Trichoderma reesei*. *Appl. Environ. Microbiol.* 83, e00535–e00517. doi: 10.1128/AEM.00535-17

Chung, D., Kwon, Y. M., and Yang, Y. (2021). Telomere-to-telomere genome assembly of asparaginase-producing *Trichoderma simmonsii*. *BMC Genomics* 22, 830. doi: 10.1186/s12864-021-08162-4

Chung, D., Kwon, Y. M., and Yang, Y. (2022). The complete mitochondrial genome of *Trichoderma simmonsii* (Hypocreales: Hypocreaceae) from the southern coast of Korea. *Mitochondrial DNA B Resour* 7, 640–641. doi: 10.1080/23802359.2022.2060766

Chun, J., Na, B., and Kim, D. H. (2020). Characterization of a novel dsRNA mycovirus of *Trichoderma atroviride* NFCF377 reveals a member of "Fusagraviridae" with changes in antifungal activity of the host fungus. *J. Microbiol.* 58, 1046–1053. doi: 10.1007/s12275-020-0380-1

Chun, J., So, K. K., Ko, Y. H., and Kim, D. H. (2022). Molecular characteristics of a novel hypovirus from *Trichoderma harzianum*. *Arch. Virol.* 167, 233–238. doi: 10.1007/s00705-021-05253-1

Chun, J., Yang, H. E., and Kim, D. H. (2018a). Identification and molecular characterization of a novel partitivirus from *Trichoderma atroviride* NFCF394. *Viruses* 10(11):578. doi: 10.3390/v10110578

Chun, J., Yang, H. E., and Kim, D. H. (2018b). Identification of a novel partitivirus of *Trichoderma harzianum* NFCF319 and evidence for the related antifungal activity. *Front. Plant Sci.* 9, 1699. doi: 10.3389/fpls.2018.01699

Clark-Walker, G. D. (1991). Contrasting mutation rates in mitochondrial and nuclear genes of yeasts versus mammals. *Curr. Genet.* 20, 195–198. doi: 10.1007/BF00326232

Compant, S., Gerbore, J., Antonielli, L., Brutel, A., and Schmoll, M. (2017). Draft genome sequence of the root-colonizing fungus *Trichoderma harzianum* B97. *Genome Announc* 5(13):e00137-17. doi: 10.1128/genomeA.00137-17

Crucello, A., Sforca, D. A., Horta, M. A., Dos Santos, C. A., Viana, A. J., Beloti, L. L., et al. (2015). Analysis of genomic regions of *Trichoderma harzianum* IOC-3844 related to biomass degradation. *PloS One* 10, e0122122. doi: 10.1371/journal.pone.0122122

Daskalov, A., Heller, J., Herzog, S., Fleissner, A., and Glass, N. L. (2017). Molecular mechanisms regulating cell fusion and heterokaryon formation in filamentous fungi. *Microbiol. Spectr.* 5(2). doi: 10.1128/9781555819583.ch10

Dattenböck, C., Tisch, D., Schuster, A., Monroy, A. A., Hinterdobler, W., and Schmoll, M. (2018). Gene regulation associated with sexual development and female fertility in different isolates of *Trichoderma reesei*. *Fungal Biol. Biotechnol.* 5, 9. doi: 10.1186/s40694-018-0055-4

Davolos, D., Russo, F., Canfora, L., Malusa, E., Tartanus, M., Furmanczyk, E. M., et al. (2021). A genomic and transcriptomic study on the DDT-resistant *Trichoderma hamatum* FBL 587: first genetic data into mycoremediation strategies for DDT-polluted sites. *Microorganisms* 9(8):1680. doi: 10.3390/microorganisms9081680

Dawe, A., and Nuss, D. L. (2013). Hypovirus molecular biology: from koch's postulates to host self-recognition genes that restrict virus transmission. *Adv. Virus Res.* 86, 109–147. doi: 10.1016/B978-0-12-394315-6.00005-2

Debuchy, R., Berteaux-Lecellier, V., and Silar, P. (2010). "Mating systems and sexual morphogenesis in ascomycetes," in *Cellular and molecular biology of filamentous fungi*. Eds. K. A. Borkovich and D. J. Ebbole (Washington, DC: ASM Press), 501–535.

Dell'Anno, F., Rastelli, E., Buschi, E., Barone, G., Beolchini, F., and Dell'anno, A. (2022). Fungi can be more effective than bacteria for the bioremediation of marine sediments highly contaminated with heavy metals. *Microorganisms* 10(5):993. doi: 10.3390/microorganisms10050993

Derntl, C., Guzman-Chavez, F., Mello-De-Sousa, T. M., Busse, H. J., Driessen, A. J. M., Mach, R. L., et al. (2017). *In vivo* study of the sorbicillinoid gene cluster in *Trichoderma reesei*. Front. Microbiol. 8, 2037. doi: 10.3389/fmicb.2017.02037

Derntl, C., Rassinger, A., Srebotnik, E., Mach, R. L., and Mach-Aigner, A. R. (2016). Identification of the main regulator responsible for synthesis of the typical yellow pigment produced by *Trichoderma reesei*. Appl. Environ. Microbiol. 82, 6247–6257. doi: 10.1128/AEM.01408-16

Druzhinina, I. S., Chenthamara, K., Zhang, J., Atanasova, L., Yang, D., Miao, Y., et al. (2018). Massive lateral transfer of genes encoding plant cell wall-degrading enzymes to the mycoparasitic fungus *Trichoderma* from its plant-associated hosts. *PloS Genet.* 14, e1007322. doi: 10.1371/journal.pgen.1007322

Druzhinina, I. S., Komon-Zelazowska, M., Atanasova, L., Seidl, V., and Kubicek, C. P. (2010). Evolution and ecophysiology of the industrial producer *Hypocrea jecorina* (anamorph *Trichoderma reesei*) and a new sympatric agamospecies related to it. *PloS One* 5, e9191. doi: 10.1371/journal.pone.0009191

Druzhinina, I., and Kubicek, C. (2013). "Ecological genomics of trichoderma," in *The ecological genomics of fungi* Hoboken, New Jersey, USA. Ed. F. Martin (John Wiley & Sons Inc), 89–116.

Druzhinina, I. S., Kubicek, E. M., and Kubicek, C. P. (2016). Several steps of lateral gene transfer followed by events of 'birth-and-death' evolution shaped a fungal sorbicillinoid biosynthetic gene cluster. *BMC Evol. Biol.* 16, 269. doi: 10.1186/s12862-016-0834-6

Druzhinina, I. S., Seidl-Seiboth, V., Herrera-Estrella, A., Horwitz, B. A., Kenerley, C. M., Monte, E., et al. (2011). *Trichoderma*: the genomics of opportunistic success. *Nat. Rev. Microbiol.* 9, 749–759. doi: 10.1038/nrmicro2637

Duan, C., Wang, S., Huo, R., Li, E., Wang, M., Ren, J., et al. (2022). Sorbicillinoid derivatives with the radical scavenging activities from the marine-derived fungus *Acremonium chrysogenum* C10. *J. Fungi (Basel)* 8(5):530. doi: 10.3390/jof8050530

Eusebio-Cope, A., Sun, L., Tanaka, T., Chiba, S., Kasahara, S., and Suzuki, N. (2015). The chestnut blight fungus for studies on virus/host and virus/virus interactions: from a natural to a model host. *Virology* 477, 164–175. doi: 10.1016/j.virol.2014.09.024

Fanelli, F., Liuzzi, V. C., Logrieco, A. F., and Altomare, C. (2018). Genomic characterization of *Trichoderma atrobrunneum* (*T. harzianum* species complex) ITEM 908: insight into the genetic endowment of a multi-target biocontrol strain. *BMC Genomics* 19, 662. doi: 10.1186/s12864-018-5049-3

Febbraio, F. (2017). Biochemical strategies for the detection and detoxification of toxic chemicals in the environment. *World J. Biol. Chem.* 8, 13–20. doi: 10.4331/wjbc.v8.i1.13

Ferreira Filho, J. A., Horta, M., Beloti, L. L., Dos Santos, C. A., and De Souza, A. P. (2017). Carbohydrate-active enzymes in *Trichoderma harzianum*: a bioinformatic analysis bioprospecting for key enzymes for the biofuels industry. *BMC Genomics* 18, 779. doi: 10.1186/s12864-017-4181-9

Ferreira Filho, J. A., Horta, M., Dos Santos, C. A., Almeida, D. A., Murad, N. F., Mendes, J. S., et al. (2020). Integrative genomic analysis of the bioprospection of regulators and accessory enzymes associated with cellulose degradation in a filamentous fungus (*Trichoderma harzianum*). *BMC Genomics* 21, 757. doi: 10.1186/s12864-020-07158-w

Fonseca, P. L. C., Badotti, F., De-Paula, R. B., Araujo, D. S., Bortolini, D. E., Del-Bem, L. E., et al. (2020). Exploring the relationship among divergence time and coding and non-coding elements in the shaping of fungal mitochondrial genomes. *Front. Microbiol.* 11, 765. doi: 10.3389/fmicb.2020.00765

Ford, R. E., Foster, G. D., and Bailey, A. M. (2022b). Exploring fungal RiPPs from the perspective of chemical ecology. *Fungal Biol. Biotechnol.* 9, 12. doi: 10.1186/s40694-022-00144-9

Ford, H. V., Jones, N. H., Davies, A. J., Godley, B. J., Jambeck, J. R., Napper, I. E., et al. (2022a). The fundamental links between climate change and marine plastic pollution. *Sci. Total Environ.* 806, 150392. doi: 10.1016/j.scitotenv.2021.150392

Frisvad, J. C., Moller, L. L. H., Larsen, T. O., Kumar, R., and Arnau, J. (2018). Safety of the fungal workhorses of industrial biotechnology: update on the mycotoxin and secondary metabolite potential of *Aspergillus niger*, *Aspergillus oryzae*, and *Trichoderma reesei*. *Appl. Microbiol. Biotechnol.* 102, 9481–9515. doi: 10.1007/s00253-018-9354-1

Gaderer, R., Bonazza, K., and Seidl-Seiboth, V. (2014). Cerato-platanins: a fungal protein family with intriguing properties and application potential. *Appl. Microbiol. Biotechnol.* 98, 4795–4803. doi: 10.1007/s00253-014-5690-y

Gaderer, R., Lamdan, N. L., Frischmann, A., Sulyok, M., Krska, R., Horwitz, B. A., et al. (2015). Sm2, a paralog of the *Trichoderma* cerato-platanin elicitor Sm1, is also highly important for plant protection conferred by the fungal-root interaction of *Trichoderma* with maize. *BMC Microbiol.* 15, 2. doi: 10.1186/s12866-014-0333-0

Gaillardin, C., Neuveglise, C., Kerscher, S., and Nicaud, J. M. (2012). Mitochondrial genomes of yeasts of the *Yarrowia* clade. *FEMS Yeast Res.* 12, 317–331. doi: 10.1111/j.1567-1364.2011.00782.x

Gao, R., Ding, M., Jiang, S., Zhao, Z., Chenthamara, K., Shen, Q., et al. (2020). The evolutionary and functional paradox of cerato-platanins in fungi. *Appl. Environ. Microbiol.* 86(13):e00696-20. doi: 10.1128/AEM.00696-20

Garber, R. C., and Yoder, O. C. (1983). Isolation of DNA from filamentous fungi and separation into nuclear, mitochondrial, ribosomal, and plasmid components. *Anal. Biochem.* 135, 416–422. doi: 10.1016/0003-2697(83)90704-2

Gazis, R., and Chaverri, P. (2010). Diversity of fungal endophytes in leaves and stems of wild rubber trees (*Hevea brasiliensis*) in Peru. *Fungal Ecol.* 3, 240–254. doi: 10.1016/j.funeco.2009.12.001

Ghabrial, S. A., Caston, J. R., Jiang, D., Nibert, M. L., and Suzuki, N. (2015). 50-plus years of fungal viruses. *Virology* 479-480, 356–368. doi: 10.1016/j.virol.2015.02.034

Ghabrial, S. A., and Suzuki, N. (2009). Viruses of plant pathogenic fungi. *Annu. Rev. Phytopathol.* 47, 353–384. doi: 10.1146/annurev-phyto-080508-081932

Gilbert, K. B., Holcomb, E. E., Allscheid, R. L., and Carrington, J. C. (2019). Hiding in plain sight: New virus genomes discovered *via* a systematic analysis of fungal public transcriptomes. *PloS One* 14, e0219207. doi: 10.1371/journal.pone.0219207

Gladyshev, E. (2017). Repeat-induced point mutation and other genome defense mechanisms in fungi. *Microbiol. Spectr.* 5(4), 10.1128/microbiolspec.FUNK-0042-2017. doi: 10.1128/9781555819583.ch33

Gladyshev, E., and Kleckner, N. (2014). Direct recognition of homology between double helices of DNA in *Neurospora crassa*. *Nat. Commun.* 5, 3509. doi: 10.1038/ncomms4509

Glass, N. L., Schmoll, M., Cate, J. H., and Coradetti, S. (2013). Plant cell wall deconstruction by ascomycete fungi. *Annu. Rev. Microbiol.* 67, 477–498. doi: 10.1146/annurev-micro-092611-150044

Gomez, I., Chet, I., and Herrera-Estrella, A. (1997). Genetic diversity and vegetative compatibility among *Trichoderma harzianum* isolates. *Mol. Gen. Genet.* 256, 127–135. doi: 10.1007/s004380050554

Gortikov, M., Wang, Z., Steindorff, A. S., Grigoriev, I. V., Druzhinina, I. S., Townsend, J. P., et al. (2022). Sequencing and analysis of the entire genome of the mycoparasitic bioeffector fungus *Trichoderma asperelloides* strain T 203 (Hypocreales). *Microbiol. Resour Announc* 11, e0099521. doi: 10.1128/mra.00995-21

Gruber, S., Omann, M., and Zeilinger, S. (2013). Comparative analysis of the repertoire of G protein-coupled receptors of three species of the fungal genus *Trichoderma*. *BMC Microbiol.* 13, 108. doi: 10.1186/1471-2180-13-108

Guangtao, Z., Hartl, L., Schuster, A., Polak, S., Schmoll, M., Wang, T., et al. (2009). Gene targeting in a nonhomologous end joining deficient *Hypocrea jecorina*. *J. Biotechnol.* 139, 146–151. doi: 10.1016/j.jbiotec.2008.10.007

Gudynaite-Savitch, L., and White, T. C. (2016). "Fungal biotechnology for industrial enzyme production: Focus on (hemi)cellulase production strategies, advances and challenges," in *Gene expression systems in fungi: Advancements and applications*. Eds. M. Schmoll and C. Dattenböck (Switzerland: Springer International Publishing Switzerland), 395–435.

Gutierrez, S., Mccormick, S. P., Cardoza, R. E., Kim, H. S., Yugueros, L. L., Vaughan, M. M., et al. (2021). Distribution, function, and evolution of a gene essential for trichothecene toxin biosynthesis in *Trichoderma*. *Front. Microbiol.* 12, 791641. doi: 10.3389/fmicb.2021.791641

Guzman-Chavez, F., Salo, O., Nygard, Y., Lankhorst, P. P., Bovenberg, R., and Driessen, A. J. M. (2017). Mechanism and regulation of sorbicillin biosynthesis by *Penicillium chrysogenum*. *Microb. Biotechnol.* 10, 958–968. doi: 10.1111/1751-7915.12736

Guzman-Guzman, P., Aleman-Duarte, M. I., Delaye, L., Herrera-Estrella, A., and Olmedo-Monfil, V. (2017). Identification of effector-like proteins in *Trichoderma* spp. and role of a hydrophobin in the plant-fungus interaction and mycoparasitism. *BMC Genet.* 18, 16. doi: 10.1186/s12863-017-0481-y

Guzman-Guzman, P., Porras-Troncoso, M. D., Olmedo-Monfil, V., and Herrera-Estrella, A. (2019). *Trichoderma* species: Versatile plant symbionts. *Phytopathology* 109, 6–16. doi: 10.1094/PHYTO-07-18-0218-RVW

Hafiz, F. B., Moradtalab, N., Goertz, S., Rietz, S., Dietel, K., Rozhon, W., et al. (2022). Synergistic effects of a root-endophytic *Trichoderma* fungus and *Bacillus* on early root colonization and defense activation against *Verticillium longisporum* in rapeseed. *Mol. Plant Microbe Interact.* 35, 380–392. doi: 10.1094/MPMI-11-21-0274-R

Hager, K. M., and Yanofsky, C. (1990). Genes expressed during conidiation in *Neurospora crassa*: molecular characterization of *con-13*. *Gene* 96, 153–159. doi: 10.1016/0378-1119(90)90247-O

Hammond, T. M., Andrewski, M. D., Roossinck, M. J., and Keller, N. P. (2008). *Aspergillus* mycoviruses are targets and suppressors of RNA silencing. *Eukaryot Cell* 7, 350–357. doi: 10.1128/EC.00356-07

Han, J., Xue, Y., Li, M., Li, Y., Liu, J., Gan, L., et al. (2020). Effect of VIB gene on cellulase production of *Trichoderma orientalis* EU7-22. *Appl. Biochem. Biotechnol.* 191, 1444–1455. doi: 10.1007/s12010-020-03260-7

Hao, Z., and Su, X. (2019). Fast gene disruption in *Trichoderma reesei* using *in vitro* assembled Cas9/gRNA complex. *BMC Biotechnol.* 19, 2. doi: 10.1186/s12896-018-0498-y

Harman, G. E., Doni, F., Khadka, R. B., and Uphoff, N. (2021). Endophytic strains of trichoderma increase plants' photosynthetic capability. *J. Appl. Microbiol.* 130, 529–546. doi: 10.1111/jam.14368

Harman, G. E., Howell, C. R., Viterbo, A., Chet, I., and Lorito, M. (2004a). *Trichoderma* species–opportunistic, avirulent plant symbionts. *Nat. Rev. Microbiol.* 2, 43–56. doi: 10.1038/nrmicro797

Harman, G. E., Lorito, M., and Lynch, J. M. (2004b). Uses of *Trichoderma* spp. to alleviate or remediate soil and water pollution. *Adv. Appl. Microbiol.* 56, 313–330. doi: 10.1016/S0065-2164(04)56010-0

Harned, A. M., and Volp, K. A. (2011). The sorbicillinoid family of natural products: isolation, biosynthesis, and synthetic studies. *Nat. Prod Rep.* 28, 1790–1810. doi: 10.1039/c1np00039j

Hatvani, L., Homa, M., Chenthamara, K., Cai, F., Kocsube, S., Atanasova, L., et al. (2019). Agricultural systems as potential sources of emerging human mycoses caused by *Trichoderma*: a successful, common phylotype of *Trichoderma longibrachiatum* in the frontline. *FEMS Microbiol. Lett.* 366(21):fnz246. doi: 10.1093/femsle/fnz246

Hinterdobler, W., Beier, S., Monroy, A. A., Berger, H., Dattenbock, C., and Schmoll, M. (2020a). The G-protein coupled receptor GPR8 regulates secondary metabolism in *Trichoderma reesei*. *Front. Bioeng Biotechnol.* 8, 558996. doi: 10.3389/fbioe.2020.558996

Hinterdobler, W., Beier, S., S., K., and Schmoll, M. (2020b). "Sexual development, its determinants and regulation in trichoderma reesei," in *Recent developments in trichoderma research*. Eds. S. Zeilinger, I. Druzhinina, H. B. Singh and V. K. Gupta (Amsterdam, The Netherlands: Elsevier), 185–206.

Hinterdobler, W., Li, G., Spiegel, K., Basyouni-Khamis, S., Gorfer, M., and Schmoll, M. (2021a). *Trichoderma reesei* isolated from Austrian soil with high potential for biotechnological application. *Front. Microbiol.* 12, 552301. doi: 10.3389/fmicb.2021.552301

Hinterdobler, W., Li, G., Turra, D., Schalamun, M., Kindel, S., Sauer, U., et al. (2021b). Integration of chemosensing and carbon catabolite repression impacts fungal enzyme regulation and plant associations. *bioRxiv.* doi: 10.1101/2021.1105.1106.442915

Hitzenhammer, E., Büschl, C., Sulyok, M., Schuhmacher, R., Kluger, B., Wischnitzki, E., et al. (2019). YPR2 is a regulator of light modulated carbon and secondary metabolism in *Trichoderma reesei*. *BMC Genomics* 20, 211. doi: 10.1186/s12864-019-5574-8

Hoof, J. B., Nodvig, C. S., and Mortensen, U. H. (2018). Genome editing: CRISPR-Cas9. *Methods Mol. Biol.* 1775, 119–132. doi: 10.1007/978-1-4939-7804-5_11

Hou, X., Zhang, X., Xue, M., Zhao, Z., Zhang, H., Xu, D., et al. (2022). Recent advances in sorbicillinoids from fungi and their bioactivities (Covering 2016-2021). *J. Fungi (Basel)* 8(1):62. doi: 10.3390/jof8010062

Ivanova, C., Ramoni, J., Aouam, T., Frischmann, A., Seiboth, B., Baker, S. E., et al. (2017). Genome sequencing and transcriptome analysis of *Trichoderma reesei* QM9978 strain reveals a distal chromosome translocation to be responsible for loss of *vib1* expression and loss of cellulase induction. *Biotechnol. Biofuels* 10, 209. doi: 10.1186/s13068-017-0897-7

Jaklitsch, W. M., and Voglmayr, H. (2015). Biodiversity of *Trichoderma* (Hypocreaceae) in southern Europe and macaronesia. *Stud. Mycol* 80, 1–87. doi: 10.1016/j.simyco.2014.11.001

Jom-in, S., and Akarapisan, A. (2009). Characterization of double stranded RNA in *Trichoderma* spp. isolates in Chiang mai province. *J. Agric. Technol.* 5, 261–270.

Jourdier, E., Baudry, L., Poggi-Parodi, D., Vicq, Y., Koszul, R., Margeot, A., et al. (2017). Proximity ligation scaffolding and comparison of two *Trichoderma reesei* strains genomes. *Biotechnol. Biofuels* 10, 151. doi: 10.1186/s13068-017-0837-6

Juraschek, L. M., Kappenberg, A., and Amelung, W. (2022). Mycotoxins in soil and environment. *Sci. Total Environ.* 814, 152425. doi: 10.1016/j.scitotenv.2021.152425

Kabani, M., Beckerich, J.-M., and Brodsky, J. L. (2002). Nucleotide exchange factor for the yeast Hsp70 molecular chaperone Ssa1p. *Mol. Cell. Biol.* 22, 4677–4689. doi: 10.1128/MCB.22.13.4677-4689.2002

Kannan, C., Divya, M., Rekha, G., Barbadikar, K. M., Maruthi, P., Hajira, S. K., et al. (2022). Whole genome sequencing data of native isolates of *Bacillus* and *Trichoderma* having potential biocontrol and plant growth promotion activities in rice. *Data Brief* 41, 107923. doi: 10.1016/j.dib.2022.107923

Karimi Aghcheh, R., Druzhinina, I. S., and Kubicek, C. P. (2013). The putative protein methyltransferase LAE1 of *Trichoderma atroviride* is a key regulator of asexual development and mycoparasitism. *PloS One* 8, e67144. doi: 10.1371/journal.pone.0067144

Karwehl, S., and Stadler, M. (2016). Exploitation of fungal biodiversity for discovery of novel antibiotics. *Curr. Top. Microbiol. Immunol.* 398, 303–338. doi: 10.1007/82_2016_496

Kashyap, P. L., Rai, P., Srivastava, A. K., and Kumar, S. (2017). *Trichoderma* for climate resilient agriculture. *World J. Microbiol. Biotechnol.* 33, 155. doi: 10.1007/s11274-017-2319-1

Kawamori, M., Morikawa, Y., and Takasawa, S. (1985). Inductive formation of celluases by l-sorbose in *Trichoderma reesei*. *Appl. Microbiol. Biotechnol.* 22, 235–236. doi: 10.1007/BF00253616

Kessler, S. C., and Chooi, Y. H. (2022). Out for a RiPP: challenges and advances in genome mining of ribosomal peptides from fungi. *Nat. Prod Rep.* 39, 222–230. doi: 10.1039/D1NP00048A

Khalifa, M. E., and MacDiarmid, R. M. (2019). A novel totivirus naturally occurring in two different fungal genera. *Front. Microbiol.* 10, 2318. doi: 10.3389/fmicb.2019.02318

Konstantinovas, C., De Oliveira Mendes, T. A., Vannier-Santos, M. A., and Lima-Santos, J. (2017). Modulation of human immune response by fungal biocontrol agents. *Front. Microbiol.* 8, 39. doi: 10.3389/fmicb.2017.00039

Kour, D., Kaur, T., Devi, R., Yadav, A., Singh, M., Joshi, D., et al. (2021). Beneficial microbiomes for bioremediation of diverse contaminated environments for environmental sustainability: present status and future challenges. *Environ. Sci. pollut. Res. Int.* 28, 24917–24939. doi: 10.1007/s11356-021-13252-7

Kouzminova, E., and Selker, E. U. (2001). *dim-2* encodes a DNA methyltransferase responsible for all known cytosine methylation in *Neurospora*. *EMBO J.* 20, 4309–4323. doi: 10.1093/emboj/20.15.4309

Kredics, L., Antal, Z., Doczi, I., Manczinger, L., Kevei, F., and Nagy, E. (2003). Clinical importance of the genus trichoderma. a review. *Acta Microbiol. Immunol. Hung* 50, 105–117. doi: 10.1556/AMicr.50.2003.2-3.1

Kredics, L., Chen, L., Kedves, O., Buchner, R., Hatvani, L., Allaga, H., et al. (2018). Molecular tools for monitoring *Trichoderma* in agricultural environments. *Front. Microbiol.* 9, 1599. doi: 10.3389/fmicb.2018.01599

Krumlauf, R., and Marzluf, G. A. (1980). Genome organization and characterization of the repetitive and inverted repeat DNA sequences in *Neurospora crassa*. *J. Biol. Chem.* 255, 1138–1145. doi: 10.1016/S0021-9258(19)86153-7

Kubicek, C. P., Baker, S., Gamauf, C., Kenerley, C. M., and Druzhinina, I. S. (2008). Purifying selection and birth-and-death evolution in the class II hydrophobin gene families of the ascomycete *Trichoderma/Hypocrea*. *BMC Evol. Biol.* 8, 4. doi: 10.1186/1471-2148-8-4

Kubicek, C. P., Herrera-Estrella, A., Seidl-Seiboth, V., Martinez, D. A., Druzhinina, I. S., Thon, M., et al. (2011). Comparative genome sequence analysis underscores mycoparasitism as the ancestral life style of Trichoderma. *Genome Biol.* 12(4), R40. doi: 10.1186/gb-2011-12-4-r40

Kubicek, C. P., Steindorff, A. S., Chenthamara, K., Manganiello, G., Henrissat, B., Zhang, J., et al. (2019). Evolution and comparative genomics of the most common *Trichoderma* species. *BMC Genomics* 20, 485. doi: 10.1186/s12864-019-5680-7

Kuo, H. C., Wang, T. Y., Chen, P. P., Chen, R. S., and Chen, T. Y. (2015). Genome sequence of *Trichoderma virens* FT-333 from tropical marine climate. *FEMS Microbiol. Lett.* 362(7):fnv036. doi: 10.1093/femsle/fnv036

Kwak, Y. (2020). Complete mitochondrial genome of the fungal biocontrol agent *Trichoderma atroviride*: genomic features, comparative analysis and insight into the mitochondrial evolution in *Trichoderma*. *Front. Microbiol.* 11, 785. doi: 10.3389/fmicb.2020.00785

Kwak, Y. (2021). An update on *Trichoderma* mitogenomes: complete *de novo* mitochondrial genome of the fungal biocontrol agent *Trichoderma harzianum* (Hypocreales, sordariomycetes), an ex-neotype strain CBS 226.95, and tracing the evolutionary divergences of mitogenomes in *Trichoderma*. *Microorganisms* 9(8), 1564. doi: 10.3390/microorganisms9081564

Lahlali, R., Ezrari, S., Radouane, N., Kenfaoui, J., Esmaeel, Q., El Hamss, H., et al. (2022). Biological control of plant pathogens: a global perspective. *Microorganisms* 10(3), 596. doi: 10.3390/microorganisms10030596

Landeis, A., and Schmidt-Heydt, M. (2021). Sequencing and analysis of the entire genome of the mycoparasitic fungus *Trichoderma afroharzianum*. *Microbiol. Resour Announc* 10 (15), e00211–e00221. doi: 10.1128/MRA.00211-21

Lawrence, T. J., Carper, D. L., Spangler, M. K., Carrell, A. A., Rush, T. A., Minter, S. J., et al. (2021). amPEPpy 1.0: a portable and accurate antimicrobial peptide prediction tool. *Bioinformatics.* 37 (14), 2058–2060. doi: 10.1093/bioinformatics/btaa917

Lee, S. H., Yun, S. H., Chun, J., and Kim, D. H. (2017). Characterization of a novel dsRNA mycovirus of *Trichoderma atroviride* NFCF028. *Arch. Virol.* 162, 1073–1077. doi: 10.1007/s00705-016-3214-z

Lehmann, L., Ronnest, N. P., Jorgensen, C. I., Olsson, L., Stocks, S. M., Jorgensen, H. S., et al. (2016). Linking hydrolysis performance to *Trichoderma reesei*

cellulolytic enzyme profile. *Biotechnol. Bioeng* 113, 1001–1010. doi: 10.1002/bit.25871

Li, W. C., Chen, C. L., and Wang, T. F. (2018). Repeat-induced point (RIP) mutation in the industrial workhorse fungus *Trichoderma reesei*. *Appl. Microbiol. Biotechnol.* 102, 1567–1574. doi: 10.1007/s00253-017-8731-5

Lichius, A., Bidard, F., Buchholz, F., Le Crom, S., Martin, J., Schackwitz, W., et al. (2015). Genome sequencing of the *Trichoderma reesei* QM9136 mutant identifies a truncation of the transcriptional regulator XYR1 as the cause for its cellulase-negative phenotype. *BMC Genomics* 16, 326. doi: 10.1186/s12864-015-1526-0

Lieckfeldt, E., Kullnig, C. M., Samuels, G. J., and Kubicek, C. P. (2000). Sexually competent, sucrose- and nitrate-assimilating strains of *Hypocrea jecorina* (*Trichoderma reesei*) from south American soils. *Mycologia* 92, 374–380. doi: 10.1080/00275514.2000.12061170

Li, W. C., Huang, C. H., Chen, C. L., Chuang, Y. C., Tung, S. Y., and Wang, T. F. (2017). *Trichoderma reesei* complete genome sequence, repeat-induced point mutation, and partitioning of CAZyme gene clusters. *Biotechnol. Biofuels* 10, 170. doi: 10.1186/s13068-017-0825-x

Li, W. C., Lee, C. Y., Lan, W. H., Woo, T. T., Liu, H. C., Yeh, H. Y., et al. (2021a). *Trichoderma reesei* Rad51 tolerates mismatches in hybrid meiosis with diverse genome sequences. *Proc. Natl. Acad. Sci. U.S.A.* 118(8):e2007192118. doi: 10.1073/pnas.2007192118

Li, W. C., Lin, T. C., Chen, C. L., Liu, H. C., Lin, H. N., Chao, J. L., et al. (2021b). Complete genome sequences and genome-wide characterization of *Trichoderma* biocontrol agents provide new insights into their evolution and variation in genome organization, sexual development, and fungal-plant interactions. *Microbiol. Spectr.* 9, e0066321. doi: 10.1128/Spectrum.00663-21

Li, Z., and Liu, T. (2022). High-quality genome sequence data of *Trichoderma gracile* HK011-1, a fungal antagonistic agent against plant pathogens. *Plant Dis.* 106, 1035–1038. doi: 10.1094/PDIS-09-21-2006-A

Lindo, L., Mccormick, S. P., Cardoza, R. E., Brown, D. W., Kim, H. S., Alexander, N. J., et al. (2018). Effect of deletion of a trichothecene toxin regulatory gene on the secondary metabolism transcriptome of the saprotrophic fungus *Trichoderma arundinaceum*. *Fungal Genet. Biol.* 119, 29–46. doi: 10.1016/j.fgb.2018.08.002

Linke, R., Thallinger, G. G., Haarmann, T., Eidner, J., Schreiter, M., Lorenz, P., et al. (2015). Restoration of female fertility in *Trichoderma reesei* QM6a provides the basis for inbreeding in this industrial cellulase producing fungus. *Biotechnol. Biofuels* 8, 155. doi: 10.1186/s13068-015-0311-2

Liu, W., Cai, Y., Zhang, Q., Chen, L., Shu, F., Ma, X., et al. (2020). The mitochondrial genome of *Morchella importuna* (272.2 kb) is the largest among fungi and contains numerous introns, mitochondrial non-conserved open reading frames and repetitive sequences. *Int. J. Biol. Macromol* 143, 373–381. doi: 10.1016/j.ijbiomac.2019.12.056

Liu, R., Chen, L., Jiang, Y., Zhou, Z., and Zou, G. (2015). Efficient genome editing in filamentous fungus *Trichoderma reesei* using the CRISPR/Cas9 system. *Cell Discovery* 1, 15007. doi: 10.1038/celldisc.2015.7

Liu, C., Li, M., Redda, E. T., Mei, J., Zhang, J., Wu, B., et al. (2019). A novel double-stranded RNA mycovirus isolated from *Trichoderma harzianum*. *Virol. J.* 16, 113. doi: 10.1186/s12985-019-1213-x

Liu, H. C., Li, W. C., and Wang, T. F. (2021). TSETA: A third-generation sequencing-based computational tool for mapping and visualization of SNPs, meiotic recombination products, and RIP mutations. *Methods Mol. Biol.* 2234, 331–361. doi: 10.1007/978-1-0716-1048-0_22

Losada, L., Pakala, S. B., Fedorova, N. D., Joardar, V., Shabalina, S. A., Hostetler, J., et al. (2014). Mobile elements and mitochondrial genome expansion in the soil fungus and potato pathogen *Rhizoctonia solani* AG-3. *FEMS Microbiol. Lett.* 352, 165–173. doi: 10.1111/1574-6968.12387

Macias-Rodriguez, L., Contreras-Cornejo, H. A., Adame-Garnica, S. G., Del-Val, E., and Larsen, J. (2020). The interactions of *Trichoderma* at multiple trophic levels: inter-kingdom communication. *Microbiol. Res.* 240, 126552. doi: 10.1016/j.micres.2020.126552

Malmierca, M. G., Cardoza, R. E., Alexander, N. J., McCormick, S. P., Collado, I. G., Hermosa, R. , and Gutiérrez, S. (2013). Relevance of trichothecenes in fungal physiology: disruption of *tri5* in *Trichoderma arundinaceum*. *Fungal Genet. Biol.* 53, 22–33. doi: 10.1016/j.fgb.2013.02.001.

Mandels, M., Weber, J., and Parizek, R. (1971). Enhanced cellulase production by a mutant of *Trichoderma viride*. *Appl. Microbiol.* 21, 152–154. doi: 10.1128/am.21.1.152-154.1971

Marie-Nelly, H., Marbouty, M., Cournac, A., Flot, J. F., Liti, G., Parodi, D. P., et al. (2014). High-quality genome (re)assembly using chromosomal contact data. *Nat. Commun.* 5, 5695. doi: 10.1038/ncomms6695

Marquez, L. M., Redman, R. S., Rodriguez, R. J., and Roossinck, M. J. (2007). A virus in a fungus in a plant: three-way symbiosis required for thermal tolerance. *Science* 315, 513–515. doi: 10.1126/science.1136237

Martinez, D., Berka, R. M., Henrissat, B., Saloheimo, M., Arvas, M., Baker, S. E., et al. (2008). Genome sequencing and analysis of the biomass-degrading fungus *Trichoderma reesei* (syn. *Hypocrea jecorina*). *Nat. Biotechnol.* 26, 553–560. doi: 10.1038/nbt1403

Maskey, R. P., Grun-Wollny, I., and Laatsch, H. (2005). Sorbicillin analogues and related dimeric compounds from *Penicillium notatum*. *J. Nat. Prod* 68, 865–870. doi: 10.1021/np040137t

McDonald, M. J., Rice, D. P., and Desai, M. M. (2016). Sex speeds adaptation by altering the dynamics of molecular evolution. *Nature* 531, 233–236. doi: 10.1038/nature17143

Medina-Castellanos, E., Villalobos-Escobedo, J. M., Riquelme, M., Read, N. D., Abreu-Goodger, C., and Herrera-Estrella, A. (2018). Danger signals activate a putative innate immune system during regeneration in a filamentous fungus. *PloS Genet.* 14, e1007390. doi: 10.1371/journal.pgen.1007390

Medina, R., Franco, M. E. E., Bartel, L. C., Martinez Alcantara, V., Saparrat, M. C. N., and Balatti, P. A. (2020). Fungal mitogenomes: relevant features to planning plant disease management. *Front. Microbiol.* 11, 978. doi: 10.3389/fmicb.2020.00978

Megarioti, A. H., and Kouvelis, V. N. (2020). The coevolution of fungal mitochondrial introns and their homing endonucleases (GIY-YIG and LAGLIDADG). *Genome Biol. Evol.* 12, 1337–1354. doi: 10.1093/gbe/evaa126

Mendoza-Mendoza, A., Zaid, R., Lawry, R., Hermosa, R., Monte, E., Horwitz, B., et al. (2018). Molecular dialogues between *Trichoderma* and roots: role of the fungal secretome. *Fungal Biol. Rev.* 32, 62–85. doi: 10.1016/j.fbr.2017.12.001

Meng, J., Wang, X., Xu, D., Fu, X., Zhang, X., Lai, D., et al. (2016). Sorbicillinoids from fungi and their bioactivities. *Molecules* 21(6), 715. doi: 10.3390/molecules21060715

Milgroom, M. G., and Cortesi, P. (2004). Biological control of chestnut blight with hypovirulence: a critical analysis. *Annu. Rev. Phytopathol.* 42, 311–338. doi: 10.1146/annurev.phyto.42.040803.140325

Mishra, S., Lin, Z., Pang, S., Zhang, W., Bhatt, P., and Chen, S. (2021). Recent advanced technologies for the characterization of xenobiotic-degrading microorganisms and microbial communities. *Front. Bioeng Biotechnol.* 9, 632059. doi: 10.3389/fbioe.2021.632059

Monroy, A. A., Stappler, E., Schuster, A., Sulyok, M., and Schmoll, M. (2017). A CRE1- regulated cluster is responsible for light dependent production of dihydrotrichotetronin in *Trichoderma reesei*. *PloS One*, 12 (8), e0182530. doi: 10.1371/journal.pone.0182530

Moran-Diez, M. E., Martinez De Alba, A. E., Rubio, M. B., Hermosa, R., and Monte, E. (2021). Trichoderma and the plant heritable priming responses. *J. Fungi (Basel)* 7(4), 318. doi: 10.3390/jof7040318

Myers, J. M., and James, T. Y. (2022). Mycoviruses. *Curr. Biol.* 32, R150–R155. doi: 10.1016/j.cub.2022.01.049

Nerva, L., and Chitarra, W. (2021). "Mycoviruses: A hidden world within fungi," in *Encyclopedia of mycology*. Eds. Ó. Zaragoza and A. Casadevall (Oxford: Elsevier), 134–141.

Nerva, L., Varese, G. C., Falk, B. W., and Turina, M. (2017). Mycoviruses of an endophytic fungus can replicate in plant cells: evolutionary implications. *Sci. Rep.* 7, 1908. doi: 10.1038/s41598-017-02017-3

Nevalainen, K. M., and Palva, E. T. (1978). Production of extracellular enzymes in mutants isolated from *Trichoderma viride* unable to hydrolyze cellulose. *Appl. Environ. Microbiol.* 35, 11–16. doi: 10.1128/aem.35.1.11-16.1978

Nevalainen, H., Suominen, P., and Taimisto, K. (1994). On the safety of *Trichoderma reesei*. *J. Biotechnol.* 37, 193–200. doi: 10.1016/0168-1656(94)90126-0

Nogueira-Lopez, G., Padilla-Arizmendi, F., Inwood, S., Lyne, S., Steyaert, J. M., Nieto-Jacobo, M. F., et al. (2019). TrichoGate: An improved vector system for a large scale of functional analysis of *Trichoderma* genes. *Front. Microbiol.* 10, 2794. doi: 10.3389/fmicb.2019.02794

Pachauri, S., Sherkhane, P. D., Kumar, V., and Mukherjee, P. K. (2020). Whole genome sequencing reveals major deletions in the genome of M7, a gamma ray-induced mutant of *Trichoderma virens* that is repressed in conidiation, secondary metabolism, and mycoparasitism. *Front. Microbiol.* 11, 1030. doi: 10.3389/fmicb.2020.01030

Paloheimo, M., Haarmann, T., Mäkinen, S., and Vehmaanperä, J. (2016). "Production of industrial enzymes in trichoderma reesei," in *Gene expression systems in fungi: Advancements and applications*. Eds. M. Schmoll and C. Dattenböck (Heidelberg: Springer International), 23–58.

Pang, A. P., Zhang, F., Hu, X., Luo, Y., Wang, H., Durrani, S., et al. (2021). Glutamine involvement in nitrogen regulation of cellulase production in fungi. *Biotechnol. Biofuels* 14, 199. doi: 10.1186/s13068-021-02046-1

Peterson, R., and Nevalainen, H. (2012). *Trichoderma reesei* RUT-C30 - thirty years of strain improvement. *Microbiology* 158, 58–68. doi: 10.1099/mic.0.054031-0

Pfordt, A., Schiwek, S., Karlovsky, P., and Von Tiedemann, A. (2020). *Trichoderma afroharzianum* ear rot–a new disease on maize in Europe. *Front. Agron.* 2. doi: 10.3389/fagro.2020.547758

Pilgaard, B., Vuillemin, M., Munk, L., Holck, J., Meier, S., Wilkens, C., et al. (2022). Discovery of a novel glucuronan lyase system in *Trichoderma parareesei*. *Appl. Environ. Microbiol.* 88, e0181921. doi: 10.1128/AEM.01819-21

Porciuncula Jde, O., Furukawa, T., Mori, K., Shida, Y., Hirakawa, H., Tashiro, K., et al. (2013). Single nucleotide polymorphism analysis of a *Trichoderma reesei* hyper-cellulolytic mutant developed in Japan. *Biosci. Biotechnol. Biochem.* 77, 534–543. doi: 10.1271/bbb.120794

Pramateftaki, P. V., Kouvelis, V. N., Lanaridis, P., and Typas, M. A. (2006). The mitochondrial genome of the wine yeast *Hanseniaspora uvarum*: a unique genome organization among yeast/fungal counterparts. *FEMS Yeast Res.* 6, 77–90. doi: 10.1111/j.1567-1364.2005.00018.x

Proctor, R. H., Mccormick, S. P., Kim, H. S., Cardoza, R. E., Stanley, A. M., Lindo, L., et al. (2018). Evolution of structural diversity of trichothecenes, a family of toxins produced by plant pathogenic and entomopathogenic fungi. *PloS Pathog.* 14, e1006946. doi: 10.1371/journal.ppat.1006946

Ramirez-Valdespino, C. A., Casas-Flores, S., and Olmedo-Monfil, V. (2019). Trichoderma as a model to study effector-like molecules. *Front. Microbiol.* 10, 1030. doi: 10.3389/fmicb.2019.01030

Rantasalo, A., Czeizler, E., Virtanen, R., Rousu, J., Lahdesmaki, H., Penttila, M., et al. (2016). Synthetic transcription amplifier system for orthogonal control of gene expression in *Saccharomyces cerevisiae*. *PloS One* 11, e0148320. doi: 10.1371/journal.pone.0148320

Rantasalo, A., Landowski, C. P., Kuivanen, J., Korppoo, A., Reuter, L., Koivistoinen, O., et al. (2018). A universal gene expression system for fungi. *Nucleic Acids Res.* 46, e111. doi: 10.1093/nar/gky558

Rantasalo, A., Vitikainen, M., Paasikallio, T., Jantti, J., Landowski, C. P., and Mojzita, D. (2019). Novel genetic tools that enable highly pure protein production in *Trichoderma reesei*. *Sci. Rep.* 9, 5032. doi: 10.1038/s41598-019-41573-8

Rassinger, A., Gacek-Matthews, A., Strauss, J., Mach, R. L., and Mach-Aigner, A. R. (2018). Truncation of the transcriptional repressor protein Cre1 in *Trichoderma reesei* rut-C30 turns it into an activator. *Fungal Biol. Biotechnol.* 5, 15. doi: 10.1186/s40694-018-0059-0

Repas, T. S., Gillis, D. M., Boubakir, Z., Bao, X., Samuels, G. J., and Kaminskyj, S. G. W. (2017). Growing plants on oily, nutrient-poor soil using a native symbiotic fungus. *PloS One* 12, e0186704. doi: 10.1371/journal.pone.0186704

Rodriguez-Iglesias, A., and Schmoll, M. (2015). "Protoplast transformation for genome manipulation in fungi," in *Genetic transformation systems in fungi*. Eds. M. A. Van Den Berg and K. Maruthachalam (Switzerland: Springer International Publishing), 21–40.

Rozhkova, A. M., and Kislitsin, V. Y. (2021). CRISPR/Cas genome editing in filamentous fungi. *Biochem. (Mosc)* 86, S120–S139. doi: 10.1134/S0006297921140091

Rush, T. A., Shrestha, H. K., Gopalakrishnan Meena, M., Spangler, M. K., Ellis, J. C., Labbé, J. L., et al. (2021). Bioprospecting *Trichoderma*: A systematic roadmap to screen genomes and natural products for biocontrol applications. *Front. Fungal Biol.* 2. doi: 10.3389/ffunb.2021.716511

Salas-Marina, M. A., Isordia-Jasso, M. I., Islas-Osuna, M. A., Delgado-Sánchez, P., Jiménez-Bremont, J. F., Rodríguez-Kessler, M., et al. (2015). The Epl1 and Sm1 proteins from *Trichoderma atroviride* and *Trichoderma virens* differentially modulate systemic disease resistance against different life style pathogens in *Solanum lycopersicum*. *Front. Plant Sci.* 6, 77. doi: 10.3389/fpls.2015.00077

Salo, O., Guzman-Chavez, F., Ries, M. I., Lankhorst, P. P., Bovenberg, R. A., Vreeken, R. J., et al. (2016). Identification of a polyketide synthase involved in sorbicillin biosynthesis by *Penicillium chrysogenum*. *Appl. Environ. Microbiol.* 82, 3971–3978. doi: 10.1128/AEM.00350-16

Saloheimo, M., Paloheimo, M., Hakola, S., Pere, J., Swanson, B., Nyyssonen, E., et al. (2002). Swollenin, a *Trichoderma reesei* protein with sequence similarity to the plant expansins, exhibits disruption activity on cellulosic materials. *Eur. J. Biochem.* 269, 4202–4211. doi: 10.1046/j.1432-1033.2002.03095.x

Sandoval-Denis, M., Sutton, D. A., Cano-Lira, J. F., Gene, J., Fothergill, A. W., Wiederhold, N. P., et al. (2014). Phylogeny of the clinically relevant species of the emerging fungus *Trichoderma* and their antifungal susceptibilities. *J. Clin. Microbiol.* 52, 2112–2125. doi: 10.1128/JCM.00429-14

Sanna, M., Pugliese, M., Gullino, M. L., and Mezzalama, M. (2022). First report of *Trichoderma afroharzianum* causing seed rot on maize in Italy. *Plant Dis.* doi: 10.1094/PDIS-12-21-2697-PDN

Schmoll, M. (2013). "Sexual development in trichoderma - scrutinizing the aspired phenomenon," in *Trichoderma: biology and applications*. Eds. P. K. Mukherjee, B. A. Horwitz, U. S. Singh, M. Mukherjee and M. Schmoll (Oxfordshire, UK: CAB International), 67–86.

Schmoll, M. (2018a). Light, stress, sex and carbon - the photoreceptor ENVOY as a central checkpoint in the physiology of *Trichoderma reesei*. *Fungal Biol.* 122, 479–486. doi: 10.1016/j.funbio.2017.10.007

Schmoll, M. (2018b). Regulation of plant cell wall degradation by light in *Trichoderma*. *Fungal Biol. Biotechnol.* 5, 10. doi: 10.1186/s40694-018-0052-7

Schmoll, M., Dattenböck, C., Carreras-Villasenor, N., Mendoza-Mendoza, A., Tisch, D., Aleman, M. I., et al. (2016). The genomes of three uneven siblings: footprints of the lifestyles of three *Trichoderma* species. *Microbiol. Mol. Biol. Rev.* 80, 205–327. doi: 10.1128/MMBR.00040-15

Schmoll, M., Esquivel-Naranjo, E. U., and Herrera-Estrella, A. (2010). *Trichoderma* in the light of day - physiology and development. *Fungal Genet. Biol.* 47, 909–916. doi: 10.1016/j.fgb.2010.04.010

Schmoll, M., and Kubicek, C. P. (2005). *ooc1*, a unique gene expressed only during growth of *Hypocrea jecorina* (anamorph: *Trichoderma reesei*) on cellulose. *Curr. Genet.* 48, 126–133. doi: 10.1007/s00294-005-0585-1

Schmoll, M., Tisch, D., Schuster, A., Freitag, M., Pomraning, K. R., and Wang, T. F. (2013). *Introducing or inactivating female fertility in filamentous fungal cells*. CAB International: Oxfordshire, UK.

Schmoll, M., and Wang, T. F. (2016). "Sexual development in trichoderma," in *The mycota (Vol. i): Growth, differentiation and sexuality*. Ed. J. Wendland (Switzerland: Springer International Publishing), 457–474.

Schmoll, M., and Zeilinger, S. (2021). Resistance marker- and gene gun-mediated transformation of *Trichoderma reesei*. *Methods Mol. Biol.* 2234, 55–62. doi: 10.1007/978-1-0716-1048-0_4

Schmoll, M., Zeilinger, S., Mach, R. L., and Kubicek, C. P. (2004). Cloning of genes expressed early during cellulase induction in *Hypocrea jecorina* by a rapid subtraction hybridization approach. *Fungal Genet. Biol.* 41, 877–887. doi: 10.1016/j.fgb.2004.06.002

Schuster, A., Bruno, K. S., Collett, J. R., Baker, S. E., Seiboth, B., Kubicek, C. P., et al. (2012). A versatile toolkit for high throughput functional genomics with *Trichoderma reesei*. *Biotechnol. Biofuels* 5, 1. doi: 10.1186/1754-6834-5-1

Schuster, A., Kubicek, C. P., and Schmoll, M. (2011). Dehydrogenase GRD1 represents a novel component of the cellulase regulon in *Trichoderma reesei* (*Hypocrea jecorina*). *Appl. Environ. Microbiol.* 77, 4553–4563. doi: 10.1128/AEM.00513-11

Schuster, A., and Schmoll, M. (2010). Biology and biotechnology of *Trichoderma*. *Appl. Microbiol. Biotechnol.* 87, 787–799. doi: 10.1007/s00253-010-2632-1

Segers, G. C., Zhang, X., Deng, F., Sun, Q., and Nuss, D. L. (2007). Evidence that RNA silencing functions as an antiviral defense mechanism in fungi. *Proc. Natl. Acad. Sci. U.S.A.* 104, 12902–12906. doi: 10.1073/pnas.0702500104

Seidl, V., Gamauf, C., Druzhinina, I. S., Seiboth, B., Hartl, L., and Kubicek, C. P. (2008). The *Hypocrea jecorina* (*Trichoderma reesei*) hypercellulolytic mutant RUT C30 lacks a 85 kb (29 gene-encoding) region of the wild-type genome. *BMC Genomics* 9, 327. doi: 10.1186/1471-2164-9-327

Seidl, V., Seibel, C., Kubicek, C. P., and Schmoll, M. (2009). Sexual development in the industrial workhorse *Trichoderma reesei*. *Proc. Natl. Acad. Sci. U.S.A.* 106, 13909–13914. doi: 10.1073/pnas.0904936106

Seidl, V., and Seiboth, B. (2010). *Trichoderma reesei*: genetic approaches to improving strain efficiency. *Biofuels* 1, 343–354. doi: 10.4155/bfs.10.1

Selker, E. U., Cambareri, E. B., Jensen, B. C., and Haack, K. R. (1987). Rearrangement of duplicated DNA in specialized cells of *Neurospora*. *Cell* 51, 741–752. doi: 10.1016/0092-8674(87)90097-3

Sharma, P., Parakh, S. K., Singh, S. P., Parra-Saldivar, R., Kim, S. H., Varjani, S., et al. (2022). A critical review on microbes-based treatment strategies for mitigation of toxic pollutants. *Sci. Total Environ.* 834, 155444. doi: 10.1016/j.scitotenv.2022.155444

Shenouda, M. L., Ambilika, M., Skellam, E., and Cox, R. J. (2022). Heterologous expression of secondary metabolite genes in *Trichoderma reesei* for waste valorization. *J. Fungi (Basel)* 8(4):355. doi: 10.3390/jof8040355

Shenouda, M. L., and Cox, R. J. (2021). Molecular methods unravel the biosynthetic potential of *Trichoderma* species. *RSC Adv.* 11, 3622–3635. doi: 10.1039/D0RA09627J

Shoresh, M., Harman, G. E., and Mastouri, F. (2010). Induced systemic resistance and plant responses to fungal biocontrol agents. *Annu. Rev. Phytopathol.* 48, 21–43. doi: 10.1146/annurev-phyto-073009-114450

Singh, A., Taylor, L. E.2nd, Vander Wall, T. A., Linger, J., Himmel, M. E., Podkaminer, K., et al. (2015). Heterologous protein expression in *Hypocrea jecorina*: a historical perspective and new developments. *Biotechnol. Adv.* 33, 142–154. doi: 10.1016/j.biotechadv.2014.11.009

Son, M., Yu, J., and Kim, K. H. (2015). Five questions about mycoviruses. *PloS Pathog.* 11, e1005172. doi: 10.1371/journal.ppat.1005172

Sood, M., Kapoor, D., Kumar, V., Sheteiwy, M. S., Ramakrishnan, M., Landi, M., et al. (2020). *Trichoderma*: the "secrets" of a multitalented biocontrol agent. *Plants (Basel)* 9(6):762. doi: 10.3390/plants9060762

Stappler, E., Dattenböck, C., Tisch, D., and Schmoll, M. (2017). Analysis of light- and carbon-specific transcriptomes implicates a class of G-protein-coupled receptors in cellulose sensing. *mSphere* 2, e00089–e00017. doi: 10.1128/mSphere.00089-17

Stoddard, B. L. (2014). Homing endonucleases from mobile group I introns: discovery to genome engineering. *Mob DNA* 5, 7. doi: 10.1186/1759-8753-5-7

Stracquadanio, C., Luz, C., La Spada, F., Meca, G., and Cacciola, S. O. (2021). Inhibition of mycotoxigenic fungi in different vegetable matrices by extracts of *Trichoderma* species. *J. Fungi (Basel)* 7(6), 445. doi: 10.3390/jof7060445

Sun, X., Cai, Y. S., Yuan, Y., Bian, G., Ye, Z., Deng, Z., et al. (2019). Genome mining in *Trichoderma viride* J1-030: discovery and identification of novel sesquiterpene synthase and its products. *Beilstein J. Org Chem.* 15, 2052–2058. doi: 10.3762/bjoc.15.202

Tamizi, A. A., Mat-Amin, N., Weaver, J. A., Olumakaiye, R. T., Akbar, M. A., Jin, S., et al. (2022). Genome sequencing and analysis of *Trichoderma* (Hypocreaceae) isolates exhibiting antagonistic activity against the papaya dieback pathogen, *Erwinia mallotivora*. *J. Fungi (Basel)* 8(3), 246. doi: 10.3390/jof8030246

Taylor, J. T., Harting, R., Shalaby, S., Kenerley, C. M., Braus, G. H., and Horwitz, B. A. (2022). Adhesion as a focus in *Trichoderma*-root interactions. *J. Fungi (Basel)* 8(4), 372. doi: 10.3390/jof8040372

Taylor, J. T., Wang, K.-D., Horwitz, B., Kolomiets, M., and Kenerley, C. (2021). Early transcriptome response of *Trichoderma virens* to colonization of maize roots. *Front. Fungal Biol.* 2. doi: 10.3389/ffunb.2021.718557

Tisch, D., Pomraning, K. R., Collett, J. R., Freitag, M., Baker, S. E., Chen, C. L., et al. (2017). Omics analyses of *Trichoderma reesei* CBS999.97 and QM6a indicate the relevance of female fertility to carbohydrate-active enzyme and transporter levels. *Appl. Environ. Microbiol.* 83(22), e01578-17. doi: 10.1128/AEM.01578-17

Torigoi, E., Henrique-Silva, F., Escobar-Vera, J., Carle-Urioste, J. C., Crivellaro, O., El-Dorry, H., et al. (1996). Mutants of *Trichoderma reesei* are defective in cellulose induction, but not basal expression of cellulase-encoding genes. *Gene* 173, 199–203. doi: 10.1016/0378-1119(96)00219-3

Tripathi, P., Singh, P. C., Mishra, A., Chaudhry, V., Mishra, S., Tripathi, R. D., et al. (2013). *Trichoderma* inoculation ameliorates arsenic induced phytotoxic changes in gene expression and stem anatomy of chickpea (*Cicer arietinu*m). *Ecotoxicol Environ. Saf.* 89, 8–14. doi: 10.1016/j.ecoenv.2012.10.017

Tsuji, J., Frith, M. C., Tomii, K., and Horton, P. (2012). Mammalian NUMT insertion is non-random. *Nucleic Acids Res.* 40, 9073–9088. doi: 10.1093/nar/gks424

Tyskiewicz, R., Nowak, A., Ozimek, E., and Jaroszuk-Scisel, J. (2022). *Trichoderma*: The current status of its application in agriculture for the biocontrol of fungal phytopathogens and stimulation of plant growth. *Int. J. Mol. Sci.* 23(4), 2329. doi: 10.3390/ijms23042329

Uchiyama, T., Uchihashi, T., Nakamura, A., Watanabe, H., Kaneko, S., Samejima, M., et al. (2020). Convergent evolution of processivity in bacterial and fungal cellulases. *Proc. Natl. Acad. Sci. U.S.A.* 117, 19896–19903. doi: 10.1073/pnas.2011366117

van Bohemen, A. I., Ruiz, N., Zalouk-Vergnoux, A., Michaud, A., Robiou du Pont, T., Druzhinina, I., et al. (2021). Pentadecaibins I-V: 15-residue peptaibols produced by a marine-derived *Trichoderma* sp. of the *Harzianum* clade. *J. Nat. Prod.* 84 (4), 1271–1282. doi: 10.1021/acs.jnatprod.0c01355

van Wyk, S., Wingfield, B. D., De Vos, L., van der Merwe, N. A., and Steenkamp, E. T. (2020). Genome-wide analyses of repeat-induced point mutations in the ascomycota. *Front. Microbiol.* 11, 622368. doi: 10.3389/fmicb.2020.622368

Venice, F., Davolos, D., Spina, F., Poli, A., Prigione, V. P., Varese, G. C., et al. (2020). Genome sequence of *Trichoderma lixii* MUT3171, a promising strain for mycoremediation of PAH-contaminated sites. *Microorganisms* 8(9), 1258. doi: 10.3390/microorganisms8091258

Verschoor, J. A., Kusumawardhani, H., Ram, A. F. J., and De Winde, J. H. (2022). Toward microbial recycling and upcycling of plastics: prospects and challenges. *Front. Microbiol.* 13, 821629. doi: 10.3389/fmicb.2022.821629

Vicente, I., Baroncelli, R., Morán-Diez, M. E., Bernardi, R., Puntoni, G., Hermosa, R., et al. (2020). Combined comparative genomics and gene expression analyses provide insights into the terpene synthases inventory in *Trichoderma*. *Microorganisms* 8 (10), 1603. doi: 10.3390/microorganisms8101603

Vieira, A. A., Vianna, G. R., Carrijo, J., Aragão, F. J. L., and Vieira, P. M. (2021). Generation of *Trichoderma harzianum* with *pyr4* auxotrophic marker by using the CRISPR/Cas9 system. *Sci. Rep.* 11 (1), 1085. doi: 10.1038/s41598-020-80186-4

Vĺglaš, J., Dobiasova, S., Viktorova, J., Ruml, T., Repiska, V., Olejnikova, P., et al. (2021). Peptaibol-containing extracts of *Trichoderma atroviride* and the fight against resistant microorganisms and cancer cells. *Molecules* 26(19), 6025. doi: 10.3390/molecules26196025

Vignolle, G. A., Mach, R. L., Mach-Aigner, A. R., and Derntl, C. (2020). Novel approach in whole genome mining and transcriptome analysis reveal conserved RiPPs in *Trichoderma* spp. *BMC Genomics* 21, 258. doi: 10.1186/s12864-020-6653-6

Vignolle, G. A., Schaffer, D., Zehetner, L., Mach, R. L., Mach-Aigner, A. R., and Derntl, C. (2021). FunOrder: A robust and semi-automated method for the identification of essential biosynthetic genes through computational molecular co-evolution. *PloS Comput. Biol.* 17, e1009372. doi: 10.1371/journal.pcbi.1009372

Wallen, R. M., and Perlin, M. H. (2018). An overview of the function and maintenance of sexual reproduction in dikaryotic fungi. *Front. Microbiol.* 9, 503. doi: 10.3389/fmicb.2018.00503

Wang, Q., and Coleman, J. J. (2019). Progress and challenges: Development and implementation of CRISPR/Cas9 technology in filamentous fungi. *Comput. Struct. Biotechnol. J.* 17, 761–769. doi: 10.1016/j.csbj.2019.06.007

Wang, H., Sivonen, K., and Fewer, D. P. (2015b). Genomic insights into the distribution, genetic diversity and evolution of polyketide synthases and nonribosomal peptide synthetases. *Curr. Opin. Genet. Dev.* 35, 79–85. doi: 10.1016/j.gde.2015.10.004

Wang, G., Wang, H., Xiong, X., Chen, S., and Zhang, D. (2015a). Mitochondria thioredoxin's backup role in oxidative stress resistance in *Trichoderma reesei*. *Microbiol. Res.* 171, 32–38. doi: 10.1016/j.micres.2015.01.005

Wang, Q., Zhao, Q., Liu, Q., He, X., Zhong, Y., Qin, Y., et al. (2021). CRISPR/Cas9-mediated genome editing in *Penicillium oxalicum* and *Trichoderma reesei* using 5S rRNA promoter-driven guide RNAs. *Biotechnol. Lett.* 43, 495–502. doi: 10.1007/s10529-020-03024-7

Wilson, D. B. (2009). Cellulases and biofuels. *Curr. Opin. Biotechnol.* 20, 295–299. doi: 10.1016/j.copbio.2009.05.007

Wu, C., Chen, Y., Qiu, Y., Niu, X., Zhu, N., Chen, J., et al. (2020). A simple approach to mediate genome editing in the filamentous fungus *Trichoderma reesei* by CRISPR/Cas9-coupled *in vivo* gRNA transcription. *Biotechnol. Lett.* 42, 1203–1210. doi: 10.1007/s10529-020-02887-0

Wu, B., and Hao, W. (2019). Mitochondrial-encoded endonucleases drive recombination of protein-coding genes in yeast. *Environ. Microbiol.* 21, 4233–4240. doi: 10.1111/1462-2920.14783

Wu, M., Jin, F., Zhang, J., Yang, L., Jiang, D., and Li, G. (2012). Characterization of a novel bipartite double-stranded RNA mycovirus conferring hypovirulence in the phytopathogenic fungus *Botrytis porri*. *J. Virol.* 86, 6605–6619. doi: 10.1128/JVI.00292-12

Xie, J., and Jiang, D. (2014). New insights into mycoviruses and exploration for the biological control of crop fungal diseases. *Annu. Rev. Phytopathol.* 52, 45–68. doi: 10.1146/annurev-phyto-102313-050222

Xiong, Y., Sun, J., and Glass, N. L. (2014). VIB1, a link between glucose signaling and carbon catabolite repression, is essential for plant cell wall degradation by *Neurospora crassa*. *PloS Genet.* 10, e1004500. doi: 10.1371/journal.pgen.1004500

Yadav, A. N., Kour, D., Kaur, T., Devi, R., and Yadav, A. (2022). Endophytic fungal communities and their biotechnological implications for agro-environmental sustainability. *Folia Microbiol. (Praha)* 67, 203–232. doi: 10.1007/s12223-021-00939-0

You, J., Zhou, K., Liu, X., Wu, M., Yang, L., Zhang, J., et al. (2019). Defective RNA of a novel mycovirus with high transmissibility detrimental to biocontrol properties of *Trichoderma* spp. *Microorganisms* 7(11), 507. doi: 10.3390/microorganisms7110507

Yun, S. H., Lee, S. H., So, K. K., Kim, J. M., and Kim, D. H. (2016). Incidence of diverse dsRNA mycoviruses in *Trichoderma* spp. causing green mold disease of shiitake *Lentinula edodes*. *FEMS Microbiol. Lett.* 363(19), fnw220. doi: 10.1093/femsle/fnw220

Zafra, G., and Cortes-Espinosa, D. V. (2015). Biodegradation of polycyclic aromatic hydrocarbons by *Trichoderma* species: a mini review. *Environ. Sci. pollut. Res. Int.* 22, 19426–19433. doi: 10.1007/s11356-015-5602-4

Zeilinger, S., Schmoll, M., Pail, M., Mach, R. L., and Kubicek, C. P. (2003). Nucleosome transactions on the *Hypocrea jecorina* (*Trichoderma reesei*) cellulase promoter *cbh2* associated with cellulase induction. *Mol. Genet. Genomics* 270, 46–55. doi: 10.1007/s00438-003-0895-2

Zhang, H., Xie, J., Fu, Y., Cheng, J., Qu, Z., Zhao, Z., et al. (2020). A 2-kb mycovirus converts a pathogenic fungus into a beneficial endophyte for *Brassica* protection and yield enhancement. *Mol. Plant* 13, 1420–1433. doi: 10.1016/j.molp.2020.08.016

Zhang, T., Zeng, X., Cai, X., Liu, H., and Zeng, Z. (2018). Molecular characterization of a novel double-stranded RNA mycovirus of *Trichoderma asperellum* strain JLM45-3. *Arch. Virol.* 163, 3433–3437. doi: 10.1007/s00705-018-3988-2

Zhou, Y., Wang, Y., Chen, K., Wu, Y., Hu, J., Wei, Y., et al. (2020). Near-complete genomes of two *Trichoderma* species: A resource for biological control of plant pathogens. *Mol. Plant Microbe Interact.* 33, 1036–1039. doi: 10.1094/MPMI-03-20-0076-A

Zou, G., Xiao, M., Chai, S., Zhu, Z., Wang, Y., and Zhou, Z. (2021). Efficient genome editing in filamentous fungi *via* an improved CRISPR-Cas9 ribonucleoprotein method facilitated by chemical reagents. *Microb. Biotechnol.* 14, 2343–2355. doi: 10.1111/1751-7915.13652

Zou, G., and Zhou, Z. (2021). CRISPR/Cas9-mediated genome editing of *Trichoderma reesei*. *Methods Mol. Biol.* 2234, 87–98. doi: 10.1007/978-1-0716-1048-0_8

Chapter 2: RGS4 impacts carbohydrate and siderophore metabolism in *Trichoderma reesei*

Miriam Schalamun[1], Eva Maria Molin[1] and Monika Schmoll[1,2]

[1] AIT Austrian Institute of Technology, Center for Health and Bioresources GmbH, Tulln, Austria

[2] Department of Microbiology and Ecosystem Science, Division of Terrestrial Ecosystem Research, University of Vienna, Vienna, Austria

RGS4 impacts carbohydrate and siderophore metabolism in *Trichoderma reesei*

Miriam Schalamun[1], Eva Maria Molin[1] and Monika Schmoll[1,2*]

Abstract

Background Adaptation to complex, rapidly changing environments is crucial for evolutionary success of fungi. The heterotrimeric G-protein pathway belongs to the most important signaling cascades applied for this task. In *Trichoderma reesei,* enzyme production, growth and secondary metabolism are among the physiological traits influenced by the G-protein pathway in a light dependent manner.

Results Here, we investigated the function of the SNX/H-type regulator of G-protein signaling (RGS) protein RGS4 of *T. reesei*. We show that RGS4 is involved in regulation of cellulase production, growth, asexual development and oxidative stress response in darkness as well as in osmotic stress response in the presence of sodium chloride, particularly in light. Transcriptome analysis revealed regulation of several ribosomal genes, six genes mutated in RutC30 as well as several genes encoding transcription factors and transporters. Importantly, RGS4 positively regulates the siderophore cluster responsible for fusarinine C biosynthesis in light. The respective deletion mutant shows altered growth on nutrient sources related to siderophore production such as ornithine or proline in a BIOLOG phenotype microarray assay. Additionally, growth on storage carbohydrates as well as several intermediates of the D-galactose and D-arabinose catabolic pathway is decreased, predominantly in light.

Conclusions We conclude that RGS4 mainly operates in light and targets plant cell wall degradation, siderophore production and storage compound metabolism in *T. reesei*.

Keywords *Trichoderma reesei*, *Hypocrea jecorina*, Regulator of G-protein signaling, Cellulase, Nutrient sensing, Light response, Storage carbohydrates, Iron homeostasis, Siderophore

Background

Fungi have to adapt to their environment to survive and succeed in competition. Such environmental cues might be the available nutrients, light, defense against competitors or finding a mating partner. Therefore, complex sensing and signaling pathways exist, one of the most important one being heterotrimeric G-protein signaling [1], which profoundly impacts physiological reactions and adaptation to the environment of fungi, from growth and reproduction to secondary metabolism and pathogenicity [2, 3].

The steps of signal transmission from sensing at the plasma membrane to the actual output in terms of enzyme or secondary metabolite production, growth or accumulation of storage compounds and other physiological adaptations are complex and integrate reactions to multiple environmental cues. Thereby, the individual connections from receptors to transmitters to kinases and ultimately transcription factors are only known for very few pathways and mostly only in one model organism. Especially the contributions of RNA- and protein

*Correspondence:
Monika Schmoll
monika.schmoll@univie.ac.at
[1] AIT Austrian Institute of Technology GmbH, Bioresources Unit, Center for Health & Bioresources, Konrad Lorenz Strasse 24, Tulln 3430, Austria
[2] Division of Terrestrial Ecosystem Research, Centre of Microbiology and Ecosystem Science, University of Vienna, Djerassiplatz 1, Vienna 1030, Austria

Schalamun *et al. BMC Genomics* (2023) 24:372

Page 2 of 17

stability, posttranscriptional and posttranslational regulations are often difficult to interpret and integrate into a mechanistic model.

The filamentous ascomycete *Trichoderma reesei* [4, 5] is among the most prolific producers of homologous and heterologous enzymes, especially plant cell wall degrading carbohydrate active enzymes (CAZys), and performance proteins in industry [6, 7]. Recent genome sequencing efforts of the prototypical wild-type QM6a yielded a complete high quality genome [8, 9] and evolutionary analyses revealed an unexpectedly high proportion of CAZyme genes to be acquired to *Trichoderma* through horizontal gene transfer (HGT) [10, 11]. *T. reesei* has become a model organism for plant cell wall degradation in fungi [4, 12], but also for light modulated substrate degradation and enzyme production [13, 14]. The latter phenomenon was investigated in detail in *T. reesei* and connections of light response to the heterotrimeric G-protein pathway, growth, sexual development [15] and secondary metabolism were detected [13, 16, 17]. The light response pathway of *T. reesei* comprises the photoreceptors BLR1 and BLR2, which represent GATA-type transcription factors as well as ENV1, a PAS/LOV domain protein [18, 19]. To achieve its widespread impacts on fungal physiology, diverse signaling pathways are integrated with light response, which involves influences on epigenetic events, posttranscriptional and posttranslational modifications (especially phosphorylation) and protein stability [20, 21].

The function of the G-protein pathway in enzyme biosynthesis was shown to be light dependent [13], which is in agreement with the crucial function of numerous protein kinases, including the cAMP dependent protein kinase A, in light response [22, 23]. The nodes of interaction between the light response pathway and nutrient- and mating partner sensing by the G-protein pathway are still under investigation, although the phosducin-like protein PhLP1 and adenylate cyclase [24] were proposed to play a role in signal integration.

As in most ascomycetes, the G-protein complex in *T. reesei* consists of three alpha-, one beta- and one gamma-subunit [25]. Upon binding of a ligand to a G-protein coupled receptor (GPCRs) the confirmation of the heterotrimeric G-protein complex changes and G-alpha bound GDP is exchanged to GTP [26]. The activated G-proteins dissociate, leading to a free alpha subunit and beta-gamma complex which are now able to transmit downstream signals. The intrinsic GTPase activity of the G-alpha subunits causes GTP hydrolysis to GDP and reassociation of the complex and termination of signal [27, 28].

Regulator of G-protein signaling (RGS) proteins modulate the activity of the heterotrimeric G-protein pathway

by accelerating the GTPase activity of the G-alpha subunits [29, 30]. This GTPase activity leads to deactivation of the G-alpha subunit and hence to termination of the transmitted signal [30–32].

RGS proteins are typically regulated at the level of transcription, epigenetic regulation, expression, localization and stability, but not through binding of a ligand. Thereby, phosphorylation by protein kinase A influences localization and stability of RGS proteins. Additionally, feedback mechanisms due to interactions of RGS proteins with their regulating transcription factors are proposed [33]. Besides the impact of RGS proteins on G-alpha subunits, also functions outside this pathway, including activation of MAPkinase signaling are known [34].

In *T. reesei*, the G-protein signaling cascade is well described with respect to its role in enzyme production with characterizations of the G-alpha, -beta and -gamma subunits and a few GPCRs [35–40]. Additionally, G-protein mediated signaling involves more regulators such as GTPase activating proteins, phosducins and other proteins fine-tuning this pathway [41]. The genome of *T. reesei* comprises seven RGS domain containing proteins, of which four represent RGS proteins and three proteins are related to RGS-domain containing GprK-type GPCRs [42]. All RGS proteins of *T. reesei* contain a RGS box (130 amino acid motif; IPR016137) which is important for G-alpha binding [41].

Generally, the functions of RGS proteins in fungi range from pheromone response, growth and sporulation, pathogenicity [43, 44] and toxin production [45] to nematode trapping by *Athrobotrys* [46]. Due to their central functions in the physiology of fungi, they emerged also as important drug targets [47]. *T. reesei* RGS4 is related to *Aspergillus fumigatus* RgsC which is involved in vegetative growth and development, stress tolerance and virulence [48]. The *A. fumigatus rgsC* deletion mutant shows significantly decreased conidiophore formation and slower colony growth on plates but elevated spore germination on different carbon sources suggesting an involvement in the control of the cAMP/PKA pathway as well as a decreased tolerance to oxidative stress [48]. The down-regulation of gliotoxin (GT) genes and decreased GT production in *A. fumigatus* in mutants lacking *rgsC* might be due to the regulation of a global secondary metabolite regulator LaeA by RgsC [48].

In this study, we aimed to gain insight into the network of nutrient sensing and light response in *T. reesei*. Therefore, we investigated the role of RGS4, as a potential modulator of the activity of one or more of the three G-alpha subunits of *T. reesei*. We show here, that RGS4 impacts the physiology of *T. reesei* on multiple levels and that its major function occurs in light. RGS4 supports

Schalamun *et al. BMC Genomics*   (2023) 24:372

Page 3 of 17

cellulase production, contributes to regulation of growth on several carbon sources and importantly it is required for proper gene regulation targeting iron homeostasis in light.

Results

T. reesei RGS4 is a typical member of the SNX/H group of RGS proteins

In *T. reesei* RGS4 (TrG0496W/TR_65607) is the homolog to *A. nidulans* RgsC and similar to other fungal proteins of this group (Additional file 1, Figure S1). The protein RGS4 contains two transmembrane regions (297–314 and 321–343 aa), a RGS domain (703–843 aa, E-value: 1.65e-19), a coiled coil (1108–1146 aa) and a PhoX homologous (PX) domain (1156–1269 aa, *E*-value 8.55e-25). This domain structure identifies RGS4 as a member of the subfamily of SNX/H RGS proteins [49]. If the Gs-alpha specificity is conserved in fungi, it is likely specific to the G-alpha s subunit GNA3 of *T. reesei* [37]. Hence, deletion of RGS4 may lead to enhanced or prolonged activation of GNA3. Checking available transcriptome data showed that *rgs4* is not significantly regulated in response to light, different carbon sources or during mating [24, 40, 50–52].

The regulation mechanism via phosphorylation is reflected in the amino acid sequence of RGS4 in that it comprises numerous protein kinase C (PKC) and casein kinase II (CKII) phosphorylation sites, both of which are associated also with light response processes [22, 53, 54]. The presence of four cAMP dependent protein

kinase A (PKA) sites supports a potential connection to light signaling, since PKA is known as a priming kinase for casein kinase phosphorylation associated with light response [23]. RGS4 comprises three overlapping sites for PKA and CKII, which suggests a function of PKA as a priming kinase with RGS4, since PKA showed a light dependent function in cellulase regulation as well as generally in gene regulation also in *T. reesei* [55, 56]. However, this connection remains to be confirmed.

RGS4 has its main function in light and is required for proper growth on glucose

We deleted *rgs4* in the QM6a wild-type background, which resulted in viable deletion strains. G-protein signaling influences growth and the transmission of a cellulose related signal which is received via the class XIII GPCRs CSG1 and CSG2 and regulated by light in *T. reesei* [35]. Therefore, we analyzed hyphal apical extension rates of Δ*rgs4* on rich medium (3% malt extract, MEX) versus minimal medium (MA-medium) complemented with carboxymethyl cellulose (CMC) or glucose as the carbon source in constant light and constant darkness (Fig. 1). On malt extract we did not see any difference (Fig. 1A – C), whereas the deletion of *rgs4* led to a significantly decreased colony size on cellulose and glucose in light. In darkness, a small decrease (to 90%) in apical extension of Δ*rgs4* was detected. In light, colony sizes reached 70 to 80% of the wildtype on glucose or cellulose, respectively (Fig. 1D, E).
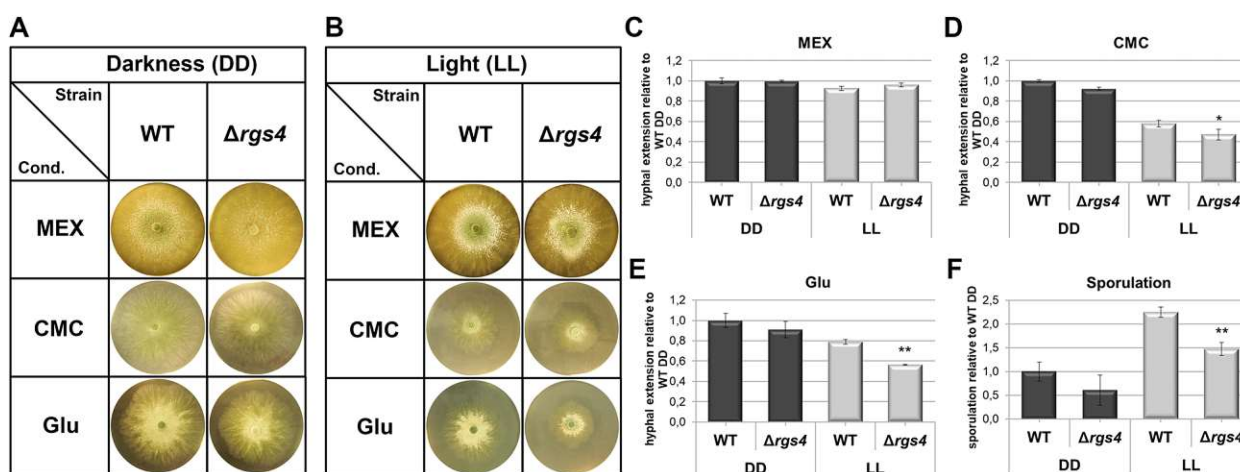
Fig. 1 Influence of RGS4 on growth and asexual development. **A-E** Hyphal extension of wild-type (QM6a) and Δ*rgs4* on 3% malt extract (MEX) and Mandels-Adreotti minimal (MA) medium with 1% glucose and 1% carboxymethyl cellulose (CMC) as carbon source after 48 h in constant darkness (DD) and constant light (LL; 1700 lx). **F** Average sporulation measured after 48 h at 28 °C in DD and LL on 3% MEX. Measurements were taken from 3 biological replicates and statistical significance was calculated for the respective light condition (DD or LL) between WT and mutant using Student's T-test. * = *p*-value < 0.05, ** = *p*-value < 0.01)

Schalamun *et al. BMC Genomics*   (2023) 24:372

Page 4 of 17

RGS4 is involved in regulation of asexual development

It is well known that the cAMP and the heterotrimeric G-protein pathway play a crucial role in sporulation in fungi [57, 58]. In *T. reesei* QM6a sporulation is enhanced in light compared to dark grown cultures. We found that deletion of *rgs4* led to significantly decreased sporulation in light (Fig. 1F), whereas, in darkness, a negative trend was observed. We conclude that RGS4 is required for normal sporulation in *T. reesei*.

RGS4 is required for proper stress response

For the RGS4 homologue in *A. fumigatus*, RgsC, hypersensitivity to oxidative stress on menadione, a natural organic compound that exerts its toxicity through the generation of reactive oxygen species (ROS), and reduced

tolerance to the presence of H_2O_2 or paraquat was shown [48]. Therefore, we were interested in the role of RGS4 in oxidative stress response in *T. reesei* and found a significant decrease ($p < 0.05$) in resistance to menadione. In Δ*rgs4* the hyphal apical extension was significantly decreased in light and darkness compared to wild-type after 96 h on MA-CMC plates supplemented with 0.25 mM menadione (Fig. 2A). Since the control without menadione (Fig. 1D) did not show a significant growth defect under these conditions in darkness, RGS4 is concluded to contribute to resistance against oxidative stress in darkness. In light, the growth defect of Δ*rgs4* upon growth in the presence of menadione is in the range of the growth defect without oxidative stress (around 80% in both cases; Fig. 1D). Consequently, if there is
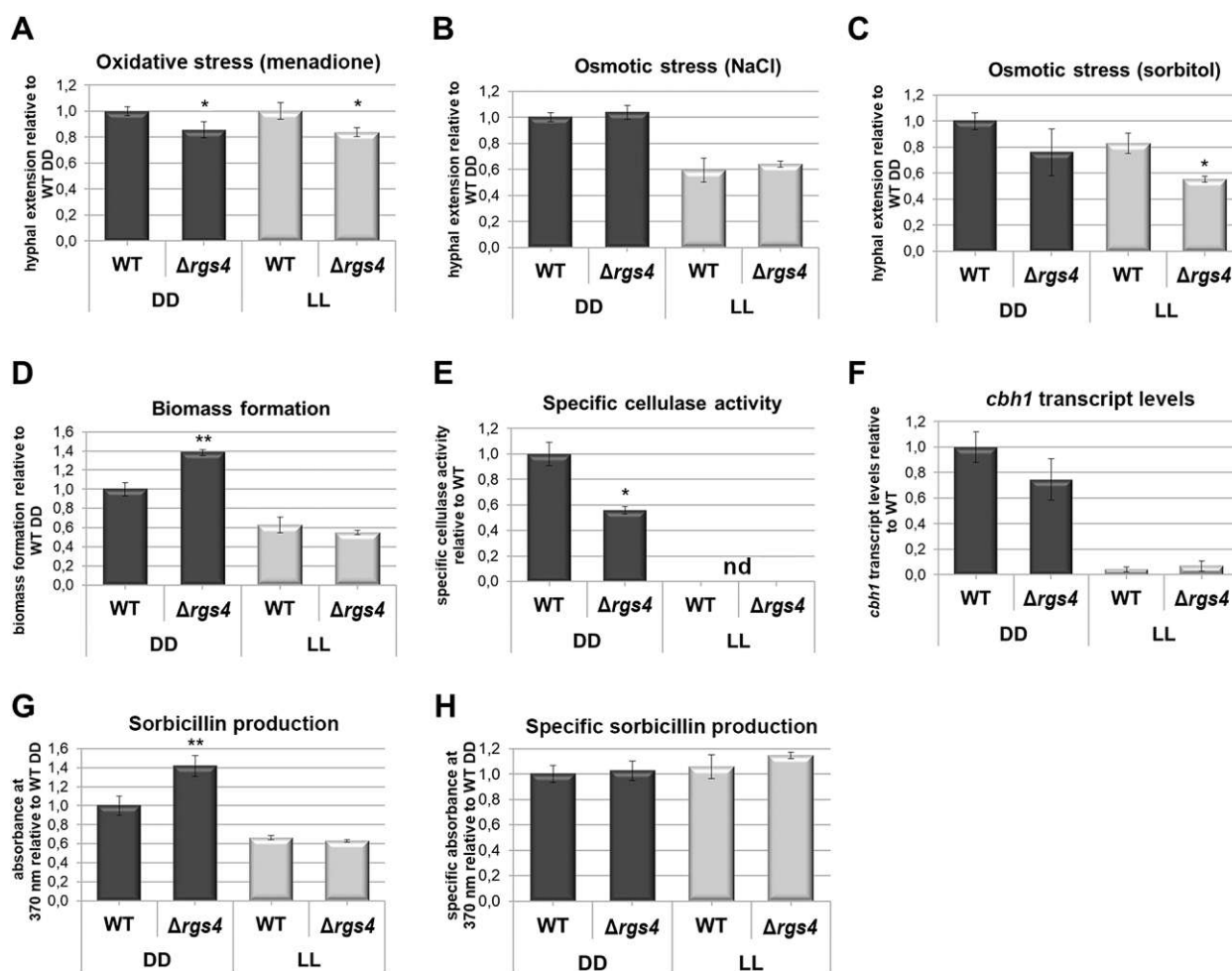
Fig. 2 Relevance of RGS4 for stress response, growth, enzyme production and secondary metabolite biosynthesis. **A**-**C** Average hyphal extension after 96 h at 28 °C in constant darkness (DD) and light (LL) on MA-medium with 1% cellulose (CMC) as carbon source and supplemented with **A** 0.25 mM menadione or **B** 1 M NaCl or **C** 1 M sorbitol to test for reaction to oxidative or osmotic stress respectively. **D**-**H** Liquid cultivation at 28 °C after 96 h in constant light (LL) and darkness (DD). **D** Average biomass formation, **E** specific cellulase activity, **F** *cbh1* transcript levels (RT-qPCR) and **G** sorbicillin production represented as absorbances at 370 nm [59]. **H** Specific sorbicillin abundance in supernatant related to biomass formation upon growth on 1% cellulose. Measurements were taken from 3 biological replicates and statistical significance was calculated for the respective light condition (DD or LL) between WT and mutant using Student's T-test.. * = *p*-value < 0.05)

a contribution of RGS4 to oxidative stress response in light, it is rather minor.

In *T. reesei* an involvement in sensitivity to osmotic stress by the G-protein pathway was shown previously [38]. To test the role of RGS4 we measured hyphal extension rates after 96 h on MA-CMC plates supplemented with 1 M NaCl or 1 M sorbitol. Interestingly the deletion of *rgs4* caused increased sensitivity to sorbitol but not to NaCl in light (Fig. 2B, C). Comparison with growth in the absence of osmotic stress on CMC (Fig. 1D) showed a more severe growth defect of Δ*rgs4* in the presence of 1 M sorbitol in both light and darkness. In case of osmotic stress applied by 1 M NaCl, the growth defect seen in the control (Fig. 1D) without stress is alleviated upon deletion of *rgs4*. Hence RGS4 is involved in the reaction of *T. reesei* to osmotic stress, particularly in the presence of NaCl (salt stress) in light.

RGS4 impacts biomass formation and cellulase activity in constant darkness

Environmental sensing in microbes is essential for an optimal distribution of resources between growth (biomass formation), enzyme production and biosynthesis of secondary metabolites, among others. Therefore, we asked whether RGS4 contributes to one or more of these tasks. Upon growth in liquid media with cellulose in light, no difference in growth was observed, whereas in darkness biomass formation of Δ*rgs4* significantly increased by almost 40% (Fig. 2D). Specific cellulase activity was below the sensitivity limit for all samples in light, indicating that the deletion of *rgs4* does not alleviate the block of cellulase formation in light. For dark grown cultures, we found that RGS4 is required for high level cellulase formation (Fig. 2E). Accordingly, transcript abundance of the major cellobiohydrolase *cbh1/cel7a* showed a negative trend in darkness (*p*-value 0.108) (Fig. 2F).

Trichoderma reesei secretes sorbicillin derivates which are responsible for the characteristic yellow color of cultivation supernatants and plates [60, 61]. Since production of these pigments as well as regulation of the responsible SOR cluster is carbon source and light dependent [16], we tested whether RGS4 might be involved in this regulation. We found that deletion of *rgs4* increased the amount of yellow pigment in darkness, however, this increase rather can be explained by the increased biomass formation under these conditions (Fig. 2G, H). Our transcriptome analysis showed that all seven genes of the sorbicillin cluster [16, 36, 60], including the transcription factors *ypr1* (TrE0665C/TR_102499) and *ypr2* (TrE0663W/TR_102497), were up-regulated between 1.4- and 2.3-fold in Δ*rgs4* (see below). But this can only be considered a positive trend, because the threshold set for statistical significance was mostly not met (padj < 0.05).

This result is hence in agreement with the lack of alteration of yellow pigment formation in Δ*rgs4.*

RGS4 impacts gene regulation mainly in light

Phenotypic analyses revealed that RGS4 differentially affects physiology of *T. reesei* in light and darkness. Moreover, clear light dependent effects were shown for the influence of the heterotrimeric G-protein signaling pathway on regulation of plant cell wall degradation [13]. We were hence interested which role RGS4 plays in this mechanism connecting light response and reaction to available nutrients. Therefore, we cultivated Δ*rgs4* on minimal medium with cellulose as carbon source in constant light and constant darkness and assessed alterations in gene expression compared to the wild-type in both conditions.

In Δ*rgs4* we found a total of 210 genes significantly differentially regulated (> 1.5-fold, padj < 0.05) of which 16 genes were up- and 48 down-regulated in darkness, and 34 up- and 112 down-regulated in light (Fig. 3A). Of those, three genes were regulated both in light and darkness by RGS4: a SANT domain transcriptional regulator TrB0388C/TR_4124 potentially involved in chromatin modification, which is significantly up-regulated on cellulose [35] and strongly down-regulated in light and a mutant lacking the sorbicillin transcription factor YPR2 [62] in darkness; a duf341 domain protein TrC1432W/TR_59368 with a comparable regulation pattern to TrB0388C/TR_4124 in light and on cellulose and an unknown unique secreted protein TrF0745W/ TR_121883, which shows only minor light dependent regulation but an up-regulation on cellulose versus repressing/non inducing carbon sources [35].

For six of the differentially regulated genes, phosphorylation association with induction of plant cell wall degrading enzymes was detected [63]. They include genes encoding two predicted amino acid transporters (TrB0212C/TR_123718 up- and TrA0392C/TR_47175 down-regulated in light), a predicted plasma membrane H + ATPase (TrA2081W/TR_76238 up-regulated in light) and a ribosomal protein (TrB0953C/TR_47795 down-regulated in light). Additionally, four genes which are mutated in RutC30 (TrF004C/TR_79726, TrF0028C/ TR_109211 and TrF0013C/TR_43418) including a muconate cycloisomerase gene (TrC0885C/TR_55887) showing regulation specific to cellulase inducing conditions [35] and two genes mutated in QM9123 (TrC0611W/ TR_2439 and TrD0796W/TR_43191) were found among the genes down-regulated by RGS4 (Additional file 2).

In light, RGS4 is involved in regulation of transcript abundance of ribosomal protein genes. There were six ribosomal protein encoding genes down-regulated around twofold in the deletion mutant in light. Among
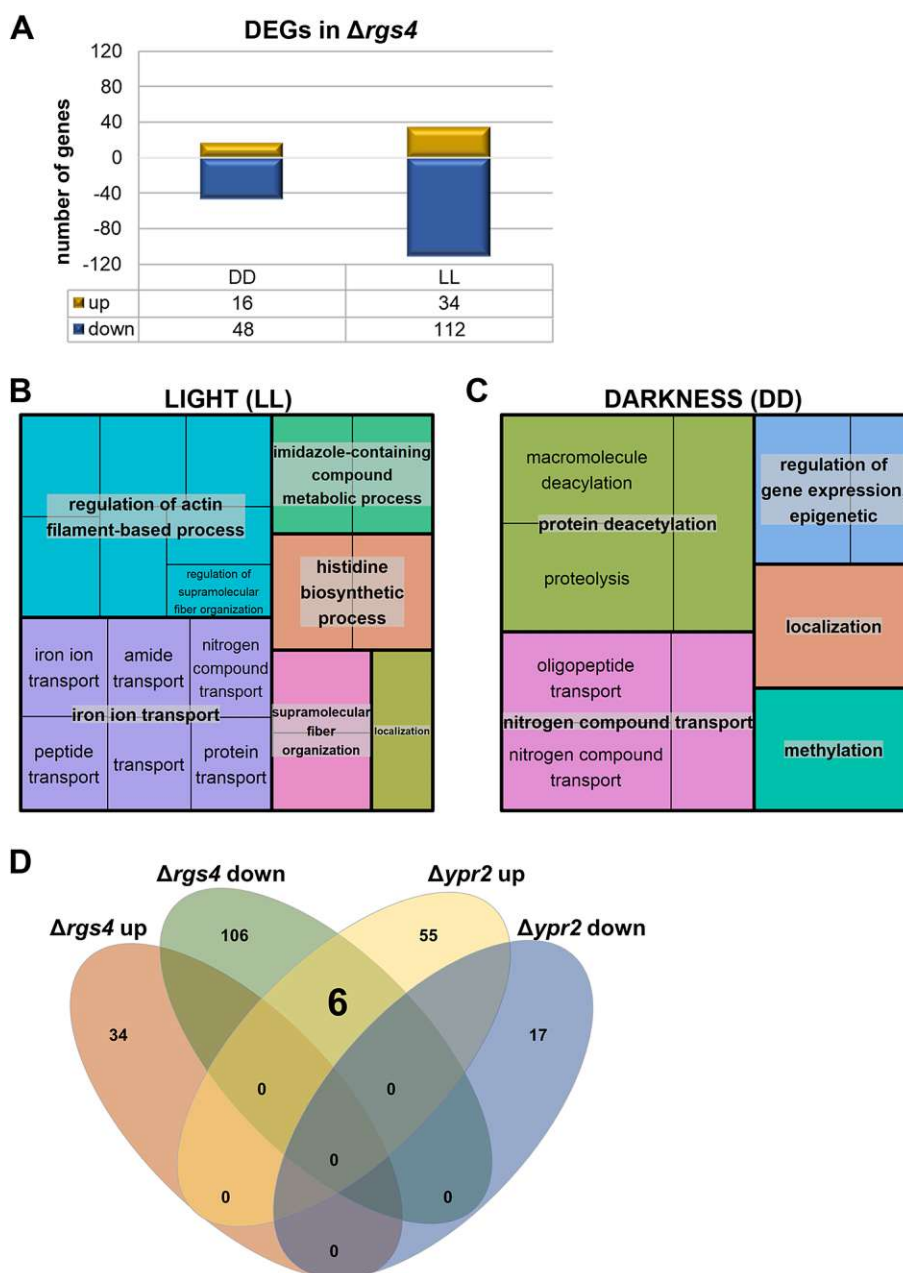
Fig. 3 Gene regulation by RGS4 on cellulose in light and darkness. **A** Number of differentially expressed genes (DEGs) in Δ*rgs4*. **B**, **C** GO enrichment of DEGs visualized with REVIGO. **D** Number and overlap of DEGs in Δ*rgs4* and Δ*ypr2* in light

which there were two 60S ribosomal protein genes *rla1* (TrB1847W/TR_123850) and *rla2* (TrD0208W/TR_123202), two potential small ribosomal protein genes *rps21* (TrB0594C/TR_78233) and *rps28* (TrC1311W/TR_106039), a potential mitochondrial ribosomal protein gene (TrC1283C/TR_121219) and a ribosomal protein gene TrB0953C/TR_47795. Additionally, we found a small nuclear ribonucleoprotein

(snRNP) (TrA2076W/TR_43225) and a snRNA associated protein TrA1443W/TR_76073.

In constant darkness there are less genes differentially regulated in Δ*rgs4* as compared to in constant light but among those, categories involved in transport and localization stand out and can also be observed in the functional enrichment analysis (Fig. 3B, C). Out of 16 up-regulated genes in darkness, seven are transporters (also

Schalamun *et al. BMC Genomics*   (2023) 24:372

Page 7 of 17

permeases or transferases) of which three are annotated as glutathione S-transferases (GST) [64]. Glutathione transferases belong to a protein family conserved across plants and animals, of detoxifying enzymes which are able to catalyze the conjugation of glutathione to form more soluble non-toxic compounds [65]. The number of GSTs in fungi correlates with the ability to degrade complex organic compounds and *T. reesei* was listed with the second highest number of GST genes present in the genome among fungi [66]. Among the down-regulated genes in darkness are two glycoside hydrolase genes (TrA0299W/TR_47268 (*bgl3i*) and TrF0168W/TR_65162) which is likely to contribute to the lower specific cellulase activity in Δ*rgs4*.

RGS4 regulates a secondary metabolite cluster associated with siderophore production

Among the down-regulated genes in light we found all six genes of a siderophore biosynthetic cluster (Fig. 4A, B): TrE0011C/TR_71005, TrE0012W/TR_112590, TrE0013C/TR_71010, TrE0014C/TR_82628, TrE0015W/TR_6085 and TrE0016W/TR_71008 (3.7 – 6.4-fold significantly down-regulated; Fig. 4C-H). TrE0015W is the homologue to *A. fumigatus* sidH, a mevalonyl CoA dehydratase, annotated in *T.reesei* as SID8, followed by a transacylase, SID6 (TrE0014C) and the NRPS siderophore synthase SID4 (TrE0011C) in the biosynthetic pathway. The genome of *T. reesei* does not comprise an N^2-transacetylase gene, which would be responsible for acetylation of fusarinine C to triacetylfusarinine C (TAFC) (*A. fumigatus* sidG). However, for *A. fumigatus,* the production of fusarinine C seems to be sufficient as the major siderophore [67]. Additionally, also a siderophore transporter (TrE0016W) and an MDR type ABC transporter (TrE0013C) belong to this cluster and were found to be down-regulated as well as the iron transporter TrD0323C/TR_38812, not member of this cluster but indicative of an involvement of RGS4 in iron transport/synthesis in light, which is supported by the enriched functional category "iron transport" as well (Fig. 3B). In support of this hypothesis, also one of the multicopper oxidases of the reductive iron transport system, Fet3b (TrD0040C/TR_5119) was up-regulated in

light. Regulation of an RGS protein in association with iron homeostasis has been shown for mammalian RGS19, which possesses a consensus iron-sulfur binding motif (CXXCXXC) [68, 69]. However, such a motif is not present in *T. reesei* RGS4.

On cellulose, already previously a light dependent regulation of this siderophore cluster upon growth on cellulose was found in the *ypr2* deletion mutant *in T. reesei* [62]. Therefore, we were interested if there is an overlap in regulatory targets between RGS4 and YPR2. YPR2 is a transcription factor located in the sorbicillin (SOR) cluster [60] and when deleted, the entire siderophore cluster was up-regulated in light, which contrasts with Δ*rgs4* where the siderophore cluster was down-regulated in light (Figs. 3D and 4C-H) [62]. Nevertheless, we did not detect mutual regulation of *ypr2* by RGS4 or vice versa. Interestingly, the six genes of the siderophore cluster were the only ones up-regulated in Δ*ypr2* and down-regulated in Δ*rgs4* in light (Fig. 3D). Consequently, the regulatory pathways involving YPR2 and RGS4 act in opposite directions concerning siderophore regulation.

To support the relevance of RGS4 for siderophore production we analyzed their presence in the supernatants of cellulose grown cultures. However, we saw that siderophore production upon growth on cellulose appears to be only slightly above the detection limit of the method and while we did observe a negative trend for Δ*rgs4* in light (data not shown), we consider gene regulation and growth patterns as more relevant evidence (see below).

RGS4 impacts growth on diverse carbon sources

As our transcriptome analysis indicated that RGS4 is involved in regulation of metabolism, we asked whether this impact extends to regulation of growth. We therefore applied the BIOLOG FF Phenotype microarray system and tested growth on 95 carbon sources in constant light and constant darkness (Additional file 3). Measurements were taken from 72 to 144 h to cover peak biomass values for most of the carbon sources. Results were considered relevant if at least two consecutive measurements

(See figure on next page.)

Fig. 4 Regulation of a siderophore biosynthetic cluster by RGS4. **A** Schematic representation of the siderophore cluster in *T. reesei*. Model designations below the scheme taken from http://genome.jgi.doe.gov/Trire2/Trire2.home.html and if annotated, *T. reesei* protein names from Druzhinina et al. 2016 [64] and homologues names for *A. fumigatus* from https://fungidb.org/fungidb/app. NRPS (non-ribosomal peptide synthase), SE (siderophore esterase), ABC (ABC transporter), AT (acetyltransferase), Co (enoyl CoA hydratase), TRA (siderophore transporter). SID4/TrE0011C was former also known as TEX20. **B** Schematic representation of siderophore pathway and involved enzymes in *T. reesei*. Carbon sources analyzed by the BIOLOG Phenotype FF microarrays are given in black letters in grey boxes, compounds not analyzed are written in white. Downward pointing triangles indicate decreased growth in Δ*rgs4*, upwards pointing triangles indicate increased growth. Yellow triangles show growth differences in light (LL). Pathways and enzymes were taken from KEGG [64, 70, 71]. Model designations with the gene names taken from http://genome.jgi.doe.gov/Trire2/Trire2.home.html and if annotated, *T. reesei* protein names from Druzhinina et al. 2016 [64] and homologues names for *A. fumigatus* from https://fungidb.org/fungidb/app. **C-H** LogCPM normalized counts of siderophore cluster genes in wild-type and Δ*rgs4* in constant light (LL). Error bars show standard deviations. Statistical significance was calculated using Student's T-test. *=*p*-value < 0.05

Schalamun *et al. BMC Genomics*   (2023) 24:372

Page 8 of 17

Fig. 4 (See legend on previous page.)

Schalamun *et al. BMC Genomics*   (2023) 24:372

Page 9 of 17
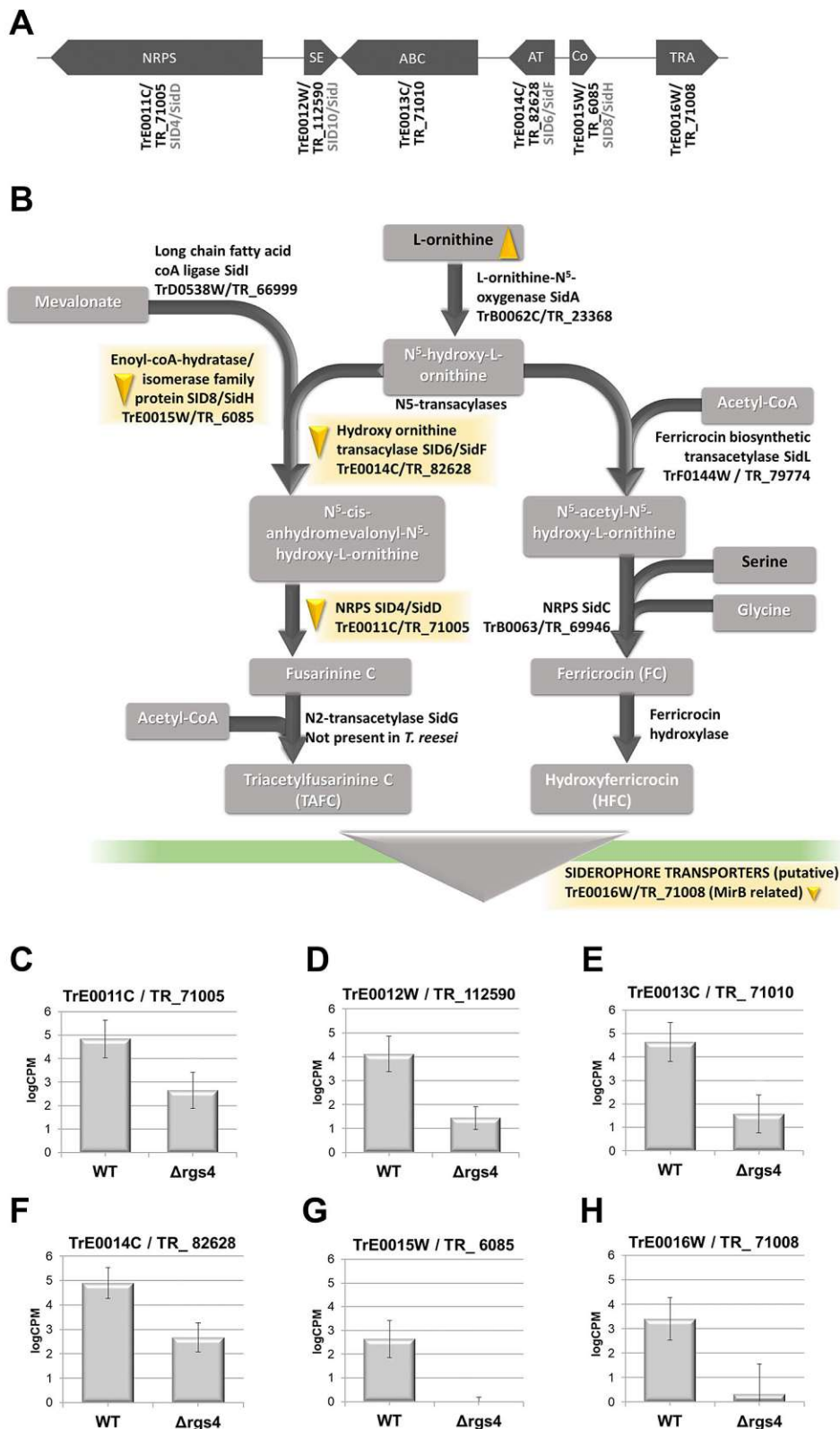
showed statistically significant differences to the wild-type (*p*-value < 0.05).

We found that growth on several storage carbohydrates is decreased in Δ*rgs4*. Growth defects in Δ*rgs4* were observed on dextrin, glycogen and trehalose, as is growth on the intermediate maltose, mostly in light upon lack of RGS4 (Fig. 5A-D). This finding suggests, that RGS4 promotes carbon storage degradation for increasing its biomass production. The decreased growth may hence reflect rerouting of these resources to other metabolic needs.

The observed growth patterns further suggest that RGS4 is involved in regulation of D-xylose, L-arabinose and D-galactose catabolism, as Δ*rgs4* grows more slowly on several intermediate carbohydrates of this pathway (Fig. 5A, E–G). In particular, growth on xylitol decreased in the dark, but increased in light (Fig. 5E), reflecting a light dependent regulation of the involved pathways by RGS4. Interestingly, this is not the case for D-xylose (Fig. 5F), which is converted to xylitol (Fig. 5A), as this shows the opposite effect in light (Fig. 5F). Consequently, we assume that due to the function of RGS4, xylitol conversion is promoted and upon deletion of *rgs4*, this intermediate is available for biomass production. In case of D-galactose, L-arabitol and D-mannitol (Fig. 5A), decreased growth was observed in both darkness and light, hinting at a more general effect of RGS4 targeting growth on these carbon sources.

Screening the transcriptome data for correlations of gene regulation with these growth patterns, we did not find regulations of the genes involved in the degradation pathways of these carbon sources. Consequently, we assume an impact of RGS4 is likely not at the transcriptional level but rather on a posttranscriptional level or that the targeted pathways are not operative or regulated upon growth on cellulose.

RGS4 impacts growth on siderophore related carbon sources

The most interesting finding of the BIOLOG assay was the detection of carbon source utilization patterns supporting regulation of siderophore biosynthesis and indirectly iron homeostasis by RGS4 (Fig. 6). Importantly,

growth on L-ornithine, the central precursor of siderophores, decreased in light, but not in darkness (Fig. 6A). Also, growth on L-proline decreased in light (Fig. 6B), although growth on glutamate only decreased in darkness. Since growth on putrescine, which is the intermediate in the metabolic pathway yielding polyamines, did not change in Δ*rgs4*, we assume that lack of *rgs4* decreases the consumption of proline, which may free resources for biomass production on ornithine. As an organic compound, the amino acid proline can be used as carbon and nitrogen source. In *A. fumigatus*, deletion of *rgsC*, the homologue of *rgs4*, resulted in restricted growth with proline as nitrogen source [48]. This is in agreement with our data, considering a role of proline as carbon source as well.

Additionally, decrease of transcript abundance and hence likely decrease of expression of the siderophore biosynthetic gene cluster and its operation in light also decreases conversion of ornithine for their production, again liberating resources for growth (Fig. 6C).

Inspection of the assay plates at the end of the experiment did not indicate significant differences in sporulation on one of the specific carbon sources tested.

Discussion
It is crucial for fungi to sense and quickly adapt to their environment which relies on efficient signal transmission pathways. One of those pathways involves heterotrimeric G-protein signaling which is conserved in eukaryotes with its main components: the heterotrimeric G-proteins, G-protein coupled receptors (GPCRs) and regulators of G-protein signaling (RGS) [3, 74]. In *T. reesei*, roles of the G-protein α, β and γ subunits and a few GPCRs in the regulation of carbon or secondary metabolism in a light dependent manner was previously described [36–38, 40, 51]. RGSs on the other hand are still missing in this picture in *T. reesei* although they play an important role in the termination of signal from the Gα subunits. RGS proteins, just as G-proteins themselves, play important roles in the regulation of basic fungal processes such as vegetative growth, conidiation, secondary metabolite production and mating [41, 43]. In *A. fumigatus* the RGS proteins have been described in more details over the

(See figure on next page.)

Fig. 5 Biomass formation of Δ*rgs4* versus WT on carbon sources related to storage and sugar catabolism. **A** Schematic representation of carbohydrate conversion pathways and involved enzymes. Carbon sources analyzed by the BIOLOG Phenotype FF microarrays are given in black letters in grey boxes, compounds not analyzed are written in white. Downwards pointing triangles indicate decreased growth, upwards pointing triangles indicate increased growth. Blue triangles stand for growth in darkness (DD), while yellow triangles show growth differences in light (LL). Pathways and enzymes were taken from KEGG [71]. Gene model designations taken from http://genome.jgi.doe.gov/Trire2/Trire2.home.html and if annotated, *T. reesei* protein names from Druzhinina et al. 2016 [64] and homologues names for *A. fumigatus* from https://fungidb.org/fungidb/app. **B-D** Growth patterns of WT and Δ*rgs4* on storage related carbon sources i. e. **B** glycogen, **C** D-trehalose and **D** maltose in constant light (LL) or constant darkness (DD) as revealed by the BIOLOG system. **E–G** Growth patterns of WT and Δ*rgs4* on carbon sources representing intermediates of D-galactose, D-xylose or L-arabinose catabolism, i.e. **E** xylitol, **F** D-xylose or **G** D-mannitol. Error bars indicate standard deviation of three biological replicates. Asterisks show statistical significance of the difference between WT and Δ*rgs4* at a given time point (* = *p*-value < 0.05, ** = *p*-value < 0.01)

Fig. 5 (See legend on previous page.)

Fig. 6 Biomass formation of Δ*rgs4* versus WT on carbon sources related to ornithine metabolism. **A**, **B** Growth patterns of WT and Δ*rgs4* on siderophore precursor (**A**) ornithine and amino acid (**B**) proline in constant light (LL) or constant darkness (DD) as revealed by the BIOLOG system. Error bars indicate standard deviation of three biological replicates. Asterisks show statistical significance of the difference between WT and Δ*rgs4* at a given time point (* = *p*-value < 0.05, ** = *p*-value < 0.01). **C** Schematic representation of conversion pathways and involved enzymes. Carbon sources analyzed by the BIOLOG Phenotype FF microarrays are given in black letters in grey boxes, compounds not analyzed are written in white. Downwards pointing triangles indicate decreased growth, upwards pointing triangles indicate increased growth; blue triangles stand for growth in darkness (DD), while yellow triangles show growth differences in light (LL). Pathways and enzymes are taken from KEGG [71–73]

last years including *rgsC* which is involved in growth and development, tolerance to oxidative stress, gliotoxin production, expression of transporters and nutrient sensing [48]. To better understand the roles of RGS proteins specifically in light dependent regulation in *T. reesei* the current study provides insights into physiological changes and differential gene expression of RGS4 (Fig. 7). One of the most interesting findings of this study is the difference of the regulatory targets of RGS4 in light versus darkness, which was not shown before and agrees with the light dependent role of the G-protein pathway shown previously [13, 37, 38].

In a previous study, a light independent regulation of growth by the Gα subunit 1 (*gna1*) on solid media with glucose as carbon source can be seen (slightly decreased

hyphal extension of Δ*gna1* on glucose) [38]. Interestingly for Δ*rgs4* the effect is stronger in light and abolished in darkness indicating that RGS4 is light dependently required for the transmission of a glucose signal. In the same study [38] a light dependent involvement of GNA1 in the reaction to oxidative stress by menadione was shown. In constant light, deletion of *rgs4* caused a similar phenotype with decreased growth due to menadione, like the constitutive activation of GNA1, whereas in darkness we saw opposite effects: increased tolerance in both mutants of GNA1 and decreased tolerance in Δ*rgs4*. The deletion of an RGS protein should increase the signal strength of a Gα subunit because the intrinsic GTPase activity is not accelerated, however, in *T. reesei* there are four different free RGS proteins and it is not yet known

Schalamun *et al. BMC Genomics*   (2023) 24:372

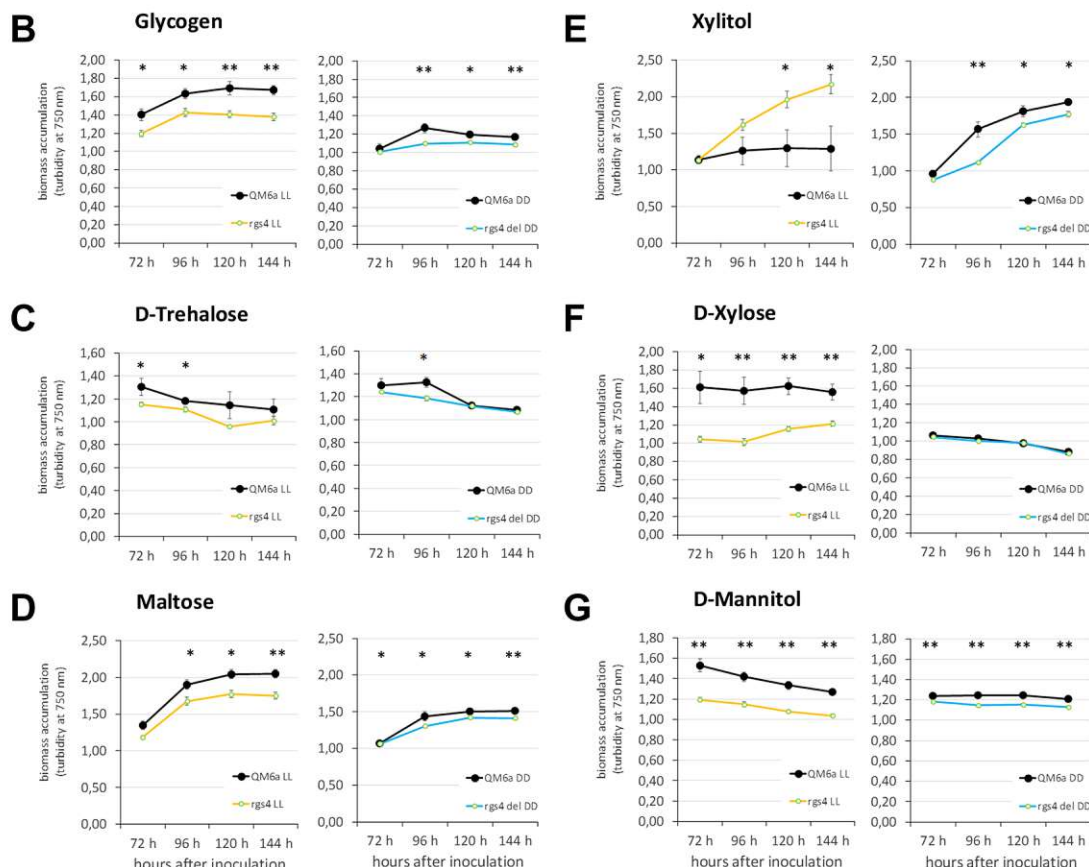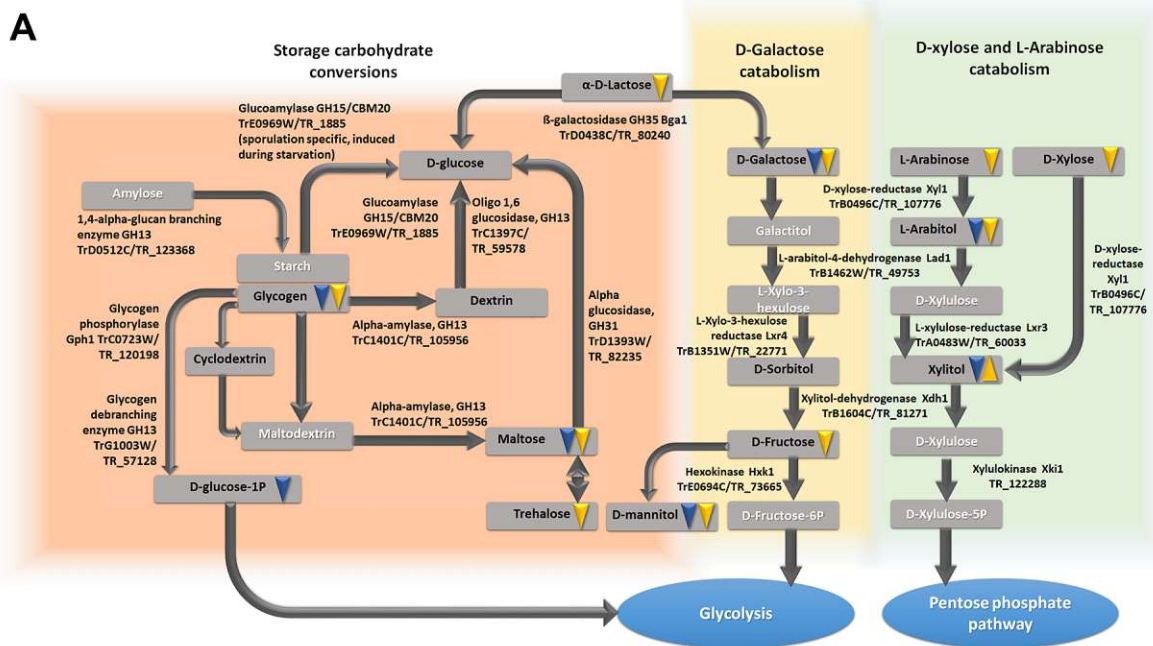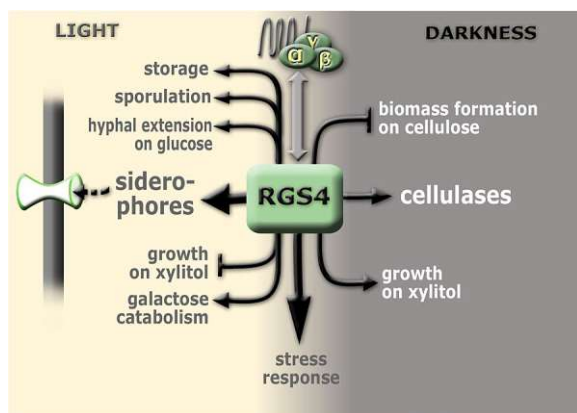Page 12 of 17

Fig. 7 Schematic representation of the regulatory role of RGS4 in light and darkness. In light, *rgs4* is required for normal expression of the siderophore cluster producing fusarinine C and for expression of (iron) transporter genes. Furthermore, *rgs4* is positively involved in growth on storage- and galactose metabolism related carbon sources, sporulation and hyphal extension on glucose but negatively effects growth on xylitol as carbon source. In darkness on the other hand *rgs4* positively influences growth on xylitol and specific cellulase activity but decreases biomass formation on cellulose. In both, light and darkness, *rgs4* contributes to resistance against oxidative stress

whether their functions are redundant and how specific their interaction with the respective G-alpha subunits is. Considering the domain composition of RGS4, it would be predicted to act on the G-alpha s protein GNA3 rather than on GNA1 [49]. If this would be the case, strains lacking *rgs4* should have a phenotype resembling that of a constitutive activation of GNA3 (GNA3QL), which was reported earlier [37]. However, despite the confirmed function of RGS4 in cellulase regulation, the strong increase in transcript levels of the major cellulolytic enzyme encoding gene *cbh1* in light, which was earlier observed for GNA3QL [37] was not observed in Δ*rgs4.* This finding either suggests that the role of RGS protein in fungi is not entirely conserved or rather that investigation of G-protein function in the background of the high-cellulase random mutant QM9414 and its derivative TU-6 may be slightly different from that in the wild-type QM6a.

A light and carbon source dependent involvement of a GPCR, i.e. *gpr8,* in regulation of secondary metabolism was investigated previously, showing a decrease in transcript levels of SOR cluster genes and secondary metabolites produced in darkness on cellulose [36]. In part, the regulation patterns of GPR8 overlap with those of YPR2, a transcription factor located in the SOR cluster, but targeting a broad range of secondary metabolite biosynthesis genes [62]. Interestingly, in darkness two thirds of all of the genes differentially regulated in Δ*rgs4* are also differentially regulated in Δ*ypr2* but only six genes overlap

in light, which all belong to the same siderophore cluster. This indicates a contribution of RGS4 in the initiation of a cascade that involves YPR2. The effect on siderophore regulation in light is opposite in both deletion mutants: RGS4 is required for siderophore gene cluster expression and YPR2 down regulates the cluster. Until now no direct correlation between RGS and iron transport has been shown in fungi, but in HELA cells the role of a RGS protein in the signaling cascade of iron chelation was shown [68].

Iron is essential for all eukaryotes and abundant on earth, but in an aerobic environment usually present in its oxidized form of ferric oxide hydrate complexes (Fe_2O_3 x nH_2O) which has a low solubility of 10^{-9} to 10^{-18} M at neutral pH [67, 75]. Therefore, microbes had to develop different strategies for efficient iron uptake. One such a mechanism is siderophore-mediated Fe^{3+} uptake. Siderophores are low molecular mass iron chelators which help with the transport and storage of iron in the cell [76]. *A. fumigatus* acquires extracellular iron by a mechanism called reductive iron assimilation (RIA) [70]. During lack of extracellular and intracellular siderophores, *A. fumigatus* operates the RIA pathway, where ferric iron gets reduced to its ferrous form and is taken up by the FtrA/FetC complex [77, 78]. Defects in the RIA pathway cause an increase of siderophore production in *A. fumigatus* [79]. The genome of *T. reesei* comprises two Ftr1/Fet3 pairs, which are each located in vicinity to each other [62]. The respective gene pairs encoding FET3a/FTR1a and FET3b/FTR1b are co-regulated and *fet3a/ftr1a* show increased transcript levels in light on cellulose, while *fet3b/ftr1b* transcript abundance is decreased in light [62]. These data indicate that the two distinct gene pairs involved in the reductive iron uptake system in *T. reesei* confer light dependent specificity of this process, which likely also influence siderophore regulation. In our study, only *fet3b* was up-regulated in light in Δ*rgs4.* We conclude that an influence of RGS4 on siderophore production and precursor metabolism in light but not in darkness is in agreement with the hypothesis of a light dependent relevance of iron as a nutrient, but also as a signal.

Phosphorylation is considered the currency of signal transduction cascades [80]. In recent years it was confirmed that fungi react to the presence of plant cell wall carbohydrates with phosphorylation of diverse proteins, including those within signal transduction cascades [81, 82]. This response happens within minutes of recognition of altered environmental conditions and is both transient and dependent on the sensed carbon source [81, 82]. Although RGS4 does not regulate protein kinases at the transcriptional level, we found several genes encoding proteins specifically phosphorylated upon detection of

Schalamun *et al. BMC Genomics*   (2023) 24:372

Page 13 of 17

residues associated with plant cell wall degradation [63] among the targets of RGS4.

As generally with phosphorylation [83], this posttranslational modification of transporters may impact activity, stability or conformation/sensitivity in dependence of the substrate to be transported. Interestingly, the *S. cerevisiae* homologue of one of the predicted amino acid transporters (TrA0390C/

TR_47175), Avt3p, is phosphorylated by the kinase Atg1p [84], hence supporting a conserved relevance of this modification. Considering that for only around 8% of predicted proteins of *T. reesei* phosphorylation (of one or more peptides) was detected [63], the finding of six genes with plant cell wall degradation associated phosphorylation among the targets of RGS4 only in light (3 up-regulated, 3 down-regulated) is remarkable.

With functions in stress response and regulation of the metabolism of storage carbohydrates, RGS4 modulates physiologically crucial mechanisms intimately associated with survival. Moreover, in both cases a role in reaction to changing or deteriorating environmental conditions is implicated by this function and as with other functions of RGS4, it is connected to a light dependent relevance. The decreased growth upon degradation of extracellular glycogen, dextrin or trehalose hints to a lower expression or secretion of the respective enzymes and a function of RGS4 balancing growth with storage of carbohydrates in response to the environment.

Materials and methods
Strains and cultivation conditions
For the genotype of all strains used in this study see Table 1. The wild-type strain referred to in this study is *T. reesei* QM6a [85] which was used as a parental strain to construct the recombinant strain QM6aΔ*rgs4.*

Liquid cultivation was performed in Mandels Adreotti minimal medium (MA medium; [87]) containing 1% (w/v) microcrystalline cellulose (Alfa Aesar, Karlsruhe, Germany) and 0.1% (w/v) peptone to induce germination in constant dark and constant light (1700 lx) for 96 h at 200 rpm and 28° C. Strains for cultivation (QM6a and Δ*rgs4*) were revived from glycerol stocks and then

grown on 3% (w/v) malt extract agar (MEX) for 14 days in constant darkness which prevents interference of circadian rhythmicity with the analyses. 10^9 conidia/L were used for the inoculation of 50 mL MA medium in shake flasks in triplicates. For harvest in darkness a very low red safety light (darkroom lamp, Philips PF712E, red, 15W) was used.

Phenotypic plate assays were analyzed after 48 h at 28° C under constant light (1700 lx) and constant darkness. Sporulation was measured in triplicates at 600 nm, which correlates with microscopic spore counts. After excision of an agar piece of defined size (2×1.77 cm^2) from malt extract plates (3% w/v) spores were collected in 4 mL spore solution (0.8% w/v NaCl and 0.05% w/v Tween 80 in purified water) and photometrically analyzed at 600 nm against a standard curve of pre-counted spores.

Hyphal extension assays were analyzed upon growth on MA medium supplemented with either 1% w/v carboxymethyl cellulose (CMC) or 1% w/v glucose (Glc). For growth under stress, MA-CMC was supplemented with either 1 M sorbitol or 1 M NaCl for osmotic stress or 0.25 mM menadione (Sigma-Aldrich, St. Louis, Missouri, USA) for oxidative stress and measured after 96 h.

Construction of Δ*rgs4*
The deletion mutant Δ*rgs4* was created by recombinant cloning using a hygromycin phosphotransferase (*hph*) marker cassette with 1 kilobases (kb) flanking regions produced by yeast recombination as described previously [88] and protoplast transformation was performed with selection plates supplemented with 50 µg/mL hygromycin B as selection reagent (Roth, Karlsruhe, Germany) [89]. Successful deletion was confirmed by PCR. For primer sequences see Table 2. Copy number determination by qPCR as described previously [52] indicated two copies of the *rgs4* deletion cassette. Consequently, we aimed to confirm that the observed effects are due to the deletion of RGS4 rather than random effects of transformation. We performed crosses of Δ*rgs4* with female fertile FF1 to obtain progeny carrying the deletion. Analysis of these strains lacking *rgs4* as well as progeny from this crossing in which the deletion had been restored,

Table 1 Strains used in this study

Strain	Code	Characteristics	Source
QM6a	WT	Wild-type	[85]
FF1	FF1	Female fertile derivative of QM6a (MAT1-1)	[86]
FF2	FF2	Female fertile derivative of QM6a (MAT1-2)	[86]
QM6aΔ*rgs4*	Δ*rgs4*	Δ*rgs4*::hph$^+$ in QM6a background	This study
FF2rgs4_P5, FF2rgs4_P7, FF2rgs4_P11	FF2Δ*rgs4*	backcrossed Δ*rgs4* with FF1, carrying the deletion	This study
FF2rgs4_DR_3, FF2rgs4_DR_4	FF2*rgs4*DR	backcrossed Δ*rgs4* with FF1, not carrying the deletion	This study

Schalamun *et al. BMC Genomics*   (2023) 24:372

Page 14 of 17

Table 2 Oligonucleotides used in this study

Name	Sequence 5′—3′	Purpose
Rgs4_65607_5F	GTAACGCCAGGGTTTTCCCAGTCACGACGCCTGTTCAGAGCCTTATTCC	forward primer for 5′flank
Rgs4_65607_5R	ATCCACTTAACGTTACTGAAATCTCCAACGTACCGAGTACAAAACGTCG	reverse primer for 5′flank
Rgs4_65607_3F	CTCCTTCAATATCATCTTCTGTCTCCGACGAACCTGGTGTGATTTGAAGG	forward primer for 3′flank
Rgs4_65607_3R	GCGGATAACAATTTCACACAGGAAACAGCGGCATCCGTCCATAGTGAG	reverse primer for 3′flank
Rgs4_65607_qF	CGTGATACAGGAGAGCGATA	Internal primer
Rgs4_65607_qR	TTGGTGCAGTTCGTGAAAC	Internal primer
EF1-728F	CATCGAGAAGTTCGAGAAGG	Internal primer
TEF1 rev	GCCATCCTTGGAGATACCAGC	Internal primer
SAR RTF1	TGGATCGTCAACTGGTTCTACGA	RT qPCR
SAR RTR1	GCATGTGTAGCAACGTGGTCTTT	RT qPCR
RTcbh1F	ACCGTTGTCACCCAGTTCG	RT qPCR
RTcbh1R	ATCGTTGAGCTCGTTGCCAG	RT qPCR

confirmed that the characteristic growth defect of Δ*rgs4* on glucose segregated with the deletion (Additional file 1, Figure S2) hence confirming the validity of the strain used for analyses.

Isolation and manipulation of nucleic acids

DNA for screening of mutants was extracted using a rapid mini preparation method for fungal DNA [90]. For the isolation of total RNA, the mycelium from liquid cultivation was filtered through miracloth and frozen in liquid nitrogen prior to extraction with the RNeasy Plant mini kit (Qiagen, Heidelberg, Germany). Quality control of total RNA and RT-qPCR for investigation of *cbh1* transcript levels was performed as described earlier [91, 92]. *Sar1* was used as reference gene. Oligonucleotide sequences of all primers used in this study are listed in Table 2.

Biomass determination and specific cellulase activity

Biomass was determined as described earlier [93]. Briefly, frozen mycelia from liquid cultivation were ground in liquid nitrogen, incubated in 0.1 M NaOH and sonicated to break up cells. The liberated protein content was then measured using the Bradford method as a means reflecting biomass content.

For the analysis of cellulases in the cultivation supernatant, after centrifugation to remove residual cellulose, the CMC-cellulose kit (S-ACMC-L Megazyme) was used to measure endo-1,4-ß-D-glucanases. For the specific cellulase activity, the cellulase activity was normalized to the biomass produced.

Sorbicillin analysis at 370 nm

Absorbance at 370 nm reflects sorbicillin content [59] and was hence applied to quantitatively assess the amount of yellow pigment, indicative for sorbicillin and its derivatives in liquid media. Supernatants of liquid cultivation were centrifuged to remove residual cellulose and absorbance at 370 nm indicative for sorbicillin measured from biological triplicates.

BIOLOG phenotype microplate assay

Growth on different carbon sources were analyzed using BIOLOG FF Microplate assay (Biolog Inc., Hayward, CA) as described previously [94]. Inoculated microplates were incubated at 28 °C in constant dark or constant light (1700 lx) for up to 144 h and absorbances measured at 750 nm reflecting biomass accumulation in 24 h intervals starting at 72 h. Analyses were repeated in triplicates for each strain. Statistical significance of growth differences was analyzed by the T-test (p-value threshold ≤ 0.05) as implemented in Excel 2016 (Microsoft, Redmond, USA).

Transcriptome analysis and bioinformatics

We submitted total RNA in biological triplicates for each strain and condition. Library preparation, including ribo-depletion for the removal of rRNA and sequencing was conducted at the Next Generation Sequencing Facility (Vienna Biocenter Core Facilities GmbH, Austria) on a NovaSeq 6000 in paired-end (PE) and 150 bp mode, which resulted in an average of 29 million reads per sample. Quality filtering (Q30) and adapter trimming was done using bbduk version 38.18 [95]. For mapping, we used the most recent *T. reesei* QM6a reference genome [8] using HISAT2 version 2.2.1 [96], with an average overall alignment of 99.0% on average. For further data processing we used samtools version 1.10 [97] and examined the quality of mapping with QualiMap version 2.2.2 before applying featureCounts version 2.0.1 [98]. For differential gene expression (DEG) analysis in R version

Schalamun *et al. BMC Genomics*   (2023) 24:372

Page 15 of 17

4.0.3 [99], DESeq2 version 1.3.1 [100] was used with a threshold for significantly differentially regulated genes of log2fold change |>0.58| and p-adj<0.05. Resulting DEGs were further filtered with the LFCshrink function (type: apeglm) [101]. The gene annotations were done using available annotations for *T. reesei*, *T. virens* and *T. atroviride* [42] and *T. reesei* [64]. For count normalization the DESeq2 variance stabilizing transformation (VST) function was applied. Functional enrichment of a set of DEGs was performed using the Fisher's exact test using R package topGO version 2.42.0 [102] visualized with REVIGO [103].

Statistics

Statistical significance for phenotypic analysis was calculated in R using Student's T-test (compare means, ggpubr version 0.4.0) ** = p-value < 0.01, * = p-value < 0.05.

Phylogenetic analysis was performed using clustalX [104] for the alignment and MEGA11 for minimum evolution analysis [105, 106].

Supplementary Information

The online version contains supplementary material available at https://doi.org/10.1186/s12864-023-09467-2.

Additional file 1.

Additional file 2.

Additional file 3.

Authors' contributions
MiS performed experimental work and bioinformatic analysis and drafted the manuscript and figures. EMM supported and supervised bioinformatic analysis and edited the manuscript. MoS conceived the study, contributed to analysis and interpretation of results and wrote the final version of the manuscript. All authors read and approved the final manuscript.

Availability of data and materials
The datasets generated and analyzed during the current study are included in this article and its additional files and under GenBank accession number GSE216955 (https://www.ncbi.nlm.nih.gov/geo/query/acc.cgi?acc=GSE216955).

Declarations

Ethics approval and consent to participate
Not applicable.

Consent for publication
Not applicable.

Competing interests
The authors declare no competing interests.

References

1. Shpakov A. Heterotrimeric G proteins. In: Brenner's Encyclopedia of Genetics: 2nd Edition. 2013: 454–456.
2. Lengeler KB, Davidson RC, D'Souza C, Harashima T, Shen WC, Wang P, Pan X, Waugh M, Heitman J. Signal transduction cascades regulating fungal development and virulence. Microbiol Mol Biol Rev. 2000;64(4):746–85.
3. Li L, Wright SJ, Krystofova S, Park G, Borkovich KA. Heterotrimeric G protein signaling in filamentous fungi. Annu Rev Microbiol. 2007;61:423–52.
4. Druzhinina IS, Kubicek CP. Familiar stranger: ecological genomics of the model saprotroph and industrial enzyme producer *Trichoderma reesei* breaks the stereotypes. Adv Appl Microbiol. 2016;95:69–147.
5. Schmoll M. *Trichoderma reesei*. Trends Microbiol. 2022;30(4):403–4.
6. Tomico-Cuenca I, Mach RL, Mach-Aigner AR, Derntl C. An overview on current molecular tools for heterologous gene expression in *Trichoderma*. Fungal Biol Biotechnol. 2021;8(1):11.
7. Bischof RH, Ramoni J, Seiboth B. Cellulases and beyond: the first 70 years of the enzyme producer *Trichoderma reesei*. Microb Cell Fact. 2016;15(1):106.
8. Li WC, Huang CH, Chen CL, Chuang YC, Tung SY, Wang TF. *Trichoderma reesei* complete genome sequence, repeat-induced point mutation, and partitioning of CAZyme gene clusters. Biotechnol Biofuels. 2017;10:170.
9. Li WC, Lee CY, Lan WH, Woo TT, Liu HC, Yeh HY, Chang HY, Chuang YC, Chen CY, Chuang CN, et al. *Trichoderma reesei* Rad51 tolerates mismatches in hybrid meiosis with diverse genome sequences. Proc Natl Acad Sci U S Am. 2021;118(8):e2007192118.
10. Druzhinina IS, Chenthamara K, Zhang J, Atanasova L, Yang D, Miao Y, Rahimi MJ, Grujic M, Cai F, Pourmehdi S, et al. Massive lateral transfer of genes encoding plant cell wall-degrading enzymes to the mycoparasitic fungus *Trichoderma* from its plant-associated hosts. PLoS Genet. 2018;14(4): e1007322.
11. Schalamun M, Schmoll M. *Trichoderma* – genomes and genomics as treasure troves for research towards biology, biotechnology and agriculture. Front Fungal Biol. 2022;3. https://doi.org/10.3389/ffunb.2022.1002161.
12. Glass NL, Schmoll M, Cate JH, Coradetti S. Plant cell wall deconstruction by ascomycete fungi. Annu Rev Microbiol. 2013;67:477–98.
13. Schmoll M. Regulation of plant cell wall degradation by light in *Trichoderma*. Fungal Biol Biotechnol. 2018;5:10.
14. Schmoll M, Seibel C, Tisch D, Dorrer M, Kubicek CP. A novel class of peptide pheromone precursors in ascomycetous fungi. Mol Microbiol. 2010;77(6):1483–501.
15. Seidl V, Seibel C, Kubicek CP, Schmoll M. Sexual development in the industrial workhorse *Trichoderma reesei*. Proc Natl Acad Sci USA. 2009;106(33):13909–14.
16. Monroy AA, Stappler E, Schuster A, Sulyok M, Schmoll M. A CRE1- regulated cluster is responsible for light dependent production of dihydro-trichotetronin in *Trichoderma reesei*. PLoS ONE. 2017;12: e0182530.
17. Seibel C, Tisch D, Kubicek CP, Schmoll M. ENVOY is a major determinant in regulation of sexual development in *Hypocrea jecorina* (*Trichoderma reesei*). Eukaryot Cell. 2012;11:885–90.
18. Schmoll M. Light, stress, sex and carbon - the photoreceptor ENVOY as a central checkpoint in the physiology of *Trichoderma reesei*. Fungal Biol. 2018;122(6):479–86.
19. Schmoll M, Esquivel-Naranjo EU, Herrera-Estrella A. *Trichoderma* in the light of day - physiology and development. Fungal Genet Biol. 2010;47(11):909–16.
20. Proietto M, Bianchi MM, Ballario P, Brenna A. Epigenetic and posttranslational modifications in light signal transduction and the circadian clock in *Neurospora crassa*. Int J Mol Sci. 2015;16(7):15347–83.
21. Diernfellner ACR, Brunner M. Phosphorylation timers in the *Neurospora crassa* circadian clock. J Mol Biol. 2020;432(12):3449–65.
22. Franchi L, Fulci V, Macino G. Protein kinase C modulates light responses in *Neurospora* by regulating the blue light photoreceptor WC-1. Mol Microbiol. 2005;56(2):334–45.

23. Huang G, Chen S, Li S, Cha J, Long C, Li L, He Q, Liu Y. Protein kinase A and casein kinases mediate sequential phosphorylation events in the circadian negative feedback loop. Genes Dev. 2007;21(24):3283–95.

24. Tisch D, Schuster A, Schmoll M. Crossroads between light response and nutrient signalling: ENV1 and PhLP1 act as mutual regulatory pair in *Trichoderma reesei*. BMC Genomics. 2014;15:425.

25. Schmoll M. The information highways of a biotechnological work-horse - signal transduction in *Hypocrea jecorina*. BMC Genomics. 2008;9:430.

26. Jastrzebska B. GPCR: G protein complexes - the fundamental signaling assembly. Amino Acids. 2013;45(6):1303–14.

27. Cabrera-Vera TM, Vanhauwe J, Thomas TO, Medkova M, Preininger A, Mazzoni MR, Hamm HE. Insights into G protein structure, function, and regulation. Endocr Rev. 2003;24(6):765–81.

28. Schmoll M, Hinterdobler W. Tools for adapting to a complex habitat: G-protein coupled receptors in *Trichoderma*. In: Progress in Molecular Biology and Translational Science. Academic Press; 2022: in press.

29. Stewart A, Fisher RA. Introduction: G Protein-coupled Receptors and RGS Proteins. Prog Mol Biol Transl Sci. 2015;133:1–11.

30. Watson N, Linder ME, Druey KM, Kehrl JH, Blumer KJ. RGS family members: GTPase-activating proteins for heterotrimeric G-protein alpha-subunits. Nature. 1996;383(6596):172–5.

31. Ham D, Ahn D, Ashim J, Cho Y, Kim HR, Yu W, Chung KY. Conformational switch that induces GDP release from Gi. J Struct Biol. 2021;213(1): 107694.

32. Koelle MR. A new family of G-protein regulators - the RGS proteins. Curr Opin Cell Biol. 1997;9(2):143–7.

33. Alqinyah M, Hooks SB. Regulating the regulators: Epigenetic, transcriptional, and post-translational regulation of RGS proteins. Cell Signal. 2018;42:77–87.

34. Sethakorn N, Yau DM, Dulin NO. Non-canonical functions of RGS proteins. Cell Signal. 2010;22(9):1274–81.

35. Stappler E, Dattenböck C, Tisch D, Schmoll M. Analysis of light- and carbon-specific transcriptomes implicates a class of G-protein-coupled receptors in cellulose sensing. mSphere. 2017;2(3):e00089–00017.

36. Hinterdobler W, Beier S, Monroy AA, Berger H, Dattenbock C, Schmoll M. The G-protein coupled receptor GPR8 regulates secondary metabolism in *Trichoderma reesei*. Front Bioeng Biotechnol. 2020;8: 558996.

37. Schmoll M, Schuster A. do Nascimento Silva R, Kubicek CP. The G-alpha protein GNA3 of *Hypocrea jecorina* (anamorph *Trichoderma reesei*) regulates cellulase gene expression in the presence of light. Eukaryot Cell. 2009;8(3):410–20.

38. Seibel C, Gremel G, Silva RD, Schuster A, Kubicek CP, Schmoll M. Light-dependent roles of the G-protein subunit GNA1 of *Hypocrea jecorina* (anamorph *Trichoderma reesei*). BMC Biol. 2009;7(1):58.

39. Seibel C, Tisch D, Kubicek CP, Schmoll M. The role of pheromone receptors for communication and mating in *Hypocrea jecorina* (*Trichoderma reesei*). Fungal Genet Biol. 2012;49(10):814–24.

40. Tisch D, Kubicek CP, Schmoll M. The phosducin-like protein PhLP1 impacts regulation of glycoside hydrolases and light response in *Trichoderma reesei*. BMC Genomics. 2011;12:613.

41. Yu JH. Heterotrimeric G protein signaling and RGSs in *Aspergillus nidulans*. J Microbiol. 2006;44(2):145–54.

42. Schmoll M, Dattenböck C, Carreras-Villasenor N, Mendoza-Mendoza A, Tisch D, Aleman MI, Baker SE, Brown C, Cervantes-Badillo MG, Cetz-Chel J, et al. The genomes of three uneven siblings: footprints of the lifestyles of three *Trichoderma* species. Microbiol Mol Biol Rev. 2016;80(1):205–327.

43. Wang Y, Geng Z, Jiang D, Long F, Zhao Y, Su H, Zhang KQ, Yang J. Characterizations and functions of regulator of G protein signaling (RGS) in fungi. Appl Microbiol Biotechnol. 2013;97(18):7977–87.

44. Park HS, Kim MJ, Yu JH, Shin KS. Heterotrimeric G-protein signalers and RGSs in *Aspergillus fumigatus*. Pathogens. 2020;9(11):902.

45. Kim Y, Lee MW, Jun SC, Choi YH, Yu JH, Shin KS. RgsD negatively controls development, toxigenesis, stress response, and virulence in *Aspergillus fumigatus*. Sci Rep. 2019;9(1):811.

46. Ma N, Zhao Y, Wang Y, Yang L, Li D, Yang J, Jiang K, Zhang KQ, Yang J. Functional analysis of seven regulators of G protein signaling (RGSs) in the nematode-trapping fungus *Arthrobotrys oligospora*. Virulence. 2021;12(1):1825–40.

47. O'Brien JB, Wilkinson JC, Roman DL. Regulator of G-protein signaling (RGS) proteins as drug targets: Progress and future potentials. J Biol Chem. 2019;294(49):18571–85.

48. Kim Y, Heo IB, Yu JH, Shin KS. Characteristics of a Regulator of G-Protein Signaling (RGS) rgsC in *Aspergillus fumigatus*. Front Microbiol. 2017;8:2058.

49. Xie GX, Palmer PP. How regulators of G protein signaling achieve selective regulation. J Mol Biol. 2007;366(2):349–65.

50. Dattenböck C, Tisch D, Schuster A, Monroy AA, Hinterdobler W, Schmoll M. Gene regulation associated with sexual development and female fertility in different isolates of *Trichoderma reesei*. Fungal Biol Biotechnol. 2018;5:9.

51. Stappler E, Walton JD, Schmoll M. Abundance of secreted proteins of *Trichoderma reesei* is regulated by light of different intensities. Front Microbiol. 2017;8:2586.

52. Tisch D, Schmoll M. Targets of light signalling in *Trichoderma reesei*. BMC Genomics. 2013;14(1):657.

53. Allada R, Meissner RA. Casein kinase 2, circadian clocks, and the flight from mutagenic light. Mol Cell Biochem. 2005;274(1–2):141–9.

54. Mehra A, Shi M, Baker CL, Colot HV, Loros JJ, Dunlap JC. A role for casein kinase 2 in the mechanism underlying circadian temperature compensation. Cell. 2009;137(4):749–60.

55. Schuster A, Tisch D, Seidl-Seiboth V, Kubicek CP, Schmoll M. Roles of protein kinase A and adenylate cyclase in light-modulated cellulase regulation in *Trichoderma reesei*. Appl Environ Microbiol. 2012;78(7):2168–78.

56. Hinterdobler W, Schuster A, Tisch D, Ozkan E, Bazafkan H, Schinnerl J, Brecker L, Bohmdorfer S, Schmoll M. The role of PKAc1 in gene regulation and trichodimerol production in *Trichoderma reesei*. Fungal Biol Biotechnol. 2019;6:12.

57. D'Souza CA, Heitman J. Conserved cAMP signaling cascades regulate fungal development and virulence. FEMS Microbiol Rev. 2001;25(3):349–64.

58. Kronstad J, De Maria AD, Funnell D, Laidlaw RD, Lee N, de Sa MM, Ramesh M. Signaling via cAMP in fungi: interconnections with mitogen-activated protein kinase pathways. Arch Microbiol. 1998;170(6):395–404.

59. Derntl C, Rassinger A, Srebotnik E, Mach RL, Mach-Aigner AR. Identification of the main regulator responsible for synthesis of the typical yellow pigment produced by *Trichoderma reesei*. Appl Environ Microbiol. 2016;82(20):6247–57.

60. Derntl C, Guzman-Chavez F, Mello-de-Sousa TM, Busse HJ, Driessen AJM, Mach RL, Mach-Aigner AR. In Vivo Study of the Sorbicillinoid Gene Cluster in *Trichoderma reesei*. Front Microbiol. 2017;8:2037.

61. Nakari-Setala T, Aro N, Kalkkinen N, Alatalo E, Penttila M. Genetic and biochemical characterization of the *Trichoderma reesei* hydrophobin HFBI. European journal of biochemistry / FEBS. 1996;235(1–2):248–55.

62. Hitzenhammer E, Büschl C, Sulyok M, Schuhmacher R, Kluger B, Wischnitzki E, Schmoll M. YPR2 is a regulator of light modulated carbon and secondary metabolism in *Trichoderma reesei*. BMC Genomics. 2019;20(1):211.

63. Nguyen EV, Imanishi SY, Haapaniemi P, Yadav A, Saloheimo M, Corthals GL, Pakula TM. Quantitative site-specific phosphoproteomics of *Trichoderma reesei* signaling pathways upon induction of hydrolytic enzyme production. J Proteome Res. 2016;15(2):457–67.

64. Druzhinina IS, Kopchinskiy AG, Kubicek EM, Kubicek CP. A complete annotation of the chromosomes of the cellulase producer *Trichoderma reesei* provides insights in gene clusters, their expression and reveals genes required for fitness. Biotechnol Biofuels. 2016;9:75.

65. Frova C. Glutathione transferases in the genomics era: new insights and perspectives. Biomol Eng. 2006;23(4):149–69.

66. Morel M, Ngadin AA, Droux M, Jacquot JP, Gelhaye E. The fungal glutathione S-transferase system. Evidence of new classes in the wood-degrading basidiomycete *Phanerochaete chrysosporium*. Cell Mol Life Sci. 2009;66(23):3711–3725.

67. Haas H, Eisendle M, Turgeon BG. Siderophores in fungal physiology and virulence. Annu Rev Phytopathol. 2008;46:149–87.

68. Hwang J, Kim HS, Kang BS, Kim DH, Ryoo ZY, Choi SU, Lee S. RGS19 converts iron deprivation stress into a growth-inhibitory signal. Biochem Biophys Res Commun. 2015;464(1):168–75.

69. Antonkine ML, Koay MS, Epel B, Breitenstein C, Gopta O, Gartner W, Bill E, Lubitz W. Synthesis and characterization of de novo designed peptides modelling the binding sites of [4Fe-4S] clusters in photosystem I. Biochem Biophys Acta. 2009;1787(8):995–1008.

70. Schrettl M, Bignell E, Kragl C, Sabiha Y, Loss O, Eisendle M, Wallner A, Arst HN Jr, Haynes K, Haas H. Distinct roles for intra- and extracellular siderophores during *Aspergillus fumigatus* infection. PLoS Pathog. 2007;3(9):1195–207.

71. Kanehisa M, Goto S. KEGG: kyoto encyclopedia of genes and genomes. Nucleic Acids Res. 2000;28(1):27–30.

72. Dzikowska A, Grzelak A, Gawlik J, Szewczyk E, Mrozek P, Borsuk P, Koper M, Empel J, Szczęsny P, Piłsyk S, et al. KAEA (SUDPRO), a member of the ubiquitous KEOPS/EKC protein complex, regulates the arginine catabolic pathway and the expression of several other genes in Aspergillus nidulans. Gene. 2015;573(2):310–20.

73. Misslinger M, Hortschansky P, Brakhage AA, Haas H. Fungal iron homeostasis with a focus on Aspergillus fumigatus. Biochimica et Biophysica Acta (BBA) - Mol Cell Res. 2021;1868(1):118885.

74. Syrovatkina V, Alegre KO, Dey R, Huang XY. Regulation, signaling, and physiological functions of G-proteins. J Mol Biol. 2016;428(19):3850–68.

75. Miethke M, Marahiel MA. Siderophore-based iron acquisition and pathogen control. Microbiol Mol Biol Rev. 2007;71(3):413–51.

76. Wilson BR, Bogdan AR, Miyazawa M, Hashimoto K, Tsuji Y. Siderophores in iron metabolism: From mechanism to therapy potential. Trends Mol Med. 2016;22(12):1077–90.

77. Stearman R, Yuan DS, Yamaguchi-Iwai Y, Klausner RD, Dancis A. A permease-oxidase complex involved in high-affinity iron uptake in yeast. Science (New York, NY) 1996; 271(5255):1552–1557.

78. Misslinger M, Hortschansky P, Brakhage AA, Haas H. Fungal iron homeostasis with a focus on *Aspergillus fumigatus*. Biochim Biophys Acta Mol Cell Res. 2021;1868(1): 118885.

79. Schrettl M, Bignell E, Kragl C, Joechl C, Rogers T, Arst HN Jr, Haynes K, Haas H. Siderophore biosynthesis but not reductive iron assimilation is essential for *Aspergillus fumigatus* virulence. J Exp Med. 2004;200(9):1213–9.

80. Dickman MB, Yarden O. Serine/threonine protein kinases and phosphatases in filamentious fungi. Fungal Genet Biol. 1999;26(2):99–117.

81. Horta MAC, Thieme N, Gao Y, Burnum-Johnson KE, Nicora CD, Gritsenko MA, Lipton MS, Mohanraj K, de Assis LJ, Lin L, et al. Broad substrate-specific phosphorylation events are associated with the initial stage of plant cell wall recognition in *Neurospora crassa*. Front Microbiol. 2019;10:2317.

82. Nguyen QB, Kadotani N, Kasahara S, Tosa Y, Mayama S, Nakayashiki H. Systematic functional analysis of calcium-signalling proteins in the genome of the rice-blast fungus, *Magnaporthe oryzae*, using a high-throughput RNA-silencing system. Mol Microbiol. 2008;68(6):1348–65.

83. Humphrey SJ, James DE, Mann M. Protein phosphorylation: A major switch mechanism for metabolic regulation. Trends Endocrinol Metab. 2015;26(12):676–87.

84. Ptacek J, Devgan G, Michaud G, Zhu H, Zhu X, Fasolo J, Guo H, Jona G, Breitkreutz A, Sopko R, et al. Global analysis of protein phosphorylation in yeast. Nature. 2005;438(7068):679–84.

85. Martinez D, Berka RM, Henrissat B, Saloheimo M, Arvas M, Baker SE, Chapman J, Chertkov O, Coutinho PM, Cullen D *et al*: Genome sequencing and analysis of the biomass-degrading fungus *Trichoderma reesei* (syn. *Hypocrea jecorina*). Nat Biotechnol. 2008;26(5):553–560.

86. Bazafkan H, Dattenböck C, Böhmdorfer S, Tisch D, Stappler E, Schmoll M. Mating type dependent partner sensing as mediated by VEL1 in *Trichoderma reesei*. Mol Microbiol. 2015;96(6):1103–18.

87. Mandels M, Andreotti R. Problems and challenges in the cellulose to cellulase fermentation. Proc Biochem. 1978;13:6–13.

88. Schuster A, Bruno KS, Collett JR, Baker SE, Seiboth B, Kubicek CP, Schmoll M. A versatile toolkit for high throughput functional genomics with *Trichoderma reesei*. Biotechnol Biofuels. 2012;5(1):1.

89. Gruber F, Visser J, Kubicek CP, de Graaff LH. The development of a heterologous transformation system for the cellulolytic fungus *Trichoderma reesei* based on a *pyrG*-negative mutant strain. Curr Genet. 1990;18(1):71–6.

90. Liu D, Coloe S, Baird R, Pederson J. Rapid mini-preparation of fungal DNA for PCR. J Clin Microbiol. 2000;38(1):471.

91. Bazafkan H, Beier S, Stappler E, Böhmdorfer S, Oberlerchner JT, Sulyok M, Schmoll M. SUB1 has photoreceptor dependent and independent functions in sexual development and secondary metabolism in *Trichoderma reesei*. Mol Microbiol. 2017;106(5):742–59.

92. Tisch D, Kubicek CP, Schmoll M. New insights into the mechanism of light modulated signaling by heterotrimeric G-proteins: ENVOY acts on *gna1* and *gna3* and adjusts cAMP levels in *Trichoderma reesei* (*Hypocrea jecorina*). Fungal Genet Biol. 2011;48(6):631–40.

93. Schmoll M, Franchi L, Kubicek CP. Envoy, a PAS/LOV domain protein of *Hypocrea jecorina* (Anamorph *Trichoderma reesei*), modulates cellulase gene transcription in response to light. Eukaryot Cell. 2005;4(12):1998–2007.

94. Druzhinina IS, Schmoll M, Seiboth B, Kubicek CP. Global carbon utilization profiles of wild-type, mutant, and transformant strains of *Hypocrea jecorina*. Appl Environ Microbiol. 2006;72(3):2126–33.

95. Brian B. BBMap. In.https://sourceforge.net/projects/bbmap/: Sourceforge; 2014.

96. Kim D, Paggi JM, Park C, Bennett C, Salzberg SL. Graph-based genome alignment and genotyping with HISAT2 and HISAT-genotype. Nat Biotechnol. 2019;37(8):907–15.

97. Li H, Handsaker B, Wysoker A, Fennell T, Ruan J, Homer N, Marth G, Abecasis G, Durbin R. Genome Project Data Processing S: The Sequence Alignment/Map format and SAMtools. Bioinformatics. 2009;25(16):2078–9.

98. Liao Y, Smyth GK, Shi W. featureCounts: an efficient general purpose program for assigning sequence reads to genomic features. Bioinformatics. 2013;30(7):923–30.

99. Team RC. R: A language and environment for statistical computing. In.https://www.R-project.org/: R Foundation for Statistical Computing, Vienna.

100. Love MI, Huber W, Anders S. Moderated estimation of fold change and dispersion for RNA-seq data with DESeq2. Genome Biol. 2014;15(12):550.

101. Zhu A, Ibrahim JG, Love MI. Heavy-tailed prior distributions for sequence count data: removing the noise and preserving large differences. Bioinformatics. 2019;35(12):2084–92.

102. Adrian Alexa JR. Enrichment Analysis for Gene Ontology. 2021.

103. Supek F, Bosnjak M, Skunca N, Smuc T. REVIGO summarizes and visualizes long lists of gene ontology terms. PLoS ONE. 2011;6(7): e21800.

104. Thompson JD, Gibson TJ, Plewniak F, Jeanmougin F, Higgins DG. The CLUSTAL_X windows interface: flexible strategies for multiple sequence alignment aided by quality analysis tools. Nucleic Acids Res. 1997;25(24):4876–82.

105. Tamura K, Stecher G, Kumar S. MEGA11: Molecular Evolutionary Genetics Analysis Version 11. Mol Biol Evol. 2021;38(7):3022–7.

106. Rzhetsky A, Nei M. Statistical properties of the ordinary least-squares, generalized least-squares, and minimum-evolution methods of phylogenetic inference. J Mol Evol. 1992;35(4):367–75.

Publisher's Note

Chapter 3: MAPkinases regulate secondary metabolism, sexual development and light dependent cellulase regulation in *Trichoderma reesei*

Miriam Schalamun[1], Sabrina Beier[1], Wolfgang Hinterdobler[1,2], Nicole Wanko[1], Johann Schinnerl[3], Lothar Brecker[4], Dorothea Elisa Engl[4] & Monika Schmoll[1,5]

[1]AIT Austrian Institute of Technology GmbH, Center for Health and Bioresources,

Bioresources Unit, Konrad Lorenz Strasse 24, 3430 Tulln

[2] MyPilz GmbH, Wienerbergstrasse 55/13-15, 1120 Vienna, Austria

[3] Department of Botany and Biodiversity Research, University of Vienna, Rennweg 14, 1030

Vienna, Austria

[4] Department of Organic Chemistry, University of Vienna, Währinger Strasse 38, A-1090

Vienna, Austria

[5] University of Vienna, Department of Microbiology and Ecosystem Science, Division of

Terrestrial Ecosystem Research, Djerassiplatz 1, 1030 Vienna, Austria

scientific reports

OPEN

MAPkinases regulate secondary metabolism, sexual development and light dependent cellulase regulation in *Trichoderma reesei*

Miriam Schalamun[1], Sabrina Beier[1], Wolfgang Hinterdobler[1,2], Nicole Wanko[1], Johann Schinnerl[3], Lothar Brecker[4], Dorothea Elisa Engl[4] & Monika Schmoll[1,5✉]

The filamentous fungus *Trichoderma reesei* is a prolific producer of plant cell wall degrading enzymes, which are regulated in response to diverse environmental signals for optimal adaptation, but also produces a wide array of secondary metabolites. Available carbon source and light are the strongest cues currently known to impact secreted enzyme levels and an interplay with regulation of secondary metabolism became increasingly obvious in recent years. While cellulase regulation is already known to be modulated by different mitogen activated protein kinase (MAPK) pathways, the relevance of the light signal, which is transmitted by this pathway in other fungi as well, is still unknown in *T. reesei* as are interconnections to secondary metabolism and chemical communication under mating conditions. Here we show that MAPkinases differentially influence cellulase regulation in light and darkness and that the Hog1 homologue TMK3, but not TMK1 or TMK2 are required for the chemotropic response to glucose in *T. reesei*. Additionally, MAPkinases regulate production of specific secondary metabolites including trichodimerol and bisorbibutenolid, a bioactive compound with cytostatic effect on cancer cells and deterrent effect on larvae, under conditions facilitating mating, which reflects a defect in chemical communication. Strains lacking either of the MAPkinases become female sterile, indicating the conservation of the role of MAPkinases in sexual fertility also in *T. reesei*. In summary, our findings substantiate the previously detected interconnection of cellulase regulation with regulation of secondary metabolism as well as the involvement of MAPkinases in light dependent gene regulation of cellulase and secondary metabolite genes in fungi.

To survive in a competitive habitat, organisms evolved complex signaling pathways to properly react to a changing environment while optimally balancing resources for survival and growth. Especially sunlight profoundly impacts organsims living on earth and if light perception or–response machineries are impaired, severe consequences for fitness or even survival were observed[1,2]. The conserved mitogen activated protein (MAP) kinase pathways play a central role in signal transmission and–integration in eukaryotes from fungi to mammals[3,4].

MAPkinase cascades have been subject to intense research efforts in eukaryotes, which revealed their contribution to virtually all crucial physiological processes from growth, response to hyphal injury, reproduction, stress response, secondary metabolite production to metabolism and light response[4–8].

In filamentous fungi, three major MAPkinase pathways are known: The pheromone response pathway[9], the cell wall integrity pathway[10] and the osmoregulation pathway[11]. MAPkinase pathways each consist of three protein kinases, a MAPkinase, a MAPkinase kinase (MAPKK) and a MAPkinase kinase kinase (MAPKKK) which form a phosphorylation cascade[12,13]. This 3-tiered modular construct is likely positively selected during evolution[14]. Stepwise phosphorylation enables signal integration at every stage and is required for activation. Subcellular localization of MAPkinases is crucial for their function and establishment of regulatory feedback

[1]Center for Health and Bioresources, Bioresources Unit, AIT Austrian Institute of Technology GmbH, Konrad Lorenz Strasse 24, 3430 Tulln, Austria. [2]MyPilz GmbH, Wienerbergstrasse 55/13-15, 1120 Vienna, Austria. [3]Department of Botany and Biodiversity Research, University of Vienna, Rennweg 14, 1030 Vienna, Austria. [4]Department of Organic Chemistry, University of Vienna, Währinger Strasse 38, 1090 Vienna, Austria. [5]Division of Terrestrial Ecosystem Research, Department of Microbiology and Ecosystem Science, University of Vienna, Djerassiplatz 1, 1030 Vienna, Austria. ✉email: monika.schmoll@univie.ac.at

loops[15]. Thereby, MAPkinases are known to be subject to feedback inhibition, which contributes to signal fidelity and is often achieved by phosphatases dephosphorylating and hence inactivating MAPkinases[13].

Evaluation of the functions of the pheromone MAPkinase pathway in *Aspergillus flavus* showed that its members (*steC, mkkB, mpkB* and *steD*) act as a complex and are required for aflatoxin B1 production, while in the respective deletion mutants an increase in production of leporin B and aspergillicins was observed[9]. Mechanistic investigation of the role of this pathway in aflatoxin production revealed that the regulatory impact of this kinase targeted biosynthesis of precursors rather than regulation of the aflatoxin gene cluster[16]. In contrast, deletion of the Hog1-type MAPkinase SakA in *A. flavus* caused an increase in aflatoxin production[17]. Components of the cell wall integrity pathway are involved in regulation of secondary metabolism in many fungi, where they are often required for their production[10]. Already these few examples show that regulation of secondary metabolism is a common trait for the function of MAPkinase pathways in fungi.

Fungi use chemicals to communicate with mating partners and competitors[18,19]. Importantly, a considerable part of the functions of MAPKs is aimed at appropriate communication with the environment, which is crucial not only for competition, but also for virulence and pathogenicity[7,20]. While the correct function of such a communication can be detected relatively easily by genetic screenings and microscopic analysis, the compounds responsible for this interaction—the chemical(s) eliciting the response—are much harder to identify. One example is the chemotropic growth of the phytopathogen *Fusarium oxysporum* towards plants which is regulated by the CWI MAPkinase pathway, for which a peroxidase was found to be responsible[21,22], which is however unlikely to be the chemical that is detected. Another case of chemical communication is represented by the rhythmic activation of MAPkinases upon fungal communication between *Neurospora crassa* hyphae[23]. This interaction mechanism is conserved between *N. crassa* and *B. cinerea*[24] although also here the chemical compounds mediating this interaction are not yet known.

The rotation of earth causing night and day represents one of the most important environmental cues for life, including fungi[1]. Thereby, organisms do not simply respond the the increasing light intensity in the morning, but they prepare for both dusk and dawn using a circadian clock, which keeps running even in the dark[25,26]. Light is essential for entraining the clock and a light pulse resets the clock, which impacts the whole gene regulation machinery as well[25,27]. MAPkinases play an important role in circadian rhythmicity due to their rhythmic activation and their role in phosphorylation of clock proteins[28]. They are a crucial output pathway of the circadian clock[29].

Both upon constant light conditions as well as during a time course reflecting circadian rhythmicity, discrepancies between mRNA abundance and protein abundance were observed[30,31] and also metabolism related gene oscillate during the circadian day[32]. With respect to circadian rhythmicity, it is particularly interesting, that the rhythmic activation of the osmosensing MAPK pathway influences regulation of translation in dependence of osmotic stress[33].

The Hog-pathway transmits the phytochrome-related red light signal independently of its function as a stress signaling factor in *Aspergillus nidulans*[34].

The genus *Trichoderma* comprises a diverse array of mostly benefical fungi, which comprise plant symbionts and industrial workhorses for enzyme production[35–40].

In *Trichoderma*, light profoundly influences physiology[41,42] with respect to growth[43–45], asexual and sexual development[46,47], regulation of plant cell wall degrading enzymes[48], secondary metabolism[49,50] and stress response[51–53]. Moreover, the MAPkinase encoding gene *tmk3* is induced by light in a photoreceptor dependent manner in *T. atroviride*[54] and in *T. reesei*[55] and early, transient phosphorylation of TMK3 occurs in *T. atroviride*[56]. Also the photoreceptor gene *env1* and the photolyase gene *phr1* have strongly increased transcript levels in a strain lacking *tmk3*, hence indicating a dampening effect of the HOG pathway on light response and potentially increased light sensitivity in deletion strains[56].

In *S. cerevisiae*, the MAPkinase of the pheromone pathway is Fus3[12], the homologue of *T. reesei* TMK1. Upstream of the *S. cerevisiae* MAPkinase cascade, the G-protein beta and gamma subunit mediate transmission of the pheromone signal to the MAPkinases[5]. In filamentous fungi not only Fus3 homologues, but also components of other MAPkinase pathways were shown to be required for proper sexual development. The MAPkinase mediating the cell wall integrity (CWI) pathway in *N. crassa* was found to be required for formation of protoperithecia if a strain was meant to assume the female role in a cross[57]. Moreover, Slt2 homologues are required for female fertility in *F. graminearum*[58] and *Magnaporthe grisea*[59]. In *F. graminearum*, lack of of the Hog-pathway MAPkinase blocked sexual development[60]. Crosstalk was observed among the CWI and pheromone response pathways in *N. crassa*[61]. Hence, while the pheromone response pathway has a central function in sexual development, all three MAPkinases contribute to the process of sexual reproduction.

Induction of sexual development in *T. reesei* deviates from methods in other fungi in that so far, no protoperithecia or similar early female stages were observed in this fungus[62,63]. However, due to the inability of the prominent wild-type strain QM6a to assume the female role in a cross, which is due to a defect in the scaffolding protein HAM5[64,65], is considered female sterile[67].

In *Trichoderma*, three MAPkinase pathways were detected, which are conserved in the genus[40,67]. Early investigations showed that *T. virens* TmkA and TmkB are required for full antagonistic potential against fungal phytopathogens[68,69] and TmkA is needed for inducing full systemic resistance[70]. In *T. atroviride*, lack of Tmk1 reduced mycoparasitic activity, yet higher antifungal activity attributed to low molecular weight substances including 6-pentyl-α-pyrone (6PP) and peptaibol antibiotics[71]. Recently, *T. atroviride* Tmk3 and Tmk1 were implicated in polarity stress response during hyphal interaction upon mycoparasitism and the chemotropic interaction between individual hyphae in this process[72]. Another case of antagonism was shown for *T. atroviride* with *Drosophila melanogaster* larvae, which fed on the fungal mycelium. Tmk3 was required for secondary metabolite production in *T. atroviride*, which was the reason for larvae preferentially feeding on a *tmk3* mutant, although the mortality of larvae doing so was increased compared to feeding on the wild-type[73]. Furthermore, *T. atroviride*

Tmk3 was required for proper response to cell wall stress, especially upon exposure to light[56], which suggests a certain interrelationship of the cell wall integrity pathway (represented by Tmk2) and the osmosensing pathway.

Investigation of the functions of the MAPkinase pathways in *T. reesei* as well as selected upstream signaling processes revealed roles in cell wall integrity, stress response, glycogen accumulation and asexual development[74–77]. Previously, TMK1 (Fus3-like), TMK2 (Slt2-like) and TMK3 (Hog1-like) were shown to impact regulation of cellulase gene expression: TMK3 was reported to exert a strongly positive influence on cellulase production[76], while the influence of TMK2 on transcript abundance of cellulase genes is minor, despite its negative influence on secreted cellulase activity[74]. TMK1 also negatively influences cellulase production[75,77], although a positive effect of TMK1 was shown on transcript levels of major cellulase and xylanase genes[77].

Despite the fact that the influence of light on MAPKinase dependent regulation of stress response and secondary metabolism was shown previously, this environmental cue was not considered in previous studies of the topic with *T. reesei*. Consequently, we investigated the impact of light on regulation of cellulase production and we show significant differences between growth in light and growth in darkness. Our study further revealed that MAPkinases are required for female fertility upon mating in *T. reesei* and that MAPkinases differentially impact secondary metabolite production under mating conditions, hence reflecting an influence on chemical communication.

Results

Information on environmental cues is transmitted via multiple signaling cascades in fungi, one of which are the MAPkinase cascades. Although the MAPkinase genes of *T. reesei* do not show significant regulation by light[49,78], previous work revealed an involvement of phosphorylations in general and specifically also by MAPkinase cascades in light response and circadian rhythmicity[25,28]. Additionally, we showed that the random mutant QM9414 is less light sensitive with respect to cellulase production than the wild-type strain QM6a[79]. Therefore we deleted the MAPkinase encoding genes *tmk1*, *tmk2* and *tmk3* in the wild-type background of QM6a by replacement with the hygromycin selection marker cassette[80]. Throughout our study, we investigated the phase of active growth and cellulase production of QM6a, which grows somewhat more slowly than QM9414 and produces lower levels of cellulases, but has the advantage that the machinery of cellulase regulation associated signaling and gene regulation is not altered.

MAPkinases impact growth and sporulation.
As expected, *tmk1*, *tmk2* and *tmk3* were not essential in QM6a and grew well on malt extract agar plates (Fig. 1A). Analysis of biomass formation in liquid cultivations with cellulose as carbon source revealed strikingly different impacts in constant light and constant darkness. While in darkness Δ*tmk3* formed considerably less biomass (Fig. 1B), a similar effect was observed in light for Δ*tmk2* (Fig. 1C). This clear difference in the functions of TMK2 and TMK3 in modulating growth in light and darkness strengthens the need for cultivation under controlled light conditions. Moreover, the three MAPkinase pathways of *T. reesei* obviously exert signal transmission tasks for which it is crucial whether they grow in the dark or in light.

We also found that lack of *tmk3* in the genome causes abolishment of the typical green pigmentation of spores (Fig. 1A), which is in agreement with data from *T. atroviride*[56]. Hence, we were interested whether this is due to an impact of MAPkinases on regulation of *pks4*, the polyketide synthase responsible for this pigmentation[81].

RTqPCR confirmed our hypothesis (Fig. 1D,E), showing that deletion of *tmk3*, which results in a white phenotype, also correlates with abolishment of *pks4* transcription in light and darkness. Interestingly, we also found that *pks4* transcript levels are strongly increased in a strain lacking *tmk2*, both in light and darkness and that Δ*tmk1* also shows elevated *pks4* levels only in darkness. Consequently, MAPkinases crucially impact spore pigmentation, both in light, as the preferred sporulation condition and in darkness.

TMK3 is required for chemotropic response to glucose.
Glucose represents an important nutrient for *T. reesei*, which represses cellulase gene expression and elicits carbon catabolite repression[82,83]. However, genome analysis revealed that *T. reesei* lacks a direct homologue of the prototypical glucose sensors GPR-4 or Git1[67]. Investigation of G-protein coupled receptors (GPCRs) implicated two class XIII (DUF300 domain) GPCRs, CSG1 and CSG2 in glucose sensing due to their impact on cellulase regulation on cellulose and lactose[78]. This function was supported by the requirement of CSG1 and CSG2 for chemotropic responses to specific concentrations of glucose[84]. Since also a role in chemotropic reaction to glucose was shown for FMK1, the *Fusarium oxysporum* homologue of filamentation pathway MAPkinase[22], we were interested in the role of *T. reesei* MAPkinases in chemotropic reactions to glucose.

Interestingly, in *T. reesei* TMK3, but not TMK1, the homologue of FMK1, is required for chemotropic response to glucose. As for the *F. oxysporum* homologue MPK1[22], lack of the cell wall integrity pathway MAPkinase TMK2 in *T. reesei* does not perturb chemotropic response to glucose (Fig. 2A).

Since also the GPCRs CSG1 and CSG2 are required for chemotropic reactions to glucose[84], the signaling pathway triggering this reaction in *T. reesei* might not be exclusively channeled through the G-protein pathway but may be subject to biased signaling[85].

MAPkinases regulate cellulase transcription and secreted activity differentially in light and darkness.
An involvement *of T. reesei* MAPkinases in cellulase regulation was shown previously[74–76]. However, in these studies, the relevance of light for cellulase regulation was not considered and *T. reesei* TU-6, a parental strain derived from QM9414, with decreased and probably altered light response[79] was used. Therefore, we aimed to evaluate these previous results under controlled light conditions with cellulose as carbon source and we tested for a potential relevance of MAPkinases in the strong down-regulation of cellulases in light.
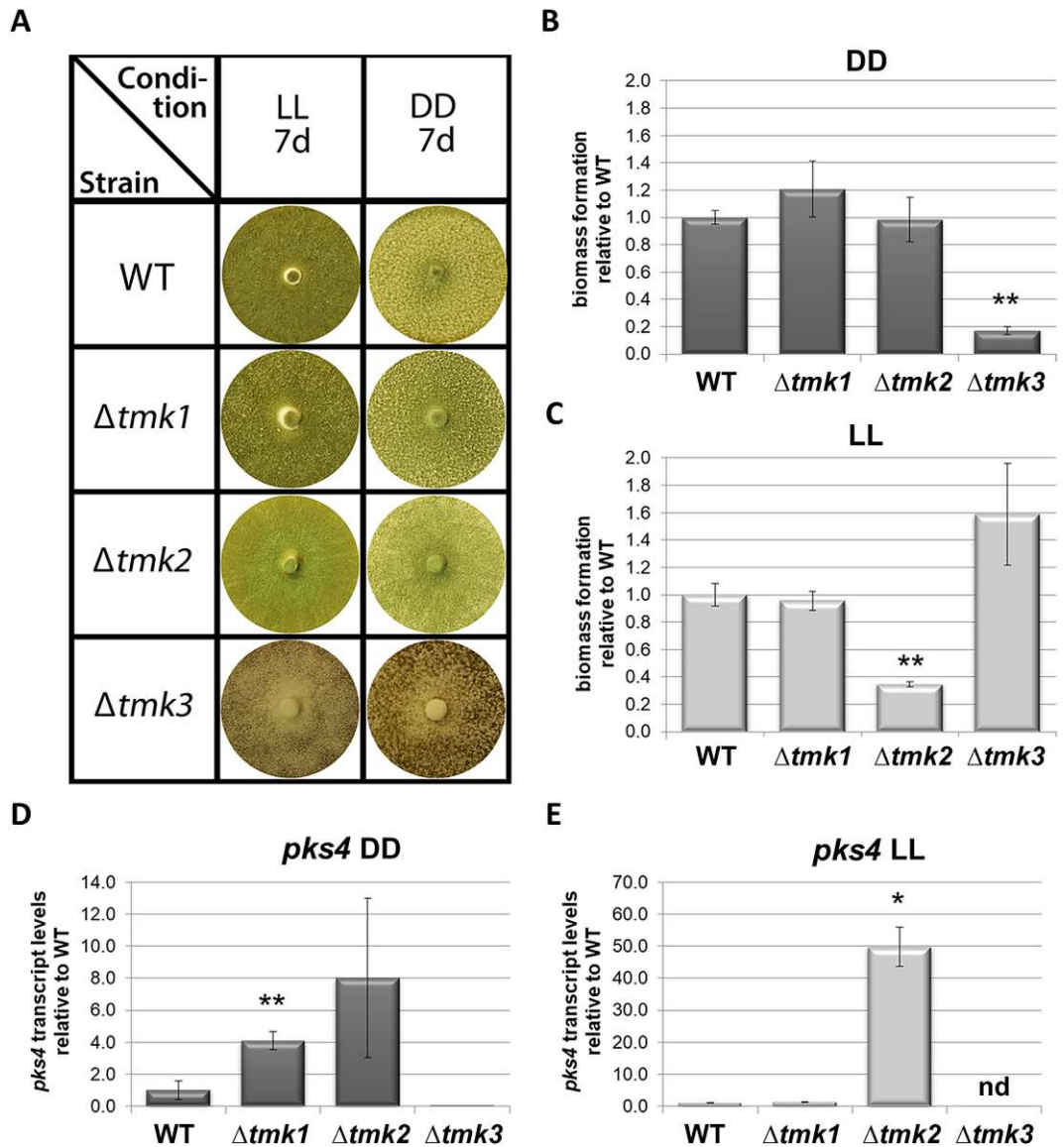
Figure 1. Relevance of MAPkinases for phenotype and biomass formation. (**A**) MAPkinase mutant strains on MEX agar plates in constant light (LL) and constant darkness (DD) after 7 days at 28 °C. (**B,C**) Biomass formation relative to wild-type (WT) QM6aΔ*ku80* upon growth on 1% cellulose in (**B**) constant darkness and (**C**) constant light. (**D,E**) Transcript levels of the polyketide synthases gene *pks4* upon growth on 1% cellulose in (**D**) constant darkness and (**E**) constant light.

We observed that lack of *tmk3* in the genome virtually abolished specific cellulase activity in darkness (Fig. 2B), which is in agreement with the strongly decreased biomass formation of Δ*tmk3* under these conditions (Fig. 1B). Due to the strong effect of TMK3 on cellulase regulation, chemotropic response to glucose and biomass formation upon growth on cellulose, we were interested whether the growth defect of Δ*tmk3* is a general phenomenon or conditions specific i.e. carbon source specific. Analysis of hyphal extension of Δ*tmk3* on malt extract medium (3% w/v) showed a colony size decreased by 48 + /− 1% (standard deviation of 3 biological replicates), on carboxymethylcellulose the decrease was considerably stronger with 86 + /− 1% and on glucose Δ*tmk3* showed no growth after the 48 h in darkness of the experiment used in parallel for the other measurements. Consequently, the growth defect caused by the lack of TMK3 is obvious on all media used, albeit the extent of the retardation is dependent on the carbon source. The more severe growth defect on carboxymethylcellulose compared to the full medium (malt extract) is in agreement with the strong decrease of cellulase expression in Δ*tmk3*. The fact that Δ*tmk3* does not chemotropically react to glucose anymore, a degradation product of cellulose is in agreement with its growth defect on glucose, as it obviously as problems to sense it, which may well be connected to perturbed cellulase regulation and the subsequent glucose liberation intra- and/or extracellularly.

Deletion of *tmk1* caused increased cellulase activity and for Δ*tmk2* we found a positive trend (Fig. 2B). In the wild-type QM6a, cellulase activity in light decreases to levels around or below the detection limit[79], which did not
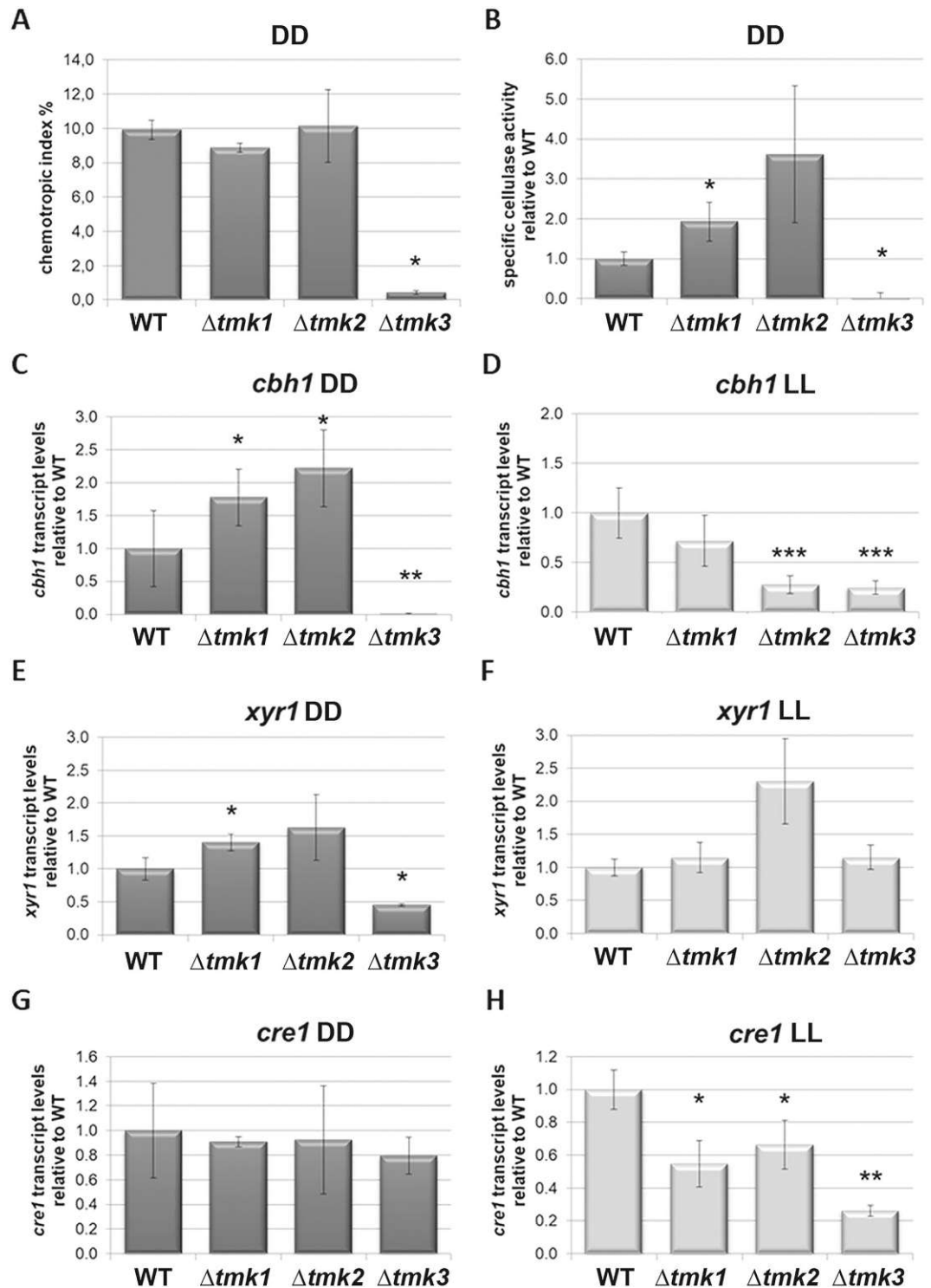
Figure 2. Relevance of MAPkinases for chemotropic response and cellulase regulation. (**A**) Chemotropic response of MAPkinase mutant strains to 1% glucose. (**B**) Specific cellulase activity upon growth on 1% cellulose in darkness. (**C,D**) Transcript levels of *cbh1* upon growth on 1% cellulose (**C**) in constant darkness and (**D**) constant light. (**E,F**) Transcript levels of *xyr1* upon growth on 1% cellulose (**E**) in constant darkness and (**F**) constant light. (**G,H**) Transcript levels of *cre1* upon growth on 1% cellulose (**G**) in constant darkness and (**H**) constant light.

change in deletion strains of *tmk1*, *tmk2* or *tmk3* (data not shown). Consequently, MAPkinases are not involved in the (posttranscriptional) mechanism responsible for the block of cellulase formation in light, although they do influence *cbh1* transcript abundance.

Transcript abundance of *cbh1*, the major cellobiohydrolase gene of *T. reesei*, correlated with the results for specific cellulase activity in darkness, with significantly increased *cbh1* levels in Δ*tmk2*, hence supporting the positive trend of cellulase activity in Δ*tmk2* (Fig. 2C). In light, *cbh1* transcript levels are decreased in all three MAPkinase mutants (Fig. 2D), reflecting a clear difference to the situation in darkness.

In darkness, transcript levels of the major cellulase transcription factor gene *xyr1* correlates with those of *cbh1* (Fig. 2E), which was shown for other conditions previously[86]. Also for *xyr1*, the situation is different in light (Fig. 2F), in that the correlation with *cbh1* was not observed and in contrast to the down-regulation of transcript levels of *cbh1* in Δ*tmk2*, *xyr1* transcript levels follow the up-regulation as seen in *cbh1* and *xyr1* in this strain in darkness. Therefore, it is tempting to speculate that TMK1 and TMK3, but not TMK2 are relevant for the function of XYR1 in cellulase regulation in light. Since XYR1 comprises MAPK phosphorylation sites[76], this would not be without precedent.

In case of the carbon catabolite repressor gene *cre1*, we also found clear differences in gene regulation by TMK1, TMK2 and TMK3 in light and darkness (Fig. 2G,H). The lack of significant regulation of *cre1* in darkness does not indicate a relevance of MAPkinases for carbon catabolite repression at the level of modulation of transcript abundance of *cre1* (Fig. 2G). In light, *cre1* transcript abundance decreases in all three deletion strains (Fig. 2H), the relevance of which is difficult to interpret, due to the very low levels of expressed cellulases in light on cellulose.

MAPkinases are involved in sorbicillin production. An involvement of MAPkinases of *T. reesei* in regulation of secondary metabolism has not been tested previously. Sorbicillin production is connected to the regulation of cellulase gene expression and carbon catabolite repression in *T. reesei*[50,87,88]. Therefore, we assessed this function with a photometric screening for yellow pigments representing mainly sorbicillin derivatives, which show a typical light absorbance maximum close to 370 nm. These compounds are biosynthetized by the products of the SOR secondary metabolite cluster[50,89,90] upon growth on liquid media with cellulose as carbon source (Fig. 3A,B).

We found that both TMK2 and TMK3 positively influence sorbicillinoid production in darkness upon growth on cellulose (Fig. 3C), which correlates with the difference in biomass production in case of Δ*tmk3*. In light, the situation is reversed for TMK2 (Fig. 3D), which has a considerably negative effect on the production of sorbicillin derivatives. This prompted us to investigate a possible influence of MAPkinases on secondary metabolism in more detail.

MAPkinases impact regulation of secondary metabolism. Among the most crucial regulators of secondary metabolism is VEL1, which regulates sexual development and secondary metabolism in *T. reesei*[91], shows a regulatory interaction with the photoreceptor ENV1[92] and is essential for cellulase gene expression[93]. Therefore, we asked whether the regulatory function of the MAPkinases might be connected to the role of VEL1 by testing transcript abundance of *vel1* in deletion strains of *tmk1*, *tmk2* and *tmk3*.

Indeed, we found a light dependent regulation of *vel1* in all MAPkinase mutants, with differential impacts either in constant light or in constant darkness (Fig. 3E,F). The regulation pattern of *vel1* did not correlate with production of sorbicillin derivatives (Fig. 3A,E) as the clear increase of *vel1* transcript abundance in Δ*tmk3* should rather result in an increased level of sorbicillinoid production in case of a direct correlation, which is not the case. Consequently, the regulatory impact of the MAPkinases on sorbicillin production is unlikely to be mediated by VEL1.

MAPkinases are required for normal sexual development. An involvement of MAPkinases in regulation of sexual development was shown previously in fungi. Since the parental strain QM6a is female sterile due to a defect in the MAPkinase scaffolding protein HAM5[64,65], we outcrossed this defect by mating with the fully fertile QM6a derivative FF1. The resulting strains with fully fertile strain background were confronted under conditions favouring sexual development. All strains were able to form fruiting bodies with the fully fertile wild-type strains CBS999.97 MAT1-1 and CBS999.97 MAT1-2 (Fig. 4). However, none of the strains lacking a MAPkinase gene could mate with a female sterile strain of the respective compatible mating type (FS69 or QM6a) or with another strain lacking a MAPkinase. Therefore, we conclude that deletion of *tmk1*, *tmk2* or *tmk3* causes female sterility.

In homozygous crosses of strains lacking TMK2 or crosses between Δ*tmk2* and Δ*tmk3* of either mating type we observed a small but visible clearing zone. This finding suggests that the clear effects in regulation of secondary metabolism under different conditions by TMK2 and TMK3 also affect chemical communication and potentially cause a retardation of growth or decrease in aerial hyphae formation prior to contact. The minor effects of TMK1 on secondary metabolism are unlikely to be relevant for chemical communication. However, it has to be noted that for example fatty acid derived secondary metabolites would not be detected in our assay and hence we cannot fully exclude an influence of TMK1 on certain compounds not observed here.

MAPkinases contribute to regulation of chemical communication. Secondary metabolite production changes under fermentative conditions in *T. reesei*, which was also shown for sorbicillinoids[94,95], which are responsible for the yellow coloration of liquid and solid media inoculated with *T. reesei* wild-types[89,90]. The involvement of TMK2 and TMK3 in regulation of secondary metabolism and the relevance of all three MAP-
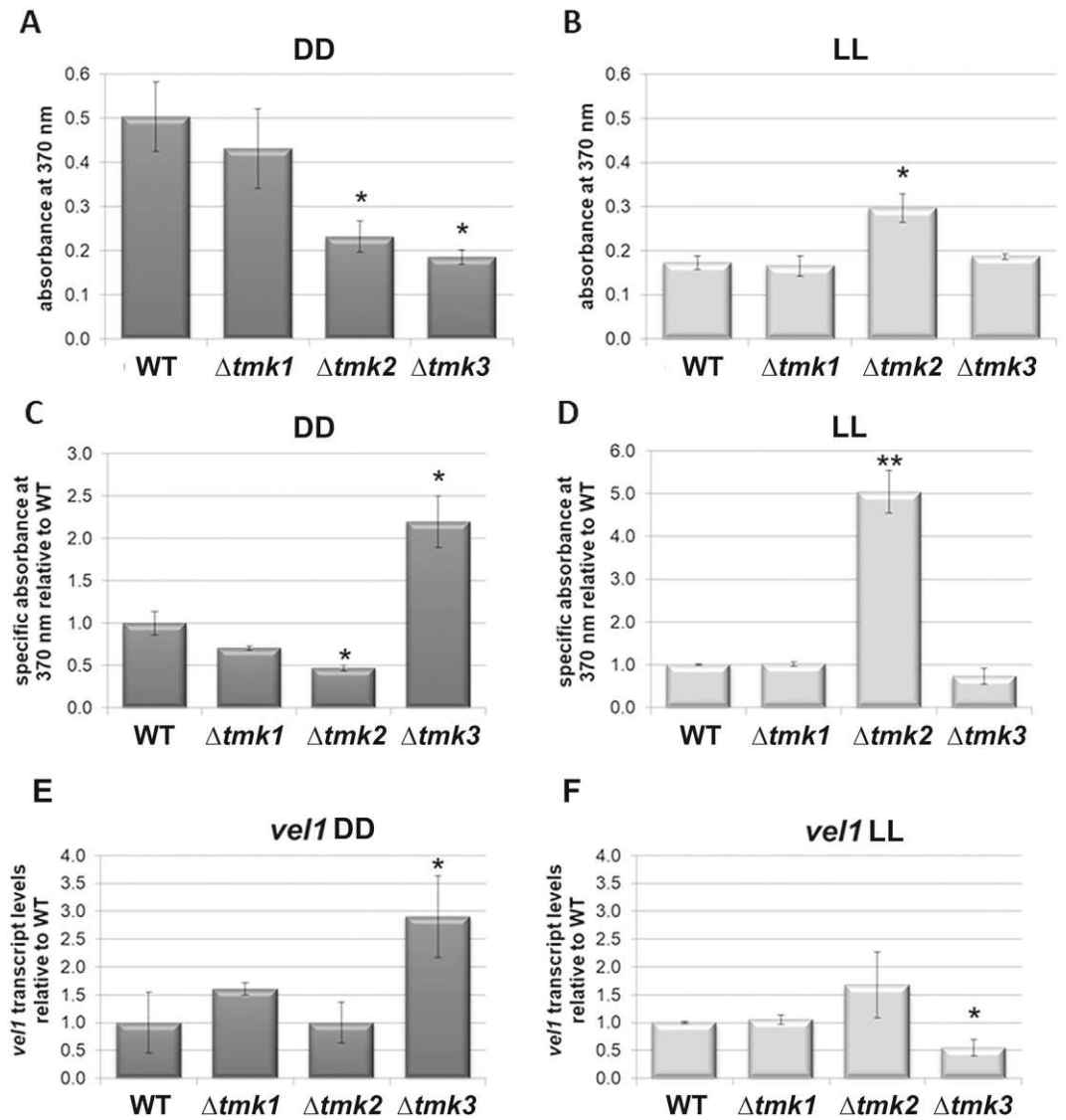
Figure 3. Relevance of MAPkinases for sorbicillin production and genes involved in secondary metabolism. (**A,B**) Evaluation of sorbicillin production as influenced by MAPkinases. Absorbances are shown for 370 nm, which is representative for sorbicillins[90]. (**C,D**) Specific sorbicillin abundance in supernatant as related to biomass formation upon growth on 1% cellulose in (**C**) constant darkness and (**D**) constant light. (**E,F**) Regulation of transcript abundance of *vel1* in MAPkinase mutant strains in (**E**) constant darkness and (**F**) constant light.

kinases for sexual development prompted us to assess their role in chemical communication under conditions facilitating mating.

Our analyses showed that TMK1 is required for production of at least one metabolite, which is also decreased upon lack of TMK3. Deletion of *tmk2* further resulted in a shift of abundance of certain secondary metabolites (Fig. 5). The most striking effect was found for Δ*tmk3* (Fig. 5A) revealing that in this strain the production of all compounds detected in the wild-type was downregulated or abolished. Using a reference compound[95], we could identify the sorbicillin derivative trichodimerol that is strongly regulated by TMK3 (Fig. 5A and Figure S1). Hence, the hypothesis that MAPkinases contribute to regulation of chemical communication of *T. reesei* by secreting (secondary) metabolites to the environment is well supported. However, although a correlation of defects in secondary metabolite secretion with perturbed mating behavior was reported previously[91,94], the precise role of these secondary metabolites in initiation of sexual development still remains to be clarified.

Considering the results for growth in liquid media with cellulose as carbon source, we conclude that MAPkinases represent important signaling cascades, differentially integrating signals with varying relevance upon growth on different carbon sources, on surfaces or submerged and in dependence of light.

MAPkinases regulate production of trichodimerol (21S)-bisorbibutenolid. Besides trichodimerol as product of the SOR cluster, also several other compounds showed alterations in one or more MAPki-
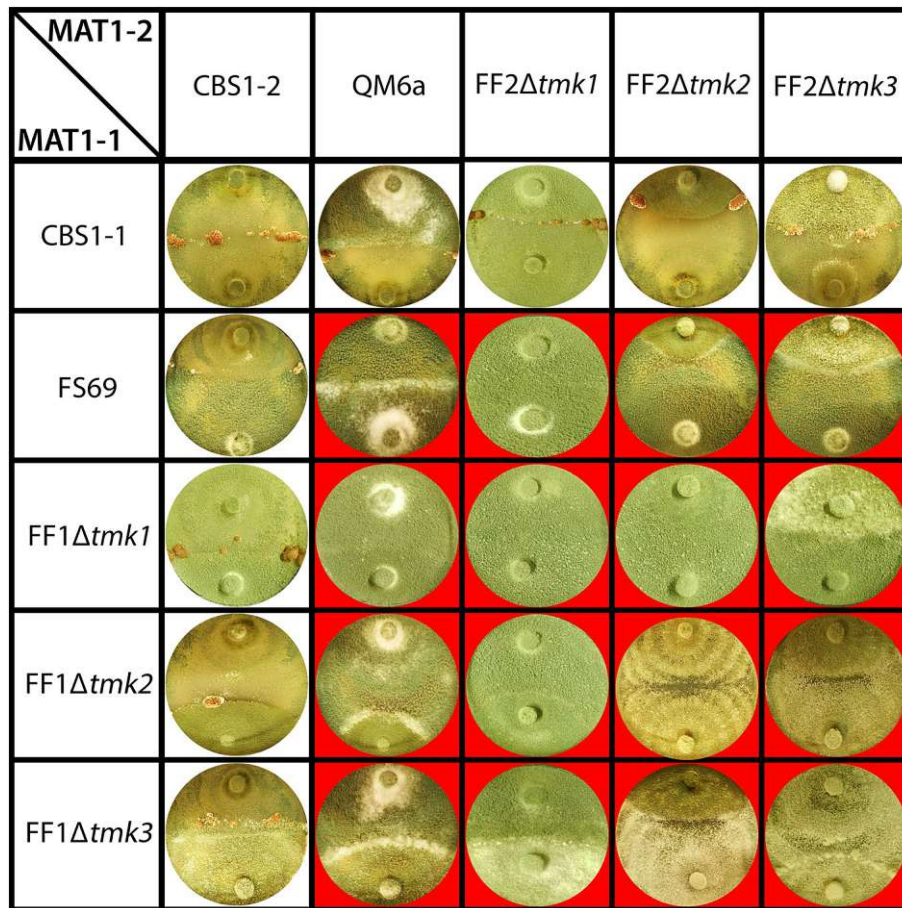
Figure 4. Involvement of MAPkinases in mating abilities. Sexual development of backcrossed MAPkinase mutant strains after 14 days grown in light cycles (12 h light, 12 h darkness) at 22 °C.
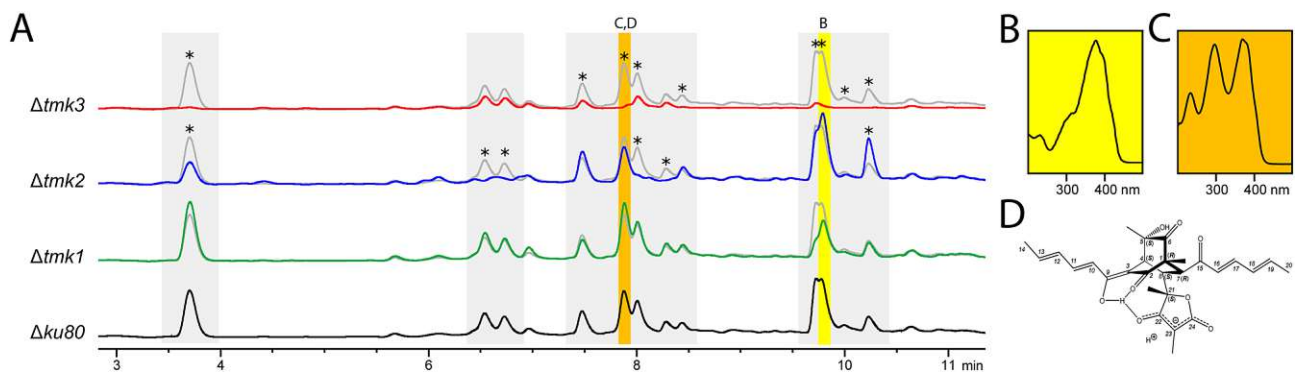
Figure 5. HPLC analysis of MAPK deletion mutants and identification of sorbicillin derivatives. (**A**) Chromatograms of wild-type (Δ*ku80*) and MAPkinase deletion mutants (Δ*tmk1-3*) at 230 nm. Wild type profile is shown in grey for better comparission. Asterisks indicate strongly regulated peaks. Trichodimerol is highlighted in yellow and (21*S*)-bisorbibutenolide in orange. (**B**) UV-spectrum of trichodimerol. (**C**) UV-spectrum of (21*S*)-bisorbibutenolide. (**D**) *(21S)-bisorbibutenolide*[98]. Numbering of protons and carbons is shown in Fig. 5D and in agreement with those used previously[98].

nase deletion strains. Hence, we were interested in the nature of these compounds and aimed at isolation and structural elucidation of one strongly regulated and hence the most interesting changing peak. Due to the complexity of different structures of sorbicillinoids, which nevertheless show similar UV spectra, we aimed to purify a compound of interest to enable unequivocal assignment of the structure.

2.8 The yellow color of the compound selected for detailed anaysis revealed that it is likely to be a sorbicilliniod and mass spectrometry indicated a similarity with bisorbibutenolide, which required more indepth investigation

for confirmation. (21S)-bisorbibutenolide (Fig. 5B–D), isolated from extract of *T. reesei*, shows in HR-ESI-TOF-MS in negative ionization a deprotonated molecular ion [M–H]$^-$ of *m/z* 495.2033, and a [M + Na]$^+$ of *m/z* 519.1980 in positive ionization mode. This correlates quite well with the calculated [M–H]$^-$ of *m/z* 495.2024 and [M + Na]$^+$ of *m/z* 519.1989 of the molecular formula $C_{28}H_{32}O_8$. 1D and 2D NMR measurements led to a total number of six methyl-, zero methylen-, eleven methine groups and eleven quaternary carbon atoms resulting in three additional non carbon bound protons. Further investigations of the UV and NMR spectroscopic as well as MS spectrometric data imply a molcular structure of an unsymetric dimer of sorbicillinol.

The central moiety of this dimer is identified as a bicyclo[2.2.2]octane sleketon. This structure can be determined in HMBC by the $^2J_{C-H}$ and $^3J_{C-H}$ couplings of protons in its positions 4, 7 and 8 as well as of the protons in two methyl substituents in positions 1 and 5 (Fig. 5B). Namely, the methyl group at position 1 shows couplings to the carbons C-1, C-2, C-6 and C-7 while the methyl group at position 5 shows couplings to C-4, C-5 and C-6. Protons H-4, H-7 and H-8 each show eight or nine C-H long range couplings to the corresponding carbons via two or three covalent bonds, respectively (Figure S2). Some of these couplings even reach to carbon atoms in substituents which are bound to the bicyclo[2.2.2]octane sleketon. Additionally, chemical shifts of δC 210.7 and 197.4 as well as the multiplicities of carbons C-2 and C-6 indicate the presence of ketone functionalities in these positions. Furthermore, the chemical shift and the multiplicity of C-5 indicate that attached apart from the methyl group there is a hydroxy group bound in this position.

A (*E,E*)-hexa-2,4-dienoyl (sorbyl) substituent is attached in position 7 to the bicyclo[2.2.2]octane. This substituent can be identified by $^3J_{H-H}$ couplings in COSY (Figure S3) as well as in HSQC by the $^{2,3}J_{C-H}$ couplings within this moity and to the methine group in position 7 (Figure S2). The *E* configurations of both double bonds result in particular from the quite large $^3J_{H-H}$ coupling constants between the sp^2 hybridised methin groups. An second (*E,E*)-hexa-2,4-dienoyl substituent can be identified to be bound in position 3. However, this moiety is predominately present as enol tautomer between C-9 and C-3, which emerges of the chemical shifts and multiplicities of these two carbon atoms. The presence of these two diene conjugated carbonyl chromophores can be confirmed by UV absorption at 372 nm (Figure S4). Furthermore, an enolized 3-oxo-2,4-dimethylbutanolide ring is bound to C-8. The carbon skeleton of this moiety can be identified by the $^2J_{C-H}$ and $^3J_{C-H}$ couplings of the protons in methyl groups bound to C-21 and C-23. The chemical shifts of C-22, C-23 and C-24 (δC 188.8, 92.3 and 180.2, respectively) further clearly indicate the enolization in this structural moiety.

The relative stereochemistry of (21S)-bisorbibutenolide was determined using NOEs recorded in the NOESY spectrum (Figure S5). The stereochemistry at positions 4, 5, 7 and 8 in the bicyclo[2.2.2]octane sleketon can especially be explained by NOEs between the CH$_3$ group at C-5 and the protons H-10 and H-11 as well as by the missing NOEs from this methyl group to H-7 and H-8. Furthermore, H-8 shows an NOE to H-16 as well as H-7 has an NOE to the methyl group at position 21. The absolute stereochemistry was deduced on the stereochemistry of *S*-sorbicillinol, which is yet only repored enantiomer of this natural product[96] (Scifinder, 2022). It results in the (1R,4S,5S,7R,8S)-bisorbibutenolide for the stereocenters in the central moiety (Fig. 5C), which are in agreement with those reported earlier[97,98] for the same molecular structure. Furthermore, the stereochemistry at position 21 in the butanolide moiety was determined with regard to Maskey et al.[98]. They have shown that an 21S configuration causes the deprotonation of the OH group in position 22 with a concomitant enolisation of C-22, C-23 and C-24. This is caused by a spatial proximity of the deprotonated hydroxy group at C-22 to the hydroxy group at C-9 as well as to the ketone at C-3. In case of a 21R configuration, such deprotonation occures to a significantly lesser extent, since the described spatial proximity between C-3, C-9 and C-22 is not possible.

Overall, the structure is those of (21S)-bisorbutenolide, which is shown in Fig. 5D. All recorded spectroscopic data are summarized in section "Materials and Methods" and the spectra are shown in the Supplementary Material (Figures S2–S11). These data are consistent with those reported by Maskey et al.[98] for (21S)-bisorbutenolide as well as well as with those reported by[97] for the structurally identical "trichotetronine". Thus, we assume that all three independently determined structures are identical.

Discussion

Fungi have to react to multiple environmental cues to succeed in competition in order to balance resources between investment in biomass formation and colonization, reproduction and warfare—production of secondary metabolites to defend nutrients, mating partners and reproductive structures. Our study revealed that the MAPkinase pathways of *T. reesei* are central to regulation of these tasks, as they differentially integrate signals and coordinately rather than separately modulate their output pathways (Fig. 6). The different functions, which TMK1, TMK2 and TMK3 assume are all influenced by light. This is in perfect agreement with the crucial functions of their homologues in light response and circadian clocks in other fungi. Importantly, the MAPkinase pathway acts downstream of the circadian clock and hence also of the photoreceptor complex members as its core components[28,99]. Thereby, the MAPkinases obviously provide important information on the environment which are integrated with the light signals perceived by photoreceptors to achieve an appropriate response in light or darkness.

For TMK1 we see a small, but significant increase in specific cellulase activity in darkness and a corresponding trend in slightly elevated *cbh1* and *xyr1* transcript levels, while in light *cbh1* transcript levels decrease, which may have contributed to the lack of detection of an effect of TMK1 in previous work[75].

TMK2 negatively influences cellulase expression upon growth on wheat bran combined with Avicel. However, biomass formation of this strain is unclear and data on specific activity are not available in this study[74]. Deletion of *tmk2* caused decreased growth in the presence of lactose and glucose, but not glycerol in *T. reesei*[77]. We could now confirm the negative impact of TMK2 on cellulase regulation in *T. reesei* upon growth on cellulose. This regulatory effect is reflected in an increase of transcript abundance of *cbh1* and *xyr1* as well as a positive trend in specific cellulase activity in Δ*tmk2*. The previously detected only minor effect of TMK2 on *cbh1* transcript abundance
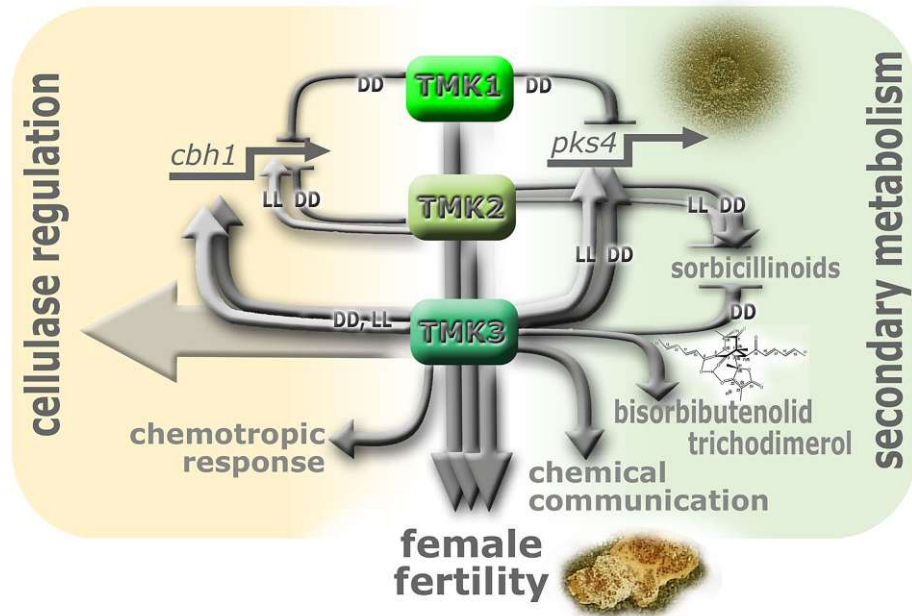
Figure 6. Schematic representation of the involvement of the MAPKinases, TMK1, TMK2 and TMK3 in sexual development (female fertility), cellulase regulation and secondary metabolism in constant light (LL) and constant darkness (DD). The figure was designed in Adobe Photoshop CS6 by MoS.

may be due to the uncontrolled light conditions during cultivation: Since we observed a clear increase of *cbh1* in Δ*tmk2* in darkness and a decrease in light, what previously was found, may well be a mixture of these effects.

In case of TMK3 our results for cellulase regulation are in agreement with previous data[76], although also here the regulation pattern we observed is more severe, with activity and transcript levels barely detectable anymore. Again, random light pulses during cultivation and harvesting may have alleviated the strongly decreased values we found.

MAPkinases are well known to act at higher levels of the signaling cascade, above the transcription factors of the downstream pathways, which may be impacted directly by phosphorylation or indirectly be regulation of positive or negative factors influencing them. However, a potential feedback regulation acting via a nutrient sensing pathway might still influence regulation of MAPkinase genes at the transcriptional level. We therefore checked available transcriptome data from comparable conditions for indications if such a feedback might exist[50,100–102], but since we did not find significant regulation of *tmk1, tmk2* or *tmk3* in these data, we conclude that this is not the case.

Interestingly, in *N. crassa* the OS pathway, corresponding to the Hog1-pathway in yeast and comprising a homologue of TMK3 has no significant influence on cellulase production[103], which is in contrast to our results.

In summary, our data obtained with experiments under controlled light conditions clearly show a light dependent regulatory function of all three MAPkinases on cellulase gene regulation and secreted cellulase activity, which is jeopardized by random light pulses.

The GPCR CSG1, which is essential for the chemotropic response of *T. reesei* to glucose[84], was shown to be required for posttranscriptional regulation of cellulase gene expression[78]. Importantly, this GPCR is not related to other known glucose sensing GPCRs like GPR-1 in *N. crassa* or Gpa2 of *S. cerevisiae*[78]. In contrast, the function of CSG1 as a member of class XIII of GPCRs was for the first time characterized as posttranscriptional regulation of cellulases[78]. Here we found that also TMK3 is needed for the chemotropic response to glucose, although here, in contrast to the situation with CSG1[78], not only cellulase activity, but also transcript abundance decrease strongly (Fig. 2B,C). Hence, we assume that perturbed chemotropic reaction to glucose does not necessarily correlate with diminished cellulase transcript abundance, but is likely to be important for regulating the amount of produced cellulases at different levels.

Interestingly, research with *F. oxysporum* showed a dependence of the chemotropic response to glucose on TMK1[22], which we did not observe and the relevance of TMK3 on this process was not studied yet. Due to the different habitats and ecological functions of these two fungi—*F. oxysporum* being a plant pathogen and *T. reesei* mainly a saprotroph—glucose sensing may have a different relevance in these fungi. However, the widespread presence and conservation of MAPkinase pathways from yeast to man rather speaks against such a hypothesis and the reason for this discrepancy remains to be investigated.

We found that the glucose signal is transmitted via the class XIII GPCR CSG1, which is also essential for the chemotropic response to glucose[84]. Our results for TMK3 reveal, that this chemotropic response is not exclusively channeled through the heterotrimeric G-protein pathway, but also through the MAPkinase pathway. Hence, a potential role of biased GPCR signaling[85] in the chemotropic response to glucose is worth exploring in *T. reesei*.

Female sterility is defined as the inability to assume the female role during sexual development and can have diverse physiological reasons[104] including a defect in hyphal fusion, for example due to mutations in the *ham5* gene[105,106]. In fungi like *N. crassa*, formation of protoperithecia is induced in the female strain prior to fertilization with conidia of the male strain to assess male and female fertility. In *T. reesei* this method is not applicable, because no growth condition is known under which such structures are formed. Consequently, tests for male or female fertility are performed by assessment of mating and fruiting body formation with strains comprising a female sterile strain background in addition to the deletion of the gene of interest or as mating partners[63]. Defects in sexual development due to lack of MAPkinases were shown for all three pathways in *N. crassa*[107] as well as in other fungi. Sexual development is consistently impacted by all three MAPkinases in *T. reesei*, which are obviously responsible for the ability to mate with a partner having a defect in female fertility such as mutations in HAM5. HAM5 acts as a scaffolding protein for MAPkinase pathways and is crucial for their function[106]. Consequently, the phenotype we see upon deletion of *tmk1*, *tmk2* and *tmk3* is in agreement with the female fertility caused by the pathway involving HAM5, which is also responsible for the sexual defect of *T. reesei* QM6a[64,65,67].

Since at least the TMK1 and TMK2 mutant strains in *S. macrospora* and *N. crassa* are fusion mutants as are those lacking HAM5[105,108], it would not be without precedent if the sexual defect of the *T. reesei* MAPkinases were due to abolished ability of hyphal fusion in these strains as well.

Carbon catabolite repression was recently reported to be impacted by the high osmolarity MAPK pathway, which contributes to a protein complex regulating CreA cellular localization and dissociates upon addition of glucose[109]. In *N. crassa*, genetic and omics analyses showed that the MAPkinase pathway is not acting through the canonical carbon catabolite repressor CRE-1[103]. Hence, the minor changes in transcript abundance we found for regulation of *T. reesei cre1* by MAPkinases in light gives a hint to their relevance, but does not reflect the full mechanism of regulation, which may be considerably more significant at the protein- and interaction level also in *T. reesei*. However, the abolished chemotropic response to glucose in a strain lacking TMK3 suggests that the Hog pathway may be connected to glucose signal transmission also in *T. reesei*. Additionally, the differences between light and darkness we see in our experiments indicate that both conditions should be investigated in fungi to obtain a comprehensive picture.

As previously shown in *T. reesei*, interaction with potential mating partners of opposite mating types involves specifically changing secondary metabolite patterns[91,94]. We chose conditions enabling sexual development for our assay to enable conclusions as to altered chemical communication by strains lacking one of the MAPkinases. Among the compounds regulated via TMK3 is the sorbicillinoid bisorbibutenolide[110]. Bisorbibutenolid (or bislongiquinolide) deters the aphid *Schizaphis graminum* from feeding[111] and showed significant growth inhibitory activity against cancer cell lines through cytostatic and not cytotoxic effect[112]. The production of bisorbibutenolide is hence likely to be aimed at fending off competitors, which is in agreement with findings in *T. atroviride* on larvae preferentially feeding on *tmk3* mutants[73]. However, the SOR cluster , which is mainly responsible for sorbicillinoid production in *T. reesei*, was acquired through lateral gene transfer and is subject to strong evolutionary selection[113]. This cluster is not present in *T. atroviride* and consequently, a conservation of this phenomenon between *T. reesei* and *T. atroviride* remains to be shown.

Materials and methods

Strains and cultivation conditions.
The wild-type strain used in this study is QM6aΔ*ku80*[50] (deficient in non-homologous end joining). For analysis of gene regulation, enzymatic activity and biomass formation by TMK1, TMK2 and TMK3 strains were grown in liquid cultivation in constant light (white light; 1700 lx) or constant darkness, 200 rpm and 28 °C for 96 h. Before inoculation, strains were grown on 3% (w/v) malt extract (MEX) agar plates in constant darkness for 14 days (to exclude influences by the circadian rhythm). For liquid culture 10⁹ conidia/L were inoculated in Mandels Andreotti minimal medium[114] with 1% (w/v) microcrystalline cellulose (Alfa Aesar, Karlsruhe, Germany) as carbon source, 5 mM urea and 0.1% peptone to induce germination. After 96 h, mycelia and supernatants were harvested, for the constant darkness cultures only a very low red safety light (darkroom lamp, Philips PF712E, red, 15W) was used as single light source.

Construction of recombinant strains.
Deletion of *tmk1*, *tmk2* and *tmk3* was done in QM6aΔ*ku80* following the procedure as described previously[80] with the hygromycin (*hph*) marker cassette constructed by yeast recombination of the 1 kb flanking regions up- and downstream of the gene of interest and the *hph* marker. Transformation was done by protoplasting and 50 µg/mL hygromycin B as selection reagent (Roth, Karlsruhe, Germany)[115]. Protoplasts were isolated three to six days after transformation and subjected to a minimum of two rounds of single spore isolation. Successful deletion was confirmed by the absence of the gene by PCR (Table S1). All three mutants were confirmed to only have a single integration of the deletion cassette by copy number determination[102].

Crossing and selection for fully fertile progeny for assessment of sexual development.
All crosses for the analysis of sexual development were performed on 60 mm 2% MEX agar plates at 22 °C and 12 h light–dark cycles as previously described[116]. To obtain progeny carrying the deletion in both mating types with a functional *ham5* gene, the mutant strains in the QM6a (MAT1-2, defective *ham5* copy) background were crossed with the female fertile strain FF1 (MAT1-1, functional *ham5* copy). The FF1 strain was obtained from backcrossing the female fertile strain CBS999.97 (described in detail previously[65]) 10 times with QM6a to acquire sexual fertility while retaining the QM6a phenotype[91]. Ascospore derived progeny were analyzed for the presence of gene deletion and mating type by PCR (Table S1). The functionality of the *ham5* gene was confirmed by high resolution melt curve (HRM) analysis, performed as described previously[117].

Isolation of nucleic acids and RTqPCR.   Isolation of RNA was done from mycelia from liquid culture using the Qiagen RNeasy Plant mini kit following the manufacture's guidelines. After DNase digest (ThermoFisher) of 1 µg total RNA and cDNA synthesis (GoScript reverse transcriptase, Promega, Madison, WI, USA), RT-qPCR was performed using the GoTaq® qPCR Master Mix (Promega) as previously described with *sar1* as reference gene and other primers listed in Table S1[94,118]. For RT-qPCR three biological and three technical replicates were considered, for *cbh1*, twice three technical replicates were included and for the analysis CFX maestro analysis software was used. Isolation of DNA for mutant and progeny screening, was done following the rapid minipreparation protocol for fungal DNA as described previously[119].

Analysis of enzyme activity and biomass formation.   Enzymatic activity was measured from supernatants of liquid cultures using the CMC-cellulose kit (S-ACMC-L Megazyme) measuring endo-1, 4-ß-D-glucanases. For specific cellulase activities, the activities were correlated with the biomass produced which was determined from frozen mycelia in the presence of insoluble cellulose[45]. Shortly, mycelia were frozen in liquid nitrogen and ground with pestle and mortar before sonification and incubation in 0.1 M NaOH to break up cells. The freed protein content was measured using the Bradford method.

Chemotropic response assay.   Analysis of chemotropism assay was done essentially as described previously[22] except that the water agar was supplemented with 0.0025% peptone as optimized previously[84]. The chemoattractant (1% glucose) was applied onto the plates in comparison with water as a control on the opposite side. The orientation of germ tubes was determined under the microscope (VisiScope TL524P microscope; $200 \times$ magnification) and chemotropic indices calculated from a minimum of 3 biological replicates, counting a minimum of 400 germ tubes per plate, as previously described[22].

Photometric analysis of sorbicillinoid production.   Supernatants of liquid cultivation were centrifuged for 5 min at 10.000 g to remove residual cellulose and absorbance at 370 nm indicative yellow sorbicillinoids were measured from biological triplicates.

Isolation of (21S)-bisorbibutenolide.   The dry crude extract (350 mg) was dissolved in 2 mL pure methanol (MeOH) and the obtained suspension centrifuged ar 14,000 rpm for 3 min. The supernatant was subsequently subjected to column chromatography over Sephadex LH20 eluted isocratically with pure MeOH. A total of 30 fractions á 5 mL were collected. Fractions 17 to 21 were pooled (11.3 mg) and finally purified by preparative thin layer chromatography (precoated glass plates, silica gel 60, F_{254}, 0.25 mm thickness) developed in $CHCl_3$/MeOH (95:5). This step afforded 4.3 mg of (21S)-bisorbibutenolide. All separation steps were monitored by HPLC.

Secondary metabolite analysis by HPLC.   For the extraction of secondary metabolites, strains were grown on 3% malt extract medium in constant darkness for 14 days. For each strain three biological replicates were used. For each sample, two agar plugs of 1,8 cm^2 were taken from 3 plates. Agar plugs were collected in 15 mL tubes and 3 mL of 50% acetone in water (v/v) was added and put into an ultrasonic bath for 15 min for better dilution. Subsequently 1 mL of chloroform was added. Tubes were then centrifuged at 4 °C at 1000 g for 1 min for phase separation. The organic phase was transferred to a glass vial and chloroform extraction was repeated twice before the vials were left for evaporation over night. The dry extracts were redissolved in 140 µL methanol and stored in glass vials at − 20 °C before analysis.

Analytical HPLC measurements were performed on Agilent 1100 series coupled with UV-diode array detection at 230 nm and a Hypersil BDS column (100×4 mm, 3 µm grain size). An aq. buffer (15 mM H3PO4 and 1.5 mM Bu4NOH) (A) and MeOH (B) was used as eluents. The following elution system was applied: From 55–95% B within 8 min, and 95% B was kept for 5.0 min, with a flow rate of 0.5 mL min^{-1}. The injection volume was 5.0 µL.

Statistics.   Statistical significance was evaluated by the t-test in R-studio (compare means, ggpubr version 0.4.0) **p value < 0.01, *p value < 0.05. At least three biological replicates were considered in every assay.

NMR spectroscopy.   For NMR spectroscopic measurements (21S)-bisorbibutenolide was dissolved in CD_3OD (~ 4.2 mg in 0.7 mL) and transferred into 5 mm high precision NMR sample tubes. All spectra were measured on a Bruker DRX-600 at 600.18 MHz (^{1}H) or 150.91 MHz (^{13}C) and performed using the Topspin 3.5 software. Measurement temperature was 298 K ± 0.05 K. 1D spectra were recorded by acquisition of 64 k data points and Fourier transformed spectra were performed with a range of 7200 Hz (^{1}H) and 32,000 Hz (^{13}C), respectively. To determine the 2D COSY, TOCSY, NOESY, HMQC, and HMBC spectra 128 experiments with 2048 data points each were recorded, zero filled and Fourier transformed to 2D spectra with a range of 6000 Hz (^{1}H) and 24,000 Hz (HSQC) or 32,000 Hz (HMBC) (^{13}C), respectively. Residual CD_2HOD was used as internal standard for ^{1}H NMR measurements (δH 3.34) and CD_3OD for ^{13}C NMR measurements (δC 49.0).

Mass spectrometry.   Mass spectra were measured on a high resolution time-of-flight (hr-TOF) mass spectrometer (maXis, Bruker Daltonics) by direct infusion electrospray ionization (ESI) in positive and negative ionization mode (mass accurancy +/− 5 ppm). TOF MS measurements have been performed within the selected mass range of m/z 100–2500. ESI was made by capillary voltage of 4 kV to maintain a (capillary) current between 30 and 50 nA. Nitrogen temperature was maintained at 180 °C using a flow rate of 4.0 L min^{-1} and the N_2 nebulizer gas pressure at 0.3 bar.

Spectroscopic data for (21S)-bisorbibutenolide[98]. UV$_{max, MeOH}$, 234, 298, 372 nm; HR ESI-MS m/z 495.2033 [M–H]$^-$ (calcd for $C_{28}H_{31}O_8^-$, 495.2024), m/z 519.1980 [M + Na]$^+$ (calcd for $C_{28}H_{32}O_8Na^+$, 519.1989); ^{1}H NMR (600 MHz, CD$_3$OD): δ_H = 7.35 (1H, dd, J = 14.7, 11.7 Hz, H-11), 7.26 (1H, dd, J = 11.8, 11.0 Hz, H-17), 6.41 (1H, m, H-19), 6.40 (1H, m, H-13), 6.38 (1H, m, H-12), 6.37 (1H, m, H-18), 6.32 (1H, d, J = 14.7 Hz, H-10), 6.16 (1H, d, J = 11.8 Hz, H-16), 3.41 (1H, m, H-7), 3.35 (1H, m, H-4), 3.17 (1H, m, H-8), 1.89 (3H, d, J = 6.7 Hz, H-14), 1.88 (3H, d, J = 6.7 Hz, H-20), 1.42 (3H, s, CH$_3$-23), 1.35 (3H, s, CH$_3$-21), 1.18 (3H, s, CH$_3$-5), 0.94 (3H, s, CH$_3$-1); ^{13}C NMR (150 MHz, CD$_3$OD): δ_C = 210.7 (s, C-6), 203.9 (s, C-15), 197.4 (s, C-2), 188.8 (s, C-22)*, 180.2 (s, C-24)*, 169.4 (s, C-9), 148.0 (d, C-17), 144.8 (d, C-19), 143.1 (d, C-11), 140.3 (d, C-13), 132.4 (d, C-18), 131.7 (d, C-12), 128.9 (d, C-16), 119.2 (d, C-10), 110.4 (s, C-3), 92.3 (s, C-23), 85.0 (s, C-21), 75.9 (s, C-5), 63.8 (s, C-1), 51.8 (d, C-7), 43.9 (d, C-8), 43.7 (d, C-4), 24.0 (q, CH$_3$-5), 23.2 (q, CH$_3$-21), 19.0 (q, C-20), 18.9 (q, C-14), 11.4 (q, CH$_3$-1), 6.4 (q, CH$_3$-23); * determined via HMBC.

Numbering of protons and carbons is shown in Fig. 5D and in agreement with those used previously[98]. All data as well as the naming of the compound are in agreement with those reported earlier for this compound[97,98], (there named as "trichotetronine"). It should be noted that the naming of this compound, particularly with regard to the stereochemistry at position 21, as well as of structurally and biosynthetically closely related compounds are not entirely consistent throughout the entire literature. 1D and 2D NMR spectra are shown in Figures S2, S3 and S5–S9, HR ESI MS spectra (pos. and neg. mode) are shown in Figure S10,S11, and chromatogram as well as UV spectrum are shown in Figure S4.

Data availability

The datasets generated and analysed during the current study are available from the corresponding author on reasonable request.

References

1. Fischer, R., Aguirre, J., Herrera-Estrella, A. & Corrochano, L. M. The complexity of fungal vision. *Microbiol. Spectr.* **4**, 4–6. https://doi.org/10.1128/microbiolspec.FUNK-0020-2016 (2016).
2. Corrochano, L. M. Light in the fungal world: From photoreception to gene transcription and beyond. *Annu. Rev. Genet.* **53**, 149–170. https://doi.org/10.1146/annurev-genet-120417-031415 (2019).
3. Avruch, J. MAP kinase pathways: The first twenty years. *Biochim. Biophys. Acta* **1773**, 1150–1160. https://doi.org/10.1016/j.bbamcr.2006.11.006 (2007).
4. Martinez-Soto, D. & Ruiz-Herrera, J. Functional analysis of the MAPK pathways in fungi. *Rev. Iberoam. Micol.* **34**, 192–202. https://doi.org/10.1016/j.riam.2017.02.006 (2017).
5. Lengeler, K. B. *et al.* Signal transduction cascades regulating fungal development and virulence. *Microbiol. Mol. Biol. Rev.* **64**, 746–785 (2000).
6. Medina-Castellanos, E. *et al.* Danger signals activate a putative innate immune system during regeneration in a filamentous fungus. *PLoS Genet.* **14**, e1007390. https://doi.org/10.1371/journal.pgen.1007390 (2018).
7. Roman, E., Arana, D. M., Nombela, C., Alonso-Monge, R. & Pla, J. MAP kinase pathways as regulators of fungal virulence. *Trends Microbiol* **15**, 181–190 (2007).
8. Turra, D., Segorbe, D. & Di Pietro, A. Protein kinases in plant-pathogenic fungi: Conserved regulators of infection. *Annu. Rev. Phytopathol.* **52**, 267–288. https://doi.org/10.1146/annurev-phyto-102313-050143 (2014).
9. Frawley, D. & Bayram, O. The pheromone response module, a mitogen-activated protein kinase pathway implicated in the regulation of fungal development, secondary metabolism and pathogenicity. *Fungal Genet. Biol.* **144**, 103469. https://doi.org/10.1016/j.fgb.2020.103469 (2020).
10. Valiante, V. The cell wall integrity signaling pathway and its involvement in secondary metabolite production. *J. Fungi (Basel)* **3**, 68. https://doi.org/10.3390/jof3040068 (2017).
11. Hohmann, S. An integrated view on a eukaryotic osmoregulation system. *Curr. Genet.* **61**, 373–382. https://doi.org/10.1007/s00294-015-0475-0 (2015).
12. Gustin, M. C., Albertyn, J., Alexander, M. & Davenport, K. MAP kinase pathways in the yeast Saccharomyces cerevisiae. *Microbiol. Mol. Biol. Rev.* **62**, 1264–1300 (1998).
13. Gonzalez-Rubio, G., Fernandez-Acero, T., Martin, H. & Molina, M. Mitogen-activated protein kinase phosphatases (MKPs) in fungal signaling: Conservation, function, and regulation. *Int. J. Mol. Sci.* **20**, 1709. https://doi.org/10.3390/ijms20071709 (2019).
14. Tian, T. & Harding, A. How MAP kinase modules function as robust, yet adaptable, circuits. *Cell Cycle* **13**, 2379–2390. https://doi.org/10.4161/cc.29349 (2014).
15. Serrano, A. *et al.* Spatio-temporal MAPK dynamics mediate cell behavior coordination during fungal somatic cell fusion. *J. Cell Sci.* **131**, jcs213462. https://doi.org/10.1242/jcs.213462 (2018).
16. Ma, L. *et al.* Fus3, as a critical kinase in MAPK cascade, regulates aflatoxin biosynthesis by controlling the substrate supply in *A. flavus*, rather than the cluster genes modulation. *Microbiol. Spectr.* **10**, e0126921. https://doi.org/10.1128/spectrum.01269-21 (2022).
17. Tumukunde, E. *et al.* Osmotic-adaptation response of sakA/hogA gene to aflatoxin biosynthesis, morphology development and pathogenicity in *A. flavus*. *Toxins (Basel)* **11**, 41. https://doi.org/10.3390/toxins11010041 (2019).
18. Clark-Cotton, M. R., Jacobs, K. C. & Lew, D. J. Chemotropism and cell-cell fusion in fungi. *Microbiol. Mol. Biol. Rev.* **86**, e0016521. https://doi.org/10.1128/mmbr.00165-21 (2022).
19. Leeder, A. C., Palma-Guerrero, J. & Glass, N. L. The social network: Deciphering fungal language. *Nat. Rev. Microbiol.* **9**, 440–451. https://doi.org/10.1038/nrmicro2580 (2011).
20. Fleissner, A. & Herzog, S. Signal exchange and integration during self-fusion in filamentous fungi. *Semin. Cell Dev. Biol.* **57**, 76–83. https://doi.org/10.1016/j.semcdb.2016.03.016 (2016).
21. Nordzieke, D. E., Fernandes, T. R., El Ghalid, M., Turra, D. & Di Pietro, A. NADPH oxidase regulates chemotropic growth of the fungal pathogen *Fusarium oxysporum* towards the host plant. *New Phytol.* **224**, 1600–1612. https://doi.org/10.1111/nph.16085 (2019).
22. Turra, D., El Ghalid, M., Rossi, F. & Di Pietro, A. Fungal pathogen uses sex pheromone receptor for chemotropic sensing of host plant signals. *Nature* **527**, 521–524. https://doi.org/10.1038/nature15516 (2015).

23. Fleissner, A., Leeder, A. C., Roca, M. G., Read, N. D. & Glass, N. L. Oscillatory recruitment of signaling proteins to cell tips promotes coordinated behavior during cell fusion. *Proc. Natl. Acad. Sci. USA* **106**, 19387–19392. https://doi.org/10.1073/pnas.0907039106 (2009).

24. Haj Hammadeh, H. *et al.* A dialogue-like cell communication mechanism is conserved in filamentous ascomycete fungi and mediates interspecies interactions. *Proc. Natl. Acad. Sci. USA* **119**, e2112518119. https://doi.org/10.1073/pnas.2112518119 (2022).

25. Diernfellner, A. C. R. & Brunner, M. Phosphorylation timers in the *Neurospora crassa* circadian clock. *J. Mol. Biol.* **432**, 3449–3465. https://doi.org/10.1016/j.jmb.2020.04.004 (2020).

26. Dunlap, J. C. & Loros, J. J. Making time: Conservation of biological clocks from fungi to animals. *Microbiol. Spectr.* https://doi.org/10.1128/microbiolspec.FUNK-0039-2016 (2017).

27. Schafmeier, T. & Diernfellner, A. C. Light input and processing in the circadian clock of *Neurospora*. *FEBS Lett.* **585**, 1467–1473. https://doi.org/10.1016/j.febslet.2011.03.050 (2011).

28. Goldsmith, C. S. & Bell-Pedersen, D. Diverse roles for MAPK signaling in circadian clocks. *Adv. Genet.* **84**, 1–39. https://doi.org/10.1016/B978-0-12-407703-4.00001-3 (2013).

29. Vitalini, M. W. *et al.* Circadian rhythmicity mediated by temporal regulation of the activity of p38 MAPK. *Proc. Natl. Acad. Sci. USA* **104**, 18223–18228 (2007).

30. Hurley, J. M. *et al.* Circadian proteomic analysis uncovers mechanisms of post-transcriptional regulation in metabolic pathways. *Cell Syst.* **7**, 613-626 e615. https://doi.org/10.1016/j.cels.2018.10.014 (2018).

31. Xiong, Y. *et al.* The proteome and phosphoproteome of *Neurospora crassa* in response to cellulose, sucrose and carbon starvation. *Fungal Genet. Biol.* **72**, 21–33. https://doi.org/10.1016/j.fgb.2014.05.005 (2014).

32. Hurley, J. M., Loros, J. J. & Dunlap, J. C. The circadian system as an organizer of metabolism. *Fungal Genet. Biol.* **90**, 39–43. https://doi.org/10.1016/j.fgb.2015.10.002 (2016).

33. Caster, S. Z., Castillo, K., Sachs, M. S. & Bell-Pedersen, D. Circadian clock regulation of mRNA translation through eukaryotic elongation factor eEF-2. *Proc. Natl. Acad. Sci. USA* **113**, 9605–9610. https://doi.org/10.1073/pnas.1525268113 (2016).

34. Yu, Z., Armant, O. & Fischer, R. Fungi use the SakA (HogA) pathway for phytochrome-dependent light signalling. *Nat. Microbiol.* **1**, 16019. https://doi.org/10.1038/nmicrobiol.2016.19 (2016).

35. Bischof, R. H., Ramoni, J. & Seiboth, B. Cellulases and beyond: the first 70 years of the enzyme producer *Trichoderma reesei*. *Microb Cell Fact* **15**, 106. https://doi.org/10.1186/s12934-016-0507-6 (2016).

36. Guzman-Guzman, P., Porras-Troncoso, M. D., Olmedo-Monfil, V. & Herrera-Estrella, A. *Trichoderma* species: Versatile plant symbionts. *Phytopathology* **109**, 6–16. https://doi.org/10.1094/PHYTO-07-18-0218-RVW (2019).

37. Harman, G. E. Multifunctional fungal plant symbionts: New tools to enhance plant growth and productivity. *New Phytol.* **189**, 647–649. https://doi.org/10.1111/j.1469-8137.2010.03614.x (2011).

38. Harman, G. E., Howell, C. R., Viterbo, A., Chet, I. & Lorito, M. Trichoderma species–opportunistic, avirulent plant symbionts. *Nat. Rev. Microbiol.* **2**, 43–56 (2004).

39. Schalamun, M. & Schmoll, M. *Trichoderma*-Genomes and genomics as treasure troves for research towards biology, biotechnology and agriculture. *Front. Fungal Biol.* **in press** (2022).

40. Schmoll, M. *et al.* The genomes of three uneven siblings: Footprints of the lifestyles of three *Trichoderma* species. *Microbiol. Mol. Biol. Rev.* **80**, 205–327. https://doi.org/10.1128/MMBR.00040-15 (2016).

41. Schmoll, M., Esquivel-Naranjo, E. U. & Herrera-Estrella, A. *Trichoderma* in the light of day—Physiology and development. *Fungal Genet. Biol.* **47**, 909–916. https://doi.org/10.1016/j.fgb.2010.04.010 (2010).

42. Carreras-Villaseñor, N., Sanchez-Arreguin, J. A. & Herrera-Estrella, A. H. *Trichoderma*: Sensing the environment for survival and dispersal. *Microbiology* **158**, 3–16. https://doi.org/10.1099/mic.0.052688-0 (2012).

43. Casas-Flores, S., Rios-Momberg, M., Bibbins, M., Ponce-Noyola, P. & Herrera-Estrella, A. BLR-1 and BLR-2, key regulatory elements of photoconidiation and mycelial growth in *Trichoderma atroviride*. *Microbiology* **150**, 3561–3569 (2004).

44. Casas-Flores, S. *et al.* Cross talk between a fungal blue-light perception system and the cyclic AMP signaling pathway. *Eukaryot Cell* **5**, 499–506 (2006).

45. Schmoll, M., Franchi, L. & Kubicek, C. P. Envoy, a PAS/LOV domain protein of *Hypocrea jecorina* (Anamorph *Trichoderma reesei*), modulates cellulase gene transcription in response to light. *Eukaryot Cell* **4**, 1998–2007 (2005).

46. Chen, C. L. *et al.* Blue light acts as a double-edged sword in regulating sexual development of *Hypocrea jecorina* (*Trichoderma reesei*). *PLoS ONE* **7**, e44969. https://doi.org/10.1371/journal.pone.0044969 (2012).

47. Seibel, C., Tisch, D., Kubicek, C. P. & Schmoll, M. ENVOY is a major determinant in regulation of sexual development in *Hypocrea jecorina* (*Trichoderma reesei*). *Eukaryot Cell* **11**, 885–890 (2012).

48. Schmoll, M. Regulation of plant cell wall degradation by light in *Trichoderma*. *Fungal Biol. Biotechnol.* **5**, 10. https://doi.org/10.1186/s40694-018-0052-7 (2018).

49. Hitzenhammer, E. *et al.* YPR2 is a regulator of light modulated carbon and secondary metabolism in *Trichoderma reesei*. *BMC Genom.* **20**, 211. https://doi.org/10.1186/s12864-019-5574-8 (2019).

50. Monroy, A. A., Stappler, E., Schuster, A., Sulyok, M. & Schmoll, M. A CRE1—Regulated cluster is responsible for light dependent production of dihydrotrichotetronin in *Trichoderma reesei*. *PLoS ONE* **12**, e0182530 (2017).

51. Lokhandwala, J. *et al.* Structural biochemistry of a fungal LOV domain photoreceptor reveals an evolutionarily conserved pathway integrating light and oxidative stress. *Structure* **23**, 116–125. https://doi.org/10.1016/j.str.2014.10.020 (2015).

52. Lokhandwala, J. *et al.* A native threonine coordinates ordered water to tune light-oxygen-voltage (LOV) domain photocycle kinetics and osmotic stress signaling in *Trichoderma reesei* ENVOY. *J. Biol. Chem.* **291**, 14839–14850. https://doi.org/10.1074/jbc.M116.731448 (2016).

53. Rodriguez-Iglesias, A. & Schmoll, M. Protein phosphatases regulate growth, development, cellulases and secondary metabolism in *Trichoderma reesei*. *Sci. Rep.* **9**, 10995. https://doi.org/10.1038/s41598-019-47421-z (2019).

54. Garcia-Esquivel, M., Esquivel-Naranjo, E. U., Hernandez-Onate, M. A., Ibarra-Laclette, E. & Herrera-Estrella, A. The *Trichoderma atroviride* cryptochrome/photolyase genes regulate the expression of *blr1*-independent genes both in red and blue light. *Fungal Biol.* **120**, 500–512. https://doi.org/10.1016/j.funbio.2016.01.007 (2016).

55. Schuster, A., Kubicek, C. P., Friedl, M. A., Druzhinina, I. S. & Schmoll, M. Impact of light on *Hypocrea jecorina* and the multiple cellular roles of ENVOY in this process. *BMC Genom.* **8**, 449 (2007).

56. Esquivel-Naranjo, E. U. *et al.* A *Trichoderma atroviride* stress-activated MAPK pathway integrates stress and light signals. *Mol. Microbiol.* **100**, 860–876. https://doi.org/10.1111/mmi.13355 (2016).

57. Park, G., Pan, S. & Borkovich, K. A. Mitogen-activated protein kinase cascade required for regulation of development and secondary metabolism in *Neurospora crassa*. *Eukaryot Cell* **7**, 2113–2122. https://doi.org/10.1128/EC.00466-07 (2008).

58. Hou, Z. *et al.* A mitogen-activated protein kinase gene (*MGV1*) in *Fusarium graminearum* is required for female fertility, heterokaryon formation, and plant infection. *Mol. Plant Microbe Interact.* **15**, 1119–1127. https://doi.org/10.1094/MPMI.2002.15.11.1119 (2002).

59. Xu, J. R., Staiger, C. J. & Hamer, J. E. Inactivation of the mitogen-activated protein kinase Mps1 from the rice blast fungus prevents penetration of host cells but allows activation of plant defense responses. *Proc. Natl. Acad. Sci. USA* **95**, 12713–12718 (1998).

60. Van Thuat, N., Schafer, W. & Bormann, J. The stress-activated protein kinase FgOS-2 is a key regulator in the life cycle of the cereal pathogen *Fusarium graminearum*. *Mol. Plant Microbe Interact.* **25**, 1142–1156. https://doi.org/10.1094/MPMI-02-12-0047-R (2012).

61. Lan, N. *et al.* Coordinated regulation of protoperithecium development by MAP kinases MAK-1 and MAK-2 in *Neurospora crassa. Front. Microbiol.* **12**, 769615. https://doi.org/10.3389/fmicb.2021.769615 (2021).

62. Schmoll, M. *et al.* Introducing or inactivating female fertility in filamentous fungal cells (2013).

63. Hinterdobler, W., Beier, S., S., K. & Schmoll, M. in *Recent Developments in Trichoderma Research New and future developments in microbial biotechnology and bioengineering* (eds. S. Zeilinger, I. Druzhinina, H. B. Singh, & V. K. Gupta), Ch. 9, 185–206 (Elsevier, 2020).

64. Linke, R. *et al.* Restoration of female fertility in *Trichoderma reesei* QM6a provides the basis for inbreeding in this industrial cellulase producing fungus. *Biotechnol. Biofuels* **8**, 155. https://doi.org/10.1186/s13068-015-0311-2 (2015).

65. Tisch, D. *et al.* Omics analyses of *Trichoderma reesei* CBS99997 and QM6a indicate the relevance of female fertility to carbohydrate-active enzyme and transporter levels. *Appl. Environ. Microbiol.* **83**, e01578-17. https://doi.org/10.1128/AEM.01578-17 (2017).

66. Seidl, V., Seibel, C., Kubicek, C. P. & Schmoll, M. Sexual development in the industrial workhorse *Trichoderma reesei. Proc. Natl. Acad. Sci. USA* **106**, 13909-13914. https://doi.org/10.1073/pnas.0904936106 (2009).

67. Schmoll, M. The information highways of a biotechnological workhorse—Signal transduction in *Hypocrea jecorina. BMC Genom.* **9**, 430 (2008).

68. Kumar, A. *et al.* Overlapping and distinct functions of two *Trichoderma virens* MAP kinases in cell-wall integrity, antagonistic properties and repression of conidiation. *Biochem. Biophys. Res. Commun.* **398**, 765–770. https://doi.org/10.1016/j.bbrc.2010.07.020 (2010).

69. Mukherjee, P. K., Latha, J., Hadar, R. & Horwitz, B. A. TmkA, a mitogen-activated protein kinase of *Trichoderma virens*, is involved in biocontrol properties and repression of conidiation in the dark. *Eukaryot Cell* **2**, 446–455 (2003).

70. Viterbo, A., Harel, M., Horwitz, B. A., Chet, I. & Mukherjee, P. K. *Trichoderma* mitogen-activated protein kinase signaling is involved in induction of plant systemic resistance. *Appl. Environ. Microbiol.* **71**, 6241–6246 (2005).

71. Reithner, B. *et al.* Signaling via the *Trichoderma atroviride* mitogen-activated protein kinase Tmk1 differentially affects mycoparasitism and plant protection. *Fungal Genet. Biol.* **44**, 1123–1133 (2007).

72. Moreno-Ruiz, D., Salzmann, L., Fricker, M. D., Zeilinger, S. & Lichius, A. Stress-activated protein kinase signalling regulates mycoparasitic hyphal-hyphal interactions in *Trichoderma atroviride. J. Fungi (Basel)* **7**, 365. https://doi.org/10.3390/jof7050365 (2021).

73. Atriztan-Hernandez, K., Moreno-Pedraza, A., Winkler, R., Markow, T. & Herrera-Estrella, A. *Trichoderma atroviride* from predator to prey: Role of the mitogen-activated protein kinase Tmk3 in fungal chemical defense against fungivory by *Drosophila melanogaster* larvae. *Appl. Environ. Microbiol.* **85**, e01825-e1918. https://doi.org/10.1128/AEM.01825-18 (2019).

74. Wang, M. *et al.* Identification of the role of a MAP kinase Tmk2 in *Hypocrea jecorina* (*Trichoderma reesei*). *Sci. Rep.* **4**, 6732. https://doi.org/10.1038/srep06732 (2014).

75. Wang, M. *et al.* Role of *Trichoderma reesei* mitogen-activated protein kinases (MAPKs) in cellulase formation. *Biotechnol. Biofuels* **10**, 99. https://doi.org/10.1186/s13068-017-0789-x (2017).

76. Wang, M. *et al.* A mitogen-activated protein kinase Tmk3 participates in high osmolarity resistance, cell wall integrity maintenance and cellulase production regulation in *Trichoderma reesei. PLoS ONE* **8**, e72189. https://doi.org/10.1371/journal.pone.0072189 (2013).

77. de Paula, R. G. *et al.* The duality of the MAPK signaling pathway in the control of metabolic processes and cellulase production in *Trichoderma reesei. Sci. Rep.* **8**, 14931. https://doi.org/10.1038/s41598-018-33383-1 (2018).

78. Stappler, E., Dattenböck, C., Tisch, D. & Schmoll, M. Analysis of light- and carbon-specific transcriptomes implicates a class of G-protein-coupled receptors in cellulose sensing. *mSphere* **2**, e00089-00017. https://doi.org/10.1128/mSphere.00089-17 (2017).

79. Stappler, E., Walton, J. D. & Schmoll, M. Abundance of secreted proteins of *Trichoderma reesei* is regulated by light of different intensities. *Front. Microbiol.* **8**, 2586 (2017).

80. Schuster, A. *et al.* A versatile toolkit for high throughput functional genomics with *Trichoderma reesei. Biotechnol. Biofuels* **5**, 1. https://doi.org/10.1186/1754-6834-5-1 (2012).

81. Atanasova, L., Knox, B. P., Kubicek, C. P., Druzhinina, I. S. & Baker, S. E. The polyketide synthase gene *pks4* of *Trichoderma reesei* provides pigmentation and stress resistance. *Eukaryot Cell* **12**, 1499–1508. https://doi.org/10.1128/EC.00103-13 (2013).

82. Adnan, M. *et al.* Carbon catabolite repression in filamentous fungi. *Int. J. Mol. Sci.* **19**, 48. https://doi.org/10.3390/ijms19010048 (2017).

83. Bazafkan, H., Tisch, D. & Schmoll, M. in *Biotechnology and Biology of Trichoderma* (eds. V. K. Gupta *et al.*). 291–307 (Elsevier, 2014).

84. Hinterdobler, W. *et al.* (2021) Integration of chemosensing and carbon catabolite repression impacts fungal enzyme regulation and plant associations. *bioRxiv.* https://doi.org/10.1101/2021.05.06.442915.

85. Schmoll, M. & Hinterdobler, W. in *Progress in Molecular Biology and Translational Science* in press (Academic Press, 2022).

86. Schuster, A., Tisch, D., Seidl-Seiboth, V., Kubicek, C. P. & Schmoll, M. Roles of protein kinase A and adenylate cyclase in light-modulated cellulase regulation in *Trichoderma reesei. Appl. Environ. Microbiol.* **78**, 2168–2178. https://doi.org/10.1128/AEM.06959-11 (2012).

87. Cao, Y. *et al.* Dual regulatory role of chromatin remodeler ISW1 in coordinating cellulase and secondary metabolite biosynthesis in *Trichoderma reesei. MBio* **13**, e0345621. https://doi.org/10.1128/mbio.03456-21 (2022).

88. Zhang, W. *et al.* Influences of genetically perturbing synthesis of the typical yellow pigment on conidiation, cell wall integrity, stress tolerance, and cellulase production in *Trichoderma reesei. J. Microbiol.* **59**, 426–434. https://doi.org/10.1007/s12275-021-0433-0 (2021).

89. Derntl, C. *et al.* In Vivo study of the sorbicillinoid gene cluster in *Trichoderma reesei. Front. Microbiol.* **8**, 2037. https://doi.org/10.3389/fmicb.2017.02037 (2017).

90. Derntl, C., Rassinger, A., Srebotnik, E., Mach, R. L. & Mach-Aigner, A. R. Identification of the main regulator responsible for synthesis of the typical yellow pigment produced by *Trichoderma reesei. Appl. Environ. Microbiol.* **82**, 6247–6257. https://doi.org/10.1128/AEM.01408-16 (2016).

91. Bazafkan, H. *et al.* Mating type dependent partner sensing as mediated by VEL1 in *Trichoderma reesei. Mol. Microbiol.* **96**, 1103–1118. https://doi.org/10.1111/mmi.12993 (2015).

92. Bazafkan, H., Dattenbock, C., Stappler, E., Beier, S. & Schmoll, M. Interrelationships of VEL1 and ENV1 in light response and development in *Trichoderma reesei. PLoS ONE* **12**, e0175946. https://doi.org/10.1371/journal.pone.0175946 (2017).

93. Karimi Aghcheh, R. *et al.* The VELVET A orthologue VEL1 of *Trichoderma reesei* regulates fungal development and is essential for cellulase gene expression. *PLoS ONE* **9**, e112799. https://doi.org/10.1371/journal.pone.0112799 (2014).

94. Bazafkan, H. *et al.* SUB1 has photoreceptor dependent and independent functions in sexual development and secondary metabolism in *Trichoderma reesei. Mol. Microbiol.* **106**, 742–759. https://doi.org/10.1111/mmi.13842 (2017).

95. Hinterdobler, W. *et al.* The role of PKAc1 in gene regulation and trichodimerol production in *Trichoderma reesei. Fungal Biol. Biotechnol.* **6**, 12. https://doi.org/10.1186/s40694-019-0075-8 (2019).

96. SciFinder; Chemical Abstracts Service: Columbus, OH; https://scifinder.cas.org (Accessed September 19 2022).

97. Shitota, O. *et al.* Structural elucidation of trichotetronines: polyketides possessing a bicyclo [2.2.2.] octane skeleton with a tetronic acid moiety isolated from *Trichoderma* spp.. *J. Chem. Soc Perkin Trans.* **1**, 2961–2964 (1997).

98. Maskey, R. P., Grun-Wollny, I. & Laatsch, H. Sorbicillin analogues and related dimeric compounds from *Penicillium notatum*. *J. Nat. Prod.* **68**, 865–870. https://doi.org/10.1021/np040137t (2005).

99. de Paula, R. M., Lamb, T. M., Bennett, L. & Bell-Pedersen, D. A connection between MAPK pathways and circadian clocks. *Cell Cycle* **7**, 2630–2634. https://doi.org/10.4161/cc.7.17.6516 (2008).

100. Antonieto, A. C., dos Santos Castro, L., Silva-Rocha, R., Persinoti, G. F. & Silva, R. N. Defining the genome-wide role of CRE1 during carbon catabolite repression in *Trichoderma reesei* using RNA-Seq analysis. *Fungal Genet. Biol.* **73**, 93–103. https://doi.org/10.1016/j.fgb.2014.10.009 (2014).

101. Dos Santos Castro, L. *et al.* Understanding the role of the master regulator XYR1 in *Trichoderma reesei* by global transcriptional analysis. *Front. Microbiol* **7**, 175. https://doi.org/10.3389/fmicb.2016.00175 (2016).

102. Tisch, D. & Schmoll, M. Targets of light signalling in *Trichoderma reesei*. *BMC Genom.* **14**, 657. https://doi.org/10.1186/1471-2164-14-657 (2013).

103. Huberman, L. B., Coradetti, S. T. & Glass, N. L. Network of nutrient-sensing pathways and a conserved kinase cascade integrate osmolarity and carbon sensing in *Neurospora crassa*. *Proc. Natl. Acad. Sci. USA* **114**, E8665–E8674. https://doi.org/10.1073/pnas.1707713114 (2017).

104. Hornok, L., Waalwijk, C. & Leslie, J. F. Genetic factors affecting sexual reproduction in toxigenic Fusarium species. *Int. J. Food Microbiol.* **119**, 54–58 (2007).

105. Fu, C. *et al.* Identification and characterization of genes required for cell-to-cell fusion in *Neurospora crassa*. *Eukaryot Cell* **10**, 1100–1109. https://doi.org/10.1128/EC.05003-11 (2011).

106. Jonkers, W. *et al.* HAM-5 functions as a MAP kinase scaffold during cell fusion in *Neurospora crassa*. *PLoS Genet.* **10**, e1004783. https://doi.org/10.1371/journal.pgen.1004783 (2014).

107. Park, G. *et al.* Global analysis of serine-threonine protein kinase genes in *Neurospora crassa*. *Eukaryot Cell* **10**, 1553–1564. https://doi.org/10.1128/EC.05140-11 (2011).

108. Teichert, I. *et al.* PRO40 is a scaffold protein of the cell wall integrity pathway, linking the MAP kinase module to the upstream activator protein kinase C. *PLoS Genet.* **10**, e1004582. https://doi.org/10.1371/journal.pgen.1004582 (2014).

109. de Assis, L. J. *et al.* Multiple phosphatases regulate carbon source-dependent germination and primary metabolism in *Aspergillus nidulans*. *G3 (Bathesda)* **5**, 857–872. https://doi.org/10.1534/g3.115.016667 (2015).

110. Abe, N., Arakawa, T., Yamamoto, K. & Hirota, A. Biosynthesis of bisorbicillinoid in *Trichoderma* sp. USF-2690; evidence for the biosynthetic pathway, via sorbicillinol, of sorbicillin, bisorbicillinol, bisorbibutenolide, and bisorbicillinolide. *Biosci. Biotechnol. Biochem.* **66**, 2090–2099. https://doi.org/10.1271/bbb.66.2090 (2002).

111. Evidente, A. *et al.* Bisorbicillinoids produced by the fungus *Trichoderma citrinoviride* affect feeding preference of the aphid *Schizaphis graminum*. *J. Chem. Ecol.* **35**, 533–541. https://doi.org/10.1007/s10886-009-9632-6 (2009).

112. Balde, E. S. *et al.* Investigations of fungal secondary metabolites with potential anticancer activity. *J. Nat. Prod.* **73**, 969–971. https://doi.org/10.1021/np900731p (2010).

113. Druzhinina, I. S., Kubicek, E. M. & Kubicek, C. P. Several steps of lateral gene transfer followed by events of "birth-and-death" evolution shaped a fungal sorbicillinoid biosynthetic gene cluster. *BMC Evol. Biol.* **16**, 269. https://doi.org/10.1186/s12862-016-0834-6 (2016).

114. Mandels, M. & Andreotti, R. Problems and challenges in the cellulose to cellulase fermentation. *Proc. Biochem.* **13**, 6–13 (1978).

115. Gruber, F., Visser, J., Kubicek, C. P. & de Graaff, L. H. The development of a heterologous transformation system for the cellulolytic fungus *Trichoderma reesei* based on a *pyrG*-negative mutant strain. *Curr. Genet.* **18**, 71–76 (1990).

116. Schmoll, M. in *Trichoderma: Biology and Applications* (eds. P. K. Mukherjee *et al.*), 67–86 (CAB International, 2013).

117. Hinterdobler, W. *et al.* The G-protein coupled receptor GPR8 regulates secondary metabolism in *Trichoderma reesei*. *Front. Bioeng. Biotechnol.* **8**, 558996. https://doi.org/10.3389/fbioe.2020.558996 (2020).

118. Tisch, D., Kubicek, C. P. & Schmoll, M. New insights into the mechanism of light modulated signaling by heterotrimeric G-proteins: ENVOY acts on *gna1* and *gna3* and adjusts cAMP levels in *Trichoderma reesei* (*Hypocrea jecorina*). *Fungal Genet. Biol.* **48**, 631–640. https://doi.org/10.1016/j.fgb.2010.12.009 (2011).

119. Liu, D., Coloe, S., Baird, R. & Pederson, J. Rapid mini-preparation of fungal DNA for PCR. *J. Clin. Microbiol.* **38**, 471 (2000).

Acknowledgements

Author contributions

Mi.S. contributed to experimental work and drafting of the manuscript, S.B. performed experimental work and contributed to figure design, W.H. contributed to secondary metabolite isolation and analysis and drafting of the manuscript. N.W. contributed to secondary metabolite isolation and D.E. contributed to secondary metabolite analysis, J.S. and L.B. performed secondary metabolite analysis and contributed to drafting the manuscript. M.S. conceived the study, contributed to analysis and interpretation of results and wrote the final version of the manuscript.

Competing interests

The authors declare no competing interests.

Additional information

Supplementary Information The online version contains supplementary material available at https://doi.org/10.1038/s41598-023-28938-w.

Correspondence and requests for materials should be addressed to M.S.

Reprints and permissions information is available at www.nature.com/reprints.

Publisher's note Springer Nature remains neutral with regard to jurisdictional claims in published maps and institutional affiliations.

Chapter 4: The transcription factor STE12 influences growth on several carbon sources and production of dehydroacetic acid (DHAA) in *Trichoderma reesei*

Miriam Schalamun[1], Wolfgang Hinterdobler[1,2], Johann Schinnerl[3], Lothar Brecker[4] and Monika Schmoll[1,5]

[1] AIT Austrian Institute of Technology GmbH, Center for Health and Bioresources, Konrad Lorenz Strasse 24, 3430 Tulln, Austria

[2] MyPilz GmbH, Wienerbergstrasse 55/13-15, 1120, Vienna, Austria

[3] University of Vienna, Department of Botany and Biodiversity Research, Rennweg 14, 1030 Vienna, Austria

[4] University of Vienna, Department of Organic Chemistry, Währinger Strasse 38, 1090 Vienna, Austria

[5] University of Vienna, Department of Microbiology and Ecosystem Science, Division of Terrestrial Ecosystem Research, Djerassiplatz 1, 1030 Vienna, Austria

The transcription factor STE12 influences growth on several carbon sources and production of dehydroacetic acid (DHAA) in Trichoderma reesei

Miriam Schalamun

AIT Austrian Institute of Technology GmbH

Wolfgang Hinterdobler

AIT Austrian Institute of Technology GmbH

Johann Schinnerl

University of Vienna

Lothar Brecker

University of Vienna

Monika Schmoll (✉ monika.schmoll@univie.ac.at)

AIT Austrian Institute of Technology GmbH

Additional Declarations: No competing interests reported.

Abstract

The filamentous ascomycete *Trichoderma reesei*, known for its prolific cellulolytic enzyme production, recently also gained attention for its secondary metabolite synthesis. Both processes are intricately influenced by environmental factors like carbon source availability and light exposure. Here, we explore the role of the transcription factor STE12 in regulating metabolic pathways in *T. reesei* in terms of gene regulation, carbon source utilization and biosynthesis of secondary metabolites. We show that STE12 is involved in regulating cellulase gene expression and growth on carbon sources associated with iron homeostasis. STE12 impacts gene regulation in a light dependent manner on cellulose with modulation of several CAZyme encoding genes as well as genes involved in secondary metabolism. STE12 selectively influences the biosynthesis of the sorbicillinoid trichodimerol, while not affecting the biosynthesis of bisorbibutenolide, which was recently shown to be regulated by the MAPkinase pathway upstream of STE12 in the signaling cascade. We further report on the biosynthesis of dehydroacetic acid (DHAA) in *T. reesei*, a compound known for its antimicrobial properties, which is subject to regulation by STE12. We conclude, that STE12 exerts functions beyond development and hence contributes to balance the energy distribution between substrate consumption, reproduction and defense.

Introduction

As for all living beings, reproduction, defense and nutrient acquisition are crucial for survival and competitiveness of fungi in nature. Thereby, balancing resources among these essential tasks in order to optimize colonization and proliferation in their habitat is essential. Diverse signal transduction pathways contribute to this task by integrating sensed environmental cues, rating their relevance under the current conditions and triggering a precisely adjusted output. Fungi of the genus *Trichoderma* are particularly successful in adaptation and competition and are found almost ubiquitously on earth [1].

The filamentous ascomycete *Trichoderma reesei* represents a model organism for regulation of plant cell wall degradation [2, 3] due to its highly efficient cellulase system [4, 5]. The balance between different environmental cues and their relevance as well as regulatory interconnections are subject to research towards signal transduction pathways. Strong connections were observed for light response and regulation of plant cell wall degradation [6], but also secondary metabolism is influenced by light and carbon sources [7–9] as is sexual development [10, 11].

STE12 and STE12-like transcription factors are unique to fungi and well-known as targets of the mating/pheromone MAPkinase pathway [12, 13]. STE12 and homologous transcription factors are involved in regulation of development [13] and pathogenicity [14] in numerous fungi, indicating a well-conserved role.

Moreover, they were suggested to support environmental adaptation [15]. Accordingly, *T. atroviride* STE12 considerably influences growth on diverse carbon sources [16].

In *S. cerevisiae*, the Kss1 MAPkinase pathway exerts differential expression by binding-imposed repression and phosphorylation dependent activation together with distinct STE12-containing complexes [17]. In yeast, STE12 represents an important node in invasive growth response and mating [18]. Its dual function in these processes served as a model for investigation of signaling specificity to discriminate between pheromone signals and nutrient limitation [12, 19]. Interestingly, investigation of the evolution of STE12 and its regulatory functions revealed, that the specific interaction with DNA binding sites evolved in some species and in another lineages only indirect interaction via a binding partner occurs [20].

Activity of STE12 is predominantly controlled at the posttranslational level via phosphorylation, protein stability and protein-protein interactions in yeast [12], which is likely also the case in filamentous fungi. In many cases the zinc finger domains are dispensable for DNA binding, while the homeodomain is required [21].

In plant pathogenic fungi, the ability to penetrate the plant cell wall is crucial for virulence, which requires elevated turgor pressure and accumulation of glycerol. Additionally, nutrient sensing and plant sensing is required for communication and adaptation. In *Fusarium graminearum*, the up-stream MAPkinase targeting STE12 was found to impact activity of extracellular endonuclease, xylanolytic and proteolytic enzymes [22, 23]. A negative effect on specific cellulase activity and *cbh1* transcript

abundance was found for *T. reesei* TMK1 under controlled light conditions in darkness [24], although no effect was observed in a previous study for TMK1 under uncontrolled conditions [25]. For *F. graminearum* STE12 a positive regulation of cellulase and protease activities was detected, which is proposed to contribute to pathogenicity [22]. The biosynthesis of the mycotoxin deoxynivalenol (DON) is not affected by deletion of *ste12* in *F. graminearum* [22].

In *Trichoderma* spp. STE12 was shown to act downstream of the TMK1 MAPkinase cascade and influences mycoparasitism, hyphal avoidance, vegetative hyphal fusion, expression of cell wall degrading enzymes relevant for mycoparasitism and carbon source dependent growth of *T. atroviride* [16]. Consequently, we were interested in functions of STE12 in gene regulation upon growth on cellulose, the most important carbon source in the natural habitat of *Trichoderma*, as well as its role in carbon utilization and secondary metabolism.

Results

The domain structure of STE12 in filamentous fungi is conserved in T. reesei

In order to integrate STE12 in the context of current network knowledge, we searched for known and predicted interactors using the STRING database (Fig. 1A). The protein interaction network of STE12 in *T. reesei* revealed a connection to the mating related MAPkinase pathway and TMK1, as well as numerous genes involved in chromatin modification (Fig. 1B). Since *ste12* homologues were previously reported to be subject to alternative splicing [26, 27], we screened available transcriptome data for coverage of the *ste12* gene model, which contains two introns. For evaluation of the gene model used in our analysis for *ste12*, we checked data from growth on cellulose or glucose in constant light or darkness (Fig. 1C). We found that the predicted introns are clearly present and that *ste12* has a relatively long 5' UTR of roughly 700 bp, which comprises an upstream in-frame stop codon at position – 24. In this UTR region, neither an additional intron nor an upstream open reading frame (uORF; [28]) was detected, which might interfere with efficient *ste12*-translation. No indications for alternative splicing were detected.

The fungal STE homeodomain is highly divergent, however, in this domain also a conserved stretch of KQKVFFWFSVA resides [29]. Indeed, a related sequence is also present in *T. reesei*, albeit with three amino acid alterations: KQKVFYWYSVP. Accordingly, *T. reesei* STE12 comprises a STE like transcription factor domain (pfam02200; p-value 1.17e-78).

STE12 positively influences cellulase gene transcription

Interestingly, *ste12* shows mutations in the *T. reesei* cellulase-mutant strains NG14 and RutC30 [30, 31], suggesting a potential contribution to the efficient production of cellulose degrading enzymes in these strains. We asked whether STE12 has a function in regulation of cellulase formation upon growth on cellulose. Therefore, we first tested whether biomass formation on this carbon source would be altered. In darkness, Δ*ste12* showed similar growth as the wild-type, while in light biomass formation was significantly increased by 20% (Fig. 2A). However, while specific cellulase activity in darkness was unaltered and hence consistent with growth data, activity in light remained below detection levels (Fig. 2B). Analysis of *cbh1* transcript abundance showed a positive effect of STE12 in light, causing a decrease of *cbh1* transcript by 60% upon *ste12* deletion but no effect in darkness (Fig. 2C,D). A similar effect was detected for the carbon catabolite repressor gene *cre1*, with a 40% decrease in transcript abundance for Δ*ste12* in light (Fig. 2E,F). For the cellulase transcription factor gene *xyr1*, no significant regulation by STE12 was found, although in darkness a negative trend of transcript levels was apparent (p-value 0.071) (Fig. 2G,H). The important regulatory gene *vel1*, which is required for cellulase induction [32] and impacts secondary metabolism also in *T. reesei* [33, 34] is not significantly regulated by STE12 (Fig. 2I,J). *Pks4*, the gene encoding the polyketide synthase responsible for the green pigment in spores of *T. reesei* [35] shows a trend towards increased abundance in the mutant in constant light, albeit the respective p-value (0.092) is below our threshold for significance set at 0.05 (Fig. 2K,L). The same upregulation is observed for gene expression analysis by RNA-sequencing, which resulted in a significant 5-fold upregulation of *pks4* in constant light for Δ*ste12*, confirming the validity of the sequencing results.

Of the five MAPkinase cascades of *S. cerevisiae*, two, Fus3 and Kss1 target Ste12 [12] to transmit the pheromone signal. Since STE12 is subject to regulation by MAPkinases also in other fungi [16, 36, 37], although predominantly in terms of phosphorylation and stability, we asked whether in *T. reesei* also effects on the transcriptional level are present. Our analysis showed that *T. reesei ste12* is not subject to transcriptional regulation by MAPkinases upon growth on cellulose (Fig. 2M).

Growth on different carbon sources is altered in Δste12

A more general role of STE12 in regulation of growth and hence metabolism on diverse carbon sources was investigated using the BIOLOG phenotype microarrays [38]. We monitored growth patterns from 72 to 144 h after inoculation in constant darkness (supplementary file 1). If two consecutive time points showed statistically significant differences (p-value < 0.05, t-test) in biomass formation as analyzed by turbidimetry at 750 nm, we considered STE12 to be relevant for regulation of growth on this carbon source.

Interestingly, the differences we found for Δ*ste12* were all positive in terms of elevated growth of the mutant strain compared to the wild-type strain (Fig. 3A-E). In many cases, these differences occurred at 120 and 144 h after inoculation, when the mutant strain obviously kept growing, whilst the parental strain did not. Better growth on glycerol and glycogen suggests utilization of these carbon sources instead of storage.

Moreover, sugars including lactose, lactulose, melibiose, maltose and melezitose enable longer growth of the mutant strain, as do γ-hydroxy butyric acid, *p*-hydroxyphenylacetic acid and α-keto-glutaric acid (Fig. 3A-E).

STE12 impacts gene regulation

We investigated the regulatory impact of STE12 on gene regulation upon growth on cellulose as carbon source in constant light and constant darkness. In total, we found 203 genes to be more than 2-fold significantly (p-adj < 0.05) regulated directly or indirectly by STE12 (supplementary file 2). Functional category analysis (supplementary file 2) of these genes revealed a significant enrichment (p-value < 0.05) of genes involved in transport facilities, particularly calcium-, iron- and zinc-ion transport, carbohydrate metabolic process as well as secondary metabolism (amine- and proline catabolic process). Gene ontology (GO) analysis supported these results (Fig. 4).

Of the STE12 targets, 84 genes were up-regulated in light, including nine CAZyme encoding genes, for example a candidate chitinase (TrA0008W/TR_59791, 28.8-fold) and a subgroup beta-chitinase (TrE0823C/TR_43873, 8.8-fold), a candidate glycoside hydrolase (TrC0858W/TR_55886) and a beta-xylosidase, *bxl1* (TrC1552C/TR_121127). Other upregulated genes include the conidiation specific *con-10*, TrD0147C/TR_5084 (11.7-fold), the protein kinase gene *gin4* (TrD1202W/TR_64125*)*, which positively influences trichodimerol biosynthesis [39] a candidate cutinase transcription factor (TrA0431C/TR_106259, 26.3-fold). TR_106259 is also strongly up-regulated in a deletion mutant of the secondary metabolite regulator of the SOR-cluster, YPR2 [8, 40, 41], corroborating an indirect effect of STE12 on secondary metabolism. The same applies for a second strongly up-regulated transcription factor gene, TrF0487C/TR_112643 (12.7-fold in darkness), which is also strongly up-regulated in Δ*ypr2* [41]. Further up-regulated genes include the gene encoding the glucose transporter HXT1 (TrE0206W/TR_22912), the predicted sugar transporter gene TrD0036W/TR_50894, which was shown not to be required for growth on lactose [42] along with several other transporter genes as well as two genes encoding proteins predicted to be involved in plant surface sensing [43], the effector protein encoding TrA1330W/TR_72907 and the PTH11 type G-protein coupled receptor gene TrG0742C/TR_45573. Among the up-regulated genes in light, four genes belong to the cytochrome p450 superfamily, where TrF0040C/TR_65036 and TrA1084W/TR_75713 are potential homologues of *Aspergillus nidulans* alkane hydroxylases, catalyzing the oxidation of alkanes. The other two cytochrome p450 encoding genes are TrE0324C/TR_66453 homolog of *N. crassa ci-1*, an *ent*-kaurene oxidase, involved in the biosynthesis of gibberellins [44] and TrA0963W/TR_67377. Additionally, two polyketide synthase genes, *pks4* (TrD1440W/TR_82208), responsible for the green pigmentation of *T. reesei* conidia [35] and *pks2* (TrD0448W/TR_65891) are up-regulated (5- and 2.8-fold) in light.

The 23 genes up-regulated in darkness comprise the conidiation associated glucose repressible gene *grg-1*, TrE0533C/TR_73516, a family 5 carbohydrate esterase, the xylanase gene *xyn3* (TrF0312W/TR_54219 and

TrC0667W/TR_120229), the non-ribosomal peptide synthase (NRPS) encoding *tex2* (TrB1256C/TR_123786) responsible for paracelsin biosynthesis. Furthermore, two mitochondrial transporters TrC0706C/TR_103853 and TrF1000W/TR_121743 and a small cysteine-rich protein encoding gene TrC1533/TR_121135 (90.3-fold).

The 86 genes of the gene set down-regulated in light comprises four CAZyme encoding genes including *cbh1/ cel7a* (4.1-fold), *egl3/ cel12a* (23-fold), which is limiting for high efficiency plant cell wall degradation [45], the beta-glucosidase *bgl1/ cel3a* (45.2-fold) and a GH 99 gene, TrC1527C, TR_121136 (21.9-fold). Additionally, among the down-regulated genes in darkness are the GprK-like RGS domain containing heterotrimeric G-protein coupled receptor gene TrG0214W/TR_81383 and three transcription factor genes (TrA0076W/TR_3605, TrG1015C/TR_120363 and TrD0324W/TR_80139). The 10 down-regulated genes in darkness include a predicted oligonucleotide transporter gene related to sexual differentiation process protein ISP4 (TrA1796W/TR_124002), and a predicted MFS permease (TrB1842C/TR_68990).

Of all STE12 targets, five genes contain mutations in the high cellulase producer RutC30 (TrB1256C/TR_123786, TrG0579W/TR_56726, TrF0040C/TR_65036, TrF0049W/TR_65039 and TrC0660W/TR_120231).

Plant cell wall degradation specific phosphorylation was detected previously [46] for six STE12-regulated genes including an amino acid transporter (TrB0212C/TR_123718), *grg-1* and a putative methyltransferase gene (TrD1044C/TR_108914).

Regulation by STE12 in both light and darkness

Eight genes show light independent regulation by STE12. Up-regulation in both, light and darkness, was observed for a potential amino acid transporter gene (TrB0212C/TR_123718), the polyketide synthase gene *pks2* (TrD0448W/TR_65891), a potential carnitine *O*-acyltransferase encoding gene (TrC0399W/TR_122240) and TrE0645C/TR_54352. The putative exonuclease protein TrA1281W/TR_57424, a siderophore transporter TrG0054C/TR_82017 and TrA1279C/TR_57823 (PRE containing) were down-regulated in light and darkness. One gene, TrD0165W/TR_50793, encoding a putative homologue of QIP, a putative exonuclease protein involved in quelling with contrasting regulation in light and darkness by STE12 was found.

STE12 influences genes involved in iron homeostasis

Interestingly, several genes involved in iron homeostasis are targeted by STE12: The genes encoding the multicopper peroxidase Fet3b (TrD0040C/TR_5119) and the high affinity iron permease Ftr1b (TrD0041W/TR_80639), both belonging to the reductive iron uptake system [47], are up-regulated in light in Δ*ste12*. Moreover, a gene encoding a predicted, Fet5 related ferroxidase (TrD1438C/TR_124079) as well as a predicted siderophore transporter (TrD0541W/TR_67026) are upregulated in light. In contrast another siderophore transporter gene (TrG0054C/TR_82017) is downregulated in darkness. Additionally, a predicted iron transporter (TrD0323C/TR_38812) is 11-fold down-regulated in light. These findings suggest a contribution of STE12 to light modulated regulation of iron homeostasis.

Presence of the pheromone response element (PRE) in STE12 target promotors

The target sequence motif of STE12 was determined in *S. cerevisiae* and is called pheromone response element (PRE): 5' (A)TGAAACA 3' [29, 48]. Multimerization of *S. cerevisiae* Ste12 appears to enhance binding to pheromone response elements (PREs) and several adjacent PREs occur in strongly pheromone induced genes [49, 50], although a clear correlation was not found and pheromone responsive genes without PREs also exist [51, 52].

This sequence is also essential for Ste12 binding in *C. neoformans* [53] and in *Colletotrichum lindemuthianum* [27]. Screening the genes regulated by STE12 in *T. reesei* on cellulose, we found PREs in the promotors of five target genes (TrE0645C/TR_54352, TrA1206C/TR_104816, TrF0872C/TR_107349, TrA0569C/TR_108586 and TrA0485W /TR_121285). The reverse sequence 5' TGTTTCA 3' was present in 14 of the *T. reesei* STE12 target genes (supplementary file 2) CAZyme encoding genes, *grg-1* and a putative amino acid transporter. However, in none of these promotors we found more than one motif or a combination of forward and reverse motifs.

STE12 regulates production of dehydroacetic acid and trichodimerol

Functional category analysis of genes regulated by STE12 upon growth on cellulose revealed a significant enrichment of genes associated with secondary metabolism among its targets. Moreover, regulation of development is among the primary functions of STE12 in fungi [13, 37, 54], which is accompanied with clear alterations in secreted metabolites in *T. reesei* [33]. Consequently, we asked whether STE12 is required for proper chemical communication under conditions favoring sexual development.

Bisorbibutenolide, which was recently shown to be produced by *T. reesei* and dependent on the presence of the MAPkinase TMK3 [24], is not regulated by STE12 (Fig. 5A, highlighted in orange (D)). However, STE12 is involved in regulation of dehydroacetic acid (highlighted in green (B,C)) and also trichodimerol (highlighted in yellow (E)) in Fig. 5A.

Preparative column chromatography fractions obtained from *T. reesei* crude extracts were subjected to NMR and MS analysis and resulted in the identification of dehydroacetic acid (Fig. 5B,C). It was identified in a mixture together with the steroid ergosterol (sample A), in a further purified sample (B) and finally by comparison to a commercially available standard.

The NMR spectroscopic analysis of sample A revealed a content of approx. 90% (mol/mol) ergosterol (Fig. S1 in supplementary file 3). These NMR spectroscopic data of ergosterol are in agreement with those of a commercial reference sample as well as with previously published data of ergosterol [55]. In addition, approximately 7% (mol/mol) of the target compound could be identified from the mixture in sample A. Further purification of this smaller amount in sample A by prep TLC using silica gel 60 glass plates (Merck) yielded 0.6 mg of the target compound (sample B). It was identified as dehydroacetic acid (3-acetyl-6-methyl-3,4-dihydro-2H-pyran-2,4-dione, DHAA).

HR-ESI-TOF-MS in negative ionization of sample A (Fig. S2 in supplementary file 3) shows a deprotonated molecular ion [M-H]$^-$ of m/z 167.0343, which correlates quite well with the calculated [M-H]$^-$ of m/z 167.0350 of the molecular formula $C_8H_8O_4$. The HR-ESI-TOF-MS of sample B (Fig. S3, S4 in supplementary file 3) shows a deprotonated molecular ion [M-H]$^-$ of m/z 167.0349 in the negative ionization mode as well as a [M + Na]$^+$ of m/z 191.0309 and a [M + H]$^+$ of m/z 169.0489 in positive ionization mode. The isotopic patterns in these spectra of sample B show a weak entry of deuterium into the molecule, because it was previously dissolved in CD$_3$OD. However, all recorded monoisotopic masses fit well with calculated [M-H]$^-$ of m/z 167.0350, [M + Na]$^+$ of m/z 191.0315 and a [M + H]$^+$ of m/z 169.0495 of the molecular formula $C_8H_8O_4$. Further co-chromatographic comparison using commercially available dehydroacetic acid (Thermo Scientific, Waltham, MA; CAS Nr. 520-45-6) as standard confirmed the identity of this compound in sample B (Fig. 5).

1D and 2D NMR measurements of the 7% (mol/mol) dehydroacetic acid in sample A further confirmed the structure of the target compound (Fig. S5 in supplementary file 3). The spectra led to a total number of two methyl-, zero methylen-, one methine groups and five quaternary carbon atoms, resulting in one additional non carbon bound proton. The ^{1}H NMR signal of the methyl group at pos. 8 (δ_H 2.58 ppm / δ_C 30.7 ppm) shows in HMBC a $^2J_{H-C}$ coupling to the keto function at C-7 (δ_C 206.7 ppm) and a $^3J_{H-C}$ coupling to the quaternary C-3 (δ_C 100.9 ppm). Furthermore, the ^{1}H NMR signal of the methyl group in pos. 9 (δ_H 2.28 ppm / δ_C 21.2 ppm) shows a $^2J_{H-C}$ to C-6 (δ_C 171.7 ppm) and a $^3J_{H-C}$ on the of the methylene group at C-5 (δ_H 6.14 ppm / δ_C 102.2 ppm). The corresponding H-5 shows a further $^2J_{H-C}$ to C-4 (δ_C 180.4 ppm), while the ^{13}C NMR signal from C-2 cannot be determined in HMBC and is assumed to be as weak signal at 162.4 ppm. All these chemical shifts and couplings are in good agreement with those reported earlier [56, 57]. Numbering of protons and carbons as well all chemical shifts and couplings are shown in Fig. S6 in supplementary file 3.

Discussion

We explored the role of STE12 in regulation of metabolic pathways, which are crucial to application of the industrial workhorse *T. reesei*. Ste12 is a transcription factor that was first described in the yeast *S. cerevisiae* where it acts downstream of the mating and invasive growth response pathways which are controlled by the Fus3 and Kss1 MAPkinases respectively [13]. In other *Trichoderma* species like *T. atroviride*, Ste12 is also linked to the Fus3/Kss1 homolog Tmk1, and several Tmk1-mediated processes, including mycoparasitism, hyphal growth, and carbon source utilization, are regulated through Ste12 [16]. Hence, we

were also interested in overlapping functions of MAPkinases and STE12 in *T. reesei*. Interestingly, we did not detect a regulation of transcript abundance of *ste12* by any of the three MAPkinases in *T. reesei* upon growth on cellulose. Consequently, the MAPkinase cascades either do not regulate STE12 on cellulose or this regulation occurs at a posttranscriptional or posttranslational level.

Given the previous findings indicating that various functions regulated by MAPkinases in *T. reesei* are light-dependent [24], we regarded light as a critical environmental factor when exploring the role of STE12. Indeed, we found varying gene expression regulation for constant light and constant darkness by STE12 on cellulose, the carbon source closest to its natural habitat. In light, deletion of *ste12* leads to an up-regulation of CAZyme encoding genes, specifically chitinases and glycosidases, which resembles the observations in *T. atroviride* where chitinase encoding genes were upregulated upon growth on chitin [16]. Whereas other CAZyme genes such as the prominent cellobiohydrolase *cbh1* gene and the beta-glucosidase gene *bgl1* are downregulated.

When comparing this regulation in Δ*ste12* to the MAPkinases in *T. reesei*, the pattern of *cbh1* down-regulation in the presence of light aligns with the regulation pattern observed for all three MAPkinases, TMK1, TMK2, and TMK3. This observation suggests a possible involvement of STE12 in the cellulase signal transmission by all three MAPkinases in light, likely at a posttranslational level by phosphorylation. In darkness, however, there is no significant *cbh1* regulation in Δ*ste12* whereas the MAPkinases in this case show contrasting significant regulations, showcasing the complex interplay between signal transmission cascades and environmental cues in cellulase regulation. Similarly, there is an increase in biomass formation upon growth of Δ*ste12* on cellulose in light however in darkness there is no change of growth.

In *Trichoderma*, the green pigmentation of spores is attributed to the activity of polyketide synthase PKS4 [35]. In the *T. reesei* Δ*tmk3* mutant, the expression of the *pks4* gene is completely abolished, resulting in spores lacking their characteristic green color [24]. Conversely, when the MAPkinase *tmk2* is deleted, there is a significant increase in *pks4* gene expression in the presence of light [24], mirroring a similar response observed upon the deletion of *ste12.* Therefore, a contribution of STE12 to transmission of the signal regulating *pks4* by the cell integrity pathway (TMK2) in light would not be without precedent.

Our analysis of carbon source utilization, i.e. growth on diverse carbon sources in darkness, did not reveal dramatic alterations in growth of Δ*ste12*, indicating that STE12 is not essential for the considerable adaptation competence of the metabolism of *T. reesei*. Nevertheless, in several cases, lack of *ste12* appeared to result in better fitness in terms of achieving higher biomass at later time points of growth. We conclude that STE12 is involved in modulation of growth for adaptation to different nutrient conditions in *T. reesei* and that its function is rather a negative one.

Our transcriptome analysis hinted at a contribution of STE12 to regulation of secondary metabolism with respect to siderophore biosynthesis and transport as well as iron transport. Additionally, strong up-regulation of two transcription factors also up-regulated in the absence of an important sorbicillinoid regulating transcription factor, YPR2 [41] indicate a function in secondary metabolism. Previously, STE12 was found to play a role in *Athrobotrys oligospora*, a nematode trapping fungus, in secondary metabolism under trap formation conditions [58] However, in *Fusarium graminearum*, abundance of the important secondary metabolite DON (deoxynivalenol) was not influenced by STE12 [22], while other compounds were not analyzed in the respective study.

Iron is among the most important nutrients for survival of microbes and hence it is subject to competitive actions [59]. The involvement of STE12 in iron homeostasis and siderophore associated gene regulation was not reported before and is likely specific to growth on cellulose. However, we also want to note here that this effect occurred in light, where the mutant strain grows somewhat better (Fig. 2A) and may hence reach iron-limiting conditions, which facilitate siderophore production [60], earlier than the wild-type.

We could previously show that the chemical communication with mating partners is not limited to secretion and sensing of peptide pheromones, but involves further secreted metabolites [33], including the sorbicillin derivative trichodimerol [39]. Regulation of this chemical language in *T. reesei* involves different sensing and signaling factors like protein kinase A [39], the secondary metabolite regulator VEL1 [33], the photoreceptor ENV1 [61] and the transcription factor SUB1 [62]. Since the most

thoroughly investigated function of STE12 involves the regulation of development, we figured that under these conditions, also modulations of secondary metabolites, likely including those of sorbicillins should occur.

Sorbicillinoids are by now among the best studied secondary metabolites of *T. reesei* [8, 40]. The SOR-cluster, which is responsible for sorbicillinoid production, was acquired by *T. reesei* by lateral gene transfer [63, 64] and is regulated by light [8]. These compounds have anti-inflammatory, cytotoxic and antimicrobial effects [65]. HPLC analyses confirmed the connection of STE12 to sorbicillinoid production with an influence on trichodimerol production under conditions facilitating sexual development (Fig. 5). Interestingly, abundance of bisorbibutenolid, which was recently shown to be produced in *T. reesei* [24], was not altered, indicating that STE12 acts selectively on production of sorbicillinoids.

The identified compound dehydroacetic acid (DHAA) was recognized already in the 19th century as a possible intermediate of the polyketide pathway [66]. It thus belongs to this large group of natural products and is a possible intermediate and building block for larger polyketides [67]. Furthermore, the antifungal effect of DHAA was also recognized in 1947 [68] and led to an industrial production and wide use of this compound. As a result, DHAA can nowadays be found as a contaminant in various places in nature [69]. However, so far only a few reports have been described in which DHAA is isolated and described from natural sources, e.g. [70, 71], including an isolation from *Trichoderma viride* [72]. This lack of reports on isolation may be due to the fact, that DHAA is further converted in the polyketide pathway and hence not further accumulated in many organisms. The regulation of DHAA production by STE12 under conditions facilitating sexual development may hint at a function in adjusting defense during the energy consuming mating process in *T. reesei*.

In summary, we found that STE12 is involved in regulation of transcript abundance upon growth on cellulose and that its function is distinct in light and darkness. Due to the strongly negative impact on two further transcription factors, it can be assumed that STE12 not only acts directly but also indirectly on its targets. The involvement of STE12 in secondary metabolism likely includes an impact on iron homeostasis via siderophores, and a clear effect on the production of polyketide secondary metabolites in *T. reesei*. Hence, also considering the background of knowledge from other fungi, STE12 exerts important functions in primary and secondary metabolism, which are likely associated with balancing energy distribution between enzyme production, secondary metabolite production and development in response to given environmental conditions.

Materials and Methods

Strains and cultivation conditions

T. reesei QM6a [73, 74] and QM6aΔ*ku80* were used as parental strains in this study. To investigate gene regulation, enzymatic activity and biomass formation, liquid cultivation was performed under both continuous light and constant darkness conditions at 200 rpm and 28°C for 96 hours. Prior to inoculation, the strains were cultured on agar plates containing 3% (w/v) malt extract (MEX) in constant darkness for a period of 14 days to eliminate any potential effects of circadian rhythmicity. For the liquid culture, of 10^9 conidia per liter were inoculated in Mandels-Andreotti minimal medium [75] supplemented with 1% (w/v) microcrystalline cellulose (Alfa Aesar, Karlsruhe, Germany) as only carbon source. Additionally, 5mM urea and 0.1% peptone were added to induce germination. Following the 96-hour incubation, both mycelia and supernatants were collected and snap frozen in liquid nitrogen. In the case of cultures under constant darkness, only minimal red safety light was employed, specifically a darkroom lamp (Philips PF712E, red, 15W).

Construction of the ste12 deletion strain

ste12 (TrA1391C/TR_36543) was deleted in QM6aΔ*ku80* following the procedure described previously [76] using yeast recombination and the hygromycin (hph) marker cassette. The protoplasting method was used for transformation and 50 µg/mL hygromycin B as selection reagent (Roth, Karlsruhe, Germany) [77]. Successful deletion was confirmed by the absence of the gene by PCR and primers 36543_qF and 36354_qR (Table 1). DNA integrity was confirmed by a parallel PCR with primers TEF1-728F and TEF1_rev to avoid a false negative result. Copy number determination confirmed the single integration of the deletion cassette [78].

Table 1
Oligonucleotides used in this study.

Primer name	Info	Sequence 5' – 3'	target gene	Notes
pdel_36543_5F	construction of deletion cassette	GTAACGCCAGGGTTTTCCCAGTCACGACGTGTACCTGTACCTTACCACG	*ste12*	This study
pdel_36543_5R	construction of deletion cassette construction of deletion cassette	ATCCACTTAACGTTACTGAAATCTCCAACGTGTGTGTGTGAGAGAGACC	*ste12*	This study
pdel_36543_3F	construction of deletion cassette	CTCCTTCAATATCATCTTCTGTCTCCGACTCCAGTGGGATAATACCTGC	*ste12*	This study
pdel_36543_3R	construction of deletion cassette	GCGGATAACAATTTCACACAGGAAACAGCTCTCCTATTACCTGTCTACG	*ste12*	This study
RT_36543_F	internal primer	CCACATCAGCGACGACAT	*ste12*	This study
RT_36543_R	internal primer	GAGTGAGACTTGTGAGGGTAAG	*ste12*	This study
EF1-728F	internal primer	CATCGAGAAGTTCGAGAAGG	*tef1*	[91]
TEF1 rev	internal primer	GCCATCCTTGGAGATACCAGC	*tef1*	[92]
RTcbh1F	qPCR primer	ACCGTTGTCACCCAGTTCG	*cbh1*	[93]
RTcbh1R	qPCR primer	ATCGTTGAGCTCGTTGCCAG	*cbh1*	[93]
RT_VEL_R1	qPCR primer	GCAGGAACACCAGTCAGGATG	*vel1*	[33]
RT_VEL_F1	qPCR primer	CGAGGAGGGCAAGGACATTAC	*vel1*	[33]
SAR RTF1	qPCR primer	TGGATCGTCAACTGGTTCTACGA	*sar*	[94]
SAR RTR1	qPCR primer	GCATGTGTAGCAACGTGGTCTTT	*sar*	[94]
RT_82208_F	qPCR primer	ACTGAAGCAGTATCGGGCAACT	*pks4*	[61]
RT_82208_R	qPCR primer	TCTTCGACGTAAAGAGCAGCCA	*pks4*	[61]
xyr1RTF	qPCR primer	CTTCCTCCTCCTGCTCATCG	*xyr1*	[95]
xyr1RTR	qPCR primer	TCGTGTGCCCTAACAATGGTC	*xyr1*	[95]
RT_CRE1 F	qPCR primer	GCAGCACAATACGACTCCG	*cre1*	This study
RT_CRE1 R	qPCR primer	CGGCTAATGATGTCGGTAAG	*cre1*	This study

Isolation and manipulation of nucleic acids

The Qiagen RNeasy Plant mini kit was used for the isolation of RNA from mycelia from liquid culture. RT-qPCR was performed with three biological and three technical replicates as described previously [62, 79] using the GoTaq® qPCR Master Mix (Promega) as previously described with *sar1* as reference gene and other primers listed in Table 1. For mutant screening DNA was isolated following the rapid minipreparation protocol for fungal DNA as described previously [80].

Transcriptome analysis

Total RNA was provided in biological triplicates for every strain and condition. Sequencing and library-preparation using ribo-depletion to eliminate rRNA was performed at the Next Generation Sequencing Facility (Vienna Biocenter Core Facilities GmbH (VBCF), Austria). The sequencing was carried out on a NovaSeq 6000 platform using a paired-end (PE) configuration and 150 bp mode and yielded an average of 31 million reads per sample. Data analysis was performed as previously described [24], briefly: Quality filtering (Q30) was done using bbduk version 38.18 [81], mapping to the most recent *T. reesei* QM6a reference genome [73] was done using HISAT2 version 2.2.1 [82]. Furthermore, samtools version 1.10 [83], QualiMap version 2.2.2 [84] and featureCounts version 2.0.1 [85] were used. Differential gene expression (DEG) analysis (DESeq2 version 1.3.1) [86] was performed in R version 4.0.3 (https://www.R-project.org), with a threshold for significantly differentially regulated genes with log2fold change | > 1| and p-adj < 0.05. Gene annotations were performed employing existing annotations for *T. reesei*, *T. virens* and *T. atroviride* [87] and *T. reesei* [88]. The DESeq2 variance stabilizing transformation (VST) function was applied for count normalization. Functional enrichment of a set of DEGs was performed using the Fisher's exact test using R package topGO version 2.42.0 (https://bioconductor.org/packages/topGO) visualized with the R package rrvgo (p-value < 0.1, weighted algorithm 0.7 threshold) [89]. The specific script developed for and used in this analysis is available at: https://github.com/miriamschalamun/RNA_Tricho/tree/main"

Statistics

Statistical significance for RTqPCR, cellulase activity and biomass analysis was calculated in R using Student's T-test (compare means, ggpubr version 0.4.0) ** = p-value < 0.01, * = p-value < 0.05.

BIOLOG phenotype microarray analysis

Variations in growth based on diverse carbon sources were assessed using the BIOLOG FF Microplate assay (Biolog Inc., Hayward, CA), as described previously [90]. Inoculated microplates were incubated at 28°C in constant darkness, spanning a timeframe of up to 144 hours. Measurements of absorbance at 750 nm, indicative of biomass accumulation, were taken at 24-hour intervals, starting at 72-hours. To evaluate the statistical significance of growth differences, a T-test was employed (with a threshold p-value of ≤ 0.05) using Excel 2016 (Microsoft, Redmond, USA).

Secondary metabolite analysis

Secondary metabolites were extracted from strains grown on 3% malt extract medium in constant darkness for 14 days in triplicates as described previously [24, 39]. Samples were prepared from each two agar plugs of 1.8 cm² from 3 plates. Extraction was done in 15 mL tubes by adding 3 mL of 50% acetone in water (v/v) and ultrasonication for 15 min. Thereafter, 1 mL of chloroform was added. For phase separation, tubes were centrifuged at 4°C at 1000 g for 1 min. The organic phase was transferred to glass vials and left for evaporation overnight. This step was repeated two times. The dry extracts were redissolved in 140 μL MeOH for HPLC analysis.

Analytical HPLC-UV-DAD measurements were done on Agilent 1100 series coupled with UV-diode array detection at 230 nm and a Hypersil BDS column (100 × 4 mm, 3 μm particle size). An aq. buffer containing 15 mM H_3PO_4 and 1.5 mM tetrabutylammonium hydroxide (A) and MeOH (B) were used as eluents. The following elution system was applied: From 55–95% B within 8 min, and 95% B was kept for 5.0 min, with a flow rate of 0.5 mL min^{-1}. The injection volume was 5.0 μL.

HR-ESI-TOF-MS spectra were obtained on a maXis UHR ESI-Qq-TOF mass spectrometer (Bruker Daltonics, Bremen, Germany). Samples were dissolved and further diluted in ACN/MeOH/H_2O in the ratio of 99:99:2 (v/v/v) and directly infused into the ESI source with a syringe pump. The ESI ion source was operated as follows: capillary voltage: 4.0-4.5 kV, nebulizer: 0.4 bar (N_2), dry gas flow: 4 L/min (N_2), and dry temperature: 180°C. Mass spectra were recorded in the range of m/z 50–1900 in the positive- and negative ion mode. The sum formulae of the detected ions were determined using Bruker Compass DataAnalysis 1 based on the mass accuracy ($\Delta m/z \leq 5$ ppm) and isotopic pattern matching (SmartFormula algorithm).

Sample A was dissolved in deuterated solvent (acetone-d_6, 5 mg in 0.6 mL) and transferred into a 5 mm high precision NMR sample tube for NMR spectroscopic measurements. 1D and 2D NMR spectra were recorded on a Bruker AVIII 600 spectrometer (Bruker, Rheinstetten, Germany) at 600.13 MHz (^{1}H) and 150.91 MHz (^{13}C), respectively and processed with Topspin 4.1. Chemical shifts (δ) are reported in ppm; for ^{1}H relative to residual acetone-d_5 (δ_H = 2.05 ppm) as well as for ^{13}C relative to acetone-d_6, (δ_C = 29.8 and 206.3).

Purification and identification of dehydroacetic acid

In the course of preparative isolation and purification of *T. reesei* secondary metabolites a lipophilic extract (696 mg) of mutant strains was suspended in approx. 5 mL of a mixture consisting of 30% *n*-heptane in ethyl acetate and adsorbed on 3 g silica gel 60 (0.2−0.5 mm grain size). After the solvent disappeared the dry silica gel powder was subjected to column chromatography over 24 g silica gel 60, 40−63 µm grain size, eluted with *n*-heptane: ethyl acetate mixtures in ratios of 95:5, 90:10, 85:15, 80:20, 75:25, 70:30 and 45:55 (100 mL each; fraction size 50 mL). The fractions eluted with 80:20 were pooled after HPLC analysis (38 mg) and subjected to size exclusion chromatography over Sephadex LH20 (GE Healthcare) eluted with acetone which afforded in total 6 mg of a mixture of the target compound and a steroid in higher quantities, determined by MS and NMR (sample A).

A Merck Silica gel 60 glass plate were used for preparative thin layer chromatography (TLC) to obtain sample B. This plate was developed in *n*-heptane/ ethyl acetate 70:30 (v/v).

Declarations

Author Contribution

MiS performed transcriptome analysis, RTqPCR and BIOLOG analysis. WH, LB and JS performed secondary metabolite analyses. LB, JS identified dehydroacetic acid. MoS conceived the study, contributed to data analysis and interpretation. MiS, WH, LB and MoS contributed to drafting the manuscript. MiS and MoS wrote the final version of the manuscript. All authors read the final version of the manuscript and agreed to publication.

Acknowledgements

Data availability statement

The datasets generated and analyzed during the current study are included in this article and its additional files and under GenBank accession number GSE222127 (https://www.ncbi.nlm.nih.gov/geo/query/acc.cgi?&acc=GSE222127).

References

1. Woo, S.L. *et al.* (2022) *Trichoderma*: a multipurpose, plant-beneficial microorganism for eco-sustainable agriculture. Nat Rev Microbiol. 10.1038/s41579-022-00819-5
2. Bischof, R.H. *et al.* (2016) Cellulases and beyond: the first 70 years of the enzyme producer *Trichoderma reesei*. Microb Cell Fact 15, 106. 10.1186/s12934-016-0507-6

3. Glass, N.L. *et al.* (2013) Plant cell wall deconstruction by ascomycete fungi. Annu Rev Microbiol 67, 477–498. 10.1146/annurev-micro-092611-150044

4. Druzhinina, I.S. and Kubicek, C.P. (2016) Familiar stranger: ecological genomics of the model saprotroph and industrial enzyme producer *Trichoderma reesei* breaks the stereotypes. Adv Appl Microbiol 95, 69–147. 10.1016/bs.aambs.2016.02.001

5. Gupta, V.K. *et al.* (2016) The post-genomic era of *Trichoderma reesei*: What's next? Trends Biotechnol 34, 970–982. 10.1016/j.tibtech.2016.06.003

6. Schmoll, M. (2018) Regulation of plant cell wall degradation by light in *Trichoderma*. Fungal Biol Biotechnol 5, 10. 10.1186/s40694-018-0052-7

7. Yu, W. *et al.* (2023) Light regulation of secondary metabolism in fungi. J Biol Eng 17, 57. 10.1186/s13036-023-00374-4

8. Monroy, A.A. *et al.* (2017) A CRE1- regulated cluster is responsible for light dependent production of dihydrotrichotetronin in *Trichoderma reesei*. PLoS One, e0182530

9. Atoui, A. *et al.* (2010) Cross-talk between light and glucose regulation controls toxin production and morphogenesis in *Aspergillus nidulans*. Fungal Genet Biol 47, 962–972. 10.1016/j.fgb.2010.08.007

10. Debuchy, R. *et al.* (2010) Mating systems and sexual morphogenesis in ascomycetes. In *Cellular and Molecular Biology of Filamentous Fungi* (Borkovich, K.A. and Ebbole, D.J., eds), pp. 501–535, ASM Press

11. Hinterdobler, W. *et al.* (2020) Sexual development, its determinants and regulation in *Trichoderma reesei*. In *Recent Developments in Trichoderma Research* (Zeilinger, S. *et al.*, eds), pp. 185–206, Elsevier

12. Rispail, N. and Di Pietro, A. (2010) The homeodomain transcription factor Ste12: Connecting fungal MAPK signalling to plant pathogenicity. Commun Integr Biol 3, 327–332. 10.4161/cib.3.4.11908

13. Wong Sak Hoi, J. and Dumas, B. (2010) Ste12 and Ste12-like proteins, fungal transcription factors regulating development and pathogenicity. Eukaryot Cell 9, 480–485. 10.1128/EC.00333-09

14. John, E. *et al.* (2021) Transcription factor control of virulence in phytopathogenic fungi. Mol Plant Pathol 22, 858–881. 10.1111/mpp.13056

15. Tollot, M. *et al.* (2009) An STE12 gene identified in the mycorrhizal fungus *Glomus intraradices* restores infectivity of a hemibiotrophic plant pathogen. New Phytol 181, 693–707. 10.1111/j.1469-8137.2008.02696.x

16. Gruber, S. and Zeilinger, S. (2014) The transcription factor Ste12 mediates the regulatory role of the Tmk1 MAP kinase in mycoparasitism and vegetative hyphal fusion in the filamentous fungus *Trichoderma atroviride*. PLoS One 9, e111636. 10.1371/journal.pone.0111636

17. Bardwell, L. *et al.* (1998) Repression of yeast Ste12 transcription factor by direct binding of unphosphorylated Kss1 MAPK and its regulation by the Ste7 MEK. Genes Dev 12, 2887–2898. 10.1101/gad.12.18.2887

18. Madhani, H.D. and Fink, G.R. (1997) Combinatorial control required for the specificity of yeast MAPK signaling. Science 275, 1314–1317. 10.1126/science.275.5304.1314

19. Elion, E.A. *et al.* (2005) Signal transduction. Signaling specificity in yeast. Science 307, 687–688. 10.1126/science.1109500

20. Sorrells, T.R. *et al.* (2015) Intersecting transcription networks constrain gene regulatory evolution. Nature 523, 361–365. 10.1038/nature14613

21. Nolting, N. and Poggeler, S. (2006) A STE12 homologue of the homothallic ascomycete *Sordaria macrospora* interacts with the MADS box protein MCM1 and is required for ascosporogenesis. Mol Microbiol 62, 853–868. 10.1111/j.1365-2958.2006.05415.x

22. Gu, Q. *et al.* (2015) A transcription factor FgSte12 is required for pathogenicity in *Fusarium graminearum*. Mol Plant Pathol 16, 1–13. 10.1111/mpp.12155

23. Jenczmionka, N.J. and Schafer, W. (2005) The Gpmk1 MAP kinase of *Fusarium graminearum* regulates the induction of specific secreted enzymes. Curr Genet 47, 29–36. 10.1007/s00294-004-0547-z

24. Schalamun, M. *et al.* (2023) MAPkinases regulate secondary metabolism, sexual development and light dependent cellulase regulation in *Trichoderma reesei*. *Sci Rep* 13, 1912. 10.1038/s41598-023-28938-w

25. Wang, M. *et al.* (2017) Role of *Trichoderma reesei* mitogen-activated protein kinases (MAPKs) in cellulase formation. Biotechnol Biofuels 10, 99. 10.1186/s13068-017-0789-x

26. Schamber, A. *et al.* (2010) The role of mitogen-activated protein (MAP) kinase signalling components and the Ste12 transcription factor in germination and pathogenicity of *Botrytis cinerea*. Mol Plant Pathol 11, 105–119. 10.1111/j.1364-3703.2009.00579.x

27. Wong Sak Hoi, J. *et al.* (2007) Regulation and role of a STE12-like transcription factor from the plant pathogen *Colletotrichum lindemuthianum*. Mol Microbiol 64, 68–82. 10.1111/j.1365-2958.2007.05639.x

28. Hood, H.M. *et al.* (2009) Evolutionary roles of upstream open reading frames in mediating gene regulation in fungi. Annu Rev Microbiol 63, 385–409. 10.1146/annurev.micro.62.081307.162835

29. Yuan, Y.L. and Fields, S. (1991) Properties of the DNA-binding domain of the *Saccharomyces cerevisiae* STE12 protein. Mol Cell Biol 11, 5910–5918. 10.1128/mcb.11.12.5910-5918.1991

30. Le Crom, S. *et al.* (2009) Tracking the roots of cellulase hyperproduction by the fungus *Trichoderma reesei* using massively parallel DNA sequencing. Proc Natl Acad Sci U S A 106, 16151–16156. 10.1073/pnas.0905848106

31. Peterson, R. and Nevalainen, H. (2012) *Trichoderma reesei* RUT-C30 - thirty years of strain improvement. Microbiology 158, 58–68. 10.1099/mic.0.054031-0

32. Karimi Aghcheh, R. *et al.* (2014) The VELVET A orthologue VEL1 of *Trichoderma reesei* regulates fungal development and is essential for cellulase gene expression. PLoS One 9, e112799. 10.1371/journal.pone.0112799

33. Bazafkan, H. *et al.* (2015) Mating type dependent partner sensing as mediated by VEL1 in *Trichoderma reesei*. Mol Microbiol 96, 1103–1118. 10.1111/mmi.12993

34. Liu, K. *et al.* (2016) Regulation of cellulase expression, sporulation, and morphogenesis by velvet family proteins in *Trichoderma reesei*. Appl Microbiol Biotechnol 100, 769–779. 10.1007/s00253-015-7059-2

35. Atanasova, L. *et al.* (2013) The polyketide synthase gene *pks4* of *Trichoderma reesei* provides pigmentation and stress resistance. Eukaryot Cell 12, 1499–1508. 10.1128/EC.00103 – 13

36. Rispail, N. and Di Pietro, A. (2009) *Fusarium oxysporum* Ste12 controls invasive growth and virulence downstream of the Fmk1 MAPK cascade. Mol Plant Microbe Interact 22, 830–839. 10.1094/MPMI-22-7-0830

37. Li, D. *et al.* (2005) A mitogen-activated protein kinase pathway essential for mating and contributing to vegetative growth in *Neurospora crassa*. Genetics 170, 1091–1104

38. Atanasova, L. and Druzhinina, I.S. (2010) Global nutrient profiling by Phenotype MicroArrays: a tool complementing genomic and proteomic studies in conidial fungi. J Zhejiang Univ Sci B 11, 151–168. 10.1631/jzus.B1000007

39. Hinterdobler, W. *et al.* (2019) The role of PKAc1 in gene regulation and trichodimerol production in *Trichoderma reesei*. *Fungal Biol Biotechnol* 6, 12. 10.1186/s40694-019-0075-8

40. Derntl, C. *et al.* (2017) In vivo study of the sorbicillinoid gene cluster in *Trichoderma reesei*. *Front Microbiol* 8, 2037. 10.3389/fmicb.2017.02037

41. Hitzenhammer, E. *et al.* (2019) YPR2 is a regulator of light modulated carbon and secondary metabolism in *Trichoderma reesei*. BMC Genomics 20, 211. 10.1186/s12864-019-5574-8

42. Ivanova, C. *et al.* (2013) Systems analysis of lactose metabolism in *Trichoderma reesei* identifies a lactose permease that is essential for cellulase induction. PLoS One 8, e62631. 10.1371/journal.pone.0062631

43. Van Dijck, P. *et al.* (2017) Nutrient sensing at the plasma membrane of fungal cells. Microbiol Spectr 5. 10.1128/microbiolspec.FUNK-0031-2016

44. Kawaide, H. (2006) Biochemical and molecular analyses of gibberellin biosynthesis in fungi. Biosci Biotechnol Biochem 70, 583–590. 10.1271/bbb.70.583

45. Lehmann, L. *et al.* (2016) Linking hydrolysis performance to *Trichoderma reesei* cellulolytic enzyme profile. Biotechnol Bioeng 113, 1001–1010. 10.1002/bit.25871

46. Nguyen, E.V. *et al.* (2016) Quantitative site-specific phosphoproteomics of *Trichoderma reesei* signaling pathways upon induction of hydrolytic enzyme production. J Proteome Res 15, 457–467. 10.1021/acs.jproteome.5b00796

47. Haas, H. *et al.* (2008) Siderophores in fungal physiology and virulence. Annu Rev Phytopathol 46, 149–187. 10.1146/annurev.phyto.45.062806.094338

48. Hagen, D.C. *et al.* (1991) Pheromone response elements are necessary and sufficient for basal and pheromone-induced transcription of the FUS1 gene of *Saccharomyces cerevisiae*. Mol Cell Biol 11, 2952–2961

49. Chou, S. *et al.* (2006) Regulation of mating and filamentation genes by two distinct Ste12 complexes in *Saccharomyces cerevisiae*. Mol Cell Biol 26, 4794–4805. 10.1128/MCB.02053-05

50. Su, T.C. *et al.* (2010) Organizational constraints on Ste12 *cis*-elements for a pheromone response in *Saccharomyces cerevisiae*. FEBS J 277, 3235–3248. 10.1111/j.1742-4658.2010.07728.x

51. Zheng, W. *et al.* (2010) Genetic analysis of variation in transcription factor binding in yeast. Nature 464, 1187–1191. 10.1038/nature08934

52. Roberts, C.J. *et al.* (2000) Signaling and circuitry of multiple MAPK pathways revealed by a matrix of global gene expression profiles. Science 287, 873–880. 10.1126/science.287.5454.873

53. Chang, Y.C. *et al.* (2004) Regulatory roles for the homeodomain and C2H2 zinc finger regions of *Cryptococcus neoformans* Ste12alphap. Mol Microbiol 53, 1385–1396. 10.1111/j.1365-2958.2004.04188.x

54. Deng, F. *et al.* (2007) Ste12 transcription factor homologue CpST12 is down-regulated by hypovirus infection and required for virulence and female fertility of the chestnut blight fungus *Cryphonectria parasitica*. Eukaryot Cell 6, 235–244. 10.1128/EC.00302-06

55. Zhao, J. *et al.* (2010) Antimicrobial metabolites from the endophytic fungus *Pichia guilliermondii* isolated from *Paris polyphylla* var. *yunnanensis*. *Molecules* 15, 7961–7970. 10.3390/molecules15117961

56. Chalaça, M.Z. and Figueroa-Villar, J.D. (2000) A theoretical and NMR study of the tautomerism of dehydroacetic acid. Journal of Molecular Structure 554, 225–231. https://doi.org/10.1016/S0022-2860(00)00674-8

57. Tan, S.-F. *et al.* (1982) 1H, 13C, and 15N nuclear magnetic resonance studies on the tautomerism of the Schiff's bases of 3-acetyl-6-methyl-2H-pyran-2,4(3H)-dione and 3,5-diacetyltetrahydropyran-2,4,6-trione. Journal of the Chemical Society, Perkin Transactions *2*, 513–521. 10.1039/P29820000513

58. Bai, N. *et al.* (2023) AoSte12 is required for mycelial development, conidiation, trap morphogenesis, and secondary metabolism by regulating hyphal fusion in nematode-trapping fungus *Arthrobotrys oligospora*. Microbiol Spectr 11, e0395722. 10.1128/spectrum.03957-22

59. Liu, Y. *et al.* (2023) Iron in the symbiosis of plants and microorganisms. Plants (Basel) 12. 10.3390/plants12101958

60. Haas, H. (2014) Fungal siderophore metabolism with a focus on *Aspergillus fumigatus*. Nat Prod Rep 31, 1266–1276. 10.1039/c4np00071d

61. Bazafkan, H. *et al.* (2017) Interrelationships of VEL1 and ENV1 in light response and development in *Trichoderma reesei*. PLoS One 12, e0175946. 10.1371/journal.pone.0175946

62. Bazafkan, H. *et al.* (2017) SUB1 has photoreceptor dependent and independent functions in sexual development and secondary metabolism in *Trichoderma reesei*. Mol Microbiol 106, 742–759. 10.1111/mmi.13842

63. Druzhinina, I.S. *et al.* (2018) Massive lateral transfer of genes encoding plant cell wall-degrading enzymes to the mycoparasitic fungus *Trichoderma* from its plant-associated hosts. PLoS Genet 14, e1007322. 10.1371/journal.pgen.1007322

64. Druzhinina, I.S. *et al.* (2016) Several steps of lateral gene transfer followed by events of 'birth-and-death' evolution shaped a fungal sorbicillinoid biosynthetic gene cluster. BMC Evol Biol 16, 269. 10.1186/s12862-016-0834-6

65. Hou, X. *et al.* (2022) Recent advances in sorbicillinoids from fungi and their bioactivities (covering 2016–2021). J Fungi (Basel) 8. 10.3390/jof8010062

66. Collie, N. and Myers, W.S. (1893) VII.—The formation of orcinol and other condensation products from dehydracetic acid. Journal of the Chemical Society, Transactions 63, 122–128. 10.1039/CT8936300122

67. Staunton, J. and Weissman, K.J. (2001) Polyketide biosynthesis: a millennium review. Natural Product Reports 18, 380–416. 10.1039/A909079G

68. Coleman, G.H. and Wolf, P.A. Dow Chemical Company, Midland. Making proteinaceous and fatty foods resistant to microorganisms,

69. Zhang, Y. *et al.* (2016) Sodium dehydroacetate levels in chicken tissues. Journal of Food Composition and Analysis 47, 31–37. https://doi.org/10.1016/j.jfca.2015.12.008

70. Rivera, C. *et al.* (1976) Dehydroacetic acid in anthers ofSolandra nitida (Solanaceae). Experientia 32, 1490–1490. 10.1007/BF01924409

71. Tan, W.-N. *et al.* (2022) Metabolomics Analysis and Antioxidant Potential of Endophytic Diaporthe fraxini ED2 Grown in Different Culture Media. Journal of Fungi 8, 519

72. Adachi, T. (2004) Biological active substance produced by Trichoderma viride isolated from allyl alcohol-partial sterilized soils. *Scientific Reports of the Faculty of Agriculture-Meijo University (Japan)*,

73. Li, W.C. *et al.* (2017) *Trichoderma reesei* complete genome sequence, repeat-induced point mutation, and partitioning of CAZyme gene clusters. Biotechnol Biofuels 10, 170. 10.1186/s13068-017-0825-x

74. Martinez, D. *et al.* (2008) Genome sequencing and analysis of the biomass-degrading fungus *Trichoderma reesei* (syn. *Hypocrea jecorina*). Nat Biotechnol 26, 553–560

75. Mandels, M. and Andreotti, R. (1978) Problems and challenges in the cellulose to cellulase fermentation. Proc Biochem 13, 6–13

76. Schuster, A. *et al.* (2012) A versatile toolkit for high throughput functional genomics with *Trichoderma reesei*. Biotechnol Biofuels 5, 1. 10.1186/1754-6834-5-1

77. Gruber, F. *et al.* (1990) The development of a heterologous transformation system for the cellulolytic fungus *Trichoderma reesei* based on a *pyrG*-negative mutant strain. Curr Genet 18, 71–76.

78. Tisch, D. and Schmoll, M. (2013) Targets of light signalling in *Trichoderma reesei*. BMC Genomics 14, 657. 10.1186/1471-2164-14-657

79. Tisch, D. *et al.* (2011) New insights into the mechanism of light modulated signaling by heterotrimeric G-proteins: ENVOY acts on *gna1* and *gna3* and adjusts cAMP levels in *Trichoderma reesei* (*Hypocrea jecorina*). *Fungal Genet Biol* 48, 631–640. S1087-1845(10)00245-8 [pii]10.1016/j.fgb.2010.12.009

80. Liu, D. *et al.* (2000) Rapid mini-preparation of fungal DNA for PCR. J Clin Microbiol 38, 471

81. Bushnell, B. (2014) BBMap: A fast, accurate, splice-aware aligner. Published online https://www.osti.gov/servlets/purl/1241166.

82. Kim, D. *et al.* (2019) Graph-based genome alignment and genotyping with HISAT2 and HISAT-genotype. Nat Biotechnol 37, 907–915. 10.1038/s41587-019-0201-4

83. Li, H. *et al.* (2009) The Sequence Alignment/Map format and SAMtools. Bioinformatics 25, 2078–2079. 10.1093/bioinformatics/btp352

84. García-Alcalde, F. *et al.* (2012) Qualimap: evaluating next-generation sequencing alignment data. Bioinformatics 28, 2678–2679. 10.1093/bioinformatics/bts503

85. Liao, Y. *et al.* (2014) featureCounts: an efficient general purpose program for assigning sequence reads to genomic features. Bioinformatics 30, 923–930. 10.1093/bioinformatics/btt656

86. Love, M.I. *et al.* (2014) Moderated estimation of fold change and dispersion for RNA-seq data with DESeq2. Genome Biol 15, 550. 10.1186/s13059-014-0550-8

87. Schmoll, M. *et al.* (2016) The genomes of three uneven siblings: footprints of the lifestyles of three *Trichoderma* species. Microbiol Mol Biol Rev 80, 205–327. 10.1128/MMBR.00040 – 15

88. Druzhinina, I.S. *et al.* (2016) A complete annotation of the chromosomes of the cellulase producer *Trichoderma reesei* provides insights in gene clusters, their expression and reveals genes required for fitness. Biotechnol Biofuels 9, 75. 10.1186/s13068-016-0488-z

89. Sayols, S. (2023) rrvgo: a Bioconductor package for interpreting lists of Gene Ontology terms. *MicroPubl Biol* 2023. 10.17912/micropub.biology.000811

90. Druzhinina, I.S. *et al.* (2006) Global carbon utilization profiles of wild-type, mutant, and transformant strains of *Hypocrea jecorina*. *Appl Environ Microbiol* 72, 2126–2133. 72/3/2126 [pii]10.1128/AEM.72.3.2126-2133.2006

91. Chaverri, P. *et al.* (2003) *Hypocrea/Trichoderma*: species with conidiophore elongations and green conidia. Mycologia 95, 1100–1140

92. Samuels, G.J. *et al.* (2002) *Trichoderma* species associated with the green mold epidemic of commercially grown *Agaricus bisporus*. Mycologia 94, 146–170

93. Tisch, D. *et al.* (2011) The phosducin-like protein PhLP1 impacts regulation of glycoside hydrolases and light response in *Trichoderma reesei*. BMC Genomics 12, 613

94. Steiger, M.G. *et al.* (2010) An accurate normalization strategy for RT-qPCR in *Hypocrea jecorina* (*Trichoderma reesei*). J Biotechnol 145, 30–37. 10.1016/j.jbiotec.2009.10.012

95. Schuster, A. *et al.* (2012) Roles of protein kinase A and adenylate cyclase in light-modulated cellulase regulation in *Trichoderma reesei*. Appl Environ Microbiol 78, 2168–2178. 10.1128/AEM.06959-11
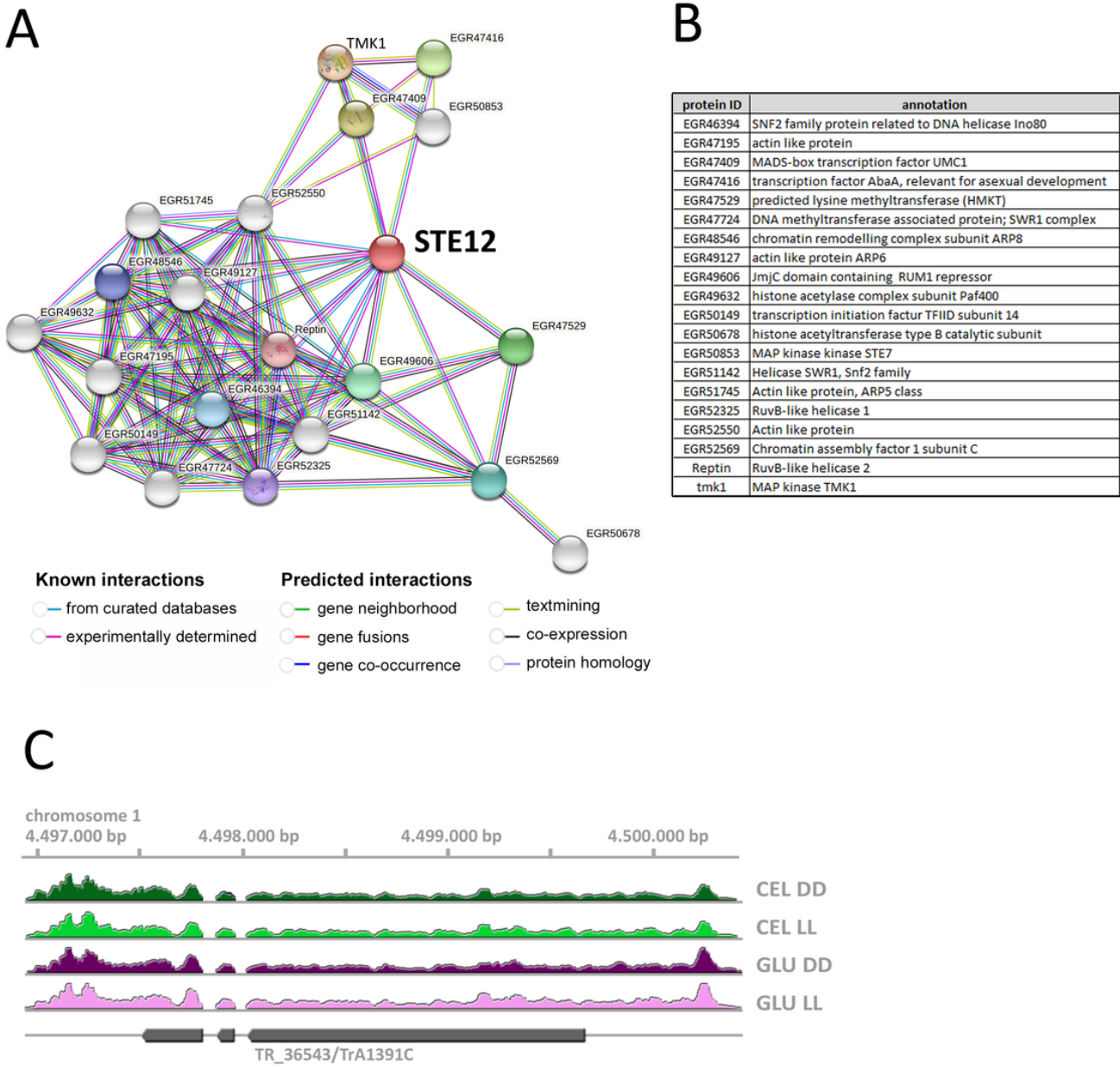
Figures

Figure 1

Characteristics of *ste12*/TR_36543/ TrA1391C and its encoded protein. (**A**) STRING network of known and predicted interaction partners. (**B**) Annotations of predicted interaction partners of STE12. (**C**) Evaluation of the protein model of STE12 by analysis of aligned reads from available transcriptome data for growth on cellulose (CEL) or glucose (GLU) in constant light (LL) or constant darkness (DD).
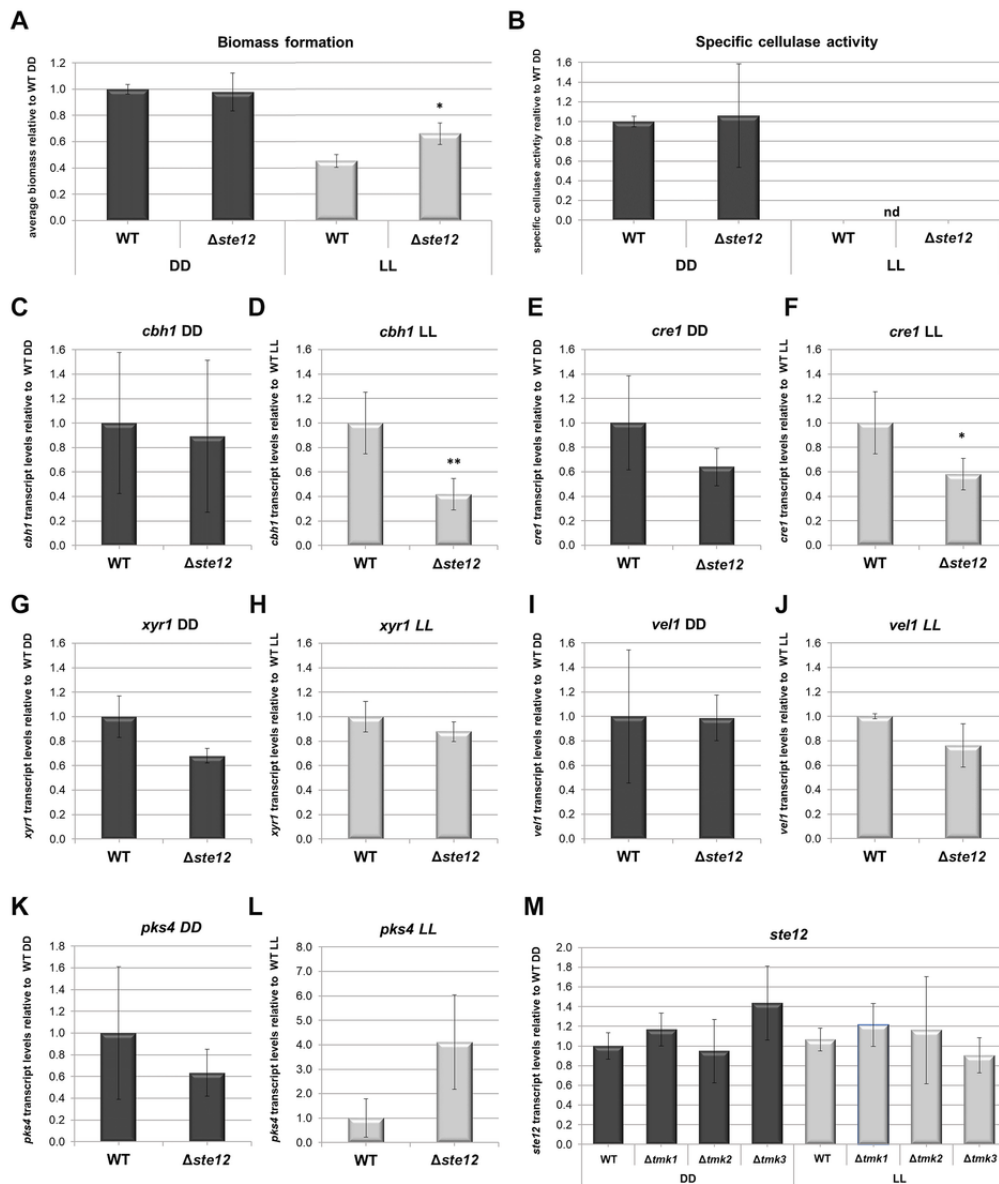
Figure 2

Relevance of STE12 for biomass formation, cellulase activity and gene regulation upon growth on 1% cellulose. (**A**) Biomass formation relative to wild-type (WT). (**B**) Specific cellulase activity. (**C,D**) Transcript levels of *cbh1* (**C**) in constant darkness and (**D**) constant light. (**E,F**) Transcript levels of *cre1* (**E**) in constant darkness and (**F**) constant light. (**G,H**) Transcript levels of *xyr1* (**G**) in constant darkness and (**H**) constant light. (**I, J**) Transcript levels of *vel1* (**I**) in constant darkness and (**J**) constant light. (**K,L**) Transcript levels of *pks4* (**K**) in constant darkness and (**L**) constant light. (**M**) Transcript levels of *ste12* in MAPKinase deletion mutants in constant darkness (DD) and light (LL).
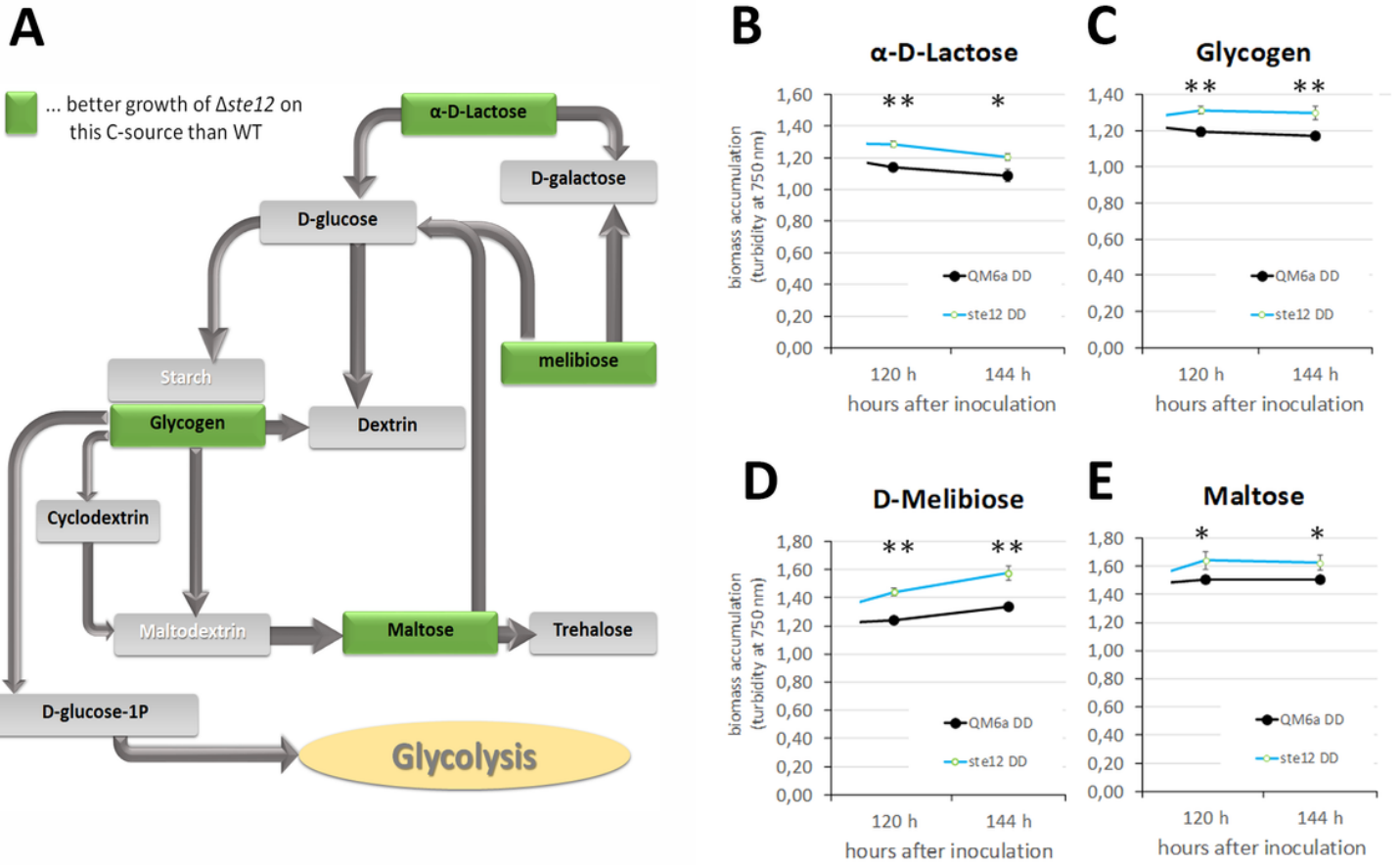
Figure 3

Analysis of carbon source utilization using the BIOLOG phenotype microassay. (A) Schematic representation of carbon sources on which Δ*ste12* grows better than the wild-type along with conversion pathways as deduced from KEGG pathways for *T. reesei*. (B,C) Growth data of the *ste12*-deletion strain as represented by turbidimetric analysis of biomass accumulation at 750 nm and compared to the wild-type strain QM6a. The analysis was done in biological triplicates with growth in darkness (DD). Statistical significance was determined by the T-test; * = p-value <0.05, ** = p-value <0.01
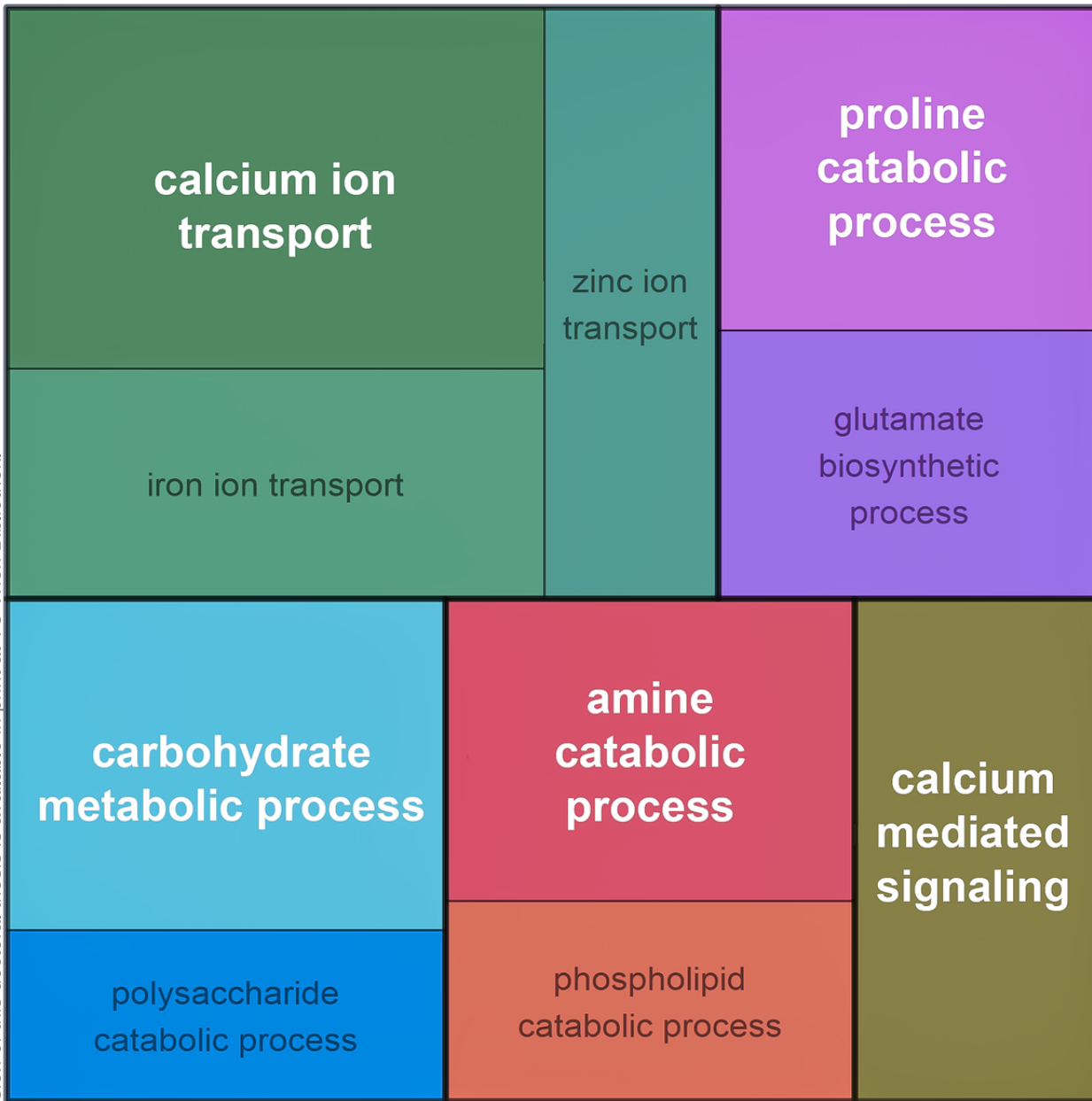
Figure 4

Gene ontology analysis of genes regulated by STE12. GO enrichment of up- and down-regulated genes for Δ*ste12* in constant darkness and light, visualized with rrvgo in R.
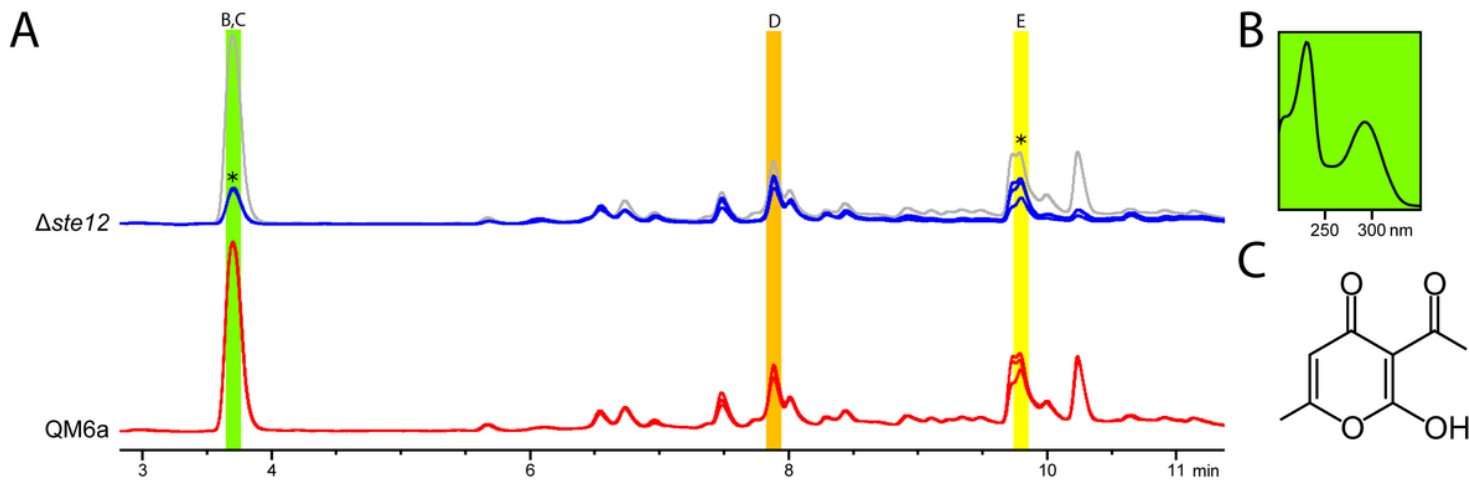
Figure 5

HPLC analysis of secondary metabolite production and identification of dehydroacetic acid. (**A**) HPLC-DAD chromatograms of QM6a and Δ*ste12* at 230 nm. QM6a profile is shown in grey for better comparison. Three biological replicates are shown. Strongly regulated peaks are indicated by asterisks. Dehydroacetic acid (B,C) is highlighted in green, (21S)-bisorbibutenolide (D) in orange and trichodimerol (E) in yellow [24]. (**B**) UV-spectrum and (**C**) chemical structure of dehydroacetic acid.

Supplementary Files

This is a list of supplementary files associated with this preprint. Click to download.

- Supplementaryfile1.xlsx
- Supplementaryfile2.xlsx
- Supplementaryfile3.pdf

Chapter 5: Plant recognition by *Trichoderma harzianum* elicits upregulation of a novel secondary metabolite cluster required for colonization

Miriam Schalamun[1], Guofen Li[1], Wolfgang Hinterdobler[1], Dominik K. Großkinsky[1], Stephane Compant[1], Assia Dreux-Zigha[2] and Monika Schmoll[1,3]

[1]AIT Austrian Institute of Technology GmbH, Center for Health and Bioresources, Konrad Lorenz Strasse 24, 3430 Tulln, Austria

[2] Greencell, 63360 St Beauzire, France

[3] University of Vienna, Department of Microbiology and Ecosystem Science, Division of Terrestrial Ecosystem Research, Djerassiplatz 1, 1030 Vienna, Austria

Plant recognition by *Trichoderma harzianum* elicits upregulation of a novel secondary metabolite cluster required for colonization

Miriam Schalamun[1], Guofen Li[1], Wolfgang Hinterdobler[1,§], Dominik K. Großkinsky[1], Stephane Compant[1], Assia Dreux-Zigha[2] and Monika Schmoll[1,3]*

[1]*AIT Austrian Institute of Technology GmbH, Center for Health and Bioresources, Konrad Lorenz Strasse 24, 3430 Tulln, Austria*

[2] *Greencell, 63360 St Beauzire, France*

[3] *University of Vienna, Department of Microbiology and Ecosystem Science, Division of Terrestrial Ecosystem Research, Djerassiplatz 1, 1030 Vienna, Austria*

Running title: Plant recognition in *T. harzianum*

*Corresponding author
Tel: +43 660 5565466

§ Current address:
MyPilz GmbH, Wienerbergstrasse 55/13-15, 1120 Vienna, Austria

Email:
Miriam Schalamun   miriam.schalamun@ait.ac.at
Guofen Li   guofen.li@ait.ac.at
Wolfgang.Hinterdobler   wolfgang.hinterdobler@mypilz.eu
Dominik Grosskinsky   dominik.grosskinsky@ait.ac.at
Stephane Compant   stephane.compant@ait.ac.at
Assia Dreux-Zigha   assiadreux@greencell.tech
Monika Schmoll   monika.schmoll@univie.ac.at

Keywords

Trichoderma harzianum, *Hypocrea lixii*, biocontrol, plant protection, plant-fungus interaction, secondary metabolism, MAMP (microbe-associated molecular pattern), interkingdom communication, PCA cluster

Summary

Trichoderma harzianum is a filamentous ascomycete frequently applied as plant beneficial agent in agriculture. While mycoparasitism and antagonism of *Trichoderma* spp. against fungal pathogens are well known, early responses of the fungus to the presence of a plant await broader investigation. In this study we analyzed these early stages of plant-fungus communication at the molecular level. We show that *T. harzianum* B97 is an efficient colonizer of plants and chemotropically responds to a plant extract. Patterns of secreted metabolites revealed that the fungus chemically responds to the presence of the plant and that the plant secrets a fungus specific metabolite as well. Hence we developed a strategy for omics analysis to simulate the conditions of the early plant recognition eliciting a chemotropic response in the fungus and found only 102 genes to be differentially regulated, including nitrate and nitrite reductases. Among them, a so far uncharacterized, presumably silent gene cluster was strongly induced upon recognition of the plant. Gene deletion of two genes of this *P*lant *C*ommunication *A*ssociated (PCA) cluster revealed that they are essential for colonization of soybean roots. Moreover, for part of the gene cluster, a DNA motif with palindromic sequence was detected. Phylogenetic analysis indicated that the PCA cluster is only present in the Harzianum clade of *Trichoderma* and was likely acquired by horizontal gene transfer (HGT) from *Metarhizium* spp., with the clustered genes originating from fungi, bacteria and plants.

We conclude that the plant recognition specific PCA cluster mediates early chemical communication between plant and fungus, is required for colonization and it is likely responsible for the high potential of *T. harzianum* and closely related species for biocontrol applications.

Significance statement

Interactions of plants with fungi – beneficial or pathogenic – are crucial for the ecological function of both partners. Yet, the chemical "language" they use and how or when they use it is still insufficiently known. We describe discovery of a novel secondary metabolite cluster, which is transcriptionally induced in the early phase of interaction, even before contact. Presence of this cluster is essential for colonization of the plant, hence reflecting the very start of an intimate plant-fungal interkingdom interaction. Acquisition of the cluster from other organisms highlights the evolutionary adaptation of *T. harzianum* to plant interaction and likely contributes to its success as plant symbiont.

Introduction

68

69

70 Natural environments harbor a complex community of microorganisms, which fulfill crucial tasks in the

71 carbon cycle and can interact with plants as symbionts (Averill et al., 2022; Harman, Lorito, et al., 2004)

72 or pathogens (Doehlemann et al., 2017). Climate change and global warming are bringing increased

73 disease pressure, abiotic stresses and promotes invasion of plant pathogens in new habitats (Bebber,

74 2015; Raza & Bebber, 2022). Hence, better understanding for knowledge based application of biocontrol

75 agents and biostimulants is required (Del Buono, 2021; Liu et al., 2022). Fungi evolved elaborated

76 mechanisms for dealing with their biotic and abiotic environment in terms of sensing and signaling

77 mechanisms as well as strategies for effective competition and antagonism (Khan et al., 2020; Syed Ab

78 Rahman et al., 2018). Fungal secondary metabolites are thereby of crucial importance for interactions

79 with other microbes, animals and also with plants (Rangel et al., 2021). The abilities of some fungi to

80 antagonize and kill their competitors is applied for protection of plants against pathogens and fungi of

81 the genus *Trichoderma* are among the most broadly applied for this purpose (Sood et al., 2020).

82 Consequently, this genus also dominates research towards mycoparasitism, plant protection and

83 biocontrol of plant pathogens (Ramirez-Valdespino et al., 2019; Tyskiewicz et al., 2022).

84

85 Fungi of the genus *Trichoderma* (Schalamun & Schmoll, 2022; Woo et al., 2022) are typical inhabitants

86 of the rhizosphere and are found in soils worldwide (Druzhinina et al., 2011). They belong to the most

87 versatile microorganisms for both agricultural and industrial applications (Mukherjee et al., 2013).

88 Several *Trichoderma* species are known as efficient biocontrol organisms and act as important

89 symbionts with plants (Guzman-Guzman et al., 2019; Harman, Howell, et al., 2004). They are studied

90 in detail for their capabilities in producing antibiotics, parasitizing other fungi – predominantly plant

91 pathogens – and to compete with deleterious plant pathogens (Druzhinina et al., 2011; Tyskiewicz et al.,

92 2022). Beneficial *Trichoderma* strains further induce root branching and can increase shoot biomass and

93 trigger systemic resistance as well as plant nutrient uptake (Contreras-Cornejo et al., 2016). One of the

94 major advantages of *Trichoderma* as biocontrol agents (BCAs) is that they can be found almost

95 ubiquitously, which enables development of regional integrated crop protection strategies, with only

96 minor interference with the natural microbial flora (Averill et al., 2022; He et al., 2021).

97

98 Among the most important functions for successful fungal plant interaction – beneficial or pathogenic -

99 is the ability to colonize plant roots (Haueisen & Stukenbrock, 2016; Tyskiewicz et al., 2022).

100 *Trichoderma* spp. are able to efficiently colonize plant roots, although they mostly remain at the outer

101 layers of the plant tissue (Contreras-Cornejo et al., 2016; Tyskiewicz et al., 2022). Nevertheless, also

102 truly endophytic strains of *Trichoderma* (Chaverri et al., 2015; Harman & Uphoff, 2019) are known to

103 associate with plants, including also some *T. harzianum* strains (Bailey & Melnick, 2013; Chaverri et

104 al., 2015). Fungi communicate with their environment using a broad array of signals (Bazafkan et al.,

105 2015; Leeder et al., 2011; Macias-Rodriguez et al., 2020). Chemical communication between fungi and

106 plants is essential for interaction and diverse secondary metabolites are known to play an important role

107 in this interplay (Macias-Rodriguez et al., 2020). Moreover, adhesion and the function of hydrophobins

108 are required for plant-fungus interaction (Taylor et al., 2022). Intriguingly, stressed plants were found

109 to secrete specific compounds attracting beneficial fungi (Lombardi et al., 2018). Overall, a considerable

110 number of effectors (Ramirez-Valdespino et al., 2019) and secondary metabolites (Contreras-Cornejo

111 et al., 2016) including volatile organic compounds (Joo & Hussein, 2022) are already known to

112 contribute to successful biocontrol. In the plant, recognition of beneficial fungi like *Trichoderma* spp.

113 leads to metabolic changes (Schweiger et al., 2021) and the onset of systemic resistance (Newman et

114 al., 2013). Acquisition of nutrients is supported by plant-fungus interactions, also if the requirements for

115 mycorrhiza are not fulfilled.

116

117 One major question of the last decades was how fungi sense the presence of a plant. Several years ago,

118 a seminal study on plant recognition by the fungal pathogen *Fusarium oxysporum* provided

119 groundbreaking insights in this respect (Turra & Di Pietro, 2015; Turra et al., 2015). It was shown that

120 this fungus chemotropically responds to the presence of a plant and that this response is dependent on a

121 pheromone receptor of the fungus, which obviously senses a peroxidase of the plant (Nordzieke et al.,

122 2019; Turra et al., 2015). This research and the developed method opens up new possibilities to study

123 plant fungus as well as other intra- and interkingdom interactions and their determinants (Turra et al.,

124 2016).

125

126 Biocontrol of plant pathogens (He et al., 2021) is a complex mechanism involving processes from

127 secretion of enzymes to production of secondary metabolites to mycoparasitism on the fungal pathogen

128 (Karlsson et al., 2017). *Trichoderma* spp. as well as other fungi applied in agriculture as plant beneficial

129 agents produce a broad array of secondary metabolites (Lehner et al., 2013; Zeilinger et al., 2016).

130 Nevertheless, these fungi (except for a few more problematic species like *T. brevicompactum*) have a

131 long history of safe application worldwide and no contamination of treated crops has been observed and

132 hardly any negative effects on plants are known. Thereby, not only the fungi themselves, but also their

133 secondary metabolites can be applied in agriculture (Vinale & Sivasithamparam, 2020). Moreover,

134 investigation of secondary metabolites of *Trichoderma* and their functions bears the opportunity to

135 identify novel, bioactive compounds potentially useful in medicine and industry (Shenouda & Cox,

136 2021). Interestingly, evolutionary analysis revealed that the core genome of *Trichoderma* species

137 comprises about 7000 genes and that a considerable number of genes crucial to their well-known

138 functions in litter degradation or secondary metabolism was acquired by horizontal gene transfer

139 (Druzhinina et al., 2018; Druzhinina et al., 2016; Schalamun & Schmoll, 2022). This successful sourcing

140 of advantageous genes by *Trichoderma* is assumed to be corroborated by their capability of

141 mycoparasitism, which brings them in contact with foreign DNA (Druzhinina et al., 2018). Acquisition

4

142 of secondary metabolite clusters can be particularly beneficial for a biocontrol agent, due to their
143 potential function in communication with the plant and/or fending of competitors or antagonizing
144 pathogens.

145

146 *Trichoderma harzianum* B97 (Compant et al., 2017) was selected for its high efficiency in stimulation
147 of plant growth. Moreover, the strain shows solubilization of phosphate and can alleviate abiotic
148 stresses. Due to its proven efficiency in agricultural applications, it was the ideal isolate for studying its
149 communication with a plant in more detail. We show that *T. harzianum* B97 chemotropically reacts to
150 the presence of a plant and chemically communicates with a living plant as well. Moreover, we found
151 that the ability of B97 to efficiently colonize plant roots depends on a secondary metabolite cluster
152 specifically induced during early plant recognition and likely acquired by horizontal gene transfer.

153

154

155 **Results**

156

157 *T. harzianum is an efficient colonizer of plant roots*

158

159 *T. harzianum* B97 was isolated from agricultural soil in France (Compant et al., 2017) and selected for
160 its plant beneficial characteristics. Good colonization of plants by the fungus would indicate efficient
161 communication with the plant (Lareen et al., 2016). Therefore we studied, whether *T. harzianum* B97
162 would be able to efficiently colonize plant roots. We analyzed colonization after co-inoculation of wheat
163 seedlings with *T. harzianum* B97. Staining of roots with wheat germ agglutinin (WGA)-AlexaFluor488
164 and confocal microscopy showed efficient colonization of roots by *T. harzianum* B97 (Figure 1A).

165

166 *T. harzianum B97 shows chemotropic response to soybean root exudates*

167

168 Recognition of the presence of the plant in the vicinity is crucial for initiation of interaction. Moreover,
169 successful interaction with different plant species is a desirable trait for biocontrol agents. Recently,
170 attraction of a *T. harzianum* strain to plant roots was shown (Lombardi et al., 2018). Hence we wanted
171 to test first, whether *T. harzianum* B97 chemotropically reacts to the presence of root of soy plants.
172 Optimization of the assay to *T. harzianum* B97 yielded an optimal working concentration of 0.0025 %
173 peptone from casein to support germination without inducing multipolarity. We tested the response of
174 *T. harzianum* B97 to 1 % (w/v) glucose, which yielded a chemotropic index of 9.66 ±1.15 % and was
175 hence in the range seen previously for fungi (Turra et al., 2015). Subsequent analysis of chemotropic
176 response to soybean root extracts showed a chemotropic index of 8.32% ± 0.15%, representing low but
177 clearly present response (Figure 1B).

178

Secretion of secondary metabolites changes in the presence of soy bean roots

As *T. harzianum* B97 clearly reacts to the presence of the plant, we wanted to test whether chemical communication is initiated as a consequence of recognition. We used conditions as close as possible to those applied in the chemotropic assay, with a low level of carbon source (0.1 % (w/v) glucose) and minimal medium nutrients to support growth and still allow plant recognition. After 34 hours growth of *T. harzianum* B97, roots of soybean plants were placed in 3 cm distance of the fungal growth front and incubated for 13 hours in the darkness to enable communication. To ensure that communication occurs via the medium or via volatile organic compounds, but not due to direct contact, we only used plates where fungus and plants remained without physical contact at the time of harvesting. Thereafter, agar slices were excised from the area covered by the fungus for assessing changes in fungal metabolite profiles as well as from the area opposite of the plant root to analyze alterations in metabolites secreted by the plant (Figure 1C). Secondary metabolite patterns from the fungus grown without a plant and of the plant in the absence of the fungus under otherwise similar conditions were used as controls.

Indeed, after 13 hours of exposure of the fungus to the plant, we observed additional bands appearing in the high performance thin layer chromatography (HPTLC) analysis, reflecting reaction of the fungus to the plant (Figure 1D,E). Also the plant secreted additional compounds upon detection of the fungus, which were not present in the assay without the fungus (Figure 1D,E). Consequently, *T. harzianum* B97 initiates chemical communication with the soy plant roots within 13 hours of co-cultivation.

Transcriptome analysis of early stages of plant recognition

Having confirmed that plant recognition by *T. harzianum* B97 indeed occurs and elicits a two-way communication, we adapted transcriptome analysis to these conditions by covering the agar surface with cellophane to enable harvesting of the mycelium. Due to the high similarity of *T. harzianum* B97 with the previously sequenced reference strain *T. harzianum* CBS226.95 (Druzhinina et al., 2018) we refer to protein IDs from the respective public genome database at JGI (https://mycocosm.jgi.doe.gov/Triha1/Triha1.home.html) in the following.

Since transcript levels reflect investment of resources for functions important under a certain condition, we checked which functions were represented under the conditions used for secondary metabolite screening and transcriptome analyses. Functional category analysis of the 250 genes with highest transcript levels under the applied conditions showed considerable investments in metabolic functions, energy production and transport among others (Figure 2A.

Besides the expected enrichment in metabolic functions, energy metabolism and carbohydrate metabolism, we also found that the highest levels of transcript abundance were enriched in functions in stress response (p-value 1.96e-03) and unfolded protein response (p-value 7.89e-04). Additionally, also polysaccharide metabolism is significantly enriched in this highly transcribed gene set (p-value 2.49e-

216 11), with the homologues of the cellobiohydrolases *cbh1* and *cbh2* comprised in this group. These

217 patterns reflect that the chosen condition indeed represents a condition of low nutrient availability

218 inducing cellobiohydrolases likely due to starvation. Consequently, this condition closely resembles the

219 conditions present in the chemotropic assay.

220

221 *Specific gene regulation in the presence of a plant*

222

223 Comparison of genes differentially regulated between growth alone on the plate and in the presence of

224 a plant confirmed that our experimental setup captured a very early specific stage of plant recognition

225 by *T. harzianum* B97 and likely represents the onset of communication. In total, only 102 genes were

226 significantly (p-value <0.01) regulated more than 2fold (41 down, 61 up) upon recognition of the plant

227 (supplementary file 1), which share functions in energy production, metabolism and transport (Figure

228 2B). Genes upregulated in the presence of the plant were enriched in functions of C-compound and

229 carbohydrate metabolism (p-value 1.04e-03), glycolysis and gluconeogenesis (p-value 4.09e-03) and

230 electrochemical potential driven transport (p-value 4.00e-03). Interestingly, the gene set down-regulated

231 in the presence of the plant is enriched in functions in secondary metabolism (p-value 5.03e-04) and

232 drug/toxin transport (p-value 4.26e-03).

233

234 Specifically, we detected a nitrate reductase (Triha_507858) and a nitrite reductase gene (Triha_507859)

235 to be up-regulated 17fold or 4fold, respectively upon plant recognition. These genes represent the

236 homologues of the *Aspergillus nidulans* genes *niiA* and *niaD*, which share a bidirectional promotor and

237 play important roles in nitrogen uptake and metabolism (Brownlee & Arst, 1983; Johnstone et al., 1990).

238 However, the putative homologue of *crnA*, the major facilitator superfamily (MFS) transporter gene

239 associated with this cluster in *A. nidulans* (Triha1_142220) and the major transcription factor genes

240 responsible for regulation of nitrogen metabolism, *areA* (Triha1_451) and *areB* (Triha1_70872), are not

241 significantly differentially regulated under these conditions.

242

243 Considering fungus-plant interaction, also the more than 5fold up-regulation of Triha_398864, encoding

244 a homologue of Epl1/Sm1 is interesting. These ceratoplatanin-like proteins play a role in colonization

245 of plant roots and as effectors (Gao et al., 2020). In *T. harzianum*, Epl1 regulates virulence of the plant

246 pathogen *Botrytis cinerea*, mycoparasitism as well as plant immunity at early stages of root colonization

247 (Gomes et al., 2015; Gomes et al., 2017), which is in perfect agreement with our hypotheses.

248

249 Furthermore, transcript abundance of two predicted protease genes (Triha1_541862; 5.3fold down and

250 Triha1_98848; 2.2fold down) is decreased in the presence of plant roots. As two putative terpene

251 synthase genes, *tps1* (Triha1_497584; 2.8fold up) and *tps11* (Triha1_523651; 3.1fold up) are up-

252 regulated, a role of terpenoid compounds in plant interaction is worth further investigation. Additionally,

253   an as yet uncharacterized non-ribosomal peptide synthase (NRPS, Triha_155805) and a putative

254   polyketide synthase (PKS, Triha_546993) are more than 2 fold upregulated upon plant sensing.

255

256   A further, strongly upregulated gene (32fold) is Triha1_36398, which is still uncharacterized and its

257   encoded protein comprises no known domains. However, analysis of putative protein interaction

258   partners using the homologue of this protein in *T. reesei* using the STRING database ((Szklarczyk et al.,

259   2021); https://string-db.org; version 11.5) suggests a connection to a predicted ferric reductase, which

260   fits to its genomic vicinity next to a putative ferric reductase (Triha1_76871) in *T. harzianum*, which is

261   also strongly upregulated and fits to the general picture of gene regulation in B97 upon plant recognition.

262

263   We conclude that the recognition of a plant in the environment causes *T. harzianum* to modulate

264   secondary metabolism, but to also elevate certain metabolic capabilities. Although functions in C-

265   compound and carbohydrate metabolism are enriched among up-regulated genes, this gene set does not

266   include the common plant cell wall degrading enzymes. The high expression level of cellulases detected

267   in all analyzed samples (see above) is not significantly altered upon recognition of a plant.

268

269   *A secondary metabolite cluster strongly up-regulated upon plant recognition*

270

271   Despite the low number of regulated genes, we still found a strongly regulated gene cluster (Figure 3A,

272   B), which is silent when the fungus is growing alone, and strongly induced upon recognition of the plant

273   with up to 1000-fold upregulation (Figure 3B; supplementary file 1). This gene cluster is located on

274   scaffold 23: 272 000 – 286 000 in the reference strain *T. harzianum* CBS226.95 and comprises all seven

275   genes present in this area. We termed the cluster *P*lant *C*ommunication *A*ssociated (PCA) cluster which

276   is comprised of TH_323871/*pca1*, TH_513502/*pca2*, TH_513502/*pca3*, TH_99174/*pca4*,

277   TH_513504/*pca5*, TH_513505/*pca6* and TH_513506/*pca7*. None of the genes in the cluster was

278   previously characterized and hence the metabolite produced cannot be predicted.

279   Interestingly, also a further putative ferric reductase gene related to *pca1* is strongly up-regulated upon

280   plant recognition (Triha1_76871; 21.2fold) as is a copper transporter gene closely related to *pca2*

281   (Triha1_83588; 30.8fold). Both genes are not located in the genomic vicinity of the PCA cluster.

282

283   A SNP analysis of differences between *T. harzianum* B97 (Compant et al., 2017) and the publicly

284   available sequence of *T. harzianum* (*sensu stricto*) CBS226.95 (Druzhinina et al., 2018) revealed no

285   intragenic, no intergenic and no nonsynonymous SNPs in the region of the PCA cluster. Only one

286   synonymous SNP was detected in 513506 and one in 513501 in the 5' UTR, hence strengthening the

287   identification of *T. harzianum* B97 as *sensu stricto*. Consequently, we will refer to the *T. harzianum*

288   CBS226.95 protein IDs and sequences hereafter.

289   In order to gain information on the potential function of the PCA cluster, we performed domain analysis

290   and checked homologous genes in other fungi. PCA1 comprises a NADPH oxidase domain (cd06186)

291   catalyzing the generation of reactive oxygen species (ROS) as well as a ferric reductase like

292   transmembrane component (pfam01794) and is related to *A. fumigatus* FRE7, which is regulated by veA

293   (Lind et al., 2015), upon response to Fe starvation (Kurucz et al., 2018) and during hypoxia (Losada et

294   al., 2014). PCA2 contains a copper transporter domain (pfam04145), which may be involved in

295   oxidative stress protection or pigmentation and is related to putative low affinity copper transporters in

296   *Aspergilli*. PCA3 is a member of the transferase superfamily (cl23789), which comprises enzymes that

297   catalyze the first committed reaction of phytoalexin biosynthesis, but also trichothecene 3-0-

298   acetyltransferase. The *A. fumigatus* homologue, which is not closely related to PCA3, has a predicted

299   role in festuclavine biosynthesis. PCA4 contains an NAD/NADP octopine/nopaline dehydrogenase

300   (pfam02317) domain as well as a glutamate synthase or related oxidoreductase domain (cl28234), which

301   may be involved in amino acid transport and metabolism. PCA4 has no homologues in *Aspergilli*. PCA5

302   is a major facilitator superfamily transporter (pfam07690), related to a cycloheximide resistance protein.

303   PCA6 belongs to the superfamily of S-adenosylmethionine-dependent methyltransferases, class I

304   (cl17173). PCA7 has a Cytochrome P450 domain (cl12078), which may be involved in the degradation

305   of environmental toxins. The homologue of PCA7 in *A. nidulans*, STCF, is a putative sterigmatocystin

306   biosynthesis P450 monooxygenase with a predicted role in sterigmatocystin/aflatoxin biosynthesis.

307   However, we want to note here, that the genes within the PCA cluster likely originate from horizontal

308   gene transfer from other fungi or even plants (see below) and that therefore these potential functions

309   should be considered preliminary.

310

The cluster comprises multiple occurrences of a novel DNA motif

312

313   Due to the striking up-regulation of the PCA cluster genes upon plant recognition, we were interested

314   whether a common DNA motif might be present in the promotors of the genes. To this end, we analyzed

315   the promotors of all *pca* genes for promotor motifs using MEME. Interestingly, we found a palindromic

316   motif (Figure 3A,C) in the intergenic regions between *pca1* and *pca2* as well as *pca3* and *pca4*. This

317   motif is present twice in each region and was not yet characterized in fungi.

318

The PCA cluster is required for plant root colonization

320   We further asked whether the early and strong transcriptional response of the PCA cluster genes upon

321   plant recognition would be predictive of a role in colonization, which is crucial for plant-fungus

322   interaction and plant protection (Macias-Rodriguez et al., 2020). For construction of deletion strains we

323   chose *pca1*, the putative NADPH oxidase, since previous work revealed an involvement of ROS –

324   directly or indirectly – in plant-fungus interaction (Nordzieke et al., 2019; Turra et al., 2015).

325   Additionally, we prepared a null mutant of *pca5*, encoding a transporter potentially involved in signal

326   compound emission. Both mutant strains were viable and showed no striking growth defects.

327   We tested the ability to colonize plant roots by inoculating soybean seeds with the mutant strains or the

328   wildtype and evaluated the presence of fungal mycelia on young roots after 8 days (Figure 4). Confocal

329   microscopy was performed from at least three replicate assays and multiple sites per root. Roots grown

330   from uninoculated seeds were used as controls. This analysis showed that while the wildtype *T.*

331   *harzianum* B97 efficiently colonized the root surface. Neither Δ*pca1* nor Δ*pca5* were able to colonize

332   and the root grown from seeds inoculated with the mutant strains and these samples rather resembled

333   the uninoculated control (Figure 4). We conclude that the requirement of these two genes of the PCA

334   cluster is representative for the importance of this cluster and its upregulation upon plant recognition for

335   efficient colonization of plants by *T. harzianum* B97.

336

The PCA cluster is specific to Trichoderma and was likely acquired by HGT

338

339   Because of the obvious importance of the PCA cluster for plant recognition and colonization, we were

340   interested in its conservation and evolution in fungi. Since the genomic region of the cluster in B97 did

341   not comprise a notable number of SNPs in comparison with *T. harzianum* CBS226.95, we will refer to

342   the region in the latter strain in our further analyses and descriptions.

343

344   After identifying the genomic area of the PCA cluster in *T. harzianum*, we performed a blastn analysis

345   with all dikarya genome sequences available at JGI (2140 genomes). These genome sequences cover

346   the group of Sordariomycetes (528 genomes) very well, including numerous strains of the genus

347   *Trichoderma*, which would allow for association to the well-studied clades of the genus (Atanasova et

348   al., 2013). All other groups of fungi in JGI mycocosm outside dikarya (Grigoriev et al., 2014) were

349   tested as well, but did not yield homologous sequences. Surprisingly, the search results did not reflect

350   the expected relationships according to the known phylogeny of ascomycetes. Moreover, the cluster was

351   not present in many *Trichoderma* species. Neither *Trichoderma* spp. outside of the Harzianum clade nor

352   the common ancestor of the genus *Trichoderma*, *Escovopsis weberi* (de Man et al., 2016) or closely

353   related species such as *Fusarium* spp. had this cluster, as revealed by only partial coverage of the cluster

354   sequence in the genomes. Rather it was scattered among some species in the Sordariomycetes. However,

355   good coverage of the cluster area was detected for *Metarhizium* species as well as for *Pestaliopsis fici*

356   (Xylariales (Wang et al., 2015)) and *Talaromyces islandicus* (Eurotiomycetes (Schafhauser et al., 2015).

357   Using the respective nucleotide sequences covering the whole clusters for phylogenetic analysis

358   confirmed the close relationship of the cluster sequences (Figure 5). In case of *Metarhizium* spp. we

359   found coverage of the cluster for *M. anisopliae, M. robertii* and *M. brunneum*, representing the generalist

360   species of the genus (Sbaraini et al., 2016), but not in intermediate or specialist species, which is also

361   the case for other secondary metabolite clusters in specialist species of *Metarhizium* (Sbaraini et al.,

362 2016). Interestingly, the PCA cluster was not detected previously in *Metarhizium* (Donzelli & Krasnoff,

363 2016) and does not overlap with the well characterized secondary metabolite clusters responsible for

364 production of destruxin, ferricrocin or other known toxins (Donzelli & Krasnoff, 2016; Sbaraini et al.,

365 2016). Furthermore, this finding suggested, that the PCA cluster was acquired by *T. harzianum* via

366 horizontal gene transfer (HGT), likely from *Metarhizium* spp.

367

368 *Individual genes of the PCA cluster presumably originate from plants and bacteria*

369

370 Our detailed investigation of genome sequences confirmed that the full PCA cluster is indeed only

371 present in the Harzianum clade (Atanasova et al., 2013) of *Trichoderma*, but not in the more ancestral

372 Trichoderma clade or in the evolutionarily younger Longibrachiatum clade. These findings suggest that

373 the PCA cluster was gathered from other organisms by HGT, likely after the split of the Harzianum

374 clade from the Longibrachiatum clade in *Trichoderma*. We screened the identified genomic locations

375 for the presence of the seven genes of the PCA cluster and found all of them in the same order and

376 orientation in the Harzianum clade as well as in *Metarhizium* spp., which strengthens the hypothesis of

377 HGT. In *P. fici* and *T. islandicus* the cluster is not complete, with *pca1* and *pca2* or *pca3* and *pca5*

378 missing, respectively (Figure 6A). Individual genes of the cluster did show hits with blast searches in

379 *Trichoderma* spp. outside of the Harzianum clade as well as in several other species, but they were not

380 assembled in clusters.

381

382 We therefore asked whether the *pca* genes might be present in the genomes of other *Trichoderma* clades,

383 yet not assembled in clusters. We performed phylogenetic analysis using at least three blast hits (if

384 present and e-value <e-10; otherwise all available) for the predicted protein sequences encoded by each

385 *pca* gene in various organisms. This analysis allowed us to delineate, whether in these species the cluster

386 simply lost several components during evolution or if those blast hits merely represent unrelated genes

387 with similar function. We used representatives of the Harzianum species complex (Chaverri et al., 2015)

388 (*T. harzianum, T. guizhouense, T. afroharzianum*) and the Harzianum clade (*T. pleuroticola, T.

389 aggressivum* and *T. virens*) (Chaverri et al., 2015). From the further clades we picked representatives

390 from the Longibrachiatum clade (*T. reesei*), the Helicum clade (*T. helicum*) (Jaklitsch & Voglmayr,

391 2015), the Brevicompactum clade (*T. brevicompactum*) (Thomas Degenkolb et al., 2008) and the

392 Trichoderma clade (*T. atroviride*) (Kubicek et al., 2019) as well as from *M. anisopliae, P. fici* and *T.

393 islandicus* and other fungi having potential homologues in their genomes. Moreover, we added closely

394 related sequences revealed as potential homologues from plants and bacteria as detected in blastp

395 analysis using NCBI Blastp and excluding ascomycetes.

396

397 Interestingly, the latter blastp search on the NCBIdatabase yielded also highly related sequences to

398 bacteria and plants for individual PCA proteins (Figure 6B), with *Quercus suber* (cork oak, plant)

11

399   homologues as best hit for PCA1, PCA2 and PCA7, basidiomycete proteins for PCA3 and PCA5 as well

400   as bacterial proteins for PCA4 and PCA6, which was already a strong indication that the components of

401   the cluster were assembled from different donor species.

402   This first exploratory phylogenetic analysis revealed the PCA proteins presumably connected by

403   evolution and enabled us to distinguish those which clustered with proteins only similar, but not

404   homologous to the PCA proteins and hence unrelated to the cluster. Indeed, the PCA homologues from

405   species comprising the cluster formed a separate clade from those with similarity to the PCA sequences,

406   but not organized in a cluster. In a second step we then used the closest hit of respective protein

407   sequences from this sister clade for repeated phylogenetic analyses (Figure 7 A-G).

408

409   This analysis confirmed that only the *pca* genes from species having the cluster form a clade together,

410   while *pca*-related genes scattered over the genome formed separate clades. Interestingly, *T. atroviride*

411   seems to have homologues of PCA1 and PCA3 (Figure 7A, C), since the respective proteins cluster

412   closely with the genes assembled in clusters in *T. harzianum* and not outside this clade. Additionally,

413   we also found that hits from fungi outside ascomycetes, as well as those from plants or bacteria clustered

414   among the fungal sequences or as sister clades hence confirming the blastp results. Consequently,

415   acquisition of individual genes even from different kingdoms is likely, although the highly conserved

416   structure of the cluster in *Metarhizium*, *Trichoderma* and in part *P. fici* and *T. islandicus* suggests

417   assembly of the cluster in one of these genera. While we cannot provide evidence of the evolutionary

418   path and chronological order of the gene transfer, or whether a birth and death evolution as reported for

419   the SOR cluster in *T. reesei* (Druzhinina et al., 2016) has occurred, our results still strongly indicate that

420   HGT contributed to acquisition and formation of the PCA cluster.

421

422   **Discussion**

423

424   Recognition of plants by fungi is crucial if the actual cry for help in the form of root exudates (Rolfe et

425   al., 2019) is to be heard. Beneficial fungi of the genus *Trichoderma* positively impact plants at multiple

426   levels, also using chemicals for achieving their effect (Macias-Rodriguez et al., 2020), but most

427   importantly, they trigger the systemic immune response of plants (Guzman-Guzman et al., 2019;

428   Harman et al., 2020). *T. harzianum* strains produce a number of secondary metabolites (Hanson, 2005),

429   most of which are not yet assigned to specific biosynthetic gene clusters.

430   Although secondary metabolism and the gene clusters involved in biosynthesis of secondary metabolites

431   are well studied in *Trichoderma* species (Keswani et al., 2014; Zeilinger et al., 2016), the plant

432   recognition specific PCA gene cluster we found in this study was not described before. Consequently,

433   it is currently not possible to associate a metabolite that might be produced by this cluster or probably

434   modified. However, the enormous extent of the induction of this cluster, which exceeds the changes in

435   transcript abundance of all other regulated genes, indicates that communication with the plant is

436 associated with this induction, which we confirmed with investigation of two crucial genes of the cluster

437 (*pca1* and *pca5*). Moreover, the fact that the presence of a plant elicits a response in terms of secondary

438 metabolite production is in agreement with the finding that the secondary metabolite pattern of *T.*

439 *harzianum* B97 is altered in the presence of a plant.

440

441 The striking impact of deletion of members of the PCA cluster on colonization of soybean roots strongly

442 supports a function of the associated secondary metabolite(s) in plant-fungus communication. Such

443 communication is vital for beneficial interkingdom-interactions, which was also shown for *Trichoderma*

444 (Macias-Rodriguez et al., 2020). The beneficial effects of *T. harzianum* B97 on plant health are

445 extensive, facilitating commercial application, and may involve an influence of secondary metabolites

446 – including those of the PCA cluster – on innate immunity as shown previously for *Trichoderma*

447 (Newman et al., 2013). However, as root colonization is a prerequisite for efficient interaction, it can be

448 concluded that the early stage recognition and communication represents the major function of the PCA

449 cluster. This hypothesis is further strengthened by the very early induction of the cluster, within only 13

450 hours of proximity and without direct contact between plant and fungus.

451

452 A relevance of an NADPH oxidase involved in ROS production for plant-fungus interaction was

453 previously shown for *T. atroviride* (Villalobos-Escobedo et al., 2020). For *F. oxysporum*, NADPH

454 oxidase was found to be essential for chemotropic response to the presence of a plant (Nordzieke et al.,

455 2019).

456

457 Our analysis of gene regulation patterns specific for early plant recognition by *T. harzianum* B97

458 revealed a significant enrichment of genes involved in detoxification by export, which is likely achieved

459 by transporters. Therefore, we investigated the role of PCA5 in plant interaction and indeed found that

460 this transporter is crucial for colonization. This finding is in agreement with the hypothesis, that the

461 chemical communication with the plant as initiated by induction of the PCA cluster is dependent on

462 export of secondary metabolites serving as signaling molecules by PCA5.

463

464 The PCA cluster comprises also three genes putatively involved in biosynthesis or modification of

465 secondary metabolites. Among the genes regulated in response to the presence of the plant, we found

466 several more putative permeases and transporters, but no gene which might encode a transcription factor.

467 Hence, it remains to be demonstrated, how the coordinated induction of the PCA cluster genes is

468 achieved.

469

470 One striking example of horizontal gene transfer (HGT) was described for the sorbicillin biosynthetic

471 cluster in *T. reesei*, which was acquired from other fungi, but also other cases are known from this genus

472 (Druzhinina et al., 2018; Druzhinina et al., 2016; Schalamun & Schmoll, 2022). An unexpectedly high

473 number of genes, including numerous carbohydrate-active enzymes (CAZymes) and plant cell wall

474 degradation associated proteins in the *Trichoderma* genomes originates from other organisms. However,

475 for plant associated fungi, like those of the genus *Trichoderma*, HGT seems to be a rather common

476 phenomenon, especially concerning genes involved in production of secondary metabolites (Spatafora

477 & Bushley, 2015).

478

479 Currently we cannot anticipate for the biosynthesis of which compound the PCA cluster is responsible

480 and if it may be harmful or toxic, because secondary metabolite clusters related to the PCA cluster were

481 not characterized before. However, since the problematic *T. brevicompactum*, which produces harmful

482 toxins (T. Degenkolb et al., 2008), does not comprise the PCA cluster, it is unlikely that this cluster

483 causes production of harmful chemicals during early plant recognition.

484

485 Interestingly, *T. harzianum* seems to have acquired the PCA cluster from *Metarhizium* (Sheng et al.,

486 2022), which is a known endophyte (Sasan & Bidochka, 2012; Wyrebek et al., 2011) and an insect

487 pathogen infecting hundreds of species (Roberts & Hajek, 1992; St Leger, 1993). In a tripartite

488 interaction, *M. robertsii,* which comprises the PCA cluster, transfers nitrogen from insects they had

489 infected to their plant hosts (Behie et al., 2012). A comparable situation was shown for *Laccaria bicolor*

490 which associates with pine and spruce and transfers nitrogen from collembola in soil to the roots it

491 colonizes (Klironomos & Hart, 2001). Recently, an impact of a strain belonging to *T. afroharzianum*, a

492 species closely related to *T. harzianum*, on the interaction of a plant with pathogenic insect was shown

493 (Di Lelio et al., 2023; Monte, 2023). Although this interaction was rather indirect via modulation of the

494 gut microbiome, also numerous direct antagonistic effects on insects by *Trichoderma* are known

495 (Poveda, 2021). Consequently, an ecological function of *Trichoderma* comparable to that of

496 *Metarhizium* shown by Behie and colleagues (Behie et al., 2012) seems likely.

497 Since availability and uptake of different nitrogen sources considerably influences secondary

498 metabolism (Tudzynski, 2014), the upregulation of the *niiA* and *niaD* homologues upon plant

499 recognition in *T. harzianum* B97 may not only reflect nitrogen transport to the plant, but could also be

500 a sign for increased efforts for production of specific secondary metabolites for plant communication.

501 Notably, although several genes associated with secondary metabolism are down-regulated, besides the

502 strong induction of PCA cluster genes, also an NRPS encoding gene and a PKS encoding gene are

503 slightly upregulated. These obvious shifts in secondary metabolism are in agreement with the altered

504 pattern we observed due to the presence of the plant.

505

506 Species of the Harzianum complex are supposed to be the most common endophytic species in tropical

507 trees (Chaverri et al., 2011), with speciation leading to habitat preferences of soil or endophytism

508 (Chaverri et al., 2015). Among the *Trichoderma* spp of the Harzianum clade, which comprise the PCA

509 cluster, there are also endophytically growing ones like *T. endophyticum* and *T. afrasin* (Chaverri et al.,

14

510 2015). The upregulation of the *niiA* and *niaD* homologues, which are involved in nitrogen uptake upon

511 recognition of the plant (*nit3* and *nit6*) indicates that nitrogen metabolism also may play a role in the

512 interaction of *T. harzianum* with the plant, although potentially also other sources of nitrogen are used

513 than by *Metarhizium*, which degrades killed insects to deliver nitrogen to the plant (Behie et al., 2012).

514 Consequently, the PCA cluster is likely to support beneficial communication to the plant at an early

515 stage of colonization, which may involve pretending to be an arriving endophyte delivering additional

516 soil/organic nitrogen. Since the PCA cluster is crucial for colonization by *T. harzianum*, presence of this

517 cluster in the fungus is highly likely to contribute to the high efficiency of members of this clade in

518 biocontrol applications.

519 Accordingly, microbiome analysis revealed co-occurrence of *Trichoderma* and *Metarhizium* species in

520 the rhizospere at high yielding field sites (Bandara et al., 2021) or with banana plants (Ciancio et al.,

521 2022). Hence the mycoparasitism of *Trichoderma* may well have contributed to acquisition of the PCA

522 cluster as was proposed for acquisition of the SOR cluster in *T. reesei* previously (Druzhinina et al.,

523 2016).

524

525 In summary, we developed a strategy to simulate conditions of chemotropic response, which allowed us

526 to detect a secondary metabolite cluster essential for communication with a plant enabling efficient

527 colonization of the root surface (Figure 8). While revealing an intriguing new aspect of plant-fungus

528 interaction, this finding can also be applied to evaluate the specificity of this regulation for prediction

529 of high efficiency biocontrol capacity during strain screening. Thereby, the presence of the cluster as

530 well as its high induction level represent promising features for diagnostic tests in strain screening

531 programs. Additionally, identification of the compound produced by the PCA cluster, which facilitates

532 colonization may support and enhance plant-fungus interaction of diverse biocontrol agents and enable

533 plant-protection of plant varieties with otherwise insufficient response to *Trichoderma*-based biocontrol

534 agents.

535

536 **Materials and Methods**

537

538 *Strains and cultivation conditions*

539

540 *T. harzianum* B97 (Compant et al., 2017) was used throughout the study. For RNA analysis, the strain

541 was revived from long term storage on malt extract agar (3 % w/v). Plates containing modified Mandels

542 Andreotti minimal medium (Mandels & Andreotti, 1978) with 0.1 % (w/v) glucose as carbon source

543 were inoculated with 10 µl of spore solution (10^8 spores/ml) at 28 °C in constant darkness for 34 hours.

544 The modified Mandels-Andreotti medium was prepared as follows: The mineral salt solution contained

545 2.8 g/l $(NH_4)_2SO_4$ (21.19 mM) (ROTH, Karlsruhe, Germany), 4.0 g/l KH_2PO_4 (29.39 mM) (Sigma-

546 Aldrich, St. Louis, USA), 0.6 g/l $MgSO_4 \cdot 7H_2O$ (2.43 mM) (ROTH, Karlsruhe, Germany) and 0.8 g/l

15

547 CaCl$_2$·2H$_2$O (5.44 mM) (Merck, Darmstadt, Germany). The trace element solution contained 0.250 g/l

548 FeSO$_4$·7H$_2$O (0.899 mM) (Sigma-Aldrich, St. Louis, USA), 0.085 g/l MnSO$_4$·H$_2$O (0.503 mM) (Merck,

549 Darmstadt, Germany), 0.070 g/l ZnSO$_4$·7H$_2$O (0.243 mM) (Riedel-de Haen, Seelze, Germany) and

550 0.143 g/l CoCl$_2$·6H$_2$O (0.603 mM) (Sigma-Aldrich, St. Louis, USA) and the pH was adjusted to 2.0

551 with concentrated sulfuric acid. Instead of phosphate buffer, milliQ water was used. The culture medium

552 was prepared combining 500 ml mineral salt solution, 480 ml milliQ water, 20 ml trace element solution,

553 0.0025 % (w/v) peptone from casein (Merck, Darmstadt, Germany) for inducing germination, 0.1 %

554 (w/v) D-glucose (ROTH, Karlsruhe, Germany) as carbon source (see pre-test for determination of

555 glucose concentration) and 1.5 % (w/v) agar-agar (ROTH, Karlsruhe, Germany).

556 Plates were covered with cellophane in order to facilitate harvesting of mycelia. For recognition analysis,

557 the roots of soy plants, which arrived second leaf stage, (19 days old, see below) were washed 4 times

558 with sterile distilled water and were placed on the plates with *T. harzianum* B97 in 3 cm distance from

559 the growth front. After further incubation for 13 hours (corresponding to the time for recognition in the

560 chemotropic assay) in darkness, fungal mycelia were harvested for RNA isolation and agar slices from

561 the same area were excised for evaluation of secreted metabolite production. As controls, plates with

562 fungus but no plant and plates with plant but no fungus were used. Five plates each were pooled per

563 sample and three biological replicates were used.

564

565 *Construction of T. harzianum B97 deletion strains*

566

567 Vectors for deletion of *pca1* and *pca5* were constructed by yeast recombination cloning using *hph*

568 marker constructs with 1kb flanking regions as described previously (Schuster et al., 2012). Protoplast

569 transformation was used for deletions in *T. harzianum* B97 parental strain with 10 mg/ml lysing enzymes

570 (*Trichoderma harzianum*, Sigma # L-1412) and 150 µg/ml hygromycin B (Roth, Karlsruhe, Germany)

571 for selection. Absence of the gene of interest was confirmed by PCR with primers binding inside the

572 deleted region. A list of primers used is shown in Table 1.

573

574 *Surface sterilization of seeds and in-vitro culture of soybean plants*

575

576 The soybeans (*Glycine max* (L) Merr., variety ES TENOR, Die Saat, Austria) were obtained from RWA

577 Austria. For the surface sterilization, the soybeans were soaked in 70 % ethanol for 1 minute and then

578 rinsed 3 times with sterile distilled water. Afterwards, the soybeans were transferred into a sterile beaker

579 containing Danklorix (2.8 % sodium hypochlorite (w/w), Colgate-Palmolive, Vienna, Austria) and

580 Tween 20 (Roth, Karlsruhe, Germany) and stirred for 3 minutes. The soybeans were then washed five

581 times with sterile distilled water. The excess water was removed by placing soybeans on sterile paper

582 tissue.

583 For the pre-germination, the surface sterilized soybeans were placed on sterile paper tissue soaked with

584 tap water and incubated at 26 °C and 16 hours light:8 h darkness for 5 days. The seedlings were

585 transferred to the *in-vitro* culture, which contained diluted Murashige&Skoog (to 0.5 concentration;

586 Duchefa Biochemie, Haarlem, The Netherlands) and 0.8 % (w/v) Daishin Agar (Duchefa Biochemie,

587 Haarlem, The Netherlands) at pH 5.8. The *in-vitro* cultures of soybean plants were further incubated at

588 the same condition for two more weeks.

589

590 *Preparation of plant root exudates*

591

592 After surface sterilization the soybeans were planted in sterilized perlite (premium perlite 2-6, Gramoflor

593 GmbH, Germany). The soybeans were kept in a plant culture room at 26 °C with 16 hours light and 8

594 hours darkness. After approximately 3 days of emergence, the plantlets were then allowed to grow for

595 further 2 weeks till the second leaf stage arrived. The plantlets were recovered from the perlite carefully

596 and washed gently under running water to remove the perlite. Afterwards, at least 300 plantlet roots

597 were submerged in 500 ml sterile milliQ water and kept for 2 days at room temperature. The obtained

598 root exudates were filter sterilized through Thermo Scientific Nalgene Syringe Filter with 0.2 µM pore

599 size and stored at -80 °C.

600

601 *Isolation of total RNA*

602

603 For isolation of total RNA, mycelium of the growth front from 5 replicate plates was pooled and frozen

604 in liquid nitrogen. Three biological replicates were used with 5 pooled plates each. Samples were then

605 treated as described previously (Tisch et al., 2011) using the QIAGEN plant RNA kit (QIAGEN, Hilden,

606 Germany). RNA quality and integrity were checked using Bioanalyzer 2100 (Agilent). Only high quality

607 RNA was used for further analyses.

608

609 *Transcriptome analysis and bioinformatics*

610

611 Sequencing of samples along with cDNA preparation was done at VetCORE (Vienna, Austria). The

612 software BWA (Keel & Snelling, 2018) was used for mapping to the genome data of *T. harzianum* (JGI

613 mycocosm; https://genome.jgi.doe.gov/Triha1/Triha1.home.html) (Druzhinina et al., 2018). The

614 software samtools was used for data processing (Li et al., 2009) and the limma package as implemented

615 in R (Ritchie et al., 2015) was used for determination of statistically significant differential expression

616 (>2fold, p-value threshold 0.01). Besides manual annotation of differentially expressed genes,

617 annotations of bidirectional best hits with *T. reesei* and/or *T. atroviride* (Schmoll et al., 2016) were used.

618 Comparison of gene expression patterns between biological replicates yielded significance scores of

619 ≥0.979 for both sample sets. Sequence data are available at NCBI GEO (Gene expression omnibus)

620 under the accession number GSE229209.

621 HCE3.5 (Seo et al., 2006) was applied to perform hierarchical clustering with default settings and the

622 Poisson correlation coefficient as the similarity/distance measure. FunCat (Functional category) analysis

623 was done with the FungiFun2 online tool (Priebe et al., 2015) based on bidirectional best hit analysis

624 with *T. atroviride*.

625

626 *Analysis of chemotropic responses*

627

628 The freshly grown spores from a 4 days old culture were recovered and dissolved in 1 ml spore-solution

629 (0.8 % NaCl and 0.05 % Tween 80). After separation of mycelia by centrifugation through glass wool,

630 the spore solution was centrifuged at 8000 rpm for 2 minutes, the supernatant was discarded, and the

631 spore pellet was resuspended in 1 ml sterile milliQ water. For the chemotropism assay, the spore solution

632 was adjusted to 10^8 spores per ml with sterile milliQ water. The peptone from casein (Merck, Darmstadt,

633 Germany) was used as germination stimulator in 0.5 % water agar. The concentration of peptone from

634 casein was optimized to 0.0025 % (w/v). After 13 hours of incubation at 28°C in darkness, germling

635 orientation was monitored and chemotropic index was calculated as described earlier (Turra et al., 2015).

636

637 *Analysis of patterns of secreted metabolites*

638

639 Analysis for alteration of secondary metabolite patterns in the presence of a soy plant was essentially

640 done as described previously (Bazafkan et al., 2015; Hinterdobler et al., 2019). Therefore the same

641 conditions as applied for transcriptome analysis as outlined above were used. Application of high

642 performance thin layer chromatography (HPTLC) and data visualization was performed as described in

643 (Bazafkan et al., 2015) except that separation was done with chloroform and 1 mM trifluoroacetic acid

644 in methanol.

645

646 *Analysis of colonization by T. harzianum B97 and recombinant strains*

647

648 Seeds were surface sterilized in 70% ethanol for 7 minutes and rinsed for 3 minutes with sterile milliQ

649 water. Seeds were then put onto MEX (malt extract) plates containing either *T. harzianum* B97,

650 B97Δ*pca1*, B97Δ*pca5* or only MEX without fungus as negative control. Seeds were then placed in

651 sterile magenta boxes containing soil mixture (1:1:1 perlite, sand, potting soil and 25 ml of sterilized tap

652 water), which was autoclaved twice. After 8 days at 22°C under 12 hours light:12 hours darkness

653 conditions, plants were harvested, and roots stained in 15ml phosphate buffer saline (PBS, pH 7.2)

654 containing 5µg/ml wheat germ agglutinin (WGA)-AlexaFluor488 conjugate (Life Technologies, USA)

655 and incubated for 2 hours at 37 °C before rinsing three times with PBS.

656 All observations were carried out using a confocal microscope (Olympus Fluoview FV1000 with multi-
657 line laser FV5-LAMAR-2 and HeNe(G)laser FV10-LAHEG230-2, Japan). Observations with the
658 confocal microscope were done at objectives of 10x, 20x and 40x. Between 20 and 40 X, Y, Z pictures
659 containing 20 to 60 scans were separately taken at 405, 488, 549 nm wavelengths in blue/green/orange-
660 red channels respectively, with the same settings each time and normal light. The image analysis
661 software Imaris software used at the confocal microscope to visualize 3D reconstructions. X, Y, Z
662 pictures from different channels were then merged using the Image J software (version 1.47v), and Z
663 project stacks were then used to create the pictures as described earlier (Pierron et al., 2015).

665 *Phylogenetic analysis*

667 For phylogenetic analysis, protein and nucleotide sequences were obtained from the NCBI nr database
668 or the genome sequences available at JGI mycocosm. Sequences were aligned using Clustal X or
669 MEGA7 (Kumar et al., 2016; Thompson et al., 1997) with default parameters. MEGA7 was used for
670 phylogenetic analysis using standard parameters and the Maximum likelihood method and 1000
671 bootstrap cycles.

Author contributions

674 MiS performed gene deletion and confocal microscopy, GL performed chemotropism analysis and RNA
675 isolation, WH performed secondary metabolite analysis, SC supervised confocal microscopy, DG
676 supported colonization analysis, ADZ contributed to editing of the manuscript, MoS conceived the
677 study, performed transcriptome analysis and wrote the final version of the manuscript. All authors read
678 the manuscript and agreed to publication.

Conflicts of interest

692 The study was in part funded by Greencell, France.

693

Availability of data

All data used for this study are available in the manuscript, its supplementary file and at the NCBI GEO online repository under accession number GSE229209.

697

Tables

699

Table 1. Oligonucleotides used in this study

Name	Function	Sequence 5' - 3'	Protein ID	targtet gene
Bpca1del5F	creation of 5' flank of deletion cassette	5'GTAACGCCAGGGTTTTCCCAGT CACGACGATGGTGGTGATTGTTG TG 3'	323871	*pca1*
Bpca5del5R	creation of 5' flank of deletion cassette	5'ATCCACTTAACGTTACTGAAAT CTCCAACGGTAAATGCGTTTCAA AG 3'	323871	*pca1*
Bpca1del3F	creation of 3' flank of deletion cassette	5'CTCCTTCAATATCATCTTCTGTC TCCGACATTAAATGATACACAGG CTG 3'	323871	*pca1*
Bpca1del3R	creation of 3' flank of deletion cassette	5'GCGGATAACAATTTCACACAGG AAACAGCCATTGTCATCTGCAGT AGAC 3'	323871	*pca1*
Bpca1screF	confirmation of deletion	5'GGATGGACCTTACCCTTTATCG 3'	323871	*pca1*
Bpca1screR	confirmation of deletion	5'ACCACAAACGAGTGCTGAAATC 3'	323871	*pca1*
Bpca5del5F	creation of 5' flank of deletion cassette	5'GTAACGCCAGGGTTTTCCCAGT CACGACGTTGTCCGTTGTCCTATG GC 3'	513504	*pca5*
Bpca5del5R	creation of 5' flank of deletion cassette	5'ATCCACTTAACGTTACTGAAAT CTCCAACATCGCTTATTCGTTCGC AG 3'	513504	*pca5*
Bpca5del3F	creation of 3' flank of deletion cassette	5'CTCCTTCAATATCATCTTCTGTC TCCGACGGTCCATTTGATAATAG AGAAG 3'	513504	*pca5*

Bpca5del3R	creation of 3' flank of deletion cassette	5'GCGGATAACAATTTCACACAGG AAACAGCCTATTCACACCCAGAG CAC 3'	513504	*pca5*
Bpca5screF	confirmation of deletion	5'CCGACGCAGGAAAGAAAC 3'	513504	*pca5*
Bpca5screR	confirmation of deletion	5'ACAGATGTAGACGCAGCTGG 3'	513504	*pca5*

701

702

703 **References**

704

705 Atanasova, L., Druzhinina, I., & Jaklitsch, W. M. (2013). Two hundred *Trichoderma* species recognized
706   on the basis of molecular phylogeny. In P. K. Mukherjee, B. A. Horwitz, U. S. Singh, M.
707   Mukherjee, & M. Schmoll (Eds.), *Trichoderma - Biology and Applications* (pp. 10-42). CAB
708   International.

709 Averill, C., Anthony, M. A., Baldrian, P., Finkbeiner, F., van den Hoogen, J., Kiers, T., Kohout, P., Hirt,
710   E., Smith, G. R., & Crowther, T. W. (2022). Defending Earth's terrestrial microbiome. *Nat*
711   *Microbiol*. https://doi.org/10.1038/s41564-022-01228-3

712 Bailey, B., & Melnick, R. (2013). *The endophytic Trichoderma*. CABI International.
713   https://doi.org/10.1079/9781780642475.0152

714 Bandara, A. Y., Weerasooriya, D. K., Trexler, R. V., Bell, T. H., & Esker, P. D. (2021). Soybean roots
715   and soil from high- and low-yielding field sites have different microbiome composition. *Front*
716   *Microbiol*, *12*, 675352. https://doi.org/10.3389/fmicb.2021.675352

717 Bazafkan, H., Dattenböck, C., Böhmdorfer, S., Tisch, D., Stappler, E., & Schmoll, M. (2015). Mating
718   type dependent partner sensing as mediated by VEL1 in *Trichoderma reesei*. *Mol Microbiol*,
719   *96*(6), 1103-1118. https://doi.org/10.1111/mmi.12993

720 Bebber, D. P. (2015). Range-expanding pests and pathogens in a warming world. *Annu Rev Phytopathol*,
721   *53*, 335-356. https://doi.org/10.1146/annurev-phyto-080614-120207

722 Behie, S. W., Zelisko, P. M., & Bidochka, M. J. (2012). Endophytic insect-parasitic fungi translocate
723   nitrogen directly from insects to plants. *Science*, *336*(6088), 1576-1577.
724   https://doi.org/10.1126/science.1222289

725 Brownlee, A. G., & Arst, H. N., Jr. (1983). Nitrate uptake in *Aspergillus nidulans* and involvement of
726   the third gene of the nitrate assimilation gene cluster. *J Bacteriol*, *155*(3), 1138-1146.
727   http://www.ncbi.nlm.nih.gov/pubmed/6350263

728 Chaverri, P., Branco-Rocha, F., Jaklitsch, W., Gazis, R., Degenkolb, T., & Samuels, G. J. (2015).
729   Systematics of the *Trichoderma harzianum* species complex and the re-identification of
730   commercial biocontrol strains. *Mycologia*, *107*(3), 558-590. https://doi.org/10.3852/14-147

731 Chaverri, P., Gazis, R. O., & Samuels, G. J. (2011). *Trichoderma amazonicum*, a new endophytic species
732   on *Hevea brasiliensis* and *H. guianensis* from the Amazon basin. *Mycologia*, *103*(1), 139-151.
733   https://doi.org/10.3852/10-078

734 Ciancio, A., Rosso, L. C., Lopez-Cepero, J., & Colagiero, M. (2022). Rhizosphere 16S-ITS
735   metabarcoding profiles in banana crops are affected by nematodes, cultivation, and local
736   climatic variations. *Front Microbiol*, *13*, 855110. https://doi.org/10.3389/fmicb.2022.855110

737 Compant, S., Gerbore, J., Antonielli, L., Brutel, A., & Schmoll, M. (2017). Draft genome sequence of
738   the root-colonizing fungus *Trichoderma harzianum* B97. *Genome Announc*, *5*(13).
739   https://doi.org/10.1128/genomeA.00137-17

740 Contreras-Cornejo, H. A., Macias-Rodriguez, L., del-Val, E., & Larsen, J. (2016). Ecological functions
741   of *Trichoderma* spp. and their secondary metabolites in the rhizosphere: interactions with plants.
742   *FEMS Microbiol Ecol*, *92*(4), fiw036. https://doi.org/10.1093/femsec/fiw036

743 de Man, T. J., Stajich, J. E., Kubicek, C. P., Teiling, C., Chenthamara, K., Atanasova, L., Druzhinina, I.
744   S., Levenkova, N., Birnbaum, S. S., Barribeau, S. M., Bozick, B. A., Suen, G., Currie, C. R., &
745   Gerardo, N. M. (2016). Small genome of the fungus *Escovopsis weberi*, a specialized disease
746   agent of ant agriculture. *Proc Natl Acad Sci U S A*, *113*(13), 3567-3572.
747   https://doi.org/10.1073/pnas.1518501113

748 Degenkolb, T., Dieckmann, R., Nielsen, K. F., Gräfenhan, T., Theis, C., Zafari, D., Chaverri, P., Ismaiel,
749   A., Brückner, H., von Döhren, H., Thrane, U., Petrini, O., & Samuels, G. J. (2008). The
750   *Trichoderma brevicompactum* clade: a separate lineage with new species, new peptaibiotics,
751   and mycotoxins. *Mycological Progress*, *7*(3), 177-219. https://doi.org/10.1007/s11557-008-
752   0563-3

753 Degenkolb, T., von Döhren, H., Nielsen, K. F., Samuels, G. J., & Brückner, H. (2008). Recent advances
754   and future prospects in peptaibiotics, hydrophobin, and mycotoxin research, and their
755   importance for chemotaxonomy of *Trichoderma* and *Hypocrea*. *Chem Biodivers*, *5*(5), 671-680.
756   https://doi.org/10.1002/cbdv.200890064

757 Del Buono, D. (2021). Can biostimulants be used to mitigate the effect of anthropogenic climate change
758   on agriculture? It is time to respond. *Sci Total Environ*, *751*, 141763.
759   https://doi.org/10.1016/j.scitotenv.2020.141763

760 Di Lelio, I., Forni, G., Magoga, G., Brunetti, M., Bruno, D., Becchimanzi, A., De Luca, M. G., Sinno,
761   M., Barra, E., Bonelli, M., Frusciante, S., Diretto, G., Digilio, M. C., Woo, S. L., Tettamanti,
762   G., Rao, R., Lorito, M., Casartelli, M., Montagna, M., & Pennacchio, F. (2023). A soil fungus
763   confers plant resistance against a phytophagous insect by disrupting the symbiotic role of its gut
764   microbiota. *Proc Natl Acad Sci U S A*, *120*(10), e2216922120.
765   https://doi.org/10.1073/pnas.2216922120

766 Doehlemann, G., Okmen, B., Zhu, W., & Sharon, A. (2017). Plant pathogenic fungi. *Microbiol Spectr*,
767   *5*(1). https://doi.org/10.1128/microbiolspec.FUNK-0023-2016

768 Donzelli, B. G., & Krasnoff, S. B. (2016). Molecular genetics of secondary chemistry in *Metarhizium*
769   fungi. *Adv Genet*, *94*, 365-436. https://doi.org/10.1016/bs.adgen.2016.01.005

770 Druzhinina, I. S., Chenthamara, K., Zhang, J., Atanasova, L., Yang, D., Miao, Y., Rahimi, M. J., Grujic,
771   M., Cai, F., Pourmehdi, S., Salim, K. A., Pretzer, C., Kopchinskiy, A. G., Henrissat, B., Kuo,
772   A., Hundley, H., Wang, M., Aerts, A., Salamov, A., . . . Kubicek, C. P. (2018). Massive lateral
773   transfer of genes encoding plant cell wall-degrading enzymes to the mycoparasitic fungus
774   *Trichoderma* from its plant-associated hosts. *PLoS Genet*, *14*(4), e1007322.
775   https://doi.org/10.1371/journal.pgen.1007322

776 Druzhinina, I. S., Kubicek, E. M., & Kubicek, C. P. (2016). Several steps of lateral gene transfer
777   followed by events of 'birth-and-death' evolution shaped a fungal sorbicillinoid biosynthetic
778   gene cluster. *BMC Evol Biol*, *16*(1), 269. https://doi.org/10.1186/s12862-016-0834-6

779 Druzhinina, I. S., Seidl-Seiboth, V., Herrera-Estrella, A., Horwitz, B. A., Kenerley, C. M., Monte, E.,
780   Mukherjee, P. K., Zeilinger, S., Grigoriev, I. V., & Kubicek, C. P. (2011). *Trichoderma*: the
781   genomics of opportunistic success [Research Support, Non-U.S. Gov't
782 Review]. *Nat Rev Microbiol*, *9*(10), 749-759. https://doi.org/10.1038/nrmicro2637

783 Gao, R., Ding, M., Jiang, S., Zhao, Z., Chenthamara, K., Shen, Q., Cai, F., & Druzhinina, I. S. (2020).
784   The evolutionary and functional paradox of cerato-platanins in fungi. *Appl Environ Microbiol*,
785   *86*(13). https://doi.org/10.1128/AEM.00696-20

786 Gomes, E. V., Costa Mdo, N., de Paula, R. G., de Azevedo, R. R., da Silva, F. L., Noronha, E. F., Ulhoa,
787   C. J., Monteiro, V. N., Cardoza, R. E., Gutierrez, S., & Silva, R. N. (2015). The cerato-platanin
788   protein Epl-1 from *Trichoderma harzianum* is involved in mycoparasitism, plant resistance
789   induction and self cell wall protection. *Sci Rep*, *5*, 17998. https://doi.org/10.1038/srep17998

790 Gomes, E. V., Ulhoa, C. J., Cardoza, R. E., Silva, R. N., & Gutierrez, S. (2017). Involvement of
791   *Trichoderma harzianum* Epl-1 protein in the regulation of *Botrytis* virulence- and tomato
792   defense-related genes. *Front Plant Sci*, *8*, 880. https://doi.org/10.3389/fpls.2017.00880

793 Grigoriev, I. V., Nikitin, R., Haridas, S., Kuo, A., Ohm, R., Otillar, R., Riley, R., Salamov, A., Zhao,
794   X., Korzeniewski, F., Smirnova, T., Nordberg, H., Dubchak, I., & Shabalov, I. (2014).
795   MycoCosm portal: gearing up for 1000 fungal genomes. *Nucleic Acids Res*, *42*(Database issue),
796   D699-704. https://doi.org/10.1093/nar/gkt1183

797 Guzman-Guzman, P., Porras-Troncoso, M. D., Olmedo-Monfil, V., & Herrera-Estrella, A. (2019).
798   *Trichoderma* species: Versatile plant symbionts. *Phytopathology*, *109*(1), 6-16.
799   https://doi.org/10.1094/PHYTO-07-18-0218-RVW

800 Hanson, J. R. (2005). The chemistry of the bio-control agent, *Trichoderma harzianum*. *Sci Prog*, *88*(Pt
801   4), 237-248. https://doi.org/10.3184/003685005783238372

802 Harman, G., Khadka, R., Doni, F., & Uphoff, N. (2020). Benefits to plant health and productivity from
803   enhancing plant microbial symbionts. *Front Plant Sci*, *11*, 610065.
804   https://doi.org/10.3389/fpls.2020.610065

805 Harman, G. E., Howell, C. R., Viterbo, A., Chet, I., & Lorito, M. (2004). *Trichoderma* species--
806   opportunistic, avirulent plant symbionts. *Nat Rev Microbiol*, *2*(1), 43-56.
807   http://www.ncbi.nlm.nih.gov/entrez/query.fcgi?cmd=Retrieve&db=PubMed&dopt=Citation&l
808   ist_uids=15035008

809 Harman, G. E., Lorito, M., & Lynch, J. M. (2004). Uses of *Trichoderma* spp. to alleviate or remediate
810   soil and water pollution. *Adv Appl Microbiol*, *56*, 313-330. https://doi.org/10.1016/S0065-
811   2164(04)56010-0

812 Harman, G. E., & Uphoff, N. (2019). Symbiotic root-endophytic soil microbes improve crop
813 productivity and provide environmental benefits. *Scientifica (Cairo)*, *2019*, 9106395.
814 https://doi.org/10.1155/2019/9106395

815 Haueisen, J., & Stukenbrock, E. H. (2016). Life cycle specialization of filamentous pathogens -
816 colonization and reproduction in plant tissues. *Curr Opin Microbiol*, *32*, 31-37.
817 https://doi.org/10.1016/j.mib.2016.04.015

818 He, D. C., He, M. H., Amalin, D. M., Liu, W., Alvindia, D. G., & Zhan, J. (2021). Biological control of
819 plant diseases: an evolutionary and eco-economic consideration. *Pathogens*, *10*(10).
820 https://doi.org/10.3390/pathogens10101311

821 Hinterdobler, W., Schuster, A., Tisch, D., Ozkan, E., Bazafkan, H., Schinnerl, J., Brecker, L.,
822 Bohmdorfer, S., & Schmoll, M. (2019). The role of PKAc1 in gene regulation and trichodimerol
823 production in *Trichoderma reesei*. *Fungal Biol Biotechnol*, *6*, 12.
824 https://doi.org/10.1186/s40694-019-0075-8

825 Jaklitsch, W. M., & Voglmayr, H. (2015). Biodiversity of *Trichoderma* (Hypocreaceae) in Southern
826 Europe and Macaronesia. *Stud Mycol*, *80*, 1-87. https://doi.org/10.1016/j.simyco.2014.11.001

827 Johnstone, I. L., McCabe, P. C., Greaves, P., Gurr, S. J., Cole, G. E., Brow, M. A., Unkles, S. E.,
828 Clutterbuck, A. J., Kinghorn, J. R., & Innis, M. A. (1990). Isolation and characterisation of the
829 *crnA-niiA-niaD* gene cluster for nitrate assimilation in *Aspergillus nidulans*. *Gene*, *90*(2), 181-
830 192. https://doi.org/10.1016/0378-1119(90)90178-t

831 Joo, J. H., & Hussein, K. A. (2022). Biological control and plant growth promotion properties of Volatile
832 Organic Compound-producing antagonistic *Trichoderma* spp. *Front Plant Sci*, *13*, 897668.
833 https://doi.org/10.3389/fpls.2022.897668

834 Karlsson, M., Atanasova, L., Jensen, D. F., & Zeilinger, S. (2017). Necrotrophic mycoparasites and their
835 genomes. *Microbiol Spectr*, *5*(2). https://doi.org/10.1128/microbiolspec.FUNK-0016-2016

836 Keel, B. N., & Snelling, W. M. (2018). Comparison of Burrows-Wheeler Transform-Based Mapping
837 Algorithms Used in High-Throughput Whole-Genome Sequencing: Application to Illumina
838 Data for Livestock Genomes. *Front Genet*, *9*, 35. https://doi.org/10.3389/fgene.2018.00035

839 Keswani, C., Mishra, S., Sarma, B. K., Singh, S. P., & Singh, H. B. (2014). Unraveling the efficient
840 applications of secondary metabolites of various *Trichoderma* spp. *Appl Microbiol Biotechnol*,
841 *98*(2), 533-544. https://doi.org/10.1007/s00253-013-5344-5

842 Khan, R. A. A., Najeeb, S., Mao, Z., Ling, J., Yang, Y., Li, Y., & Xie, B. (2020). Bioactive secondary
843 metabolites from *Trichoderma* spp. against phytopathogenic bacteria and root-knot nematode.
844 *Microorganisms*, *8*(3). https://doi.org/10.3390/microorganisms8030401

845 Klironomos, J. N., & Hart, M. M. (2001). Food-web dynamics. Animal nitrogen swap for plant carbon.
846 *Nature*, *410*(6829), 651-652. https://doi.org/10.1038/35070643

847 Kubicek, C. P., Steindorff, A. S., Chenthamara, K., Manganiello, G., Henrissat, B., Zhang, J., Cai, F.,
848 Kopchinskiy, A. G., Kubicek, E. M., Kuo, A., Baroncelli, R., Sarrocco, S., Noronha, E. F.,

25

849   Vannacci, G., Shen, Q., Grigoriev, I. V., & Druzhinina, I. S. (2019). Evolution and comparative
850   genomics of the most common *Trichoderma* species. *BMC Genomics*, *20*(1), 485.
851   https://doi.org/10.1186/s12864-019-5680-7

852   Kumar, S., Stecher, G., & Tamura, K. (2016). MEGA7: Molecular evolutionary eenetics analysis
853   version 7.0 for bigger datasets. *Mol Biol Evol*, *33*(7), 1870-1874.
854   https://doi.org/10.1093/molbev/msw054

855   Kurucz, V., Krüger, T., Antal, K., Dietl, A. M., Haas, H., Pócsi, I., Kniemeyer, O., & Emri, T. (2018).
856   Additional oxidative stress reroutes the global response of *Aspergillus fumigatus* to iron
857   depletion. *BMC Genomics*, *19*(1), 357. https://doi.org/10.1186/s12864-018-4730-x

858   Lareen, A., Burton, F., & Schafer, P. (2016). Plant root-microbe communication in shaping root
859   microbiomes. *Plant Mol Biol*, *90*(6), 575-587. https://doi.org/10.1007/s11103-015-0417-8

860   Leeder, A. C., Palma-Guerrero, J., & Glass, N. L. (2011). The social network: deciphering fungal
861   language [Research Support, U.S. Gov't, Non-P.H.S.

862   Review]. *Nat Rev Microbiol*, *9*(6), 440-451. https://doi.org/10.1038/nrmicro2580

863   Lehner, S. M., Atanasova, L., Neumann, N. K., Krska, R., Lemmens, M., Druzhinina, I. S., &
864   Schuhmacher, R. (2013). Isotope-assisted screening for iron-containing metabolites reveals a
865   high degree of diversity among known and unknown siderophores produced by Trichoderma
866   spp. *Appl Environ Microbiol*, *79*(1), 18-31. https://doi.org/10.1128/AEM.02339-12

867   Li, H., Handsaker, B., Wysoker, A., Fennell, T., Ruan, J., Homer, N., Marth, G., Abecasis, G., Durbin,
868   R., & Genome Project Data Processing, S. (2009). The Sequence Alignment/Map format and
869   SAMtools. *Bioinformatics*, *25*(16), 2078-2079. https://doi.org/10.1093/bioinformatics/btp352

870   Lind, A. L., Wisecaver, J. H., Smith, T. D., Feng, X., Calvo, A. M., & Rokas, A. (2015). Examining the
871   evolution of the regulatory circuit controlling secondary metabolism and development in the
872   fungal genus *Aspergillus*. *PLoS Genet*, *11*(3), e1005096.
873   https://doi.org/10.1371/journal.pgen.1005096

874   Liu, X., Le Roux, X., & Salles, J. F. (2022). The legacy of microbial inoculants in agroecosystems and
875   potential for tackling climate change challenges. *iScience*, *25*(3), 103821.
876   https://doi.org/10.1016/j.isci.2022.103821

877   Lombardi, N., Vitale, S., Turra, D., Reverberi, M., Fanelli, C., Vinale, F., Marra, R., Ruocco, M.,
878   Pascale, A., d'Errico, G., Woo, S. L., & Lorito, M. (2018). Root exudates of stressed plants
879   stimulate and attract *Trichoderma* soil fungi. *Mol Plant Microbe Interact*.
880   https://doi.org/10.1094/MPMI-12-17-0310-R

881   Losada, L., Barker, B. M., Pakala, S., Pakala, S., Joardar, V., Zafar, N., Mounaud, S., Fedorova, N.,
882   Nierman, W. C., & Cramer, R. A. (2014). Large-scale transcriptional response to hypoxia in
883   *Aspergillus fumigatus* observed using RNAseq identifies a novel hypoxia regulated ncRNA.
884   *Mycopathologia*, *178*(5-6), 331-339. https://doi.org/10.1007/s11046-014-9779-8

885 Macias-Rodriguez, L., Contreras-Cornejo, H. A., Adame-Garnica, S. G., Del-Val, E., & Larsen, J.
886   (2020). The interactions of *Trichoderma* at multiple trophic levels: inter-kingdom
887   communication. *Microbiol Res*, *240*, 126552. https://doi.org/10.1016/j.micres.2020.126552

888 Mandels, M., & Andreotti, R. (1978). Problems and challenges in the cellulose to cellulase fermentation.
889   *Proc Biochem*, *13*, 6 - 13.

890 Monte, E. (2023). The sophisticated evolution of *Trichoderma* to control insect pests. *Proc Natl Acad*
891   *Sci U S A*, *120*(12), e2301971120. https://doi.org/10.1073/pnas.2301971120

892 Mukherjee, P. K., Horwitz, B. A., Herrera-Estrella, A., Schmoll, M., & Kenerley, C. M. (2013).
893   *Trichoderma* research in the genome era. *Annu Rev Phytopathol*, *51*, 105-129.
894   https://doi.org/10.1146/annurev-phyto-082712-102353

895 Newman, M. A., Sundelin, T., Nielsen, J. T., & Erbs, G. (2013). MAMP (microbe-associated molecular
896   pattern) triggered immunity in plants. *Front Plant Sci*, *4*, 139.
897   https://doi.org/10.3389/fpls.2013.00139

898 Nordzieke, D. E., Fernandes, T. R., El Ghalid, M., Turra, D., & Di Pietro, A. (2019). NADPH oxidase
899   regulates chemotropic growth of the fungal pathogen *Fusarium oxysporum* towards the host
900   plant. *New Phytol*, *224*(4), 1600-1612. https://doi.org/10.1111/nph.16085

901 Pierron, R., Gorfer, M., Berger, H., Jacques, A., Sessitsch, A., Strauss, J., & Compant, S. (2015).
902   Deciphering the Niches of Colonisation of *Vitis vinifera* L. by the Esca-Associated Fungus
903   *Phaeoacremonium aleophilum* Using a gfp Marked Strain and Cutting Systems. *PLoS One*,
904   *10*(6), e0126851. https://doi.org/10.1371/journal.pone.0126851

905 Poveda, J. (2021). *Trichoderma* as biocontrol agent against pests: New uses for a mycoparasite.
906   *Biological Control*, *159*, 104634.
907   https://doi.org/https://doi.org/10.1016/j.biocontrol.2021.104634

908 Priebe, S., Kreisel, C., Horn, F., Guthke, R., & Linde, J. (2015). FungiFun2: a comprehensive online
909   resource for systematic analysis of gene lists from fungal species. *Bioinformatics*, *31*(3), 445-
910   446. https://doi.org/10.1093/bioinformatics/btu627

911 Ramirez-Valdespino, C. A., Casas-Flores, S., & Olmedo-Monfil, V. (2019). *Trichoderma* as a model to
912   study effector-like molecules. *Front Microbiol*, *10*, 1030.
913   https://doi.org/10.3389/fmicb.2019.01030

914 Rangel, L. I., Hamilton, O., de Jonge, R., & Bolton, M. D. (2021). Fungal social influencers: secondary
915   metabolites as a platform for shaping the plant-associated community. *Plant J*, *108*(3), 632-645.
916   https://doi.org/10.1111/tpj.15490

917 Raza, M. M., & Bebber, D. P. (2022). Climate change and plant pathogens. *Curr Opin Microbiol*, *70*,
918   102233. https://doi.org/10.1016/j.mib.2022.102233

919 Ritchie, M. E., Phipson, B., Wu, D., Hu, Y., Law, C. W., Shi, W., & Smyth, G. K. (2015). limma powers
920   differential expression analyses for RNA-sequencing and microarray studies. *Nucleic Acids Res*,
921   *43*(7), e47. https://doi.org/10.1093/nar/gkv007

922   Roberts, D. W., & Hajek, A. E. (1992). Entomopathogenic fungi as bioinsecticides. In G. F. Leatham
923   (Ed.), *Frontiers in Industrial Mycology* (pp. 144-159). Springer US.
924   https://doi.org/10.1007/978-1-4684-7112-0_10

925   Rolfe, S. A., Griffiths, J., & Ton, J. (2019). Crying out for help with root exudates: adaptive mechanisms
926   by which stressed plants assemble health-promoting soil microbiomes. *Curr Opin Microbiol*,
927   *49*, 73-82. https://doi.org/10.1016/j.mib.2019.10.003

928   Sasan, R. K., & Bidochka, M. J. (2012). The insect-pathogenic fungus *Metarhizium robertsii*
929   (Clavicipitaceae) is also an endophyte that stimulates plant root development. *Am J Bot*, *99*(1),
930   101-107. https://doi.org/10.3732/ajb.1100136

931   Sbaraini, N., Guedes, R. L., Andreis, F. C., Junges, A., de Morais, G. L., Vainstein, M. H., de
932   Vasconcelos, A. T., & Schrank, A. (2016). Secondary metabolite gene clusters in the
933   entomopathogen fungus *Metarhizium anisopliae*: genome identification and patterns of
934   expression in a cuticle infection model. *BMC Genomics*, *17*(Suppl 8), 736.
935   https://doi.org/10.1186/s12864-016-3067-6

936   Schafhauser, T., Wibberg, D., Ruckert, C., Winkler, A., Flor, L., van Pee, K. H., Fewer, D. P., Sivonen,
937   K., Jahn, L., Ludwig-Muller, J., Caradec, T., Jacques, P., Huijbers, M. M., van Berkel, W. J.,
938   Weber, T., Wohlleben, W., & Kalinowski, J. (2015). Draft genome sequence of *Talaromyces
939   islandicus* ("*Penicillium islandicum*") WF-38-12, a neglected mold with significant
940   biotechnological potential. *J Biotechnol*, *211*, 101-102.
941   https://doi.org/10.1016/j.jbiotec.2015.07.004

942   Schalamun, M., & Schmoll, M. (2022). *Trichoderma* – genomes and genomics as treasure troves for
943   research towards biology, biotechnology and agriculture [Review]. *Frontiers in Fungal Biology*,
944   *3*. https://doi.org/10.3389/ffunb.2022.1002161

945   Schmoll, M., Dattenböck, C., Carreras-Villasenor, N., Mendoza-Mendoza, A., Tisch, D., Aleman, M.
946   I., Baker, S. E., Brown, C., Cervantes-Badillo, M. G., Cetz-Chel, J., Cristobal-Mondragon, G.
947   R., Delaye, L., Esquivel-Naranjo, E. U., Frischmann, A., Gallardo-Negrete Jde, J., Garcia-
948   Esquivel, M., Gomez-Rodriguez, E. Y., Greenwood, D. R., Hernandez-Onate, M., . . . Herrera-
949   Estrella, A. (2016). The genomes of three uneven siblings: footprints of the lifestyles of three
950   *Trichoderma* species. *Microbiol Mol Biol Rev*, *80*(1), 205-327.
951   https://doi.org/10.1128/MMBR.00040-15

952   Schuster, A., Bruno, K. S., Collett, J. R., Baker, S. E., Seiboth, B., Kubicek, C. P., & Schmoll, M. (2012).
953   A versatile toolkit for high throughput functional genomics with *Trichoderma reesei*.
954   *Biotechnol Biofuels*, *5*(1), 1. https://doi.org/10.1186/1754-6834-5-1

955   Schweiger, R., Padilla-Arizmendi, F., Nogueira-Lopez, G., Rostas, M., Lawry, R., Brown, C., Hampton,
956   J., Steyaert, J. M., Muller, C., & Mendoza-Mendoza, A. (2021). Insights into metabolic changes
957   caused by the *Trichoderma virens*-maize root interaction. *Mol Plant Microbe Interact*, *34*(5),
958   524-537. https://doi.org/10.1094/MPMI-04-20-0081-R

959 Seo, J., Gordish-Dressman, H., & Hoffman, E. P. (2006). An interactive power analysis tool for
960   microarray hypothesis testing and generation. *Bioinformatics*, *22*(7), 808-814.
961   https://doi.org/10.1093/bioinformatics/btk052

962 Sheng, H., McNamara, P. J., & St Leger, R. J. (2022). *Metarhizium*: an opportunistic middleman for
963   multitrophic lifestyles. *Curr Opin Microbiol*, *69*, 102176.
964   https://doi.org/10.1016/j.mib.2022.102176

965 Shenouda, M. L., & Cox, R. J. (2021). Molecular methods unravel the biosynthetic potential of
966   *Trichoderma* species. *RSC Adv*, *11*(6), 3622-3635. https://doi.org/10.1039/d0ra09627j

967 Sood, M., Kapoor, D., Kumar, V., Sheteiwy, M. S., Ramakrishnan, M., Landi, M., Araniti, F., & Sharma,
968   A. (2020). *Trichoderma*: the "secrets" of a multitalented biocontrol agent. *Plants (Basel)*, *9*(6).
969   https://doi.org/10.3390/plants9060762

970 Spatafora, J. W., & Bushley, K. E. (2015). Phylogenomics and evolution of secondary metabolism in
971   plant-associated fungi. *Curr Opin Plant Biol*, *26*, 37-44.
972   https://doi.org/10.1016/j.pbi.2015.05.030

973 St Leger, R. J. (1993). Biology and mechanisms of insect cuticle invation by Deuteromycete fungal
974   pathogens. In N. E. Beckage, S. N. Thompson, & B. A. Federici (Eds.), *Parasites and pathogens*
975   *of insects* (Vol. 2, pp. 211-229). Academic Press Inc.

976 Syed Ab Rahman, S. F., Singh, E., Pieterse, C. M. J., & Schenk, P. M. (2018). Emerging microbial
977   biocontrol strategies for plant pathogens. *Plant Sci*, *267*, 102-111.
978   https://doi.org/10.1016/j.plantsci.2017.11.012

979 Szklarczyk, D., Gable, A. L., Nastou, K. C., Lyon, D., Kirsch, R., Pyysalo, S., Doncheva, N. T., Legeay,
980   M., Fang, T., Bork, P., Jensen, L. J., & von Mering, C. (2021). The STRING database in 2021:
981   customizable protein-protein networks, and functional characterization of user-uploaded
982   gene/measurement sets. *Nucleic Acids Res*, *49*(D1), D605-D612.
983   https://doi.org/10.1093/nar/gkaa1074

984 Taylor, J. T., Harting, R., Shalaby, S., Kenerley, C. M., Braus, G. H., & Horwitz, B. A. (2022). Adhesion
985   as a focus in *Trichoderma*-root interactions. *J Fungi (Basel)*, *8*(4).
986   https://doi.org/10.3390/jof8040372

987 Thompson, J. D., Gibson, T. J., Plewniak, F., Jeanmougin, F., & Higgins, D. G. (1997). The
988   CLUSTAL_X windows interface: flexible strategies for multiple sequence alignment aided by
989   quality analysis tools. *Nucleic Acids Res*, *25*(24), 4876-4882.
990   http://www.ncbi.nlm.nih.gov/entrez/query.fcgi?cmd=Retrieve&db=PubMed&dopt=Citation&l
991   ist_uids=9396791

992 Tisch, D., Kubicek, C. P., & Schmoll, M. (2011). New insights into the mechanism of light modulated
993   signaling by heterotrimeric G-proteins: ENVOY acts on *gna1* and *gna3* and adjusts cAMP
994   levels in *Trichoderma reesei* (*Hypocrea jecorina*). *Fungal Genet Biol*, *48*(6), 631-640.
995   https://doi.org/S1087-1845(10)00245-8 [pii]

996   10.1016/j.fgb.2010.12.009

997   Tudzynski, B. (2014). Nitrogen regulation of fungal secondary metabolism in fungi. *Front Microbiol*,

998   *5*, 656. https://doi.org/10.3389/fmicb.2014.00656

999   Turra, D., & Di Pietro, A. (2015). Chemotropic sensing in fungus-plant interactions. *Curr Opin Plant*

1000   *Biol*, *26*, 135-140. https://doi.org/10.1016/j.pbi.2015.07.004

1001   Turra, D., El Ghalid, M., Rossi, F., & Di Pietro, A. (2015). Fungal pathogen uses sex pheromone receptor

1002   for chemotropic sensing of host plant signals. *Nature*, *527*(7579), 521-524.

1003   https://doi.org/10.1038/nature15516

1004   Turra, D., Nordzieke, D., Vitale, S., El Ghalid, M., & Di Pietro, A. (2016). Hyphal chemotropism in

1005   fungal pathogenicity. *Semin Cell Dev Biol*, *57*, 69-75.

1006   https://doi.org/10.1016/j.semcdb.2016.04.020

1007   Tyskiewicz, R., Nowak, A., Ozimek, E., & Jaroszuk-Scisel, J. (2022). *Trichoderma*: The current status

1008   of Its application in agriculture for the biocontrol of fungal phytopathogens and stimulation of

1009   plant growth. *Int J Mol Sci*, *23*(4). https://doi.org/10.3390/ijms23042329

1010   Villalobos-Escobedo, J. M., Esparza-Reynoso, S., Pelagio-Flores, R., Lopez-Ramirez, F., Ruiz-Herrera,

1011   L. F., Lopez-Bucio, J., & Herrera-Estrella, A. (2020). The fungal NADPH oxidase is an essential

1012   element for the molecular dialog between *Trichoderma* and *Arabidopsis*. *Plant J*, *103*(6), 2178-

1013   2192. https://doi.org/10.1111/tpj.14891

1014   Vinale, F., & Sivasithamparam, K. (2020). Beneficial effects of *Trichoderma* secondary metabolites on

1015   crops. *Phytother Res*, *34*(11), 2835-2842. https://doi.org/10.1002/ptr.6728

1016   Wang, X., Zhang, X., Liu, L., Xiang, M., Wang, W., Sun, X., Che, Y., Guo, L., Liu, G., Guo, L., Wang,

1017   C., Yin, W. B., Stadler, M., Zhang, X., & Liu, X. (2015). Genomic and transcriptomic analysis

1018   of the endophytic fungus *Pestalotiopsis fici* reveals its lifestyle and high potential for synthesis

1019   of natural products. *BMC Genomics*, *16*(1), 28. https://doi.org/10.1186/s12864-014-1190-9

1020   Woo, S. L., Hermosa, R., Lorito, M., & Monte, E. (2022). *Trichoderma*: a multipurpose, plant-beneficial

1021   microorganism for eco-sustainable agriculture. *Nat Rev Microbiol*.

1022   https://doi.org/10.1038/s41579-022-00819-5

1023   Wyrebek, M., Huber, C., Sasan, R. K., & Bidochka, M. J. (2011). Three sympatrically occurring species

1024   of *Metarhizium* show plant rhizosphere specificity. *Microbiology (Reading)*, *157*(Pt 10), 2904-

1025   2911. https://doi.org/10.1099/mic.0.051102-0

1026   Zeilinger, S., Gruber, S., Bansal, R., & Mukherjee, P. K. (2016). Secondary metabolism in *Trichoderma*

1027   - chemistry meets genomics. *Fungal Biology Reviews*, *30*(2), 74-90.

1028   https://doi.org/10.1016/j.fbr.2016.05.001

1029

1030   **Figures**

1031

1032   **Figure 1**

1033

1034

Figure 1. **Assessment of *T. harzianum* B97 – plant interaction**. (A) CSLM Microphotograph of uninoculated control roots (i) and roots with *T. harzianum* B97 (ii-iv) at the root hair zone and stained with WGA-Alexa Fluor488® showing B97 as green fluorescent colonizing root hairs (iii) or the root surface (iv). (B) Chemotropic indices of *T. harzianum* B97 to the presence of 1 % (w/v) glucose or root exudates of soy plant. Analyses were done in biological duplicates, at least 400 germlings were counted

31

1040   per experiment. (C) Schematic representation of the experimental setup for analysis of plant-fungus

1041   communication. Plants were allowed to interact with the fungus for 13 hours and harvesting was done

1042   before contact. Mycelia for investigation of the transcriptome was isolated from the mycelial growth

1043   front ("harvesting area B97", yellow). For secondary metabolite analysis by HPTLC the agar slice

1044   including cellophane overlay from exactly the same area was excised. For analysis of the response of

1045   the plant an agar slice on the other side of the root was excised in order to avoid interference with fungal

1046   metabolites. For control plates the setup and positioning of harvesting areas was exactly the same. (D,

1047   E) HPTLC analysis of *T. harzianum* B97 alone on the plate (TH alone), *T. harzianum* B97 in the

1048   presence of the root of soy plant (THx(S)), the root of soy plant in the presence of the fungus (Sx(TH))

1049   and the root of soy plant alone (S alone). Two different visualizations are provided (D: Visible light

1050   after anisaldehyde derivatization and E: Remission at 366 nm) and show differentially secreted

1051   metabolites between interaction partners alone and in combination.
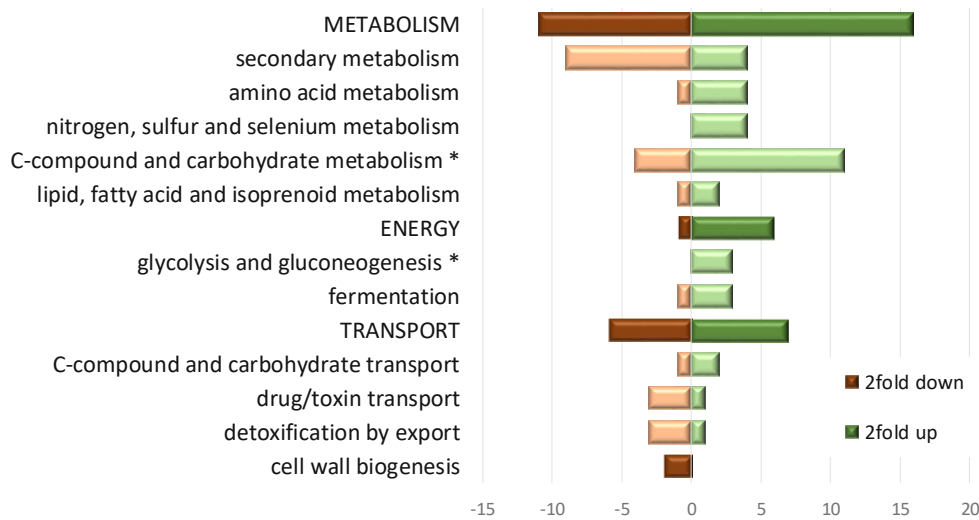
1052

1053   **Figure 2**
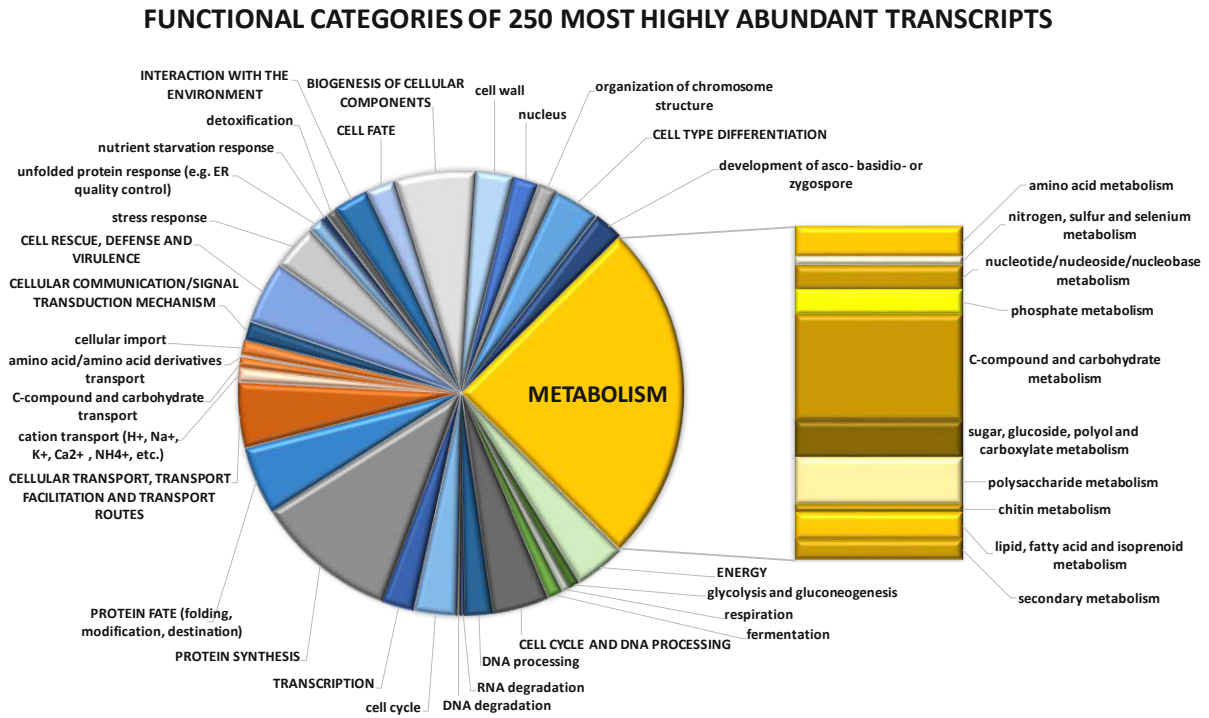
Figure 2 **Functional analysis of gene expression in *T. harzianum* B97**. (A) Functional categories represented among the 250 most abundant transcripts under the conditions of simulated chemotropic response. (B) Major functional categories assigned to genes differentially regulated in the presence of a soy plant. Significantly enriched categories are marked with an asterisk.
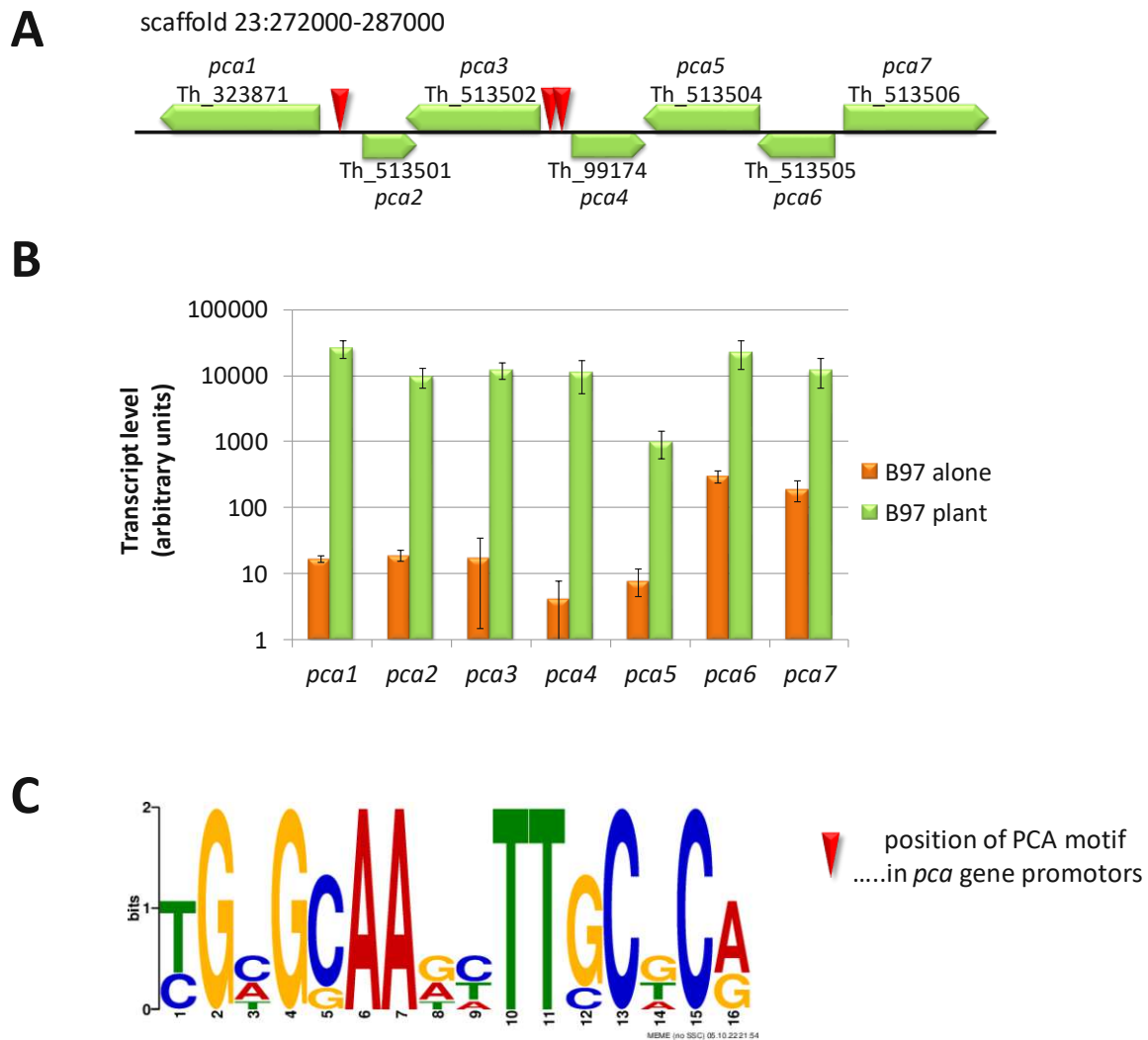
33

1060 **Figure 3**

Figure 3. **Schematic representation of the PCA cluster (A) and its regulation upon recognition of the plant (B).** (A) Localization of *pca*-genes in the *T. harzianum* genome (JGI mycocosm; https://mycocosm.jgi.doe.gov/mycocosm/home). Approximate position of the PCA-DNA motif is shown with red triangles. (B) RPKM values of transcript levels of *pca* genes upon growth alone on the plate (orange bars), where transcripts were at very low basal levels (logarithmic scale is shown). Green bars represent transcript abundance upon recognition of the plant. Values represent means of three biological replicates and error bards show standard deviations. In all cases differential regulation is statistically significant (p-value <0.01) (C) PCA motif as found in the potentially bi-directional promotors of *pca1/pca2* and *pca3/pca4*.

1072   Figure 4

1073
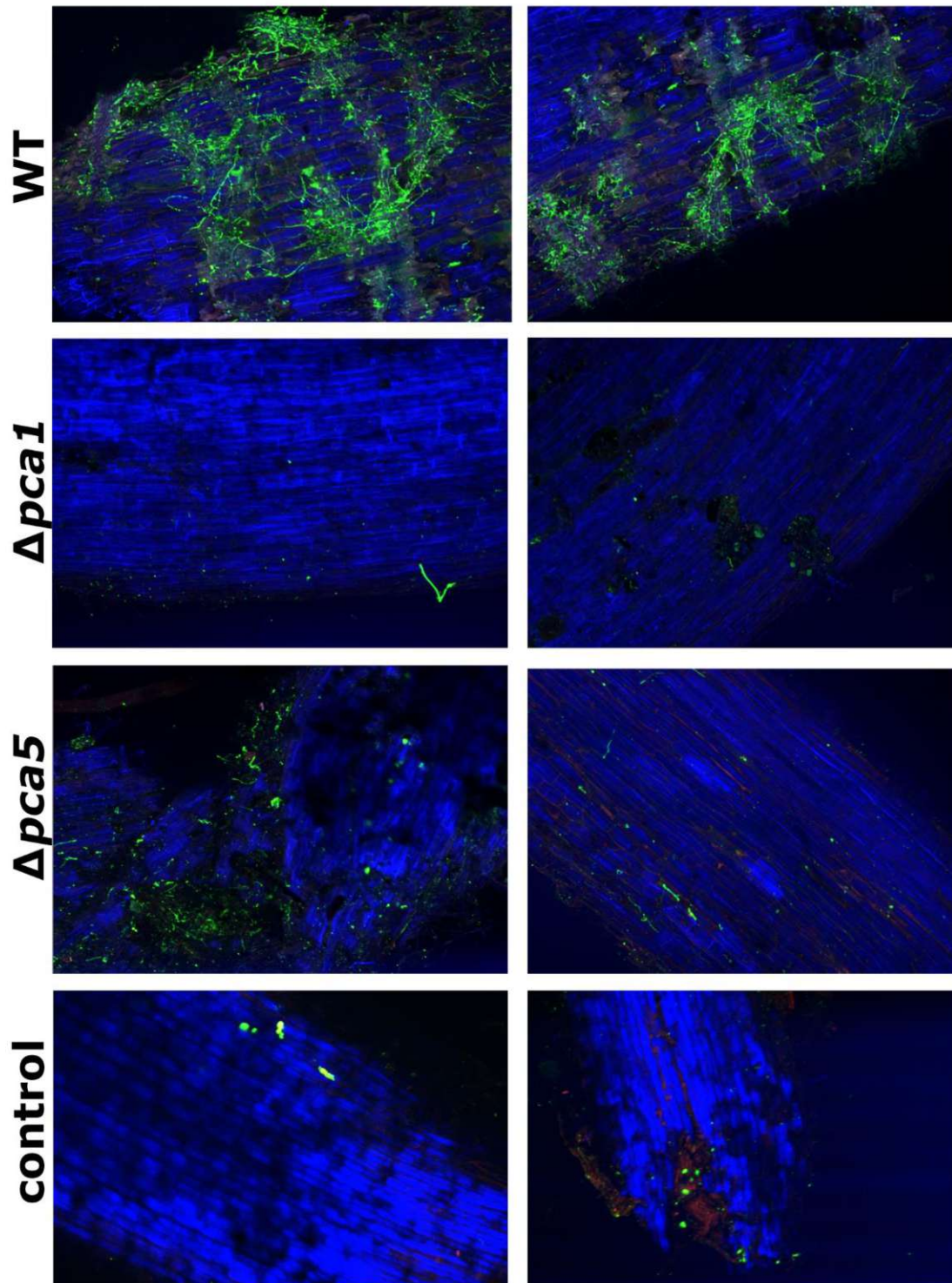
1074

1075

1076   **Figure 4**. **Colonization of soybean roots by *T. harzianum* B97 wildtype and mutant strains Δ*pca1***

1077   **and Δ*pca5***. Uninoculated roots were used as control. Fungal mycelia on the soybean roots were stained

35

1078   with WGA-Alexa Fluor488®. CLSM micrographs are showing B97 hyphae as green fluorescent

1079   colonizing the roots of wildtype but hardly detectable with both mutant strains.
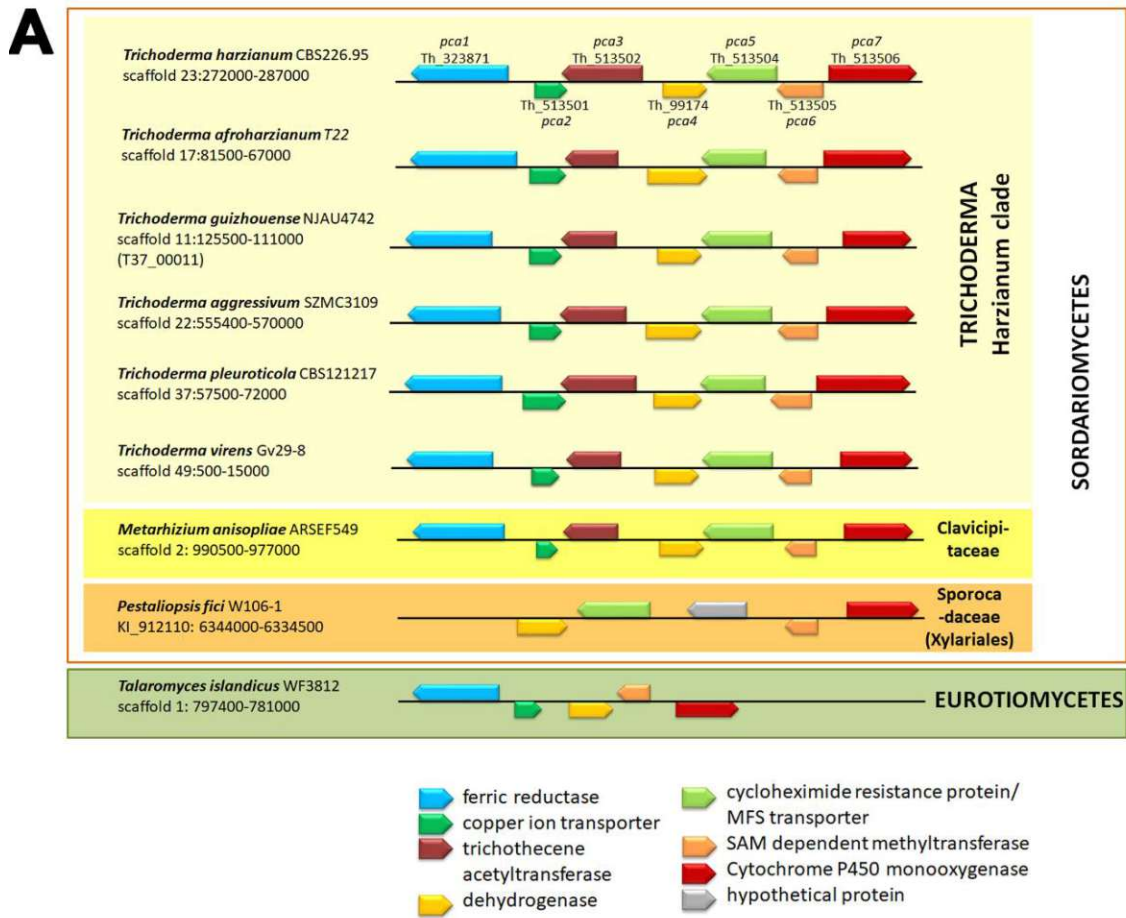
1080

1081   Figure 5

1082
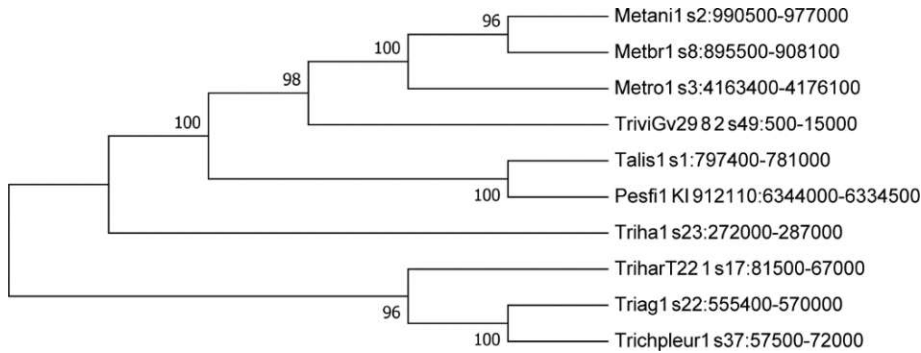
1083

1084

1085   Figure 5 **Molecular phylogenetic analysis of the cluster sequences by Maximum Likelihood**

1086   **method.**

1087   The evolutionary history was inferred by using the Maximum Likelihood method based on the Tamura-

1088   Nei model. The bootstrap consensus tree inferred from 1000 replicates is taken to represent the

1089   evolutionary history of the taxa analyzed. Branches corresponding to partitions reproduced in less than

1090   50% bootstrap replicates are collapsed. The percentage of replicate trees in which the associated taxa

1091   clustered together in the bootstrap test (1000 replicates) are shown next to the branches. Initial tree(s)

1092   for the heuristic search were obtained automatically by applying Neighbor-Join and BioNJ algorithms

1093   to a matrix of pairwise distances estimated using the Maximum Composite Likelihood (MCL) approach,

1094   and then selecting the topology with superior log likelihood value. The analysis involved 10 nucleotide

1095   sequences. Codon positions included were 1st+2nd+3rd+Noncoding. All positions with less than 95%

1096   site coverage were eliminated. That is, fewer than 5% alignment gaps, missing data, and ambiguous

1097   bases were allowed at any position. There were a total of 7697 positions in the final dataset.

1098

1099 Figure 6

1100

A

Trichoderma harzianum CBS226.95 scaffold 23:272000-287000

pca1 Th_323871 — pca3 Th_513502 — pca5 Th_513504 — pca7 Th_513506

Th_513501 pca2 — Th_99174 pca4 — Th_513505 pca6

Trichoderma afroharzianum T22 scaffold 17:81500-67000

Trichoderma guizhouense NJAU4742 scaffold 11:125500-111000 (T37_00011)

Trichoderma aggressivum SZMC3109 scaffold 22:555400-570000

Trichoderma pleuroticola CBS121217 scaffold 37:57500-72000

Trichoderma virens Gv29-8 scaffold 49:500-15000

TRICHODERMA Harzianum clade

Metarhizium anisopliae ARSEF549 scaffold 2: 990500-977000 — Clavicipitaceae

SORDARIOMYCETES

Pestaliopsis fici W106-1 KI_912110: 6344000-6334500 — Sporoca-daceae (Xylariales)

Talaromyces islandicus WF3812 scaffold 1: 797400-781000 — EUROTIOMYCETES

Legend:
- ferric reductase
- copper ion transporter
- trichothecene acetyltransferase
- dehydrogenase
- cycloheximide resistance protein/ MFS transporter
- SAM dependent methyltransferase
- Cytochrome P450 monooxygenase
- hypothetical protein

B

organism	PCA1 e-value	PCA1 id [%]	PCA1 cov [%]	PCA2 e-value	PCA2 id [%]	PCA2 cov [%]	PCA3 e-value	PCA3 id [%]	PCA3 cov [%]	PCA4 e-value	PCA4 id [%]	PCA4 cov [%]	PCA5 e-value	PCA5 id [%]	PCA5 cov [%]	PCA6 e-value	PCA6 id [%]	PCA6 cov [%]	PCA7 e-value	PCA7 id [%]	PCA7 cov [%]	
Quercus suber	0.0	55.45	99	5,E-40	54.48	74													1,E-81	36.89	88	plants
Carpinus fangiana				2,E-20	40.86	81													5,E-65	34.72	78	
Daedalea quercina	5,E-159	43.28	98																			basidiomycetes
Flammula alnicola							3,E-179	57.55	99													
Fomes fomentarium	9,E-106	34.27	99																			
Fomitiporia mediterranea													6,E-82	35.86	97				2,E-58	31.16	90	
Galerina marginata							1,E-169	53.55	100										4,E-56	31.61	92	
Laccaria bicolor													2,E-85	37.59	97							
Mycena venus	6,E-90	33.03	99										2,E-133	51.44	94							
Pleurotus eryngii													5,E-82	37.16	97				2,E-57	28.51	91	
Puccinia graminis				6,E-14	31.15	93																
Ramaria rubella							0.0	57.08	100	6,E-48	31.73	96										
Volvariella volvacea	2,E-120	36.86	99																			
Acinetobacter baumannii				9,E-19	38.46	72																bacteria
Bradyrhizobiom sp.										4,E-92	42.37	97										
Deltaproteobacteria bacterium	5,E-132	50.36	62	1,E-18	49.02	54										4,E-58	44.02	98				
Methylocaldum marinum																2,E-53	40.15	98				
Paraburkholderia sprentiae										3,E-84	39.37	95										
Sorangium cellulosum																4,E-50	39.77	98				

1101

1102 Figure 6 **The PCA cluster and proteins related to its components**. (A) Schematic representation of

1103 the clusters detected within selected representatives of *Trichoderma* spp. and outside the genus

1104 *Trichoderma*. (B) Blastp results of the respective protein sequences from *T. harzianum* B97 against the

1105 NCBI nr database with ascomycetes excluded. The top 100 hits for PCA1-7 were screened for most

1106 interesting similarities for this table.

1107

1108   Figure 7

1109

39
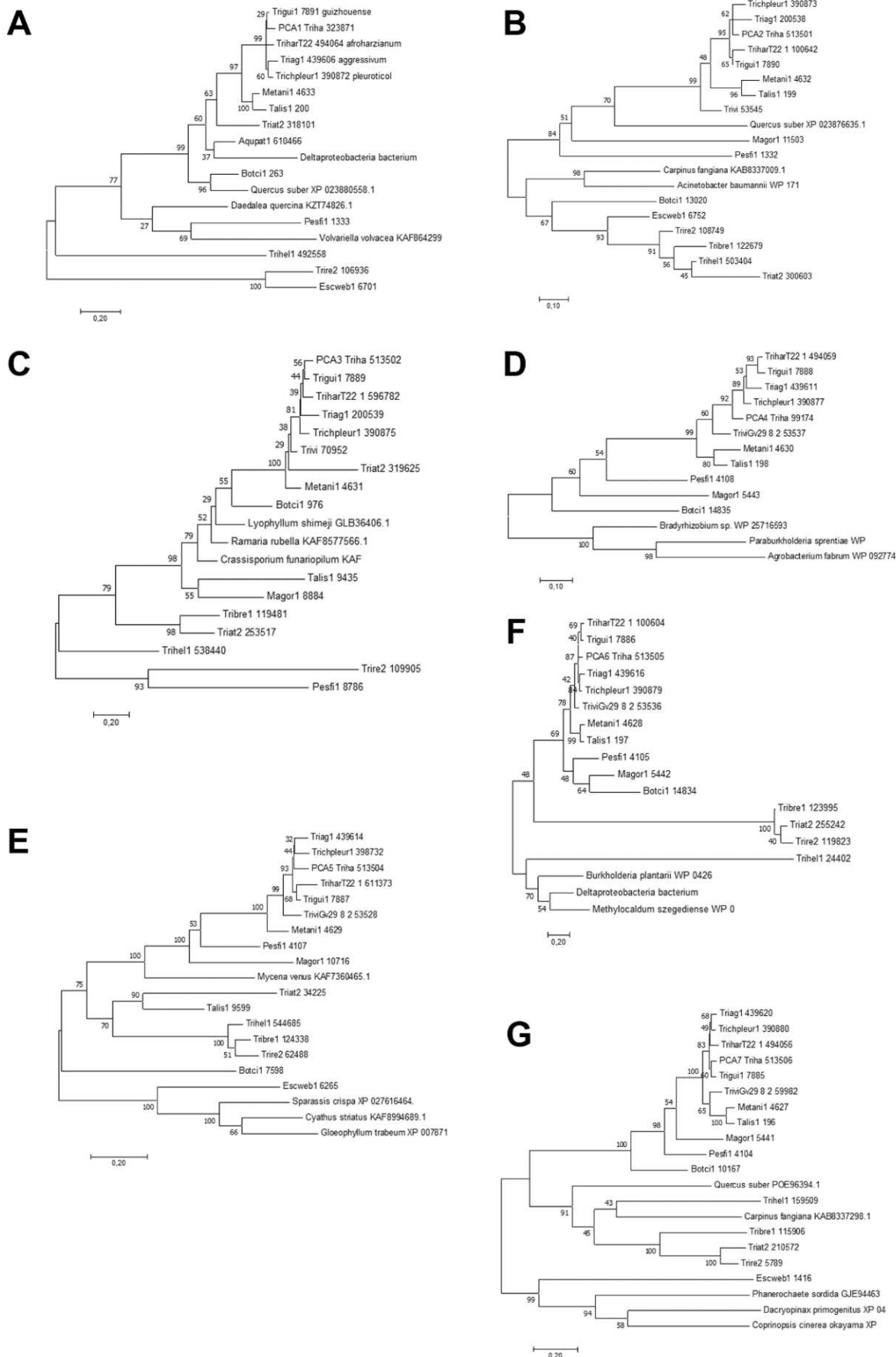
1110

Figure 7 **Molecular phylogenetic analysis of the PCA cluster genes by the Maximum Likelihood method.** Maximum likelihood trees of homologues of (A) PCA1, (B) PCA2, (C) PCA3, (D) PCA4, (E) PCA5, (F) PCA6 and (G) PCA7 are shown. The evolutionary history was inferred by using the Maximum Likelihood method based on the JTT matrix-based model. The tree with the highest log likelihood is shown. The percentage of trees in which the associated taxa clustered together is shown next to the branches. Initial tree(s) for the heuristic search were obtained automatically by applying Neighbor-Join and BioNJ algorithms to a matrix of pairwise distances estimated using a JTT model, and then selecting the topology with superior log likelihood value. The trees are drawn to scale, with branch lengths measured in the number of substitutions per site. All positions with less than 95% site coverage were eliminated. That is, fewer than 5% alignment gaps, missing data, and ambiguous bases were allowed at any position.

1122   Figure 8

1123

1124
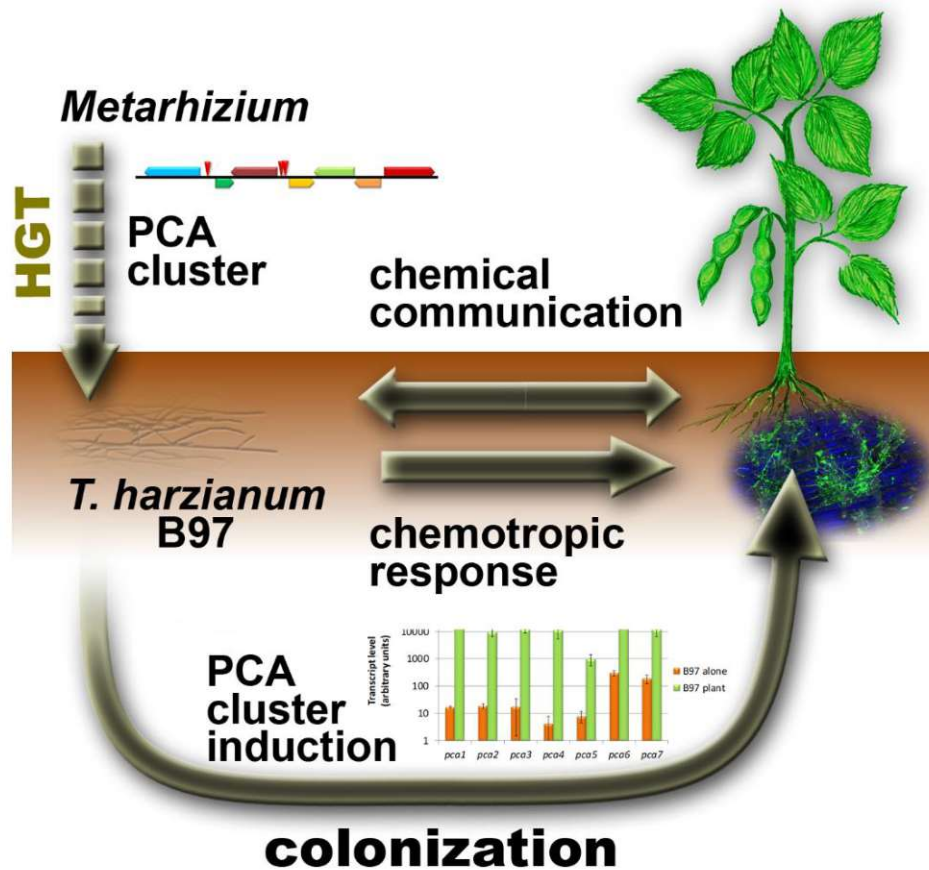
1125   Figure 8 **Schematic representation of the reaction of *T. harzianum* B97 to soy bean.** *T. harzianum*

1126   chemotropically responds to the presence of a soy plant. Chemical communication occurs both ways

1127   due to alteration of the secondary metabolite pattern of both *T. harzianum* B97 and the soy plant. The

1128   PCA gene cluster, which was likely acquired by HGT from *Metarhizium*, is strongly induced upon plant

1129   recognition and essential for effective colonization of plant roots.

Chapter 6: Differential gene expression analysis optimized for *Trichoderma reesei* RNA sequencing data

Author: Miriam Schalamun

Technical and bioinformatic advancements in the field of genomics, targeted genome manipulations and transcriptome studies have expanded our understating of regulatory mechanisms and the biotechnological potential of *T. reesei* in the last years (Li et al., 2017; Martinez et al., 2008). Transcriptome studies allow us to study the genome under specific circumstances, providing insights into gene expression patterns and cellular responses to environmental conditions. Especially for *T. reesei*, these studies shed light on gene expression patterns in response to external stimuli, examining factors such as nutrient availability, carbon source diversity, gene function, and the impact of light (Chen et al., 2021; de Paula et al., 2018; Dos Santos Castro et al., 2014; Kubicek, 2013; Tisch & Schmoll, 2013). Analyses of high throughput RNA-sequencing data requires bioinformatic algorithms and pipelines for alignment, read counting, normalization and differential gene expression (DGE) analysis (Corchete et al., 2020; Schaarschmidt et al., 2020). To ensure comparability of all datasets during the course of this study the same preprocessing pipeline for all samples were used, and they include quality filtering and adapter trimming with bbduk, aligning reads to the reference genome using HISAT2, quantifying counts with featureCounts, and quality control with QualiMap (Brian, 2014; D. Kim et al., 2019; Li et al., 2009; Liao et al., 2014). For the data analysis, the DESeq2 pipeline was adapted to our *T. reesei* RNA-sequencing datasets, including the ones for deletions of *rgs4* and *ste12* (chapter 2 and 4). For a high throughput analysis of a large number of samples, the pipeline is automated to produce publication ready figures and tables. This pipeline is publicly available at GitHub (https://github.com/miriamschalamun /RNA_Tricho

Differential gene expression analysis optimized for *Trichoderma reesei* RNA sequencing data

Miriam Schalamun 30. November 2023

Table of Contents

Introduction

This repository offers an R script for gene expression analysis, tailored for the organism *Trichoderma reesei* and based on the Bioconductor DESeq2 package. For details of the DESeq2 package please refer to the [DESeq2 Vignette] : https://www.bioconductor.org/packages/devel/bioc/vignettes/DESeq2/inst/doc/DESeq2.html.

The **RNASeq_analysis** script was created to analyze the findings for: "The transcription factor STE12 influences growth on several carbon sources and production of dehydroacetic acid (DHAA) in Trichoderma reesei".

The input data is a raw count matrix from *featureCounts* but other raw count matrixes can be used as well. The scripts include functions for differential gene expression analysis, normalization, principal component analysis (PCA), heatmaps generation, and gene ontology (GO) enrichment analysis.

Trichoderma reesei gene annotation is based on PMCID: PMC4771370 and PMC4812632.

The script was written and executed on Windows 10 and R version 4.2.2.

Requirements and Installation

Download and install R from CRAN.

Once R is installed, you can run the following commands in your R console to install the required packages:

```
install.packages("BiocManager")
BiocManager::install(c("DESeq2", "apeglm", "genefilter"))
install.packages(c("readxl", "ggplot2", "dplyr", "ggrepel", "pheatmap",
"RColorBrewer", "gplots", "tidyverse", "edgeR", "matrixStats", "xlsx",
"dendextend", "topGO", "rrvgo"))
```

Set-up

- Open the `RNASeq_analysis.Rmd` file in RStudio. Load the libraries

```
library("DESeq2")
library(stringr)
library(readxl)
library(ggplot2)
library(dplyr)
library(ggrepel)
library(apeglm)
library("pheatmap")
library("RColorBrewer")
library("genefilter")
library(gplots)
library(tidyverse)
library(edgeR)
library(matrixStats)
library("matchmaker")
library("xlsx")
library(dendextend)
library(topGO)
library(rrvgo)
```

Set up working directory, date and create required directories

Set the path to the directory where you want to perform the analysis and have all other required files stored (e.g. count files). Make sure to save the script in the same directory.

```
setwd("/path/to/script")

# Set the date, which is added to the output files
today <- Sys.Date()
today <- format(today, format = "%y%m%d", trim_ws = T)

# Creates the directories that are needed

directory <- function(name){
  if (file.exists(name)) {
    cat("the folder already exists")
  }    else {
    dir.create(name)
  }
}

directory("contrasts")
directory("contrasts/all")
directory("contrasts/significant")
directory("contrasts/strong_filtering")
directory("plots")
directory("plots/PCA")
directory("plots/clust")
directory("plots/MA")
directory("plots/heatmaps")
directory("annotation")
directory("normalized")
```

Input files

Sample input files specific to *Trichoderma reesei* are provided in this repository. They serve as templates for the format and structure data files should have.

```
# Here change the file names to your files and the ds_name to the dataset you
are working with
ds_name <- "example_data"

# Read count table from featurecounts
cts <- read.table("featurecounts_example.txt", header=TRUE, row.names = 1,
check.names = F)

# Rename every but the first (length) column by extracting only the NGS IDS (in
the example featurecounts.txt file you can see how it looks origially and
change to your needs, if you like your input names from featurecounts you don't
need to select). The first column is excluded because it is the gene length
column and we need it for the computatiotion of FPKM values later on.

colnames(cts)[-1] <- str_extract(colnames(cts)[-1], '[0-9]+')

# Add meta file
meta <- read_excel("meta_example.xlsx", col_names = TRUE)

# Load annotation file - Modified from "The Genomes of Three Uneven Siblings:
Footprints of the Lifestyles of Three Trichoderma Species"  Schmoll et al. 2016
annotation <- read_excel("path/to/Annotation_file.xlsx").
```

Compute DESeq object

The DESeq object (dds) is the DESeq2 object needed for normalization and contrasts.

```
meta$strain <- factor(meta$strain)
meta$lightregime <-factor(meta$lightregime)
sample_names <- meta$replicate
meta$replicate <- factor(meta$replicate)
rownames(meta) <- meta$replicate

# check if row names of meta table fit to colnames of countable MUST BE "TRUE"
if not there is a mistake eg sample missing and order must correspond!

all(meta$NGS_ID %in% colnames(cts)[-1])
all(colnames(cts)[-1] == meta$NGS_ID)

# ONLY PERFORM sample renaming (from NGSS_ID to sample name) if the above is
TRUE - if not than samples are switched!

if (all(colnames(cts)[-1] == meta$NGS_ID)){
  colnames(cts)[-1] <- c(sample_names)
} else {
  print("sample names don't correspond to NGS IDs")
}

write.csv2(cts, paste0("renamed_counts_", ds_name, "_", today, ".csv"))

# Here the DESeq object is computed, which allows for contrasts and comparison
of samples for more detail refer to the DESeq2 Vignette

dds <- DESeq2::DESeqDataSetFromMatrix(countData = cts[-1],
                                      colData = meta,
                                      design = ~ strain)
mcols(dds)$basepairs <- cts$Length

dds <- DESeq(dds, minReplicatesForReplace=Inf)
```

VST count normalization

In order to compare counts and visualize them, they need to be normalized first. DESeq2 has its own normalization algorithms, variance stabilizing transformations (VST) and regularized logarithm (rlog). In this example I use VST normalization.

```r
# Function to perform VST (Variance Stabilizing Transformation) and calculate
averages
process_condition <- function(dds, condition_name, ds_name, today) {
  # Perform variance stabilizing transformation
  vsd <- vst(dds, blind = FALSE)

  # Assign column names from the replicate information
  colnames(vsd) <- paste(vsd$replicate)

  # Define file name
  file_name <- paste0("normalized/vsd_normalized_", condition_name, "_",
ds_name, "_", today, ".csv")

  # Check if file exists to avoid overwriting
  if(!file.exists(file_name)) {
    write.csv2(assay(vsd), file_name)
  } else {
    message("File '", file_name, "' already exists. Skipping write.")
  }

  # Calculate the average VST-normalized counts for each strain
  unique_strains <- unique(vsd$strain)
  avvsd <- as.data.frame(matrix(0, nrow(assay(vsd)), length(unique_strains)))
  rownames(avvsd) <- rownames(assay(vsd))
  colnames(avvsd) <- unique_strains

  for(strain in unique_strains) {
    avvsd[[strain]] <- rowMeans(assay(vsd)[, vsd$strain == strain])
  }

  # Return a list containing both avvsd and vsd
  return(list(avvsd = avvsd, vsd = vsd))
}

# Process each condition and store the results in lists
results <- process_condition(dds, "", ds_name, today)

# Extracting the VST objects
vsd <- results$vsd

# Extracting the average VST-normalized counts
avvsd <- results$avvsd
```

FPKM count normalization

Fragments Per Kilobase of transcript per Million mapped reads (FPKM) and can also be used for visualizations like PCA and heatmaps.

```
fpkm <- fpkm(dds, robust = T)
head(fpkm)
colnames(fpkm) <- paste(vsd$replicate)
write.csv2(fpkm, paste0("normalized/fpkm", "_",ds_name, "_", today, "_",
".csv"))
```

PCA plot

A principal component analysis (PCA) plot shows the variation between samples based on their gene expression. Similar samples will cluster together in the plot. The plot has a standard X-Y axis layout, with the axes representing the two principal components that capture the most variation in the data. This is also a useful visualisation to check for outliers.

```
# Execute the function that automatically creates PCA plots, here you can
change e.g. the size of the plot.
# Look at the plots (in publication ready resolution) in the plots/PCA
directory
PCA_plot <- function(data, name, postfix){
 png(filename = paste0("plots/PCA/", name,"_PCA_", postfix, "_", today,
".png"), width = 1600, height = 900, res = 300)
 pcaData <- plotPCA(data, intgroup="strain", returnData=TRUE)
 percentVar <- round(100 * attr(pcaData, "percentVar"))
 print(ggplot(pcaData, aes(PC1, PC2, color=strain, label=rownames(pcaData))) +
         geom_point() +
         geom_text_repel(size=2) +
         xlab(paste0("PC1: ",percentVar[1],"% variance")) +
         ylab(paste0("PC2: ",percentVar[2],"% variance")) +
         coord_fixed())
 dev.off()
}

# This executes the PCA plot function
PCA_plot(data = vsd, name = ds_name, postfix = "")
```
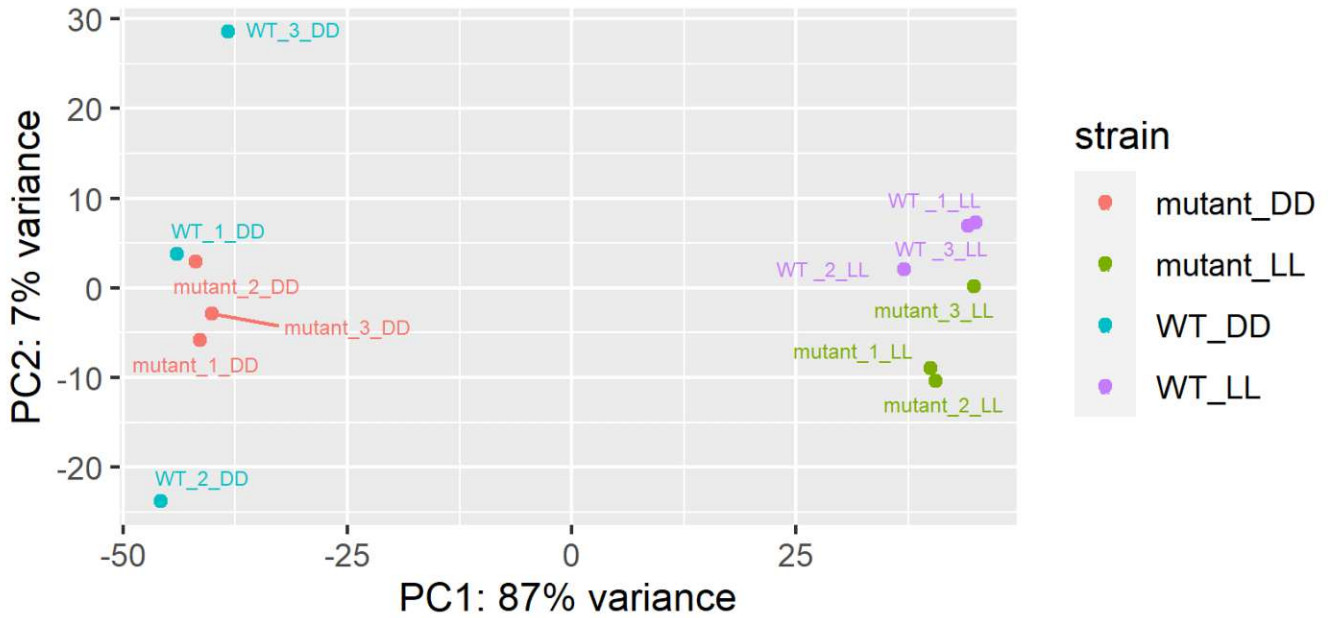
Here we see that the main variation of the dataset derives from the different ligth conditions (DD, LL) used (87% variation on x-axis (PC1)). Therefore I have to split the dataset (DESeq object) for the differential gene expression analysis (contrasts) in LL and DD so that the condition does not interfere too much with the effect of mutant vs WT.

Subset by condition

The data set I mostly used consists of different mutants under two conditions. As seen above in the PCA, most of the time the condition (light) is the strongest factor of variance therefore I need to split my data set when computing the dds element for the contrasts later on. A good indicator for that is the PCA plot, it is recommended that if PCA1 (X-axis) has a higher value than 60% and this is likely to arise from a condition and not the strains you want to analyse then it is advisable to split the data set like done here.

```r
generate_DESeq_object <- function (condition) {
  # Use grep to find columns that contain the condition (e.g., "DD" or "LL")
  matching_columns <- grep(condition, colnames(cts), value = TRUE)
  data_subset <- cts[, matching_columns]

  subset_meta <- meta %>%
    filter(lightregime == condition)
  subset_meta$strain <- factor(subset_meta$strain)

  # 'Strain' is used to subset 'meta' by matching strains

  my_colData <- subset_meta

  # Print the colData to check it
  print(my_colData)

  # Create the DESeqDataSet
  dds <- DESeqDataSetFromMatrix(countData = data_subset,
                                colData = subset_meta,
                                design = ~ strain)

  # Run DESeq analysis
  dds <- DESeq(dds, minReplicatesForReplace=Inf)

  return(dds)
}

# Generates the dds object only for condition specific samples in order to
avoid influences from condition (DD or LL)
dds_DD <- generate_DESeq_object("DD")
dds_LL <- generate_DESeq_object("LL")
```

PCA plot for separated conditions

In order to visually check if splitting the data set by condition worked we run the VST normalization and PCA plot for the split dataset.

```
# Process each condition and store the results in lists
results_DD <- process_condition(dds_DD, "DD", ds_name, today)
results_LL <- process_condition(dds_LL, "LL", ds_name, today)


# Extracting the VST objects
vsd_DD <- results_DD$vsd
vsd_LL <- results_LL$vsd

# Extracting the average VST-normalized counts data frames
avvsd_DD <- results_DD$avvsd
avvsd_LL <- results_LL$avvsd

PCA_plot(data = vsd_DD, name = ds_name, postfix = "DD")
PCA_plot(data = vsd_LL, name = ds_name, postfix = "LL")
```
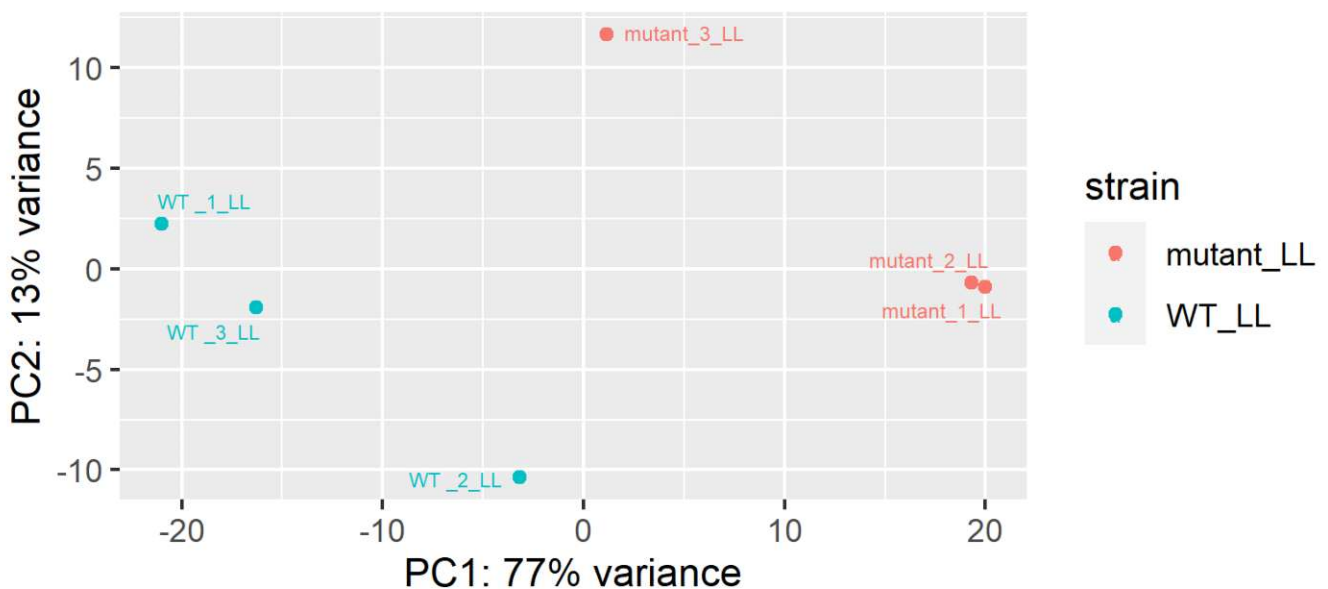
PCA for a separated dataset (LL only) and we see that now actually the mutant vs WT are the main variation of the dataset

Heatmap plot

Heatmaps are created using pheatmap and can be used to visualize clustering of samples and genes.

```r
#First execute the function
heatmap_plot <- function(data, name, postfix, rownumbers){
  avvsd_topic <- tibble::rownames_to_column(data, "gene")
  anno_topic <- annotation[,c("Geneid", "MMBR gene name", "TOPIC", "MMBR
group", "Anno Trichoderma topic")]
  topic <- right_join(anno_topic, avvsd_topic, by = c("Geneid" = "gene"))
  topic <- as.data.frame(topic)
  topic <- column_to_rownames(topic, var = "Geneid")

  row_anno <- as.data.frame(topic$`TOPIC`)
  rownames(row_anno) <- paste(row.names(topic))
  colnames(row_anno)<- c("Function")

  col_anno <- data.frame(condition = ifelse(grepl("LL",colnames(topic)),
"Light", "Dark"))
  row.names(col_anno) <- colnames(topic)

  #standard heatmap

  topVar <- head(order(-rowVars(data)), n=rownumbers)
  mat <- data[topVar, ]
  mat <- mat - rowMeans(mat)
  png(filename = paste0("plots/heatmaps/", name, "_heatmap_", rownumbers, "_",
postfix, "_", today, ".png"), width = 1600, height = 1600, res = 300)
  pheatmap(mat, color=colorRampPalette(c("blue", "white", "red"))(50),
show_rownames = F, cutree_cols = 1, cutree_rows = 1, fontsize_row = 4, fontsize
= 6, treeheight_row = 40, treeheight_col = 20, annotation_row = row_anno,
annotation_col = col_anno)
  dev.off()
}

# Enter the number of how many genes should be displayed
rownumbers <- 100

# Automatically saves the figures in the plots/heatmaps directory
heatmap_plot(data = avvsd, name = ds_name, rownumbers = 100, postfix = "")
heatmap_plot(data = avvsd_DD, name = ds_name, rownumbers = 100, postfix = "DD")
heatmap_plot(data = avvsd_LL, name = ds_name, rownumbers = 100, postfix = "LL")
```
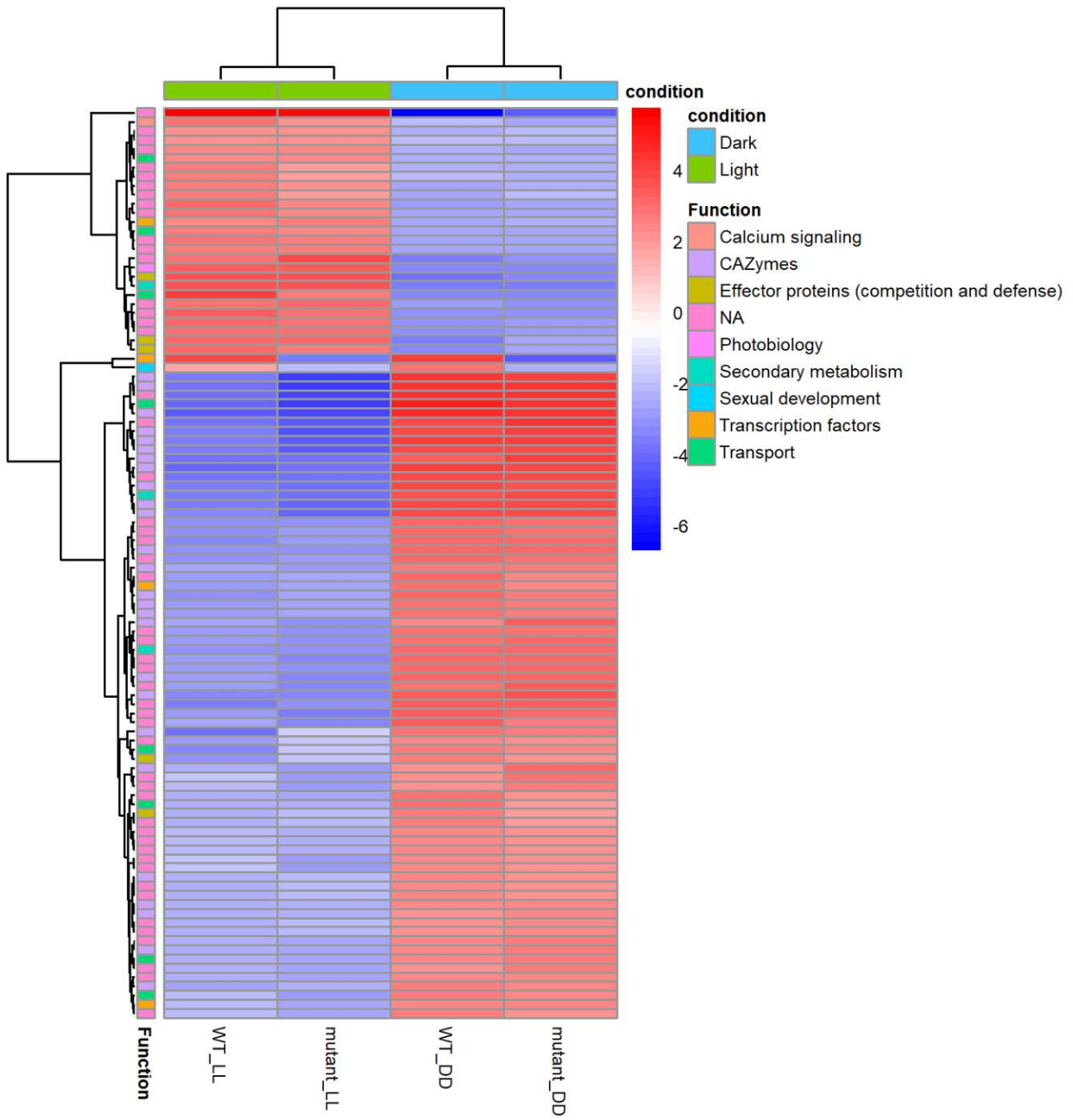
Heatmap according to pre-assigned topics

This is specific to the T. reesei annotation file and refers to different assigned "topics". Example topics: secondary metabolism, CAZymes, transcription factors, transporters..the spelling has to be exactly like in the annotation file.

```r
#First execute the function
heatmap_plot_TOPIC <- function(data, name, postfix, rownumbers, whichTOPIC){

avvsd_topic <- tibble::rownames_to_column(data, "gene")
  anno_topic <- annotation[,c("Geneid", "MMBR gene name", "TOPIC", "MMBR
group", "Anno Trichoderma topic")]
  topic <- right_join(anno_topic, avvsd_topic, by = c("Geneid" = "gene"))
  topic <- as.data.frame(topic)
  topic <- column_to_rownames(topic, var = "Geneid")

  col_anno <- data.frame(condition = ifelse(grepl("LL",colnames(topic)),
"Light", "Dark"))
  row.names(col_anno) <- colnames(topic)

  whichTOPIC <- whichTOPIC
topic_filtered <- filter(topic, TOPIC == whichTOPIC)
print(whichTOPIC)

# takes the column MMBR group for row annotation (= the groups for eg function)
# first create a "clean names" table

row_anno <- as.data.frame(topic_filtered$`MMBR group`)
rownames(row_anno) <- paste(row.names(topic_filtered))
colnames(row_anno)<- c("Function")

# column annotations (DD or LL mostly)
col_anno <- data.frame(condition = ifelse(grepl("LL",colnames(topic_filtered)),
"Light", "Dark"))
row.names(col_anno) <- colnames(topic_filtered)

# subset columns = samples (eg if more datasets combined or you only want DD or
LL and to only have the normalized counts (it doesnt work if there are the
descriptions in there ,therefore you always have to call for all the samples
you want in the heatmap))

topic_heatmap <- as.data.frame(topic_filtered[, !(colnames(topic_filtered) %in%
c("MMBR gene name", "TOPIC", "MMBR group", "Anno Trichoderma topic"))])

 topVar <- head(order(-rowVars(topic_heatmap)), n=rownumbers)
  mat <- topic_heatmap[topVar, ]
  mat <- mat - rowMeans(mat)

  png(filename = paste0("plots/heatmaps/", name, "_heatmap_", rownumbers, "_",
postfix, "_", whichTOPIC, "_", today, ".png"), width = 1600, height = 1600, res
= 300)
  pheatmap(mat, color=colorRampPalette(c("blue", "white", "red"))(50),
show_rownames = F, cutree_cols = 1, cutree_rows = 1, fontsize_row = 4, fontsize
```

```r
= 6, treeheight_row = 40, treeheight_col = 20, annotation_row = row_anno,
annotation_col = col_anno, main = whichTOPIC)
  dev.off()
}


# Filter by "TOPIC" and the type you want to filter for (eg Secondary
metabolism or CAZymes, must be written exactly as in the annotation file), the
rownumbers are the number of genes displayed.
rownumbers <- 300
whichTOPIC <- "CAZymes"

#Automatically saves the figures in the plots/heatmaps directory
heatmap_plot_TOPIC(data = avvsd, name = ds_name, rownumbers, postfix = "",
whichTOPIC)
heatmap_plot_TOPIC(data = avvsd_DD, name = ds_name, rownumbers, postfix = "DD",
whichTOPIC)
heatmap_plot_TOPIC(data = avvsd_LL, name = ds_name, rownumbers, postfix = "LL",
whichTOPIC)
```
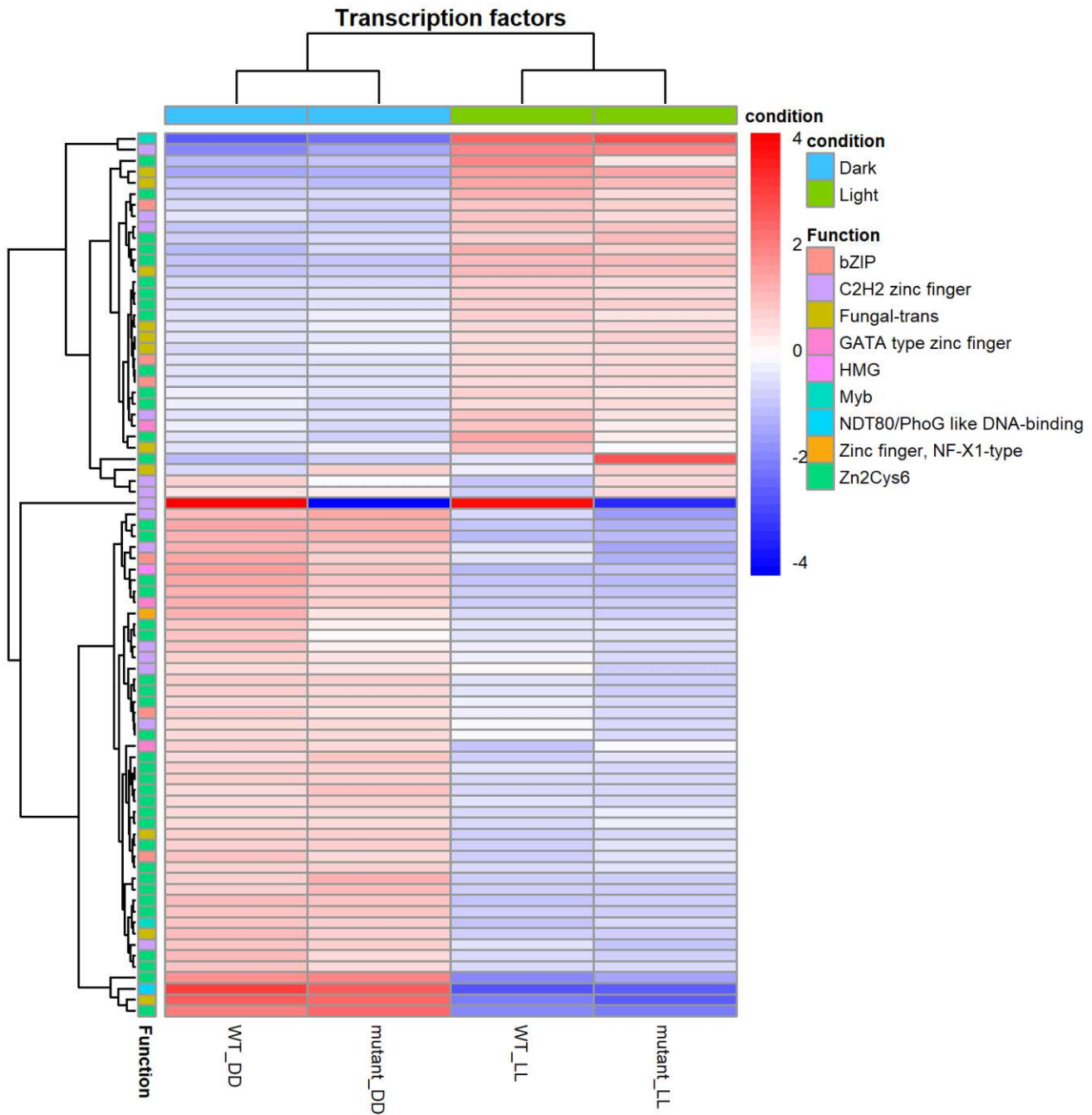
Differentially expressed genes

DEGs are created using the contrast function which results in two types of files, one in the directory conrasts/all which contains the values for all genes and in the directory contrasts/significant the files are already filtered by p-value and fold change. These values can be changed in the function. Usually I used padj < 0.05 and log2 fold change of > |1| (corresponds to a fold change > 2)

```r
# First execute the function
contrasts_function <- function(dds, mutant_base, WT_base, condition1,
condition2, padj_cutoff, log2_cutoff, today){
  # Generate file names
  contrast_name <- paste0(mutant_base, "_", condition1, "__", WT_base, "_",
condition2)
  name <- paste0("contrasts/all/", contrast_name, "_all_", today, ".csv")
  name_sig <- paste0("contrasts/significant/", contrast_name, "_sig_", today,
".csv")

  # Check if the results file already exists to avoid overwriting
  if (!file.exists(name)) {
    # Create contrast vectors
    mutant <- paste0(mutant_base, "_", condition1)
    WT <- paste0(WT_base, "_", condition2)

    # Run the DESeq2 results function
    res <- results(dds, contrast = c("strain", mutant, WT), cooksCutoff =
FALSE, independentFiltering = FALSE)
    data_padj <- subset(res, padj < padj_cutoff)
    data_LFC1 <- subset(data_padj, log2FoldChange < -log2_cutoff |
log2FoldChange > log2_cutoff)
    data_significant <- data_LFC1[order(data_LFC1$log2FoldChange),]

    # Write results to CSV
    write.csv2(res, name)
    write.csv2(data_significant, name_sig)
  } else {
    message("File ", name, " already exists. Skipping.")
  }
}

#  the names have to be exactly as in the meta file
mutant <- "mutant"
WT <- "WT"

# Run contrasts function for DD
contrasts_function(dds_DD, mutant, WT, "DD", "DD", 0.05, 1, today)

# Run contrasts function for LL
contrasts_function(dds_LL, mutant, WT, "LL", "LL", 0.05, 1, today)


# Run contrasts function for contrasts between conditions (e.g. DD vs LL)
# Out of simplicity names mutant and WT say the same here but they just refer
to the one condition you want to look at as a "background" which corresponds to
the WT and the condition which changed which corresponds to mutant here. Make
```

```
sure that always the correct values for "WT" and "mutant" are logged in.

mutant <- "mutant"
WT <- "WT"

contrasts_function(dds, mutant, WT, "LL", "DD", 0.05, 1, today)
```

Annotation

Gene annotation is performed using the T. reesei annotation file, but any other file in the same format can be used.

```r
  annotation_function <- function(data, name){
    as.data.frame(annotation)
    as.data.frame(annotation)
    as.data.frame(data)

    colnames(data) <- c("gene", "basemean", "log2FoldChange", "lfcSE", "pvalue",
"padj")
    data <- data[,c("gene", "log2FoldChange")]

    foldchange <- gtools::logratio2foldchange(data$log2FoldChange)
    as.matrix(foldchange)
    contrast_fold <- data.frame(data, foldchange)

    upregulated <- subset(contrast_fold, log2FoldChange > 1)
    up_anno <- right_join(annotation, upregulated, by = c("Geneid" = "gene"))
    up_anno <- up_anno %>% relocate(log2FoldChange, foldchange, .after =
`position in chromosome`)
    up_anno <- up_anno[order(up_anno$log2FoldChange, decreasing = T),]
    up_anno <- as.data.frame(up_anno)

    downregulated <- subset(contrast_fold, log2FoldChange < -1)
    down_anno <- right_join(annotation, downregulated, by = c("Geneid" = "gene"))
    down_anno <- down_anno %>% relocate(log2FoldChange, foldchange, .after =
`position in chromosome`)
    down_anno <- down_anno[order(down_anno$log2FoldChange),]
    down_anno <- as.data.frame(down_anno)

    write.xlsx(up_anno, file = paste0(name), sheetName = paste0("up"), row.names
= F, append = T)
    write.xlsx(down_anno, file = paste0(name), sheetName = paste0("down"),
row.names = F, append = T)

}

contrast_files <- dir(path = "contrasts/significant/", pattern = ".csv",
full.names = T, recursive = F)
for(i in contrast_files){
  data <- read.csv2(i)
  anno_name <- tools::file_path_sans_ext(base::basename(i))
  name <- paste0("annotation/", anno_name, "_anno", ".xlsx")

  if (file.exists(name)) {
      cat("the file already exists")
  }else
    annotation_function(data = data, name = name)
}
```

GO enrichment set up

Creates the directories and functions for GO enrichment and visualization. Here you don't need to change anything. Just execute.

```r
directory <- function(name){
  if (file.exists(name)) {
    cat("the folder already exists")
  }    else {
    dir.create(name)
  }
}
directory("GO")
directory("GO/rrvgo")
directory("GO/plots")
directory("GO/plots/treemap")
directory("GO/plots/treemap/BP")
directory("GO/plots/treemap/BP/weighted")
directory("GO/plots/treemap/BP/classic")
directory("GO/plots/treemap/MF")
directory("GO/plots/treemap/MF/weighted")
directory("GO/plots/treemap/MF/classic")

Gofunction <- function(data, name, rrvgo, ontology){

  as.data.frame(data)
  data <- as.character(data[,c(1)])
  geneList2 <- factor(as.integer(geneUniverse %in% data))
  names(geneList2) <- geneUniverse

# build the GOdata object, use BP (biol. proc.); MF (molec. func.) or CC (cel.
comp.)
  GOdata <- new("topGOdata", ontology = category, allGenes = geneList2,  annot
= annFUN.gene2GO, gene2GO = geneID2GO)

# Cacluate p-value using the fisher's exact test
  resultClassic <- runTest(GOdata, algorithm="classic", statistic ="fisher")

  resultweight01 <- runTest(GOdata, algorithm="weight01", statistic = "fisher")

  allRes <- GenTable(GOdata, classicFisher = resultClassic, weighted =
resultweight01, orderBy = "classicFisher", ranksOf = "classicFisher", topNodes
= length(topGO::score(resultClassic)))

  cutoff <- subset(allRes, classicFisher < 1)
  write.csv2(allRes, name, row.names = F)
  write.csv2(allRes[,c("GO.ID", "classicFisher", "weighted")], rrvgo, row.names
= F)
}

rrvgo_function_MF_classic <- function(data, name, pvalue, threshold){
  go_analysis <- data
```

```
  go_analysis$classicFisher <- (as.numeric(go_analysis$classicFisher))
  go_analysis_p <- subset(go_analysis, classicFisher < pvalue)

  simMatrix <- rrvgo::calculateSimMatrix(go_analysis_p$GO.ID, ont = "MF",
method = "Rel", orgdb = "org.Sc.sgd.db")

  scores <- setNames(-log10(go_analysis$classicFisher), go_analysis$GO.ID)

  reducedTerms <- reduceSimMatrix(simMatrix, scores, threshold, orgdb =
"org.Sc.sgd.db")

  png(filename = paste0("GO/plots/treemap/MF/classic/", name, "_p", pvalue,
"_", threshold, ".png"), width = 1600, height = 1600, res = 300)
rrvgo::treemapPlot(reducedTerms = reducedTerms)

dev.off()
}

rrvgo_function_MF_weighted <- function(data, name, pvalue, threshold){
  go_analysis <- data
  go_analysis$weighted <- (as.numeric(go_analysis$weighted))
  go_analysis_p <- subset(go_analysis, weighted < pvalue)

  simMatrix <- rrvgo::calculateSimMatrix(go_analysis_p$GO.ID, ont = "MF",
method = "Rel", orgdb = "org.Sc.sgd.db")

  scores <- setNames(-log10(go_analysis$weighted), go_analysis$GO.ID)

  reducedTerms <- reduceSimMatrix(simMatrix, scores, threshold, orgdb =
"org.Sc.sgd.db")

  png(filename = paste0("GO/plots/treemap/MF/weighted/", name, "_p", pvalue,
"_", threshold, "_weighted", ".png"), width = 1600, height = 1600, res = 300)
rrvgo::treemapPlot(reducedTerms = reducedTerms)

dev.off()
}

rrvgo_function_BP_classic <- function(data, name, pvalue, threshold){
  go_analysis <- data
  go_analysis$classicFisher <- (as.numeric(go_analysis$classicFisher))
  go_analysis_p <- subset(go_analysis, classicFisher < pvalue)


  simMatrix <- rrvgo::calculateSimMatrix(go_analysis_p$GO.ID, ont = "BP",
method = "Rel", orgdb = "org.Sc.sgd.db")

  scores <- setNames(-log10(go_analysis$classicFisher), go_analysis$GO.ID)
```

```r
  reducedTerms <- reduceSimMatrix(simMatrix, scores, threshold, orgdb =
"org.Sc.sgd.db")

  filename <- paste0("GO/plots/treemap/BP/classic/", name, "_p", pvalue, "_",
threshold, ".png")
  print(filename)
  if (file.exists(filename)) {
    cat("the file already exists")
  }else
  png(filename = filename,  width = 1600, height = 1600, res = 300)
rrvgo::treemapPlot(reducedTerms = reducedTerms)

dev.off()
}

rrvgo_function_BP_weighted <- function(data, name, pvalue, threshold){
  go_analysis <- data
  go_analysis$weighted <- (as.numeric(go_analysis$weighted))
  go_analysis_p <- subset(go_analysis, weighted < pvalue)

  simMatrix <- rrvgo::calculateSimMatrix(go_analysis_p$GO.ID, ont = "BP",
method = "Rel", orgdb = "org.Sc.sgd.db")

  scores <- setNames(-log10(go_analysis$weighted), go_analysis$GO.ID)

  reducedTerms <- reduceSimMatrix(simMatrix, scores, threshold, orgdb =
"org.Sc.sgd.db")

  filename <- paste0("GO/plots/treemap/BP/weighted/", name, "_p", pvalue, "_",
threshold, ".png")
  print(filename)
  if (file.exists(filename)) {
    cat("the file already exists")
  }else
  png(filename = filename,  width = 1600, height = 1600, res = 300)
rrvgo::treemapPlot(reducedTerms = reducedTerms)

dev.off()
}

scatterplot_function_BP_classic <- function(data, name, pvalue, threshold){
  go_analysis <- data
  go_analysis$classicFisher <- (as.numeric(go_analysis$classicFisher))
  go_analysis_p <- subset(go_analysis, classicFisher < pvalue)

  simMatrix <- rrvgo::calculateSimMatrix(go_analysis_p$GO.ID, ont = "BP",
method = "Rel", orgdb = "org.Sc.sgd.db")
```

```
    scores <- setNames(-log10(go_analysis$classicFisher), go_analysis$GO.ID)

    reducedTerms <- reduceSimMatrix(simMatrix, scores, threshold, orgdb =
"org.Sc.sgd.db")

    png(filename = paste0("GO/plots/scatterplot/BP/", "scatter_", name, "_p",
pvalue, "_", threshold, ".png"), width = 1600, height = 1600, res = 300)
rrvgo::scatterPlot(simMatrix, reducedTerms, size = "score")

    dev.off()
}
```

GO enrichment

Performs GO enrichment using topGO.

```r
BPterms <- ls(GOBPTerm)
MFterms <- ls(GOMFTerm)

# Load custom annotation file
geneID2GO <- readMappings(file = "directory/GOterms.txt")

# I needed in a format that I have one gene ID and listed next to it the GO
terms
GO2geneID <- inverseList(geneID2GO)
geneID2GO <- inverseList(GO2geneID)
str(head(geneID2GO))

# set names of all genes that we have for the GOterms
geneNames <- names(geneID2GO)
geneUniverse <- names(geneID2GO)

# automatically loads all significant contrasts and performs the Gofunction -
might take a few minutes, so this means in this cas you perform the go
enrichment only on the significantly differntially regulated genes

contrast_files <- dir(path = "contrasts/significant/", full.names = T,
recursive = F)

## Here you can change which category you want BP (biological process) or MF
(molecular function)
category <- "MF"

for(i in contrast_files){
  data <- read.csv2(i)
  GO_name <- tools::file_path_sans_ext(base::basename(i))
  ontology <- category
  name <- paste0("GO/","GO_", GO_name, "_", ontology, ".csv")
  rrvgo <- paste0("GO/rrvgo/","rrvgo_", GO_name, ontology, ".csv")
  if (file.exists(name)) {
      cat("the file already exists ")
  }else

Gofunction(data = data, name = name, rrvgo=rrvgo, ontology = category)
}
```

GO visualization

Visualize using rrvgo and the yeast database for terms. Run the tests to determine p-values for each go term using different algorithms ("classic fisher" or "weighted"). Classic: each GO term is tested independently not taking the GO hierachy into account. weight01:a mix between

"weighted" and "elim" (Alexa et al 2006 - Improved scoring of functional groups..).
I am using weight01 for most of my figures

```r
# yeast db:
library("org.Sc.sgd.db")

for(i in contrast_files){
  data <- read.csv2(i)
  GO_name <- tools::file_path_sans_ext(base::basename(i))
  ontology <- category
  name <- paste0("GO/","GO_", GO_name, "_", ontology, ".csv")
  rrvgo <- paste0("GO/rrvgo/","rrvgo_", GO_name, ontology, ".csv")
  if (file.exists(name)) {
      cat("the file already exists ")
  }else

Gofunction(data = data, name = name, rrvgo=rrvgo, ontology = category)
}

# Biological Process category (BP)

rrvgo_files_BP <- dir(path = "GO/rrvgo", pattern = ".csv", full.names = T,
recursive = F)

threshold <- "0.7"
pvalue <- "0.1"

# classic algorithm
for(i in rrvgo_files_BP){
  data <- read.csv2(i)
  GO_name <- tools::file_path_sans_ext(base::basename(i))
  name <- paste0(GO_name)
  threshold <- paste0(threshold)
  pvalue <- paste0(pvalue)
rrvgo_function_BP_classic(data, name, pvalue, threshold)
}

#weighted algorithm (more stringent but might loose info)
for(i in rrvgo_files_BP){
  data <- read.csv2(i)
  GO_name <- tools::file_path_sans_ext(base::basename(i))
  name <- paste0(GO_name)
  threshold <- paste0(threshold)
  pvalue <- paste0(pvalue)

rrvgo_function_BP_weighted(data, name, pvalue, threshold)
}

# Molecular Function category (MF)
rrvgo_files_MF <- dir(path = "GO/rrvgo/", pattern = "MF.csv", full.names = T,
```
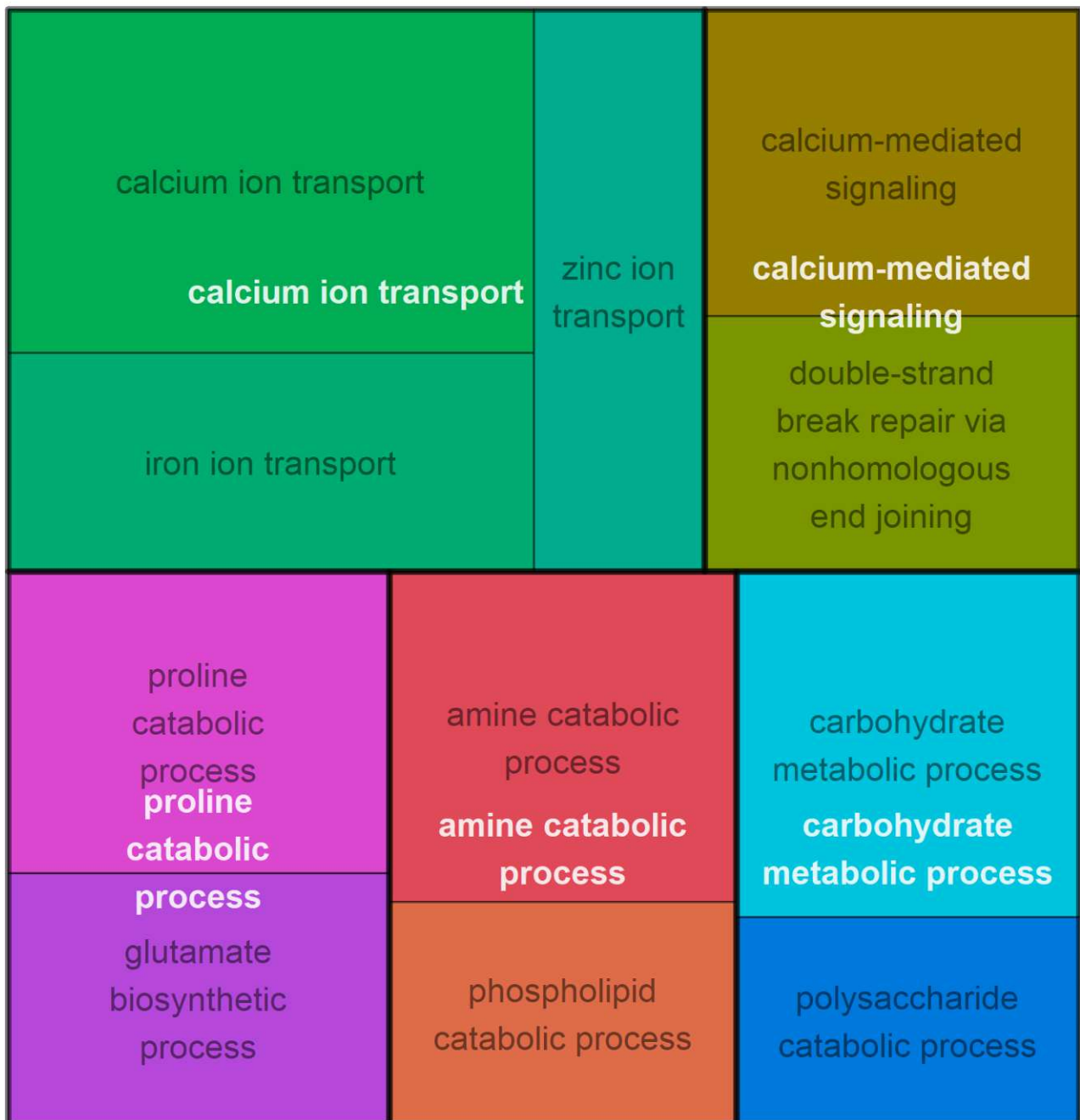
```
recursive = F)

for(i in rrvgo_files_MF){
  data <- read.csv2(i)
  GO_name <- tools::file_path_sans_ext(base::basename(i))
  name <- paste0(GO_name)
  threshold <- paste0(threshold)
  pvalue <- paste0(pvalue)

rrvgo_function_MF_weighted(data, name, pvalue, threshold)
}
```

Discussion

Every organism is governed by the need to efficiently use its available resources and energy for survival and propagation. In fungi, the breakdown of complex substrates such as plant biomass, requires the production of specialized enzymes which is energy intensive. When simpler carbon sources like sugars are available, this energy can more efficiently be used in other processes like growth or reproduction. Similarly, investing in the production of secondary metabolites at the right moment to attract a mating partner or to repel a competitor has significant consequences on survival and propagation. The aim of this thesis is to further unravel how fungi so quickly make and dictate these decisions by analyzing the signaling roles of RGS4, MAPkinases, and STE12 in *T. reesei*, alongside the investigation of the PCA secondary metabolite gene cluster in *T. harzianum*.

For *T. reesei*, understanding the underlying mechanisms that regulate cellulolytic enzyme production is essential to find the genetic and environmental factors that control its physiological responses. Previously it was shown that cell surface receptors, particularly GPCRs, along with G-protein subunits, play a pivotal role in the light-dependent detection of cellulose signals, which modulate cellulase gene expression and enzyme activity (Hinterdobler et al., 2020; Schmoll et al., 2009; Seibel et al., 2009; Stappler, Dattenböck, et al., 2017; Tisch et al., 2014). Since RGS proteins accelerate the termination of the G-protein signal, the deletion of RGS4 is proposed to resemble the phenotype of a constitutive activation of a G-alpha subunit, in this case the G-alpha s protein GNA3 (Xie & Palmer, 2007). The constitutive activation of GNA3 (GNA3QL) strongly increases transcript levels of the major cellulolytic enzyme encoding gene, *cbh1* in constant light (Schmoll et al., 2009). While RGS4 is involved in cellulase regulation, this *cbh1* upregulation is not observed, concluding that there are other regulatory processes or RGS proteins involved in the cellulase regulation by GNA3. In constant darkness however, gene expression profiles reveal that RGS4 deletion and GNA3QL share common differentially expressed genes, and they exhibit similar patterns in hierarchical clustering, pointing towards at least a partial, probably light dependent regulation of GNA3 by RGS4 (Schalamun et. al, in preparation). Additionally, growth on glucose and under oxidative stress reveal overlapping functions of RGS4 and another G-alpha subunit, GNA1, indicating

that the roles of the different RGS proteins act redundantly and are not specific to a single G-alpha subunit.

Cellulase gene expression and secretion in *T. reesei* is prone to a complex regulatory system, where not only G-proteins are involved but also MAPkinases play a crucial role (de Paula et al., 2018; Wang et al., 2014; Wang et al., 2017; M. Wang et al., 2013). Specifically, TMK3 emerges as a key mediator for cellulase signaling. Upon *tmk3* deletion and cultivation in constant darkness, expression of *cbh1* and the consequent cellulase activity are completely abolished under inducing conditions on cellulose. The same effect was observed for deletions of GNA1 and GNB1, suggesting the requirement of these signaling proteins for the transmission of the cellulase signal in darkness and a light dependent overlap of these signaling cascades for cellulase regulation (Schalamun et. al, in preparation). TMK1, the MAPkinase in the pheromone response pathway and TMK2, in the cell wall integrity pathway both negatively influence cellulase gene transcription in darkness but not in light, pointing out the importance of controlled light conditions in cellulase regulation studies (Wang et al., 2017). In other *Trichoderma* species like *T. atroviride*, the transcription factor Ste12 is linked to Tmk1, and several Tmk1-mediated processes, including the expression of host cell wall degrading enzymes (Gruber & Zeilinger, 2014). Similarly, in *T. reesei*, we observed a concurrent reduction in *cbh1* expression in constant light in both, MAPkinase and STE12 deletion mutants, hinting at STE12's potential role in cellulase signaling mediated by all three MAPkinases. Conversely, in the absence of light, Δ*ste12* does not exhibit significant *cbh1* expression changes, while the MAPkinases display distinct regulatory patterns. Overall, the G-proteins GNA1, GNB1 and the MAPkinase TMK3 are most crucial for cellulase gene transcription and activity, TMK1 and TMK2 have a negative influence and STE12 and RGS4 are not directly involved in the cellulase signal transmission. In light, where overall cellulase gene transcription and activity are strongly decreased as compared to darkness, GNA1, TMK2, TMK3 and STE12 are required for the signal transmission and the increased *cbh1* expression due to GNA3 constitutive activation is not due to RGS4 activity, revealing the complex interplay between signaling pathways and environmental factors in cellulase regulation.

The G-protein and MAPkinase cascades are both fundamental in fungal signal transmission, hence it was not surprising to discover distinct regulatory roles in different secondary metabolism involving processes in *T. reesei*. These metabolites and organic compounds

produced by fungi play essential roles in communication, development, and competition with other organisms (Rangel et al., 2021).

The gene cluster responsible for the biosynthesis of sorbicillinoids, the SOR-cluster, is starting to emerge as a thoroughly examined model for secondary metabolite production in *T. reesei* (Derntl et al., 2017; Derntl et al., 2016; Hinterdobler et al., 2020; Hinterdobler et al., 2019; Hitzenhammer et al., 2019; Monroy et al., 2017). Sorbicillin compounds are known for their bioactive properties, including antimicrobial and anti-inflammatory activities (Meng et al., 2016).

Here, we found that all three MAPkinases and STE12, are involved in the production of secondary metabolites. The deletions of TMK1 and TMK3, along with STE12, reduce or eliminate the production of trichodimerol, with Δ*tmk3* also abolishing the production of (21S)-bisorbibutenolide. Dehydroacetic acid, another metabolite with potent antimicrobial properties (Tang et al., 2018; Zhang et al., 2012), is regulated by TMK2, TMK3, and STE12, but not by TMK1.This suggests that STE12's regulation is not exclusively governed by TMK1, and other components are involved in TMK1 signal transmission in *T. reesei*. The production of these secondary metabolites proposes the potential to fend off competitors, including other fungi, bacteria and insects (Balde et al., 2010; Derntl et al., 2017; Evidente et al., 2009). On the other hand, it was shown that alteration of secondary metabolite profiles influences chemical communication with potential mating partners during sexual development in *T. reesei* (Bazafkan et al., 2017; Bazafkan et al., 2015). Given that and the mating defects observed in *N. crassa* linked to MAPkinase activity, we explored similar connections in *T. reesei*. Our results indicate that sexual development requires all three MAPkinases, with mating deficiencies due to mutations in HAM5, a scaffolding protein essential for MAPkinase pathway functionality (Jonkers et al., 2014). Hence, it remains to be investigated if secondary metabolites as produced by MAPkinases are involved in the alteration of sexual development in *T. reesei*. Components of the heterotrimeric G-protein complex also play essential roles in sexual development and the production of soribicillinoids (manuscript in preparation), which will be an interesting topic to look at, particularly in the regulatory role of RGS4, an aspect that is yet to be explored. In RGS4 however we found a transcriptional regulation of a siderophore gene cluster in the presence of light. Siderophores are iron chelators involved in iron transport and

storage in the cell and in the protection against oxidative stress (Mukherjee et al., 2012; Wilson et al., 2016).

Similar to *T. reesei*, *T. harzianum* produces a wide array of secondary metabolites to not only defend against other organisms (Macias-Rodriguez et al., 2020; Manganiello et al., 2018), but also to facilitate communication with plants. *T. harzianum* B97 chemotropically responds to soybean roots, which consequentially changes secondary metabolite profiles of both, the fungus and the plant. We show that the PCA gene cluster is activated upon plant detection and is vital for an effective root colonization which points to a complex, chemical communication between *T. harzianum* B97 and plants. Understanding these interactions helps in driving advancements in biocontrol applications.

To conclude, the complexities of fungal biology and their strategic resource distribution underlines the adaptability of these organisms to their environments. This thesis highlights the roles of cellular signaling via G-proteins and MAPkinases in governing the processes of carbon- and secondary metabolism, as well plant interactions. Looking ahead, deciphering the influence of these signaling networks on the expression of secondary metabolite clusters and their impact on biocontrol and plant symbiosis, and on cellulase secretion for an efficient biomass conversion offer a promising opportunity for research, with promising future applications in agriculture and biotechnology.

References

Alberti, F., Foster, G. D., & Bailey, A. M. (2017). Natural products from filamentous fungi and production by heterologous expression. *Appl Microbiol Biotechnol*, *101*(2), 493-500. https://doi.org/10.1007/s00253-016-8034-2

Avruch, J. (2007). MAP kinase pathways: the first twenty years. *Biochim Biophys Acta*, *1773*(8), 1150-1160. https://doi.org/10.1016/j.bbamcr.2006.11.006

Balde, E. S., Andolfi, A., Bruyere, C., Cimmino, A., Lamoral-Theys, D., Vurro, M., Damme, M. V., Altomare, C., Mathieu, V., Kiss, R., & Evidente, A. (2010). Investigations of fungal secondary metabolites with potential anticancer activity. *J Nat Prod*, *73*(5), 969-971. https://doi.org/10.1021/np900731p

Bar-On, Y. M., Phillips, R., & Milo, R. (2018). The biomass distribution on Earth. *Proc Natl Acad Sci U S A*, *115*(25), 6506-6511. https://doi.org/10.1073/pnas.1711842115

Bardwell, L. (2004). A walk-through of the yeast mating pheromone response pathway [Research Support, U.S. Gov't, P.H.S.
Review]. *Peptides*, *25*(9), 1465-1476. https://doi.org/10.1016/j.peptides.2003.10.022

Bayram, O., Bayram, O. S., Ahmed, Y. L., Maruyama, J., Valerius, O., Rizzoli, S. O., Ficner, R., Irniger, S., & Braus, G. H. (2012). The Aspergillus nidulans MAPK module AnSte11-Ste50-Ste7-Fus3 controls development and secondary metabolism. *PLoS Genet*, *8*(7), e1002816. https://doi.org/10.1371/journal.pgen.1002816

Bazafkan, H., Beier, S., Stappler, E., Böhmdorfer, S., Oberlerchner, J. T., Sulyok, M., & Schmoll, M. (2017). SUB1 has photoreceptor dependent and independent functions in sexual development and secondary metabolism in *Trichoderma reesei*. *Mol Microbiol*, *106*(5), 742-759. https://doi.org/10.1111/mmi.13842

Bazafkan, H., Dattenböck, C., Böhmdorfer, S., Tisch, D., Stappler, E., & Schmoll, M. (2015). Mating type dependent partner sensing as mediated by VEL1 in *Trichoderma reesei*. *Mol Microbiol*, *96*(6), 1103-1118. https://doi.org/10.1111/mmi.12993

Belal, E. B. (2013). Bioethanol production from rice straw residues. *Braz J Microbiol*, *44*(1), 225-234. https://doi.org/10.1590/S1517-83822013000100033

Bennett, L. D., Beremand, P., Thomas, T. L., & Bell-Pedersen, D. (2013). Circadian activation of the mitogen-activated protein kinase MAK-1 facilitates rhythms in clock-controlled genes in Neurospora crassa. *Eukaryot Cell*, *12*(1), 59-69. https://doi.org/10.1128/EC.00207-12

Benocci, T., Aguilar-Pontes, M. V., Zhou, M., Seiboth, B., & de Vries, R. P. (2017). Regulators of plant biomass degradation in ascomycetous fungi. *Biotechnol Biofuels*, *10*, 152. https://doi.org/10.1186/s13068-017-0841-x

Bischof, R. H., Ramoni, J., & Seiboth, B. (2016). Cellulases and beyond: the first 70 years of the enzyme producer *Trichoderma reesei*. *Microb Cell Fact*, *15*(1), 106. https://doi.org/10.1186/s12934-016-0507-6

Brian, B. (2014). *BBMap*. https://sourceforge.net/projects/bbmap/

Brown, N. A., Ries, L. N. A., & Goldman, G. H. (2014). How nutritional status signalling coordinates metabolism and lignocellulolytic enzyme secretion. *Fungal Genet Biol*, *72*, 48-63. https://doi.org/10.1016/j.fgb.2014.06.012

Cabrera-Vera, T. M., Vanhauwe, J., Thomas, T. O., Medkova, M., Preininger, A., Mazzoni, M. R., & Hamm, H. E. (2003). Insights into G protein structure, function, and regulation. *Endocrine reviews*, *24*(6), 765-781. https://doi.org/10.1210/er.2000-0026

Canessa, P., Schumacher, J., Hevia, M. A., Tudzynski, P., & Larrondo, L. F. (2013). Assessing the effects of light on differentiation and virulence of the plant pathogen *Botrytis cinerea*: characterization of the White Collar Complex. *PLoS One*, *8*(12), e84223. https://doi.org/10.1371/journal.pone.0084223

Carreras-Villaseñor, N., Sanchez-Arreguin, J. A., & Herrera-Estrella, A. H. (2012). *Trichoderma*: sensing the environment for survival and dispersal. *Microbiology*, *158*(Pt 1), 3-16. https://doi.org/10.1099/mic.0.052688-0

Chen, X., Song, B., Liu, M., Qin, L., & Dong, Z. (2021). Understanding the Role of Trichoderma reesei Vib1 in Gene Expression during Cellulose Degradation. *J Fungi (Basel)*, *7*(8). https://doi.org/10.3390/jof7080613

Compant, S., Gerbore, J., Antonielli, L., Brutel, A., & Schmoll, M. (2017). Draft genome sequence of the root-colonizing fungus *Trichoderma harzianum* B97. *Genome Announc*, *5*(13). https://doi.org/10.1128/genomeA.00137-17

Corchete, L. A., Rojas, E. A., Alonso-Lopez, D., De Las Rivas, J., Gutierrez, N. C., & Burguillo, F. J. (2020). Systematic comparison and assessment of RNA-seq procedures for gene expression quantitative analysis. *Sci Rep*, *10*(1), 19737. https://doi.org/10.1038/s41598-020-76881-x

Cupertino, F. B., Virgilio, S., Freitas, F. Z., Candido Tde, S., & Bertolini, M. C. (2015). Regulation of glycogen metabolism by the CRE-1, RCO-1 and RCM-1 proteins in Neurospora crassa. The role of CRE-1 as the central transcriptional regulator. *Fungal Genet Biol*, *77*, 82-94. https://doi.org/10.1016/j.fgb.2015.03.011

de Assis, L. J., Silva, L. P., Bayram, O., Dowling, P., Kniemeyer, O., Kruger, T., Brakhage, A. A., Chen, Y., Dong, L., Tan, K., Wong, K. H., Ries, L. N. A., & Goldman, G. H. (2021). Carbon Catabolite Repression in Filamentous Fungi Is Regulated by Phosphorylation of the Transcription Factor CreA. *MBio*, *12*(1). https://doi.org/10.1128/mBio.03146-20

de Paula, R. G., Antonieto, A. C. C., Carraro, C. B., Lopes, D. C. B., Persinoti, G. F., Peres, N. T. A., Martinez-Rossi, N. M., Silva-Rocha, R., & Silva, R. N. (2018). The duality of the MAPK signaling pathway in the control of metabolic processes and cellulase production in *Trichoderma reesei*. *Sci Rep*, *8*(1), 14931. https://doi.org/10.1038/s41598-018-33383-1

Derntl, C., Guzman-Chavez, F., Mello-de-Sousa, T. M., Busse, H. J., Driessen, A. J. M., Mach, R. L., & Mach-Aigner, A. R. (2017). In Vivo Study of the Sorbicillinoid Gene Cluster in

Trichoderma reesei. *Front Microbiol*, *8*, 2037. https://doi.org/10.3389/fmicb.2017.02037

Derntl, C., Rassinger, A., Srebotnik, E., Mach, R. L., & Mach-Aigner, A. R. (2016). Identification of the main regulator responsible for synthesis of the typical yellow pigment produced by *Trichoderma reesei*. *Appl Environ Microbiol*, *82*(20), 6247-6257. https://doi.org/10.1128/AEM.01408-16

Dos Santos Castro, L., Pedersoli, W. R., Antonieto, A. C., Steindorff, A. S., Silva-Rocha, R., Martinez-Rossi, N. M., Rossi, A., Brown, N. A., Goldman, G. H., Faca, V. M., Persinoti, G. F., & Silva, R. N. (2014). Comparative metabolism of cellulose, sophorose and glucose in *Trichoderma reesei* using high-throughput genomic and proteomic analyses. *Biotechnol Biofuels*, *7*(1), 41. https://doi.org/10.1186/1754-6834-7-41

El-Gendi, H., Saleh, A. K., Badierah, R., Redwan, E. M., El-Maradny, Y. A., & El-Fakharany, E. M. (2021). A Comprehensive Insight into Fungal Enzymes: Structure, Classification, and Their Role in Mankind's Challenges. *J Fungi (Basel)*, *8*(1). https://doi.org/10.3390/jof8010023

Evidente, A., Andolfi, A., Cimmino, A., Ganassi, S., Altomare, C., Favilla, M., De Cristofaro, A., Vitagliano, S., & Agnese Sabatini, M. (2009). Bisorbicillinoids produced by the fungus Trichoderma citrinoviride affect feeding preference of the aphid Schizaphis graminum. *J Chem Ecol*, *35*(5), 533-541. https://doi.org/10.1007/s10886-009-9632-6

Frawley, D., & Bayram, O. (2020). The pheromone response module, a mitogen-activated protein kinase pathway implicated in the regulation of fungal development, secondary metabolism and pathogenicity. *Fungal Genet Biol*, *144*, 103469. https://doi.org/10.1016/j.fgb.2020.103469

Glass, N. L., Schmoll, M., Cate, J. H., & Coradetti, S. (2013). Plant cell wall deconstruction by ascomycete fungi. *Annu Rev Microbiol*, *67*, 477-498. https://doi.org/10.1146/annurev-micro-092611-150044

Gonzalez-Rubio, G., Fernandez-Acero, T., Martin, H., & Molina, M. (2019). Mitogen-Activated Protein Kinase Phosphatases (MKPs) in Fungal Signaling: Conservation, Function, and Regulation. *Int J Mol Sci*, *20*(7). https://doi.org/10.3390/ijms20071709

Gruber, S., & Zeilinger, S. (2014). The transcription factor Ste12 mediates the regulatory role of the Tmk1 MAP kinase in mycoparasitism and vegetative hyphal fusion in the filamentous fungus *Trichoderma atroviride*. *PLoS One*, *9*(10), e111636. https://doi.org/10.1371/journal.pone.0111636

Gustin, M. C., Albertyn, J., Alexander, M., & Davenport, K. (1998). MAP kinase pathways in the yeast Saccharomyces cerevisiae. *Microbiol Mol Biol Rev*, *62*(4), 1264-1300. http://www.ncbi.nlm.nih.gov/entrez/query.fcgi?cmd=Retrieve&db=PubMed&dopt=Citation&list_uids=9841672

Henriquez-Urrutia, M., Spanner, R., Olivares-Yanez, C., Seguel-Avello, A., Perez-Lara, R., Guillen-Alonso, H., Winkler, R., Herrera-Estrella, A., Canessa, P., & Larrondo, L. F. (2022). Circadian oscillations in Trichoderma atroviride and the role of core clock components

in secondary metabolism, development, and mycoparasitism against the phytopathogen Botrytis cinerea. *Elife*, *11*. https://doi.org/10.7554/eLife.71358

Hermosa, R., Viterbo, A., Chet, I., & Monte, E. (2012). Plant-beneficial effects of *Trichoderma* and of its genes. *Microbiology-Sgm*, *158*, 17-25. https://doi.org/10.1099/Mic.0.052274-0

Herrera-Estrella, A., & Horwitz, B. A. (2007). Looking through the eyes of fungi: molecular genetics of photoreception. *Mol Microbiol*, *64*(1), 5-15. http://www.ncbi.nlm.nih.gov/entrez/query.fcgi?cmd=Retrieve&db=PubMed&dopt=Citation&list_uids=17376067

Hinterdobler, W., Beier, S., Monroy, A. A., Berger, H., Dattenbock, C., & Schmoll, M. (2020). The G-protein coupled receptor GPR8 regulates secondary metabolism in *Trichoderma reesei*. *Front Bioeng Biotechnol*, *8*, 558996. https://doi.org/10.3389/fbioe.2020.558996

Hinterdobler, W., Li, G., Turrà, D., Schalamun, M., Kindel, S., Sauer, U., Beier, S., Iglesias, A. R., Compant, S., Vitale, S., Pietro, A. D., & Schmoll, M. (2021). Integration of chemosensing and carbon catabolite repression impacts fungal enzyme regulation and plant associations. *bioRxiv*, 2021.2005.2006.442915. https://doi.org/10.1101/2021.05.06.442915

Hinterdobler, W., Schuster, A., Tisch, D., Ozkan, E., Bazafkan, H., Schinnerl, J., Brecker, L., Bohmdorfer, S., & Schmoll, M. (2019). The role of PKAc1 in gene regulation and trichodimerol production in *Trichoderma reesei*. *Fungal Biol Biotechnol*, *6*, 12. https://doi.org/10.1186/s40694-019-0075-8

Hitzenhammer, E., Büschl, C., Sulyok, M., Schuhmacher, R., Kluger, B., Wischnitzki, E., & Schmoll, M. (2019). YPR2 is a regulator of light modulated carbon and secondary metabolism in *Trichoderma reesei*. *BMC Genomics*, *20*(1), 211. https://doi.org/10.1186/s12864-019-5574-8

Hohmann, S. (2015). An integrated view on a eukaryotic osmoregulation system. *Curr Genet*, *61*(3), 373-382. https://doi.org/10.1007/s00294-015-0475-0

Ilmen, M., Thrane, C., & Penttila, M. (1996). The glucose repressor gene *cre1* of *Trichoderma*: isolation and expression of a full-length and a truncated mutant form. *Mol Gen Genet*, *251*(4), 451-460.

Jin, K., Han, L., & Xia, Y. (2014). MaMk1, a FUS3/KSS1-type mitogen-activated protein kinase gene, is required for appressorium formation, and insect cuticle penetration of the entomopathogenic fungus Metarhizium acridum. *J Invertebr Pathol*, *115*, 68-75. https://doi.org/10.1016/j.jip.2013.10.014

Jonkers, W., Leeder, A. C., Ansong, C., Wang, Y., Yang, F., Starr, T. L., Camp, D. G., 2nd, Smith, R. D., & Glass, N. L. (2014). HAM-5 functions as a MAP kinase scaffold during cell fusion in *Neurospora crassa*. *PLoS Genet*, *10*(11), e1004783. https://doi.org/10.1371/journal.pgen.1004783

Kim, D., Paggi, J. M., Park, C., Bennett, C., & Salzberg, S. L. (2019). Graph-based genome alignment and genotyping with HISAT2 and HISAT-genotype. *Nat Biotechnol*, *37*(8), 907-915. https://doi.org/10.1038/s41587-019-0201-4

Kim, Y., Heo, I. B., Yu, J. H., & Shin, K. S. (2017). Characteristics of a Regulator of G-Protein Signaling (RGS) rgsC in Aspergillus fumigatus. *Front Microbiol*, *8*, 2058. https://doi.org/10.3389/fmicb.2017.02058

Kim, Y., Lee, M. W., Jun, S. C., Choi, Y. H., Yu, J. H., & Shin, K. S. (2019). RgsD negatively controls development, toxigenesis, stress response, and virulence in Aspergillus fumigatus. *Sci Rep*, *9*(1), 811. https://doi.org/10.1038/s41598-018-37124-2

Kubicek, C. P. (2013). Systems biological approaches towards understanding cellulase production by Trichoderma reesei. *J Biotechnol*, *163*(2), 133-142. https://doi.org/10.1016/j.jbiotec.2012.05.020

Kuhad, R. C., Gupta, R., & Singh, A. (2011). Microbial cellulases and their industrial applications. *Enzyme Res*, *2011*, 280696. https://doi.org/10.4061/2011/280696

Kunitake, E., Uchida, R., Asano, K., Kanamaru, K., Kimura, M., Kimura, T., & Kobayashi, T. (2022). cAMP signaling factors regulate carbon catabolite repression of hemicellulase genes in Aspergillus nidulans. *AMB Express*, *12*(1), 126. https://doi.org/10.1186/s13568-022-01467-x

Lamb, T. M., Goldsmith, C. S., Bennett, L., Finch, K. E., & Bell-Pedersen, D. (2011). Direct transcriptional control of a p38 MAPK pathway by the circadian clock in *Neurospora crassa*. *PLoS One*, *6*(11), e27149. https://doi.org/10.1371/journal.pone.0027149

Lange, L. (2017). Fungal Enzymes and Yeasts for Conversion of Plant Biomass to Bioenergy and High-Value Products. *Microbiol Spectr*, *5*(1). https://doi.org/10.1128/microbiolspec.FUNK-0007-2016

Lengeler, K. B., Davidson, R. C., D'Souza, C., Harashima, T., Shen, W. C., Wang, P., Pan, X., Waugh, M., & Heitman, J. (2000). Signal transduction cascades regulating fungal development and virulence. *Microbiol Mol Biol Rev*, *64*(4), 746-785. http://www.ncbi.nlm.nih.gov/entrez/query.fcgi?cmd=Retrieve&db=PubMed&dopt=Citation&list_uids=11104818

Li, H., Handsaker, B., Wysoker, A., Fennell, T., Ruan, J., Homer, N., Marth, G., Abecasis, G., Durbin, R., & Genome Project Data Processing, S. (2009). The Sequence Alignment/Map format and SAMtools. *Bioinformatics*, *25*(16), 2078-2079. https://doi.org/10.1093/bioinformatics/btp352

Li, L., Wright, S. J., Krystofova, S., Park, G., & Borkovich, K. A. (2007). Heterotrimeric G protein signaling in filamentous fungi. *Annu Rev Microbiol*, *61*, 423-452. http://www.ncbi.nlm.nih.gov/entrez/query.fcgi?cmd=Retrieve&db=PubMed&dopt=Citation&list_uids=17506673

Li, W. C., Huang, C. H., Chen, C. L., Chuang, Y. C., Tung, S. Y., & Wang, T. F. (2017). *Trichoderma reesei* complete genome sequence, repeat-induced point mutation, and partitioning of

CAZyme gene clusters. *Biotechnol Biofuels*, *10*, 170. https://doi.org/10.1186/s13068-017-0825-x

Liao, Y., Smyth, G. K., & Shi, W. (2014). featureCounts: an efficient general purpose program for assigning sequence reads to genomic features. *Bioinformatics*, *30*(7), 923-930. https://doi.org/10.1093/bioinformatics/btt656

Ma, L., Li, X., Xing, F., Ma, J., Ma, X., & Jiang, Y. (2022). Fus3, as a critical kinase in MAPK cascade, regulates aflatoxin biosynthesis by controlling the substrate supply in *Aspergillus flavus*, rather than the cluster genes modulation. *Microbiol Spectr*, *10*(1), e0126921. https://doi.org/10.1128/spectrum.01269-21

Ma, N., Zhao, Y., Wang, Y., Yang, L., Li, D., Yang, J., Jiang, K., Zhang, K. Q., & Yang, J. (2021). Functional analysis of seven regulators of G protein signaling (RGSs) in the nematode-trapping fungus Arthrobotrys oligospora. *Virulence*, *12*(1), 1825-1840. https://doi.org/10.1080/21505594.2021.1948667

Macias-Rodriguez, L., Contreras-Cornejo, H. A., Adame-Garnica, S. G., Del-Val, E., & Larsen, J. (2020). The interactions of *Trichoderma* at multiple trophic levels: inter-kingdom communication. *Microbiol Res*, *240*, 126552. https://doi.org/10.1016/j.micres.2020.126552

Manganiello, G., Sacco, A., Ercolano, M. R., Vinale, F., Lanzuise, S., Pascale, A., Napolitano, M., Lombardi, N., Lorito, M., & Woo, S. L. (2018). Modulation of Tomato Response to Rhizoctonia solani by Trichoderma harzianum and Its Secondary Metabolite Harzianic Acid. *Front Microbiol*, *9*, 1966. https://doi.org/10.3389/fmicb.2018.01966

Martinez, D., Berka, R. M., Henrissat, B., Saloheimo, M., Arvas, M., Baker, S. E., Chapman, J., Chertkov, O., Coutinho, P. M., Cullen, D., Danchin, E. G., Grigoriev, I. V., Harris, P., Jackson, M., Kubicek, C. P., Han, C. S., Ho, I., Larrondo, L. F., de Leon, A. L., . . . Brettin, T. S. (2008). Genome sequencing and analysis of the biomass-degrading fungus *Trichoderma reesei* (syn. *Hypocrea jecorina*). *Nat Biotechnol*, *26*(5), 553-560.

Martinez-Soto, D., & Ruiz-Herrera, J. (2017). Functional analysis of the MAPK pathways in fungi. *Rev Iberoam Micol*, *34*(4), 192-202. https://doi.org/10.1016/j.riam.2017.02.006

Martzy, R., Mello-de-Sousa, T. M., Mach, R. L., Yaver, D., & Mach-Aigner, A. R. (2021). The phenomenon of degeneration of industrial Trichoderma reesei strains. *Biotechnol Biofuels*, *14*(1), 193. https://doi.org/10.1186/s13068-021-02043-4

Medina-Castellanos, E., Villalobos-Escobedo, J. M., Riquelme, M., Read, N. D., Abreu-Goodger, C., & Herrera-Estrella, A. (2018). Danger signals activate a putative innate immune system during regeneration in a filamentous fungus. *PLoS Genet*, *14*(11), e1007390. https://doi.org/10.1371/journal.pgen.1007390

Mendoza-Mendoza, A., Pozo, M. J., Grzegorski, D., Martinez, P., Garcia, J. M., Olmedo-Monfil, V., Cortes, C., Kenerley, C., & Herrera-Estrella, A. (2003). Enhanced biocontrol activity of *Trichoderma* through inactivation of a mitogen-activated protein kinase. *Proc Natl Acad Sci U S A*, *100*(26), 15965-15970. https://doi.org/10.1073/pnas.2136716100

Meng, J., Wang, X., Xu, D., Fu, X., Zhang, X., Lai, D., Zhou, L., & Zhang, G. (2016). Sorbicillinoids from fungi and their bioactivities. *Molecules*, *21*(6). https://doi.org/10.3390/molecules21060715

Meyer, V., Basenko, E. Y., Benz, J. P., Braus, G. H., Caddick, M. X., Csukai, M., de Vries, R. P., Endy, D., Frisvad, J. C., Gunde-Cimerman, N., Haarmann, T., Hadar, Y., Hansen, K., Johnson, R. I., Keller, N. P., Krasevec, N., Mortensen, U. H., Perez, R., Ram, A. F. J., . . . Wosten, H. A. B. (2020). Growing a circular economy with fungal biotechnology: a white paper. *Fungal Biol Biotechnol*, *7*, 5. https://doi.org/10.1186/s40694-020-00095-z

Monroy, A. A., Stappler, E., Schuster, A., Sulyok, M., & Schmoll, M. (2017). A CRE1- regulated cluster is responsible for light dependent production of dihydrotrichotetronin in *Trichoderma reesei*. *PLoS One*(12), e0182530.

Moreno-Ruiz, D., Fuchs, A., Missbach, K., Schuhmacher, R., & Zeilinger, S. (2020). Influence of Different Light Regimes on the Mycoparasitic Activity and 6-Pentyl-alpha-pyrone Biosynthesis in Two Strains of Trichoderma atroviride. *Pathogens*, *9*(10). https://doi.org/10.3390/pathogens9100860

Moreno-Ruiz, D., Salzmann, L., Fricker, M. D., Zeilinger, S., & Lichius, A. (2021). Stress-activated protein kinase signalling regulates mycoparasitic hyphal-hyphal interactions in *Trichoderma atroviride*. *J Fungi (Basel)*, *7*(5). https://doi.org/10.3390/jof7050365

Mukherjee, P. K., Horwitz, B. A., & Kenerley, C. M. (2012). Secondary metabolism in *Trichoderma* - a genomic perspective. *Microbiology*, *158*(Pt 1), 35-45. https://doi.org/10.1099/mic.0.053629-0

Mukherjee, P. K., Latha, J., Hadar, R., & Horwitz, B. A. (2003). TmkA, a mitogen-activated protein kinase of *Trichoderma virens*, is involved in biocontrol properties and repression of conidiation in the dark. *Eukaryot Cell*, *2*(3), 446-455. http://www.ncbi.nlm.nih.gov/entrez/query.fcgi?cmd=Retrieve&db=PubMed&dopt=Citation&list_uids=12796289

Park, H. S., Kim, M. J., Yu, J. H., & Shin, K. S. (2020). Heterotrimeric G-protein signalers and RGSs in Aspergillus fumigatus. *Pathogens*, *9*(11). https://doi.org/10.3390/pathogens9110902

Peterson, R., & Nevalainen, H. (2012). *Trichoderma reesei* RUT-C30 - thirty years of strain improvement. *Microbiology*, *158*(Pt 1), 58-68. https://doi.org/10.1099/mic.0.054031-0

Rangel, L. I., Hamilton, O., de Jonge, R., & Bolton, M. D. (2021). Fungal social influencers: secondary metabolites as a platform for shaping the plant-associated community. *Plant J*, *108*(3), 632-645. https://doi.org/10.1111/tpj.15490

Rassinger, A., Gacek-Matthews, A., Strauss, J., Mach, R. L., & Mach-Aigner, A. R. (2018). Truncation of the transcriptional repressor protein Cre1 in Trichoderma reesei Rut-C30 turns it into an activator. *Fungal Biol Biotechnol*, *5*, 15. https://doi.org/10.1186/s40694-018-0059-0

Reithner, B., Schuhmacher, R., Stoppacher, N., Pucher, M., Brunner, K., & Zeilinger, S. (2007). Signaling via the *Trichoderma atroviride* mitogen-activated protein kinase Tmk1 differentially affects mycoparasitism and plant protection. *Fungal Genet Biol*. http://www.ncbi.nlm.nih.gov/entrez/query.fcgi?cmd=Retrieve&db=PubMed&dopt=Citation&list_uids=17509915

Rispail, N., Soanes, D. M., Ant, C., Czajkowski, R., Grunler, A., Huguet, R., Perez-Nadales, E., Poli, A., Sartorel, E., Valiante, V., Yang, M., Beffa, R., Brakhage, A. A., Gow, N. A., Kahmann, R., Lebrun, M. H., Lenasi, H., Perez-Martin, J., Talbot, N. J., . . . Di Pietro, A. (2009). Comparative genomics of MAP kinase and calcium-calcineurin signalling components in plant and human pathogenic fungi. *Fungal Genet Biol*, *46*(4), 287-298. https://doi.org/10.1016/j.fgb.2009.01.002

Rush, T. A., Shrestha, H. K., Gopalakrishnan Meena, M., Spangler, M. K., Ellis, J. C., Labbé, J. L., & Abraham, P. E. (2021). Bioprospecting *Trichoderma*: A systematic roadmap to screen genomes and natural products for biocontrol applications [Systematic Review]. *Frontiers in Fungal Biology*, *2*. https://doi.org/10.3389/ffunb.2021.716511

Salo, O., Guzman-Chavez, F., Ries, M. I., Lankhorst, P. P., Bovenberg, R. A., Vreeken, R. J., & Driessen, A. J. (2016). Identification of a polyketide synthase involved in sorbicillin biosynthesis by *Penicillium chrysogenum*. *Appl Environ Microbiol*, *82*(13), 3971-3978. https://doi.org/10.1128/AEM.00350-16

Saravanakumar, K., & Kathiresan, K. (2014). Bioconversion of lignocellulosic waste to bioethanol by Trichoderma and yeast fermentation. *3 Biotech*, *4*(5), 493-499. https://doi.org/10.1007/s13205-013-0179-4

Saravanan, P., Muthuvelayudham, R., & Viruthagiri, T. (2012). Application of Statistical Design for the Production of Cellulase by Trichoderma reesei Using Mango Peel. *Enzyme Res*, *2012*, 157643. https://doi.org/10.1155/2012/157643

Schaarschmidt, S., Fischer, A., Zuther, E., & Hincha, D. K. (2020). Evaluation of Seven Different RNA-Seq Alignment Tools Based on Experimental Data from the Model Plant Arabidopsis thaliana. *Int J Mol Sci*, *21*(5). https://doi.org/10.3390/ijms21051720

Schmoll, M. (2008). The information highways of a biotechnological workhorse - signal transduction in *Hypocrea jecorina*. *BMC Genomics*, *9*, 430. http://www.ncbi.nlm.nih.gov/entrez/query.fcgi?cmd=Retrieve&db=PubMed&dopt=Citation&list_uids=18803869

Schmoll, M. (2018a). Light, stress, sex and carbon - the photoreceptor ENVOY as a central checkpoint in the physiology of *Trichoderma reesei*. *Fungal Biol*, *122*(6), 479-486. https://doi.org/https://doi.org/10.1016/j.funbio.2017.10.007

Schmoll, M. (2018b). Regulation of plant cell wall degradation by light in *Trichoderma*. *Fungal Biol Biotechnol*, *5*, 10. https://doi.org/10.1186/s40694-018-0052-7

Schmoll, M., Dattenböck, C., Carreras-Villasenor, N., Mendoza-Mendoza, A., Tisch, D., Aleman, M. I., Baker, S. E., Brown, C., Cervantes-Badillo, M. G., Cetz-Chel, J., Cristobal-Mondragon, G. R., Delaye, L., Esquivel-Naranjo, E. U., Frischmann, A., Gallardo-Negrete

Jde, J., Garcia-Esquivel, M., Gomez-Rodriguez, E. Y., Greenwood, D. R., Hernandez-Onate, M., . . . Herrera-Estrella, A. (2016). The genomes of three uneven siblings: footprints of the lifestyles of three *Trichoderma* species. *Microbiol Mol Biol Rev*, *80*(1), 205-327. https://doi.org/10.1128/MMBR.00040-15

Schmoll, M., Esquivel-Naranjo, E. U., & Herrera-Estrella, A. (2010). *Trichoderma* in the light of day - physiology and development. *Fungal Genet Biol*, *47*(11), 909-916. https://doi.org/10.1016/j.fgb.2010.04.010

Schmoll, M., Franchi, L., & Kubicek, C. P. (2005). Envoy, a PAS/LOV domain protein of *Hypocrea jecorina* (Anamorph *Trichoderma reesei*), modulates cellulase gene transcription in response to light. *Eukaryot Cell*, *4*(12), 1998-2007. http://www.ncbi.nlm.nih.gov/entrez/query.fcgi?cmd=Retrieve&db=PubMed&dopt=Citation&list_uids=16339718

Schmoll, M., & Hinterdobler, W. (2022). Tools for adapting to a complex habitat: G-protein coupled receptors in *Trichoderma*. In *Progress in Molecular Biology and Translational Science*. Academic Press. https://doi.org/https://doi.org/10.1016/bs.pmbts.2022.06.003

Schmoll, M., Schuster, A., do Nascimento Silva, R., & Kubicek, C. P. (2009). The G-alpha protein GNA3 of *Hypocrea jecorina* (anamorph *Trichoderma reesei*) regulates cellulase gene expression in the presence of light. *Eukaryot Cell*, *8*(3), 410 - 420. https://doi.org/EC.00256-08 [pii]
10.1128/EC.00256-08

Schuster, A., Kubicek, C. P., Friedl, M. A., Druzhinina, I. S., & Schmoll, M. (2007). Impact of light on *Hypocrea jecorina* and the multiple cellular roles of ENVOY in this process. *BMC Genomics*, *8*(1), 449. http://www.ncbi.nlm.nih.gov/entrez/query.fcgi?cmd=Retrieve&db=PubMed&dopt=Citation&list_uids=18053205

Schuster, A., Tisch, D., Seidl-Seiboth, V., Kubicek, C. P., & Schmoll, M. (2012). Roles of protein kinase A and adenylate cyclase in light-modulated cellulase regulation in *Trichoderma reesei*. *Appl Environ Microbiol*, *78*(7), 2168-2178. https://doi.org/10.1128/AEM.06959-11

Seibel, C., Gremel, G., Silva, R. D., Schuster, A., Kubicek, C. P., & Schmoll, M. (2009). Light-dependent roles of the G-protein subunit GNA1 of *Hypocrea jecorina* (anamorph *Trichoderma reesei*). *BMC Biol*, *7*(1), 58. http://www.ncbi.nlm.nih.gov/entrez/query.fcgi?cmd=Retrieve&db=PubMed&dopt=Citation&list_uids=19728862

Seidl, V., Gamauf, C., Druzhinina, I. S., Seiboth, B., Hartl, L., & Kubicek, C. P. (2008). The *Hypocrea jecorina* (*Trichoderma reesei*) hypercellulolytic mutant RUT C30 lacks a 85 kb (29 gene-encoding) region of the wild-type genome. *BMC Genomics*, *9*, 327. https://doi.org/10.1186/1471-2164-9-327

Serrano, A., Illgen, J., Brandt, U., Thieme, N., Letz, A., Lichius, A., Read, N. D., & Fleissner, A. (2018). Spatio-temporal MAPK dynamics mediate cell behavior coordination during fungal somatic cell fusion. *J Cell Sci*, *131*(9). https://doi.org/10.1242/jcs.213462

Stappler, E., Dattenböck, C., Tisch, D., & Schmoll, M. (2017). Analysis of Light- and Carbon-Specific Transcriptomes Implicates a Class of G-Protein-Coupled Receptors in Cellulose Sensing. *mSphere*, *2*(3). https://doi.org/10.1128/mSphere.00089-17

Stappler, E., Walton, J. D., & Schmoll, M. (2017). Abundance of secreted proteins of *Trichoderma reesei* is regulated by light of different intensities. *Front Microbiol*, 8:2586.

Syrovatkina, V., & Huang, X. Y. (2019). Signaling mechanisms and physiological functions of G-protein Galpha(13) in blood vessel formation, bone homeostasis, and cancer. *Protein Sci*, *28*(2), 305-312. https://doi.org/10.1002/pro.3531

Tang, X., Ouyang, Q., Jing, G., Shao, X., & Tao, N. (2018). Antifungal mechanism of sodium dehydroacetate against Geotrichum citri-aurantii. *World J Microbiol Biotechnol*, *34*(2), 29. https://doi.org/10.1007/s11274-018-2413-z

Tisch, D., Kubicek, C. P., & Schmoll, M. (2011a). New insights into the mechanism of light modulated signaling by heterotrimeric G-proteins: ENVOY acts on *gna1* and *gna3* and adjusts cAMP levels in *Trichoderma reesei* (*Hypocrea jecorina*). *Fungal Genet Biol*, *48*(6), 631-640.

Tisch, D., Kubicek, C. P., & Schmoll, M. (2011b). The phosducin-like protein PhLP1 impacts regulation of glycoside hydrolases and light response in *Trichoderma reesei*. *BMC Genomics*, *12*, 613.

Tisch, D., & Schmoll, M. (2010). Light regulation of metabolic pathways in fungi. *Appl Microbiol Biotechnol*, *85*(5), 1259-1277. https://doi.org/10.1007/s00253-009-2320-1

Tisch, D., & Schmoll, M. (2013). Targets of light signalling in *Trichoderma reesei*. *BMC Genomics*, *14*(1), 657. https://doi.org/10.1186/1471-2164-14-657

Tisch, D., Schuster, A., & Schmoll, M. (2014). Crossroads between light response and nutrient signalling: ENV1 and PhLP1 act as mutual regulatory pair in *Trichoderma reesei*. *BMC Genomics*, *15*, 425. https://doi.org/10.1186/1471-2164-15-425

Tong, S. M., & Feng, M. G. (2019). Insights into regulatory roles of MAPK-cascaded pathways in multiple stress responses and life cycles of insect and nematode mycopathogens. *Appl Microbiol Biotechnol*, *103*(2), 577-587. https://doi.org/10.1007/s00253-018-9516-1

Turra, D., Segorbe, D., & Di Pietro, A. (2014). Protein kinases in plant-pathogenic fungi: conserved regulators of infection. *Annu Rev Phytopathol*, *52*, 267-288. https://doi.org/10.1146/annurev-phyto-102313-050143

Valiante, V. (2017). The Cell Wall Integrity signaling Pathway and its involvement in secondary metabolite production. *J Fungi (Basel)*, *3*(4). https://doi.org/10.3390/jof3040068

van Dijk, M., Morley, T., Rau, M. L., & Saghai, Y. (2021). A meta-analysis of projected global food demand and population at risk of hunger for the period 2010-2050. *Nat Food*, *2*(7), 494-501. https://doi.org/10.1038/s43016-021-00322-9

Vasic, K., Knez, Z., & Leitgeb, M. (2021). Bioethanol Production by Enzymatic Hydrolysis from Different Lignocellulosic Sources. *Molecules*, *26*(3). https://doi.org/10.3390/molecules26030753

Vitalini, M. W., de Paula, R. M., Goldsmith, C. S., Jones, C. A., Borkovich, K. A., & Bell-Pedersen, D. (2007). Circadian rhythmicity mediated by temporal regulation of the activity of p38 MAPK. *Proc Natl Acad Sci U S A*, *104*(46), 18223-18228. http://www.ncbi.nlm.nih.gov/entrez/query.fcgi?cmd=Retrieve&db=PubMed&dopt=Citation&list_uids=17984065

Wang, M., Dong, Y., Zhao, Q., Wang, F., Liu, K., Jiang, B., & Fang, X. (2014). Identification of the role of a MAP kinase Tmk2 in *Hypocrea jecorina* (*Trichoderma reesei*). *Sci Rep*, *4*, 6732. https://doi.org/10.1038/srep06732

Wang, M., Zhang, M., Li, L., Dong, Y., Jiang, Y., Liu, K., Zhang, R., Jiang, B., Niu, K., & Fang, X. (2017). Role of *Trichoderma reesei* mitogen-activated protein kinases (MAPKs) in cellulase formation. *Biotechnol Biofuels*, *10*, 99. https://doi.org/10.1186/s13068-017-0789-x

Wang, M., Zhao, Q., Yang, J., Jiang, B., Wang, F., Liu, K., & Fang, X. (2013). A mitogen-activated protein kinase Tmk3 participates in high osmolarity resistance, cell wall integrity maintenance and cellulase production regulation in *Trichoderma reesei*. *PLoS One*, *8*(8), e72189. https://doi.org/10.1371/journal.pone.0072189

Wang, Y., Geng, Z., Jiang, D., Long, F., Zhao, Y., Su, H., Zhang, K. Q., & Yang, J. (2013). Characterizations and functions of regulator of G protein signaling (RGS) in fungi. *Appl Microbiol Biotechnol*, *97*(18), 7977-7987. https://doi.org/10.1007/s00253-013-5133-1

Wang, Y., Pierce, M., Schneper, L., Guldal, C. G., Zhang, X., Tavazoie, S., & Broach, J. R. (2004). Ras and Gpa2 mediate one branch of a redundant glucose signaling pathway in yeast. *PLoS Biol*, *2*(5), E128. https://doi.org/10.1371/journal.pbio.0020128

Wilson, B. R., Bogdan, A. R., Miyazawa, M., Hashimoto, K., & Tsuji, Y. (2016). Siderophores in Iron Metabolism: From Mechanism to Therapy Potential. *Trends Mol Med*, *22*(12), 1077-1090. https://doi.org/10.1016/j.molmed.2016.10.005

Wilson, D. B. (2009). Cellulases and biofuels [Review]. *Curr Opin Biotechnol*, *20*(3), 295-299. https://doi.org/10.1016/j.copbio.2009.05.007

Wong Sak Hoi, J., & Dumas, B. (2010). Ste12 and Ste12-like proteins, fungal transcription factors regulating development and pathogenicity. *Eukaryot Cell*, *9*(4), 480-485. https://doi.org/10.1128/EC.00333-09

Xiao, Z., Zhao, Q., Li, W., Gao, L., & Liu, G. (2023). Strain improvement of Trichoderma harzianum for enhanced biocontrol capacity: Strategies and prospects. *Front Microbiol*, *14*, 1146210. https://doi.org/10.3389/fmicb.2023.1146210

Xie, G. X., & Palmer, P. P. (2007). How regulators of G protein signaling achieve selective regulation. *J Mol Biol*, *366*(2), 349-365. https://doi.org/10.1016/j.jmb.2006.11.045

Yao, X., Guo, H., Zhang, K., Zhao, M., Ruan, J., & Chen, J. (2023). Trichoderma and its role in biological control of plant fungal and nematode disease. *Front Microbiol*, *14*, 1160551. https://doi.org/10.3389/fmicb.2023.1160551

Yu, Z., Armant, O., & Fischer, R. (2016). Fungi use the SakA (HogA) pathway for phytochrome-dependent light signalling. *Nat Microbiol*, *1*, 16019. https://doi.org/10.1038/nmicrobiol.2016.19

Yu, Z., & Fischer, R. (2019). Light sensing and responses in fungi. *Nat Rev Microbiol*, *17*(1), 25-36. https://doi.org/10.1038/s41579-018-0109-x

Zhang, Y., Du, Y., Yin, J., Hu, C., Liu, X., & Cui, W. (2012). Determination and depletion of dehydroacetic acid residue in chicken tissues. *Food Addit Contam Part A Chem Anal Control Expo Risk Assess*, *29*(6), 918-924. https://doi.org/10.1080/19440049.2012.660656

Zheng, L., Campbell, M., Murphy, J., Lam, S., & Xu, J. R. (2000). The BMP1 gene is essential for pathogenicity in the gray mold fungus Botrytis cinerea. *Mol Plant Microbe Interact*, *13*(7), 724-732. https://doi.org/10.1094/MPMI.2000.13.7.724

Curriculum Vitae

Miriam Schalamun

E-mail: miriam.schalamun@gmail.com
Phone: +4369913216941
Date of birth: 12/08/1993

Education

2020 – ongoing	**Doctoral curriculum in Natural Sciences** TU Wien, Faculty for Technical Chemistry, practical work at: AIT Austrian Institute of Technology, Health and Bioresources, Austria o Cellular Signaling in Fungi
2016 – 2019	**M.Sc. in Biotechnology** University of Natural Resources and Life Sciences, Austria
2011 – 2016	**B.Sc. in Food Sciences and Biotechnology** University of Natural Resources and Life Sciences, Austria
2009 – 2011	**International Baccalaureate** International School of Havana, Cuba

Professional Experience

04/2023 – ongoing	**MyPilz GmbH**, **Austria** Research Laboratory manager
02/2023 – 03/2023	**University of Pretoria, South Africa** Forestry and Agricultural Biotechnology Institute, South Africa Research and Innovation Staff Exchange
09/2018 – 12/2019	**Vienna Biocenter Core Facilities, Austria** Next Generation Sequencing Sequencing specialist for long read sequencing
08/2018 – 12/2019	**International Atomic Energy Agency, Austria** Animal Production and Health Section Consultant for Nanopore sequencing and data analysis
02/2018 – 07/2018	**University of Natural Resources and Life Sciences, Austria** Department of Applied Genetics and Cell Biology Student employee
08/2017 – 10/2017	**Deutsche Sammlung von Mikroorganismen und Zellkulturen, Germany** Plant Virus Division Consultant for Nanopore sequencing for the identification of plant viruses
02/2017 – 07/2017	**Australian National University, Canberra, Australia**

Master's thesis: Optimisation of high molecular weight DNA extractions from *Eucalyptus pauciflora* for MinION Nanopore sequencing

2011 – 2016   **Otis Elevator Company, Austria**
Sales and Administrative Assistant

Mentoring and coaching experience

07/2020 – 02/2021   Mentored B.Sc. students Lea Rosina and Nicole Wanko

2012 – 2013   Tutor for first semester students of B.Sc. Food Sciences and Biotechnology University of Natural Resources and Life Sciences, Austria

2014 – 2019   Organization and coaching of weekly to monthly Women Parkour Trainings Parkour-Vienna, Austria

List of Publications

Schalamun M., Hinterdobler H., Schinnerl J., Brecker L., Schmoll M. 2024 The transcription factor STE12 influences growth on several carbon sources and production of dehydroacetic acid (DHAA) in *Trichoderma reesei*. *Research Square.* https://doi.org/10.21203/rs.3.rs-3843527/v1

Schalamun M., Li G., Hinterdobler W., Großkinsky D., Compant S., Dreux-Zigha A., Schmoll M. 2023. Plant recognition by *Trichoderma harzianum* elicits upregulation of a novel secondary metabolite cluster required for colonization. *bioRXiv.* https://doi.org/10.1101/2023.04.12.536597

Schalamun M.**,** Molin E., Schmoll M. 2023. RGS4 impacts carbohydrate and siderophore metabolism in *Trichoderma reesei***.** *BMC Genomics*. 24:372. https://doi.org/10.1186/s12864-023-09467-2.

Schalamun M., Beier S., Hinterdobler W., Wanko N., Schinnerl J., Brecker L., Engl D.E., Schmoll M. 2023. MAPkinases regulate secondary metabolism, sexual development and light dependent cellulase regulation in *Trichoderma reesei*. *Scientific Reports*. 13:1912. https://doi.org/10.1186/s12864-023-09467-2

Schalamun M and Schmoll M. 2022. *Trichoderma* – genomes and genomics as treasure troves for research towards biology, biotechnology and agriculture. *Frontiers in Fungal Biology*, 3:1002161. https://doi.org/10.3389/ffunb.2022.1002161

Hinterdobler W., Li G, Turrà D., **Schalamun** M., Kindel S., Sauer U., Beier S., Iglesias AR., Compant S., Vitale S., Di Pietro A., Schmoll M. 2021. Integration of chemosensing and carbon catabolite repression impacts fungal enzyme regulation and plant associations. *bioRxiv*. https://doi.org/10.1101/2021.05.06.442915

Wang W., Das A., Kainer D., **Schalamun** M., Morales-Suarez A., Schwessinger B., Lanfear R. 2020. The draft nuclear genome assembly of *Eucalyptus pauciflora*: a pipeline to comparing de novo assemblies. *GigaScience,* 9, 2020, 1–12. https://doi.org/10.1093/gigascience/giz160

Schalamun M., Nagar R., Kainer D., Beavan E., Eccles D., Rathjen J. P., Lanfear R., Schwessinger, B. 2019. Harnessing the MinION: An example of how to establish long-read sequencing in a laboratory using challenging plant tissue from *Eucalyptus pauciflora*. *Molecular Ecology Resources,* 19: 77– 89. https://doi.org/10.1111/1755-0998.12938

Lanfear R., **Schalamun** M., Kainer D., Wang W., Schwessinger B. 2019. MinIONQC: fast and simple quality control for MinION sequencing data. *Bioinformatics,* 35(3): 523–525. https://doi.org/10.1093/bioinformatics/bty654

Wang W., **Schalamun** M., Morales-Suarez A., Kainer D., Schwessinger B., Lanfear R. 2018. Assembly of chloroplast genomes with long- and short-read data: a comparison of approaches using *Eucalyptus pauciflora* as a test case. *BMC Genomics,* 19(1). https://doi.org/10.1186/s12864-018-5348-8

List of oral and poster presentations

56. Wissenschaftliche Tagung der Deutschsprachigen Mykologischen Gesellschaft, 2022, Vienna. Presentation, Schalamun et al.

14th OEGMBT Annual Meeting - Austrian Association of Molecular Life Sciences and Biotechnology, 2022, Vienna. Presentation, Schalamun et al.

Westerdijk Spring Symposium Rise of the Fungi, 2022, Amsterdam. Poster, Schalamun et al.

Fungal Genetics Conference at Asilomar, 2022, Pacific Grove, CA. Presentation and Poster. "Genome wide insights into signal integration by the G-protein pathway for regulation of carbon- and secondary metabolism in *Trichoderma reesei*", Schalamun et al.